E-ISSN: 2148-094X

istanbul MEDICAL JOURNAL

İSTANBUL TIP DERGİSİ

VOLUME 27 • ISSUE 3 • August 2026

Editorial

Original Articles

istanbulmedicaljournal.org

galenos yayınevi

istanbul MEDICAL JOURNAL

İSTANBUL TIP DERGİSİ

galenos yayınevi

Publisher Contact
Address: Molla Gürani Mah. Kaçamak Sk. No: 21/1 34093 İstanbul, Türkiye
Phone: +90 (530) 177 30 97 / +90 (539) 307 32 03
E-mail: info@galenos.com.tr/yayin@galenos.com.tr
Web: www.galenos.com.tr
Publisher Certificate Number: 14521

Publication Date: August 2026
E-ISSN: 2148-094X
International periodical journal published four times in a year.

istanbulmedicaljournal.org

İSTANBUL MEDICAL JOURNAL
İSTANBUL TIP DERGİSİ

istanbul
MEDICAL JOURNAL
İSTANBUL TIP DERGİSİ

Pediatric Cardiovascular Surgery

Ali Can HATEMİ
Department of Pediatric Cardiovascular Surgery, University of Health Sciences Türkiye, Başakşehir Çam and Sakura City Hospital, İstanbul, Türkiye

Dermatology

Ayşe Esra KOKU AKSU
Department of Dermatology, University of Health Sciences Türkiye, İstanbul Training and Research Hospital, İstanbul, Türkiye

Mehmet Salih GÜREL
Department of Dermatology, İstanbul Medeniyet University Faculty of Medicine, İstanbul, Türkiye

Infectious Diseases and Clinical Microbiology

Nagehan Didem SARI
Department of Infectious Diseases and Clinical Microbiology, University of Health Sciences Türkiye, İstanbul Training and Research Hospital, İstanbul, Türkiye

Mustafa YILDIRIM
Department of Infectious Diseases and Clinical Microbiology, University of Health Sciences Türkiye, İstanbul Training and Research Hospital, İstanbul, Türkiye

Naim MAHROUM
Department of Infectious Diseases and Clinical Microbiology, Tel Aviv University Faculty of Medicine, Tel Aviv, İsrail

Physical Medicine and Rehabilitation

Ebru AYTEKİN
Department of Physical Medicine and Rehabilitation, University of Health Sciences Türkiye, İstanbul Training and Research Hospital, İstanbul, Türkiye

Nalan ÇAPAN
Department of Physical Therapy and Rehabilitation, İstanbul University, İstanbul Faculty of Medicine, İstanbul, Türkiye

General Surgery

Serkan SARI
Department of General Surgery, University of Health Sciences Türkiye, Başakşehir Çam and Sakura Training and Research Hospital, İstanbul, Türkiye

Mert Mahzuni SEVİNÇ
Department of General Medicine, University of Health Sciences Türkiye, İstanbul Training and Research Hospital, İstanbul, Türkiye

Ufuk Oğuz İDİZ
Department of General Medicine, University of Health Sciences Türkiye, İstanbul Training and Research Hospital, İstanbul, Türkiye

Hasan ÖKMEN
Department of General Medicine, University of Health Sciences Türkiye, İstanbul Training and Research Hospital, İstanbul, Türkiye

Chest Diseases

Erdoğan ÇETİNKAYA
Department of Chest Diseases, University of Health Sciences Türkiye, Yedikule Chest Diseases and Thoracic Surgery Training and Research Hospital, İstanbul, Türkiye

Seda TURAL ÖNÜR
Department of Chest Diseases, University of Health Sciences Türkiye, Yedikule Chest Diseases and Thoracic Surgery Training and Research Hospital, İstanbul, Türkiye

Sedat ALTIN
Department of Chest Diseases, University of Health Sciences Türkiye, Yedikule Chest Diseases and Chest Surgery Training and Research Hospital, İstanbul, Türkiye

Alexandru CORLATEANU
Department of Chest Diseases, State University of Medicine and Pharmacy, Moldova

Chest Surgery

Kemal KARAPINAR
Department of Chest Surgery, University of Health Sciences Türkiye, İstanbul Yedikule Pulmonary Diseases and Thoracic Surgery Training and Research Hospital, İstanbul, Türkiye

Levent CANSEVER
Department of Chest Surgery, University of Health Sciences Türkiye, Yedikule Chest Diseases and Chest Surgery Training and Research Hospital, İstanbul, Türkiye

Eye Diseases

Özen AYRANCI
Department of Eye Diseases, University of Health Sciences Türkiye, İstanbul Training and Research Hospital, İstanbul, Türkiye

Yusuf YILDIRIM
Department of Ophthalmology, University of Health Sciences Türkiye, İstanbul Beyoğlu Eye Training and Research Hospital, İstanbul, Türkiye

İSTANBUL MEDICAL JOURNAL
İSTANBUL TIP DERGİSİ

istanbul
MEDICAL JOURNAL
İSTANBUL TIP DERGİSİ

istanbul
MEDICAL JOURNAL
İSTANBUL TIP DERGİSİ

Please refer to the journal's webpage (**https://istanbulmedicaljournal.org/**) for "About Us" and "Instructions to Authors".

The İstanbul Medical Journal and/or its editors are members of ICMJE, COPE, WAME, CSE and EASE, and follow their recommendations.

The İstanbul Medical Journal is indexed in **Web of Science-Emerging Sources Citation Index, EBSCO, Gale, TUBITAK ULAKBIM TR Index, ProQuest, Embase, Türk Atif Dizini, Türk Medline, DOAJ, Ardi, Hinari, Goali, Oare, CAB International (CABI)** and **J-GATE**.

The journal is published online.

Owner: İstanbul Training and Research Hospital

Responsible Manager: Feray Akbaş

İSTANBUL MEDICAL JOURNAL
İSTANBUL TIP DERGİSİ

CONTENTS

İstanbul Med J 2026; 27(3): 179-80
DOI: 10.4274/imj.galenos.2026.240726

Lifestyle Medicine: From Adjunct to Core Internal Medicine Practice

Feray Akbaş

University of Health Sciences Türkiye, İstanbul Training and Research Hospital, Clinic of Internal Medicine, İstanbul, Türkiye

According to the World Health Organization, non-communicable diseases (NCDs) accounted for 75% of all non-pandemic global mortalities in 2021. Cardiovascular diseases remained the leading cause of death worldwide, followed by neoplasms, chronic respiratory diseases and diabetes mellitus, including diabetic nephropathy. The global burden and mortality of these chronic conditions are significantly exacerbated by modifiable behavioral and environmental risk factors, including atherogenic diets, physical inactivity, smoking, harmful alcohol consumption and ambient air pollution (1). Consequently, promoting and sustaining healthy lifestyle behaviours should be regarded as a fundamental pillar of the prevention and management of any chronic disease.

Lifestyle medicine encompasses several core domains, including adherence to a healthy dietary pattern—preferably one consistent with the Mediterranean diet—regular and adequate physical activity and exercise, effective stress management, restorative sleep, avoidance of health-risk substances (including tobacco, alcohol and illicit drugs), maintenance of a healthy living environment and the cultivation of strong social connections (2,3).

Healthy dietary patterns are essential for reducing the risk of chronic diseases, including type 2 diabetes mellitus, cardiovascular disease, stroke and certain types of cancer. Although healthy diets may vary according to cultural and social contexts as well as individual preferences, they should provide adequate nutrients in appropriate proportions and include a diverse selection of foods while emphasizing moderation. Ensuring food safety is also a fundamental component of a healthy diet. Furthermore, a sustainable healthy dietary pattern should prioritize a wide variety of minimally processed and unprocessed foods while limiting the consumption of foods high in unhealthy fats, free sugars, and sodium (4).

Regular physical activity is associated with substantial physical and psychological health benefits across the lifespan. Engaging in regular physical activity contributes not only to the prevention and management of chronic diseases but also to the reduction of symptoms associated with depression and anxiety, the enhancement of cognitive and brain health and the improvement of overall quality of life and well-being (5).

Psychiatric conditions—specifically major depression, anxiety and post-traumatic stress disorder—alongside maladaptive personality traits like hostility, pessimism and social isolation, are established correlates of cardiovascular morbidity. While acute stress acts as a proximal trigger for thrombotic, arrhythmic or mechanical cardiac events, chronic psychological stress primarily drives long-term cardiovascular risk by accelerating atherosclerosis. Furthermore, chronic stress indices are strongly linked to individual components of metabolic syndrome—including obesity, dysglycemia, hypertension, and dyslipidemia—as well as the syndrome as a whole. Because sustained overactivation of the neuroendocrine stress response poses a critical systemic health risk, ongoing controlled clinical trials are investigating both pharmacological and behavioral stress-reduction interventions for their efficacy in chronic disease prevention and management (6).

Sleep is influenced by a combination of biological, behavioral and environmental factors. Sleep health is not solely determined by obtaining the recommended amount of sleep; it also encompasses sleep timing, regularity, satisfaction and efficiency. Sleep disturbances are associated with increased risks of chronic diseases, impaired mental health and reduced quality of life. Therefore, healthy sleep practices should be prioritized as an essential component of disease prevention, health promotion and overall well-being (7).

Avoiding health-risk substances, including tobacco, alcohol and illicit drugs, is a critical component of chronic disease prevention, as these exposures contribute significantly to the development of cardiovascular disease, cancer, respiratory disease and other long-term health conditions (8).

The 2015 World Health Assembly resolution formally recognized air pollution as a critical risk factor driving the global burden of NCDs, specifically including ischemic heart disease, stroke, chronic obstructive pulmonary disease, asthma and various malignancies (9). Premature death and disease can be prevented to a significant extent through the creation and promotion of healthier environments. Reducing exposure to environmental risks can substantially decrease the burden of chronic diseases (10).

Social connection is a fundamental aspect of human development, health and survival. The influence of social relationships on physical health operates through multiple pathways. A substantial body of evidence demonstrates that individuals who maintain strong, high-quality social relationships have a lower risk of all-cause mortality and

Address for Correspondence: Prof. Feray Akbaş, MD, University of Health Sciences Türkiye, İstanbul Training and Research Hospital, Clinic of Internal Medicine, İstanbul, Türkiye
E-mail: atlibatur@yahoo.com **ORCID ID:** orcid.org/0000-0001-5091-9160
Cite this article as: Akbaş F. Lifestyle medicine: from adjunct to core internal medicine practice. İstanbul Med J. 2026; 27(3): 179-80

Publication Date: 03.08.2026

a reduced likelihood of developing a wide range of chronic diseases (11).

As demonstrated by the available evidence, lifestyle medicine should be recognized as a core component of internal medicine practice rather than an adjunct to conventional care. Integrating evidence-based lifestyle interventions into routine clinical practice can help prevent and manage chronic diseases, improve patient outcomes and quality of life and contribute to more sustainable healthcare systems.

References

1. World Health Organization. Noncommunicable diseases: Key facts [Internet]. Geneva: World Health Organization; 2025 Sep 25 [cited 2026 Jul 22]. Available from: https://www.who.int/news-room/fact-sheets/detail/noncommunicable-diseases
2. Parkinson MD, Stout R, Dysinger W. Lifestyle medicine: prevention, treatment, and reversal of disease. Med Clin North Am. 2023; 107: 1109-20.
3. Lippman D, Stump M, Veazey E, Guimarães ST, Rosenfeld R, Kelly JH, et al. Foundations of lifestyle medicine and its evolution. Mayo Clin Proc Innov Qual Outcomes. 2024; 8: 97-111.
4. World Health Organization. Healthy diet [Internet]. Geneva: World Health Organization; 2026 Jan 26 [cited 2026 Jul 22]. Available from: https://www.who.int/news-room/fact-sheets/detail/healthy-diet
5. World Health Organization. Physical activity [Internet]. Geneva: World Health Organization; 2024 Jun 26 [cited 2026 Jul 22]. Available from: https://www.who.int/news-room/fact-sheets/detail/physical-activity
6. Brotman DJ, Golden SH, Wittstein IS. The cardiovascular toll of stress. Lancet. 2007; 370: 1089-100.
7. Ramos AR, Wheaton AG, Johnson DA. Sleep deprivation, sleep disorders, and chronic disease. Prev Chronic Dis. 2023; 20: 77.
8. GBD 2019 Risk Factors Collaborators. Global burden of 87 risk factors in 204 countries and territories, 1990-2019: a systematic analysis for the Global Burden of Disease Study 2019. Lancet. 2020; 396: 1223-49.
9. World Health Organization. (2021). WHO global air quality guidelines: Particulate matter ($PM_{2.5}$ and PM_{10}), ozone, nitrogen dioxide, sulfur dioxide and carbon monoxide. World Health Organization. [cited 2026 Jul 22]. Available from: https://www.who.int/publications/i/item/9789240034228?utm_source=chatgpt.com
10. Preventing disease through healthy environments: a global assessment of the burden of disease from environmental risks. World Health Organization (2018). [cited 2026 Jul 22]. Available from: https://www.who.int/publications/i/item/9789241565196
11. Holt-Lunstad J, Robles TF, Sbarra DA. Advancing social connection as a public health priority in the United States. Am Psychol. 2017; 72: 517-30.

İstanbul Med J 2026; 27(3): 181-8
DOI: 10.4274/imj.galenos.2026.48276

Evaluation of Surgeons' Awareness of and Attitudes Toward Antiplatelet and Anticoagulant Medications

Muhammet Hüseyin Erkan[1], Ömer Faruk Rahman[2]

[1]Balıkesir University Faculty of Medicine, Department of Cardiovascular Surgery, Balıkesir, Türkiye
[2]İzmir Bakırçay University Faculty of Medicine, Department of Cardiovascular Surgery, İzmir, Türkiye

ABSTRACT

Introduction: This study aimed to evaluate the levels of knowledge, clinical approaches, attitudes, and recent experiences of bleeding complications among physicians in non-cardiovascular surgical disciplines regarding perioperative antithrombotic drug management.

Methods: This cross-sectional descriptive study included 176 physicians from various surgical specialties in Türkiye. Data were collected on demographic information, clinical practice preferences, and antithrombotic medication knowledge, assessed with a 13-item true/false questionnaire. Construct validity was confirmed using confirmatory factor analysis, with comparative fit index: 0.98 and root mean square error of approximation: 0.012. Descriptive statistics and non-parametric tests were used for analysis.

Results: The mean knowledge score was 7.69 out of 13. Warfarin was the drug causing the greatest preoperative concern (65.9%). During the previous six months, 47.2% of participants reported minor bleeding complications, and 11.4% reported major bleeding complications. Knowledge scores were highest among anesthesiology physicians and significantly lower among pediatric surgery, urology, and ear, nose and throat physicians ($p<0.001$). Physicians older than 51 years and those with more than 15 years of experience had significantly lower scores ($p<0.05$). Aspirin management varied considerably, with 39.8% discontinuing treatment and 40.3% consulting another specialty.

Conclusion: Physicians demonstrated moderate knowledge levels and substantial inter-specialty variability in perioperative antithrombotic management. Lower knowledge scores among more experienced physicians highlight the need for continuous education. Establishing multidisciplinary anticoagulation management teams and standardized decision-support protocols may improve patient safety and reduce complications.

Keywords: Perioperative antithrombotic management, anticoagulants, antiplatelet agents, surgical training, knowledge level

Introduction

While surgical interventions are life-saving, surgical stress can disrupt the delicate balance between bleeding and thrombosis, posing a significant perioperative risk. Patients with a history of cardiovascular and cerebrovascular disease who are therefore receiving anticoagulant or antiplatelet therapy constitute a high-risk group during the perioperative period (1). The management of antithrombotic drugs before surgery in these patients requires complex clinical decision-making. Continuing these drugs increases the risk of life-threatening bleeding complications, while discontinuing them can lead to fatal thromboembolic events such as stroke, myocardial infarction, or mechanical valve thrombosis (2).

Guidelines (American College of Chest Physicians and European Society of Cardiology) offer guidance to physicians; however, the ideal management strategy should be personalized according to the patient's thrombosis-bleeding risk profile, the pharmacokinetic properties of the medication used, the bleeding risk of the planned surgery, and the center's capabilities (3,4). There may be differences in the application of current guideline recommendations across surgical disciplines, and physicians' adherence to these recommendations may be directly influenced by their personal experience, professional seniority, and previous encounters with bleeding/thrombosis complications (5).

Few comprehensive studies have evaluated the current level of knowledge, clinical approaches, and experiences of physicians across different surgical specialties in Türkiye regarding preoperative antithrombotic drug management. Although some specialty-specific studies have been conducted -such as surveys evaluating anticoagulant and deep vein thrombosis knowledge among obstetrics and gynecology physicians- comprehensive data covering multiple surgical disciplines remain limited (6). This study aims to reveal the preoperative approaches of physicians working in surgical disciplines other than cardiovascular surgery for patients using antithrombotic drugs, their level of knowledge about these drugs, and their experience with bleeding complications.

Address for Correspondence: Asst. Prof., Muhammet Hüseyin Erkan, Balıkesir University, Department of Cardiovascular Surgery, Balıkesir, Türkiye
E-mail: mhuseyinerkan@gmail.com **ORCID ID:** orcid.org/0000-0002-8390-2493
Cite this article as: Erkan MH, Rahman ÖF. Evaluation of surgeons' awareness of and attitudes toward antiplatelet and anticoagulant medications. İstanbul Med J. 2026; 27(3): 181-8

Received: 21.01.2026
Accepted: 03.06.2026
Publication Date: 03.08.2026

Methods

This cross-sectional, descriptive survey was designed to evaluate the knowledge levels, attitudes, and clinical practices of surgical specialists regarding the management of preoperative antithrombotic drugs (antiplatelet and anticoagulant agents). Ethical approval for this study was obtained from the Necmettin Erbakan University Ethics Committee for Non-Pharmaceutical and Non-Medical Device Research (decision number: 2024/5184; meeting number: 204; date: 20.09.2024). Online informed consent was obtained from participants before data collection began; all data were collected anonymously and were used only for scientific purposes.

Study Population

A total of 176 surgeons who actively practice or are engaged in academic activities in the field of surgery participated in the study. Participants consisted of specialist physicians, assistant physicians, and academic physicians. Inclusion criteria were defined as physicians working in any surgical specialty who were involved in the management of antithrombotic drugs in surgical procedures. Those working in cardiovascular surgery and participants who did not complete the questionnaire were excluded from the study.

Data Collection Tool

Data were collected using a structured questionnaire developed by the researchers based on a literature review and expert opinions. The questionnaire was prepared online using the Google Forms platform and distributed to volunteer participants via social media channels (WhatsApp, email groups, etc.). Since the survey was distributed through voluntary online channels, a predefined sampling frame and response rate could not be calculated. The questionnaire took an average of 5-7 minutes to complete, and informed consent was obtained from participants online.

The survey consists of three sections:

1. Demographic and professional information (6 questions): Questions asking about participants' gender, age range, surgical specialty, title, length of professional experience, and average monthly number of cases.

2. Clinical practice and approach (5 questions): These questions address participants' clinical practices and attitudes, such as their caseload of patients using anticoagulants and antiplatelets, their approach to aspirin discontinuation, their concerns about specific drugs, and their experiences with minor and major bleeding complications in the last six months.

3. Knowledge level assessment (15 questions): Questions on the monitoring parameters and indications of direct oral anticoagulants (DOACs), reversal of warfarin, pharmacology of low molecular weight heparins, mechanisms of action of aspirin and clopidogrel, discontinuation periods, and bleeding risk (Table 1).

Development and Evaluation of the Knowledge Questionnaire

The antithrombotic medication knowledge questionnaire initially consisted of 15 true/false items. Based on item analysis, items 5 and 15 were removed from the scale because their discriminant indices (point biserial) were below 0.20. Following their removal, the Kuder-Richardson coefficient (KR)-20 reliability coefficient increased from 0.428 to 0.469.

Item difficulty values for the 13 items ranged from 0.307 to 0.864, with most items falling within an acceptable difficulty range. Point-biserial correlations ranged from 0.251 to 0.529, indicating variable but generally acceptable item discrimination. Biserial correlation values ranged from 0.324 to 0.665 and were above 0.3 for all items, suggesting that the items were related to the total score. The KR-20 reliability coefficient of the final 13-item scale was 0.469, indicating low internal consistency (Table 2).

Table 1. Items of the antithrombotic medication knowledge questionnaire

Question number	Question
1	The effectiveness of novel oral anticoagulants can be monitored using aPTT.
2	Novel oral anticoagulants can be safely used during pregnancy.
3	In patients with mechanical heart valves, novel oral anticoagulants can be used as an alternative to warfarin.
4	The anticoagulant effect of low-molecular-weight heparins cannot be monitored using aPTT.
6	Renal failure is a condition that requires dose adjustment during low-molecular-weight heparin therapy.
7	Warfarin is an anticoagulant that can be neutralized by protamine sulfate.
8	Platelet transfusion is required prior to emergency surgical intervention in patients with elevated INR due to warfarin use.
9	The dosage of warfarin therapy should be planned according to the patient's body weight.
10	Patients with a history of mechanical valve replacement can be managed with acetylsalicylic acid therapy during the perioperative period.
11	Although the duration of action of acetylsalicylic acid is 7-10 days, it is generally not necessary to discontinue it before surgical procedures.
12	The inhibition of platelet aggregation by acetylsalicylic acid is irreversible.
13	Clopidogrel is an anticoagulant drug that exerts its effect through inhibition of Factor V and Factor VII.
14	Discontinuation of clopidogrel therapy 5 days prior to elective surgical procedures is sufficient.

aPTT: Activated partial thromboplastin time, INR: International normalized ratio

The first-order unidimensional structure of the blood thinner medications questionnaire, comprising 13 items was tested using confirmatory factor analysis (CFA) with the RSP library in R (R Project) (Figure 1). Since the data did not meet the assumption of multivariate normality, model fit was tested using the diagonally weighted least squares (DWLS) estimation technique to assess construct validity. The CFA results are presented in Figure 1. Based on the resulting goodness-of-fit values (χ^2: 66.604, df: 65, p=0.422, root mean square error of approximation: 0.012, comparative fit index: 0.98, standardized root mean square residual: 0.063, χ^2/df: 1.025), the proposed single-factor model showed good fit with the data and was acceptable. These findings suggest that the single-factor structure of the questionnaire is acceptable in the present sample.

The final antithrombotic medication knowledge questionnaire consisted of 13 dichotomously coded items, with incorrect answers scored as 0 and correct answers scored as 1. The total score on the scale is calculated by summing the correct item responses and ranges from 0 to 13.

Statistical Analysis

In this study, the internal consistency and reliability of the questionnaire were first evaluated using the KR-20 coefficient. CFA was performed using DWLS estimation to assess construct validity. For subgroup analyses, the distribution of survey scores was tested for normality using the Kolmogorov-Smirnov test when n>50 for each group, and the Shapiro-Wilk test when n<50. The Mann-Whitney U test and the Kruskal-Wallis H test were used to compare survey scores across groups when the scores were not normally distributed. For the Kruskal-Wallis H test, pairwise comparisons to assess significant differences were conducted using the Bonferroni-corrected Dunn test and presented with a lettering method.

The analysis results were presented as mean and standard deviation (SD) (mean ± SD) for normally distributed quantitative data and as median, minimum, and maximum [median (minimum-maximum)] for non-normally distributed data. For categorical data, they were presented as frequencies (n) and percentages (%). A significance level of "p<0.05" was considered in all calculations. R software was used to obtain the findings of the analysis. The application results were obtained using the RSP package in R.

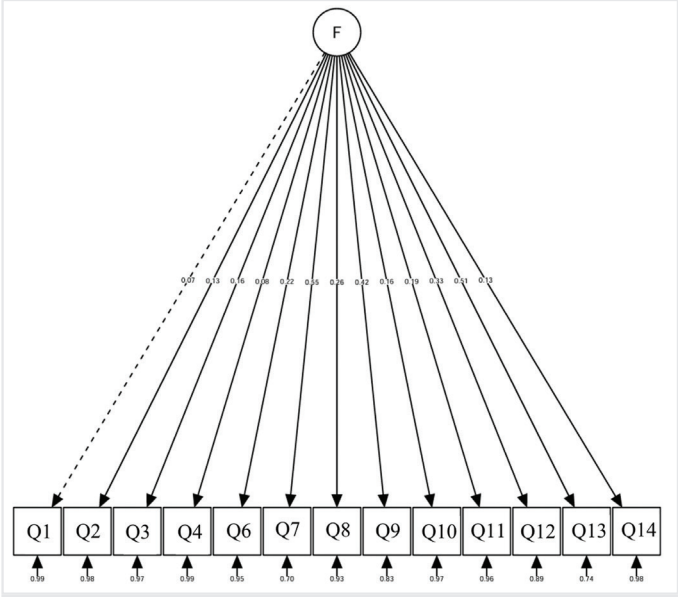

Figure 1. Confirmatory factor analysis diagram of the blood thinner medications questionnaire

Results

A total of 176 surgeons were included in the study. Examination of the age distribution of participants showed that 64.8% were in the 31-40 age range. The distribution of participants by gender showed that 60.8% were male and 39.2% were female. When the distribution by specialty was examined, the highest percentage of physicians was in general surgery (19.3%), followed by anesthesiology and resuscitation (16.5%) and orthopedics and traumatology (13.6%) (Table 3).

Examination of the distribution of titles showed that 57.4% of the participants were specialists, 28.4% were research assistants, and 14.2% were academics. Surgeons with 1-5 and 6-11 years of experience were equally represented (38.6% each), followed by those with 11-15 years (14.2%) and more than 15 years (8.5%). Regarding monthly case numbers, 26.7% of participants see more than 41 cases per month, while 17.6% see between 1 and 10 cases per month.

Half of the participants (50%) stated that the proportion of patients using antithrombotic agents in their clinics was between 0% and 25%. This was followed by 32.4% and 14.2% in the 25-50% and 50-75% ranges, respectively. Regarding aspirin use, 39.8% of surgeons stated that they discontinued aspirin before surgery, 19.9% did not discontinue it, and 40.3% consulted the relevant specialist before making a decision. Warfarin was identified as the drug of most concern in the preoperative process, with 65.9%. When the occurrence of complications during the last

Table 2. Item analysis and reliability results of the antithrombotic medication knowledge questionnaire

Question	Item difficulty	Point biserial	Biserial
Q1	0.693	0.251	0.329
Q2	0.619	0.254	0.324
Q3	0.307	0.351	0.461
Q4	0.710	0.288	0.382
Q6	0.693	0.394	0.518
Q7	0.455	0.529	0.665
Q8	0.562	0.382	0.480
Q9	0.438	0.429	0.540
Q10	0.756	0.319	0.436
Q11	0.489	0.374	0.468
Q12	0.665	0.420	0.544
Q13	0.443	0.486	0.612
Q14	0.626	0.264	0.415
Number of participants		176	
Number of item		13	
KR-20		0.469	

KR: Kuder-Richardson coefficient

Table 3. Descriptive statistics of demographic characteristics		
	n	%
Age		
25-30	36	20.5
31-40	114	64.8
41-50	18	10.2
>51	8	4.5
Gender		
Male	107	60.8
Female	69	39.2
Specialty		
Anesthesiology and reanimation	29	16.5
Neurosurgery	7	4
Pediatric surgery	4	2.3
General surgery	34	19.3
Thoracic surgery	15	8.5
Ophthalmology	11	6.3
Obstetrics and gynecology	21	11.9
Otorhinolaryngology	8	4.5
Orthopedics and traumatology	24	13.6
Plastic and reconstructive surgery	9	5.1
Urology	14	8
Title		
Research assistant	50	28.4
Specialist physician	101	57.4
Academic staff	25	14.2
Years of experience in specialty		
1-5	68	38.6
6-11	68	38.6
11-15	25	14.2
>15	15	8.5
Number of cases per month		
1-10	31	17.6
11-20	35	19.9
21-30	41	23.3
31-40	22	12.5
>41	47	26.7
Proportion of patients using blood thinners		
0-25	88	50
25-50	57	32.4
50-75	25	14.2
75-100	6	3.4
Discontinuation of aspirin before surgery		
Yes	70	39.8
No	35	19.9
Consultation with the relevant physician	71	40.3
Anticoagulant of concern in the preoperative period		
Aspirin	22	12.5
Clopidogrel	24	13.6
Warfarin	116	65.9
DOACs	14	8
Minor complications in the last 6 months		
No	93	52.8
Yes	83	47.2
Major complications in the last 6 months		
No	156	88.6
Yes	20	11.4

DOAC: Direct oral anticoagulant

six months was examined, 47.2% of participants reported experiencing minor complications, while 11.4% reported major complications.

The mean total score on the antithrombotic medication knowledge questionnaire was 7.69 (range: 2-13) (Table 4).

There was a statistically significant difference in total scores on the antithrombotic medication knowledge questionnaire between age groups ($p=0.019$). This difference was particularly evident between the scores of participants aged 51 and older and the scores of participants in other age groups. The median total score on the antithrombotic medication knowledge questionnaire was 5 for participants aged 51 and older, compared with 8 for participants in other age groups (Table 5).

A statistically significant difference in participants' total scores on the antithrombotic medication knowledge questionnaire was observed across specialties ($p<0.001$). This difference was particularly observed between the scores of participants in the anesthesiology and resuscitation specialty and those of participants in the pediatric surgery, gynecology and obstetrics, otolaryngology, and urology specialties. The median total score was 9 for anesthesiology and resuscitation, 5 for pediatric surgery, and 6 for obstetrics and gynecology, otolaryngology, and urology.

Table 4. Descriptive statistics for the total score of the antithrombotic medication knowledge questionnaire		
	Mean ± SD	Median (min-max)
Total score (n=176)	7.69±2.24	8 (2-13)

SD: Standard deviation, min: Minimum, max: Maximum

Table 5. Relationship between the antithrombotic medication knowledge questionnaire total score and demographic characteristics

	Mean ± SD	Median (min-max)	Statistic	p
Age				
25-30	7.83±1.98	8 (4-11)[a]	9.954	**0.019[h]**
31-40	7.75±2.26	8 (2-13)[a]		
41-50	8.17±2.31	8 (4-12)[a]		
>51	5.25±1.67	5 (3-8)[b]		
Gender				
Male	7.58±2.36	8 (2-13)	0.970	0.332[m]
Female	7.87±2.05	8 (3-12)		
Specialty				
Anesthesiology and reanimation	9.31±1.56	9 (6-12)[a]	42.621	**<0.001[h]**
Neurosurgery	8.57±2.07	9 (5-11)[ab]		
Pediatric surgery	4.5±1	5 (3-5)[b]		
General surgery	8.41±2.27	8 (4-13)[ab]		
Thoracic surgery	7.53±1.73	8 (5-10)[ab]		
Ophthalmology	7.82±1.99	8 (4-10)[ab]		
Obstetrics and gynecology	6.29±2.08	6 (2-10)[b]		
Otorhinolaryngology	6.25±1.98	6 (3-9)[b]		
Orthopedics and traumatology	7.54±2.08	8 (3-13)[ab]		
Plastic and reconstructive surgery	6.78±2.22	7 (4-10)[ab]		
Urology	6.93±2.16	6 (4-11)[b]		
Title				
Research assistant	7.82±1.87	8 (4-11)	4.135	0.126[h]
Specialist physician	7.83±2.21	8 (3-12)		
Academic staff	6.88±2.86	6 (2-13)		
Years of experience in specialty				
1-5	8.07±1.99	8 (4-13)[a]	9.676	**0.022[h]**
6-11	7.59±2.2	8 (2-13)[ab]		
11-15	7.92±2.58	8 (3-12)[ab]		
>15	6.07±2.34	6 (3-11)[b]		
Number of cases per month				
1-10	8.03±1.87	8 (4-11)	4.061	0.398[h]
11-20	7.46±1.85	7 (3-11)		
21-30	7.29±2.5	7 (2-13)		
31-40	7.55±2.6	7 (3-13)		
>41	8.06±2.31	9 (3-12)		
Proportion of patients using blood thinners				
0-25	7.31±2.4	7 (2-13)	5.769	0.124[h]
25-50	8.09±2.2	9 (3-12)		
50-75	8.12±1.67	8 (4-12)		
75-10	7.83±1.6	8.5 (5-9)		
Discontinuation of aspirin before surgery				
Yes	7.24±2.12	7 (3-12)	5.073	0.079[h]
No	8.2±2.42	8 (3-13)		
Consultation with the relevant physician	7.89±2.21	8 (2-13)		
Anticoagulant of concern in the preoperative period				
Aspirin	6±1.95	6 (3-9)[a]	18.152	**<0.001[h]**
Clopidogrel	8.79±2.11	9 (6-13)[b]		
Warfarin	7.76±2.16	8 (2-12)[b]		
DOACs	7.93±2.27	8 (3-13)[ab]		
Minor complications in the last 6 months				
No	7.4±2.27	7 (2-13)	1.803	0.071[m]
Yes	8.02±2.17	8 (3-13)		
Major complications in the last 6 months				
No	7.63±2.19	8 (2-13)	0.824	0.410[m]
Yes	8.15±2.64	8 (4-13)		

[m]: Mann–Whitney U test, [h]: Kruskal–Wallis H test, [a and b]: No significant difference between groups sharing the same letter (Bonferroni-corrected Dunn test), Mean: Average, SD: Standard deviation, min: Minimum, max: Maximum

Participants' total scores on the antithrombotic medication knowledge questionnaire differed significantly by length of experience in the specialty (p=0.022). This difference was particularly evident between the scores of participants with 1-5 years of experience in the specialty and those with more than 15 years of experience. The median total score for participants with 1-5 years of experience in the specialty was 8, while the median score for participants with more than 15 years of experience in the specialty was 6.

There were no statistically significant differences in participants' total scores on the antithrombotic medication knowledge questionnaire across other demographic characteristics (p>0.05).

Discussion

This study examines surgeons' knowledge, attitudes, and practices regarding the management of anticoagulant and antiplatelet drugs prior to elective surgeries and procedures and provides an overview of current clinical practice. The findings, particularly the moderate

level of knowledge, the reverse relationship with experience and age, contrary to expectations, and the differences between specialties, are consistent with trends reported in the literature, while also offering new perspectives on some details.

Guidelines on perioperative anticoagulant and antiplatelet therapy management recommend a balanced approach between bleeding and thrombosis risks and guide decisions on discontinuation and reinitiation of treatment. For example, the CHEST guidelines specify discontinuation and restart timing for vitamin K antagonists and DOACs, while recommending that most antiplatelet drugs, such as aspirin, should not be discontinued in most non-cardiac surgeries if the surgical risk is low (1). The aim of this approach is to strike a balance between preventing major thromboembolic complications and minimizing preventable bleeding complications.

In our study, surgeons' knowledge of the risk assessment and management strategies recommended in international guidelines was generally moderate. This reflects the heterogeneity in knowledge regarding the management of anticoagulant and antiplatelet drugs across many clinical settings worldwide. For example, in our study, heterogeneity in approaches to aspirin discontinuation (39.8% discontinue, 19.9% do not discontinue, 40.3% consult) indicates significant inconsistency in translating current guidelines into practice. This deviation indicates the need to disseminate guideline recommendations locally and to convert them into simple clinical decision-support tools (checklists and flowcharts). On the other hand, systematic reviews have reported that discontinuing antiplatelet therapy has varying effects on the risk of major bleeding or thrombosis across different studies (7). In this context, methodological differences in information and practice across surgical specialties and according to the bleeding risk of the procedure are to be expected.

In our study, the majority of participants (65.9%) reported warfarin as the medication of greatest concern during the preoperative period; this finding can be explained by epidemiological realities and clinical experience in Türkiye. Warfarin is a medication that has been used for decades; it is cost-effective and widely accessible. Therefore, it is used in a much wider patient population compared to DOACs, especially in specific indications such as mechanical heart valves and rheumatic valve disease (8). Consequently, surgeons more frequently encounter patients who use warfarin in their clinical practice and are therefore more exposed to bleeding complications associated with this drug. This high exposure may have created concern among physicians regarding warfarin. Furthermore, warfarin's narrow therapeutic window, numerous drug-food interactions, and challenging management process due to international normalized ratio fluctuations are another factor that increases the experience of complications (9). DOACs, on the other hand, are relatively new agents; their use is limited to more controlled indications (particularly non-valvular atrial fibrillation and venous thromboembolism), and they have a more stable pharmacokinetic profile. This may have contributed to physicians experiencing fewer complications with DOACs and, consequently, being relatively less concerned. However, the lack of routine monitoring for DOACs and the cost and accessibility issues of their emergency antidotes (idarucizumab and andexanet alfa) pose challenges to their use. However, the lack of routine monitoring of DOACs and the cost/accessibility issues of their emergency antidotes (idarucizumab, andexanet alfa) should not obscure the potential risks associated with these drugs (10). Ultimately, this finding suggests that concerns stem not only from the drug's pharmacological risks but also from its prevalence in the population and consequently, physicians accumulated clinical experience.

In this study, the fact that a significant proportion of participants (40.3%) reported consulting with a specialist physician before deciding to discontinue aspirin is an encouraging finding and can be considered a reflection of the "patient-specific, multidisciplinary approach" that forms the essence of the guidelines in practice (1). Studies exist suggesting that coordinated work between surgeons, anesthesiologists, cardiologists, and hematologists is necessary in perioperative antithrombotic management (11). Similarly, structured multidisciplinary services such as a "perioperative antithrombotic clinic" or a standard consultation pathway have been shown to increase physician confidence and reduce the rate of adverse events (12). Therefore, establishing "Perioperative Medicine Units" or "Anticoagulation Management Teams" in hospitals and implementing simple consultation algorithms, in addition to educational activities aimed at increasing knowledge, may be among the most effective ways to translate our findings into improved clinical outcomes.

The significantly high knowledge scores of physicians in the field of anesthesiology and resuscitation also support this field's role as a perioperative risk manager and a multidisciplinary bridge for surgical patients. Similar to our study, a survey involving 296 anesthesiologists and assistant physicians working in various hospitals across Türkiye showed that physicians in this specialty manage anticoagulant drugs in accordance with international guidelines (13).

In our study, advanced age and longer professional experience were associated with lower, rather than higher, knowledge scores. This finding contradicts the general assumption that "knowledge increases with experience" and emphasizes the critical importance of continuous professional development in rapidly evolving fields such as perioperative medicine. This inverse relationship can be explained by several factors. First, when more senior physicians were undergoing basic medical training, DOACs had not yet entered clinical use, and antithrombotic management was warfarin-focused. Second, physicians with established clinical practice habits may be less willing to follow current guideline recommendations or may have limited time to integrate them into practice. This situation can also be linked to the concept of "clinical inertia" (14). Third, the complexity and frequent updates of guidelines make it difficult for all physicians to keep up with these changes (15).

On the other hand, the rate at which physicians adopt new treatment protocols is generally shaped by their past prescribing habits and clinical experience. For example, physicians who prescribed almost exclusively warfarin in their practice in 2013 showed a slower increase in the adoption rate of DOACs by 2018 (16). This suggests that more senior physicians may feel more confident with warfarin management, which they are familiar with through years of experience, while newer graduates and younger physicians may be more familiar with and open to adopting these new agents because they were exposed to DOAC

protocols during their training. This finding points to the necessity of designing postgraduate training programs to target not only residents and young specialists, but physicians at all seniority levels.

The results of our study clearly demonstrate the need for structured and continuous education on perioperative antithrombotic drug management in surgical specialties. The participants' average knowledge score of 7.69 (out of 13) indicates that the correct answer rate was approximately 59%, which poses a risk to clinical decision-making. The finding that 47.2% of participants reported minor bleeding complications in the previous six months may indicate patient safety concerns; however, this result should be interpreted cautiously because it was based on self-report and not objectively verified. This educational need is not specific to surgical disciplines but is a common requirement across different areas of medicine involving drug management. Indeed, a survey conducted with dentists and specialists also reported significant knowledge gaps and educational needs regarding antithrombotic drug management (17). The literature suggests that, due to the persistence of preventable patient harm associated with anticoagulants, anticoagulation management programs structured similarly to antibiotic management should be developed, and healthcare institutions should adopt a proactive approach in this regard (18).

Study Limitations

This study has some limitations. Due to its cross-sectional design, the findings do not allow for establishing causal relationships and only reflect the level of knowledge and clinical approaches during a specific time period. The collection of data through self-reported online surveys carries the risk of social desirability and recall bias; in particular, the inability to verify experiences of complications with objective clinical records may limit the reliability of the results. Furthermore, participation based on voluntary enrollment may increase the likelihood of physicians more involved in anticoagulant and antiplatelet management being included in the study, thereby limiting the representativeness of the sample. An important limitation of this study is the relatively low internal consistency of the knowledge scale, as indicated by the KR-20 coefficient of 0.469. Although the final 13-item form showed acceptable construct validity in CFA, the total knowledge scores should be interpreted with caution. This may limit the precision of subgroup comparisons and indicates the need for further validation of the scale in larger samples. In addition, formal content validity assessment, pilot testing, and exploratory factor analysis were not performed, which limits the strength of validity claims regarding the questionnaire.

Conclusion

This exploratory study suggests that physicians working in surgical specialties other than cardiovascular surgery may have moderate knowledge levels regarding perioperative anticoagulant and antiplatelet drug management, with variability across clinical practice patterns. Heterogeneous approaches to aspirin discontinuation and practices inconsistent with guideline recommendations highlight the need for standardized decision-making processes. The higher knowledge scores of anesthesiologists and resuscitation physicians support the role of this specialty in perioperative risk management, while the association of older age and longer professional experience with lower knowledge levels emphasizes the importance of continuing professional education. These findings suggest that the development of multidisciplinary and structured antithrombotic management approaches based on current guidelines in surgical clinics is critical for patient safety.

Ethics

Ethics Committee Approval: Ethical approval for this study was obtained from the Necmettin Erbakan University Ethics Committee for Non-Pharmaceutical and Non-Medical Device Research (decision number: 2024/5184; meeting number: 204; date: 20.09.2024).

Informed Consent: Online informed consent was obtained from participants before data collection began; all data were collected anonymously and were used only for scientific purposes.

Footnotes

Authorship Contributions: Concept- M.H.E.; Design- M.H.E., Ö.F.R.; Data Collection or Processing- M.H.E., Ö.F.R.; Analysis or Interpretation- Ö.F.R.; Literature Search- M.H.E., Ö.F.R.; Writing- M.H.E., Ö.F.R.

Conflict of Interest: No conflict of interest was declared by the authors.

Financial Disclosure: The authors declared that this study received no financial support.

References

1. Douketis JD, Spyropoulos AC, Murad MH, Arcelus JI, Dager WE, Dunn AS, et al. Perioperative management of antithrombotic therapy: an American College of Chest Physicians Clinical Practice Guideline. Chest. 2022; 162: e207-43.
2. Kristensen SD, Knuuti J, Saraste A, Anker S, Bøtker HE, Hert SD, et al. 2014 ESC/ESA Guidelines on non-cardiac surgery: cardiovascular assessment and management: the joint task force on non-cardiac surgery: cardiovascular assessment and management of the European Society of Cardiology (ESC) and the European Society of Anaesthesiology (ESA). Eur Heart J. 2014; 35: 2383-431.
3. Douketis JD, Spyropoulos AC, Duncan J, Carrier M, Le Gal G, Tafur AJ, et al. Perioperative management of patients with atrial fibrillation receiving a direct oral anticoagulant. JAMA Intern Med. 2019; 179: 1469-78.
4. Steffel J, Collins R, Antz M, Cornu P, Desteghe L, Haeusler KG, et al. 2021 European Heart Rhythm Association Practical Guide on the use of non-vitamin k antagonist oral anticoagulants in patients with atrial fibrillation. Europace. 2021; 23: 1612-76. Erratum in: Europace. 2021; 23: 1676.
5. Narouze S, Benzon HT, Provenzano D, Buvanendran A, De Andres J, Deer T, et al. Interventional spine and pain procedures in patients on antiplatelet and anticoagulant medications (second edition): guidelines from the American Society of Regional Anesthesia and Pain Medicine, the European Society of Regional Anaesthesia and Pain Therapy, the American Academy of Pain Medicine, the International Neuromodulation Society, the North American Neuromodulation Society, and the World Institute of Pain. Reg Anesth Pain Med. 2018; 43: 225-62.
6. Balcı AB, Rahman ÖF, Dağdeviren E. Knowledge levels of obstetricians and gynecologists on deep vein thrombosis. Eur Res J. 2025; 11: 1098-107.
7. Shah S, Urtecho M, Firwana M, Nayfeh T, Hasan B, Nanaa A, et al. Perioperative management of antiplatelet therapy: a systematic review and meta-analysis. Mayo Clin Proc Innov Qual Outcomes. 2022; 6: 564-73.
8. Mandefro BT, Sundara SV, Lu X, Busmail H, Weerakoon S, Avula S, et al. Effectiveness and safety of direct oral anticoagulants versus warfarin in

patients with mechanical heart valves: a systematic review. Cureus. 2025; 17: e89736.

9. Limdi NA. Warfarin pharmacogenetics: challenges and opportunities for clinical translation. Front Pharmacol. 2012; 3: 183.
10. Raval AN, Cigarroa JE, Chung MK, Diaz-Sandoval LJ, Diercks D, Piccini JP, et al. Management of patients on non-vitamin K antagonist oral anticoagulants in the acute care and periprocedural setting: a scientific statement from the American Heart Association. Circulation. 2017; 135: e604-33.
11. Rossini R, Tarantini G, Musumeci G, Masiero G, Barbato E, Calabrò P, et al. A multidisciplinary approach on the perioperative antithrombotic management of patients with coronary stents undergoing surgery: surgery after stenting 2. JACC Cardiovasc Interv. 2018; 11: 417-34.
12. Douketis JD, Spyropoulos AC, Anderson JM, Arnold DM, Bates SM, Blostein M, et al. The perioperative anticoagulant use for surgery evaluation (PAUSE) study for patients on a direct oral anticoagulant who need an elective surgery or procedure: design and rationale. Thromb Haemost. 2017; 117: 2415-24.
13. Eman A, Balaban O. Perioperative use of anticoagulant and antiaggregant drugs; approaches of anesthesiology and reanimation physicians in Türkiye: a survey study. Ann Med Res. 2022; 29: 1311-6.
14. Reach G. Clinical inertia, uncertainty and individualized guidelines. Diabetes Metab. 2014; 40: 241-5.
15. Qumseya B, Goddard A, Qumseya A, Estores D, Draganov PV, Forsmark C. Barriers to clinical practice guideline implementation among physicians: a physician survey. Int J Gen Med. 2021; 14: 7591-8.
16. Wheelock KM, Ross JS, Murugiah K, Lin Z, Krumholz HM, Khera R. Clinician trends in prescribing direct oral anticoagulants for US Medicare beneficiaries. JAMA Netw Open. 2021; 4: e2137288.
17. Erçal P, Tayşi AE, Şişmanoğlu S. Knowledge and practices of dentists towards patients on antithrombotic medication therapy: a cross-sectional survey. Cerrahpaşa Med J. 2023; 1. Available from: https://cerrahpasamedj.org/index.php/pub/article/view/578
18. Burnett AE, Barnes GD. A call to action for anticoagulation stewardship. Res Pract Thromb Haemost. 2022; 6: e12757.

İstanbul Med J 2026; 27(3): 189-93
DOI: 10.4274/imj.galenos.2026.78380

Sphenoid Sinus Pneumatization Patterns in Patients With Rathke's Cleft Cysts: A Retrospective Case–Control Study

Duygu Dolen Burak[1], Cafer İkbal Gülsever[2], Sefa Öztürk[1], Yavuz Bahadır Taktak[3], Mehmet Barburoğlu[3], İlyas Dolaş[1], Altay Sencer[1], Tuğrul Cem Ünal[1]

[1]İstanbul University, İstanbul Faculty of Medicine, Department of Neurosurgery, İstanbul, Türkiye
[2]Hakkari State Hospital, Clinic of Neurosurgery, Hakkari, Türkiye
[3]İstanbul University, İstanbul Faculty of Medicine, Department of Radiology, İstanbul, Türkiye

ABSTRACT

Introduction: Rathke's cleft cysts (RCCs) are benign lesions of the pituitary region. Variations in sphenoid sinus aeration influence sellar anatomy, but their relationship to RCCs is unknown. This study examined whether specific sphenoid sinus pneumatization patterns are associated with RCCs.

Methods: A retrospective case–control study was conducted, including 126 subjects: 63 patients with magnetic resonance imaging (MRI)-confirmed RCCs and 63 control individuals matched for age and sex, who had no evidence of sellar or parasellar pathology. Computed tomography and MRIs images were evaluated to categorize sphenoid sinus aeration as conchal, presellar, incomplete sellar, or complete sellar. All imaging assessments were performed independently by two neuroradiologists (Y.B.T. and M.B.), blinded to group allocation. Statistical comparisons were made using the chi-square test.

Results: The RCCs and control groups had comparable ages (43.6±12.8 vs. 42.9±13.4 years, p=0.78) and sex distribution (61.9% vs. 58.7% female, p=0.71). Among patients with RCCs, the incomplete sellar pattern was the most frequent (58.7%), followed by complete sellar (31.7%), presellar (6.3%), and conchal (3.2%) patterns. In contrast, control subjects most commonly demonstrated complete sellar aeration (52.4%). Overall, pneumatization patterns differed significantly between groups (χ^2: 23.42, df: 3, $p<0.05$).

Conclusion: Individuals with RCCs exhibited a higher prevalence of incomplete sellar sphenoid sinus aeration compared with matched controls. This association may reflect underlying developmental or anatomical factors within the sellar-sphenoid region, potentially contributing to the formation of RCCs or to earlier symptom onset. Awareness of this relationship may support more refined radiologic assessment and improve preoperative planning for patients with cystic sellar lesions.

Keywords: Rathke's cleft cyst, sphenoid sinus, pneumatization, sellar region, pituitary

Introduction

Rathke's cleft cysts (RCCs) are epithelial cysts that develop from persistent embryologic tissue located between the anterior and posterior pituitary lobes. Although many RCCs are asymptomatic and incidentally discovered, symptomatic cases may present with headache, visual disturbances, or endocrine dysfunction from compression of adjacent structures (e.g., pituitary, optic apparatus) (1-3). Recent reviews highlight their variable natural history, noting that most uncompressed RCCs remain stable over time and advocating conservative management for selected cases (4,5). However, growth, recurrence, or symptomatic progression may occur, with recent work proposing risk models to predict which lesions will evolve (5).

The sphenoid sinus, located below the sella turcica, shows substantial interindividual variation in the degree of aeration. Sphenoid sinus pneumatization, which may extend anteriorly, posteriorly, laterally, or inferiorly, can influence both anatomical relationships and radiologic appearance of the sellar region (6). In fact, previous computed tomography (CT) investigations indicate that how the sphenoid sinus pneumatizes can influence multiple aspects of sellar morphology, as well as the protrusion or dehiscence of adjacent neurovascular structures (7). Moreover, the extent of pneumatization is not only surgically relevant (e.g., in planning transsphenoidal corridors) but may also impact biomechanical interactions between sinus cavities and the pituitary gland (8).

A preliminary version of this study was submitted as an abstract to the European Association of Neurosurgical Societies 2025 Congress (October 5-9, 2025; Vienna, Austria).

Address for Correspondence: Cafer İkbal Gülsever, MD, Hakkari State Hospital, Clinic of Neurosurgery, Hakkari, Türkiye
E-mail: cafer.gulsever@gmail.com **ORCID ID:** orcid.org/0000-0002-9246-1378

Cite this article as: Dolen Burak D, Gülsever Cİ, Öztürk S, Taktak YB, Barburoğlu M, Dolaş İ, et al. Sphenoid sinus pneumatization patterns in patients with Rathke's cleft cysts: a retrospective case–control study. İstanbul Med J. 2026; 27(3): 189-93

Received: 02.12.2025
Accepted: 04.06.2026
Publication Date: 03.08.2026

Given the embryological proximity and close spatial relationship between the sphenoid sinus and the pituitary region, it is biologically plausible that variations in pneumatization might correlate with the occurrence, growth, or morphology of RCCs. To our knowledge, no prior work has thoroughly assessed whether particular aeration patterns of the sphenoid sinus are more common among individuals with RCCs.

Therefore, this study aims to evaluate, using CT and magnetic resonance imaging (MRI), whether specific sphenoid sinus pneumatization subtypes are more frequent in patients with RCCs than in matched controls. We hypothesize that less extensive pneumatization (e.g., incomplete sellar) may be more common in RCCs, or that certain pneumatization patterns may predispose to cyst formation or facilitate detection.

Methods

Study Design and Ethical Considerations

This research used a retrospective observational design and followed the ethical standards outlined in the Declaration of Helsinki. This study was approved by the İstanbul University Non-Interventional Clinical Research Ethics Committee (decision number: 23, date: 14.11.2025) neuroradiologists (Y.B.T. and M.B.). Informed consent was waived by the Ethics Committee due to the retrospective nature of the study and the use of anonymized imaging data.

Patient Selection

The study population comprised 126 subjects: 63 with radiologically confirmed RCCs and 63 matched controls without sellar or parasellar pathology. The RCCs group consisted of patients whose diagnoses were established based on MRI findings between January 2018 and December 2023. Controls were selected from individuals who underwent cranial MRI for unrelated, non-sellar reasons (e.g., headache, dizziness) and had no radiological evidence of sellar or parasellar lesions. As this was a retrospective study conducted at a tertiary-care center, the RCC cohort likely reflects a referred, potentially symptomatic population.

Exclusion criteria for both groups included:

1. History of pituitary or sphenoid sinus surgery,

2. Presence of neoplastic or inflammatory sellar lesions,

3. Poor-quality or incomplete imaging data,

4. Congenital craniofacial malformations affecting the sphenoid region.

Imaging Acquisition and Evaluation

MRI and CT images were retrieved from İstanbul University Faculty of Medicine's Picture Archiving and Communication System. MRI scans were performed on 1.5-T or 3-T scanners (GE or Siemens Healthcare systems), using standard sellar protocols that included sagittal and coronal T1-weighted, T2-weighted, and post-contrast T1 sequences. CT images were used to evaluate the bony anatomy of the sphenoid sinus and the extent of pneumatization.

The extent of sphenoid sinus aeration was classified into four subtypes according to the extent of aeration relative to the sella turcica, as described in prior literature (9-12):

1. Conchal type–minimal aeration anterior to the sella;

2. Presellar type–pneumatization extending anteriorly but not reaching the sella;

3. Incomplete sellar type–aeration extending partially below the sella;

4. Complete sellar type–pneumatization extending fully below the sella floor (Figure 1).

Two experienced neuroradiologists (Y.B.T. and M.B.), blinded to the patient/control grouping, independently reviewed all scans. In case of disagreement, consensus was reached through joint review. Inter-

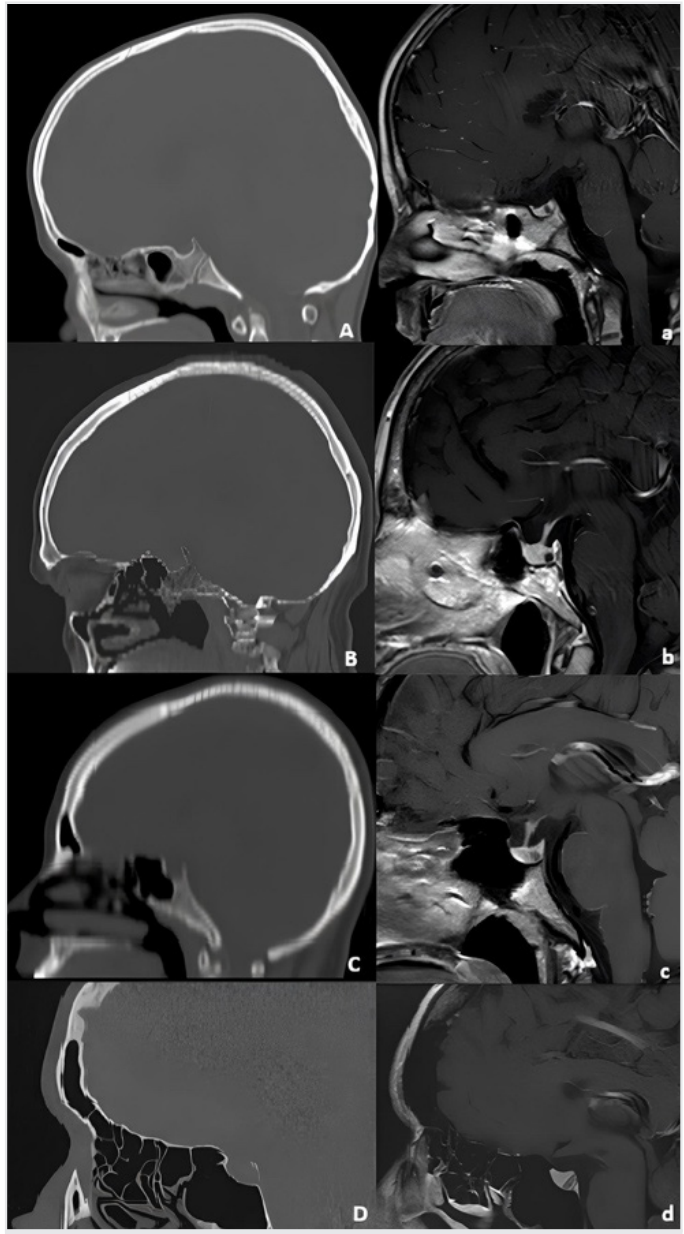

Figure 1. Representative sagittal computed tomography (left column) and corresponding magnetic resonance imaging (right column) images demonstrating the four primary sphenoid sinus pneumatization subtypes in patients with Rathke's cleft cyst. (A, a) Conchal type: minimal aeration anterior to the sella; (B, b) presellar type: aeration extending anteriorly but not reaching the sella; C, c) incomplete sellar type: partial pneumatization beneath the sella turcica; (D, d) complete sellar type: extensive pneumatization extending fully below the sellar floor

observer consistency was assessed qualitatively. All images selected for inclusion in figures were reviewed for clarity and anatomical representativeness.

Data Collection and Statistical Analysis

Demographic data (age and sex) and radiological classifications were recorded for each subject. Descriptive statistics were expressed as mean ± standard deviation for continuous variables and as frequency (percentage) for categorical variables. The chi-square (χ^2) test was used to assess the association between groups (RCCs vs. controls) and sphenoid sinus pneumatization types. Due to the relatively limited sample size and the categorical nature of the primary variables, multivariate regression analysis was not performed. A p value of <0.05 was considered statistically significant. Statistical analyses were performed using IBM SPSS Statistics version 26.0 (IBM Corp., Armonk, NY, USA).

Results

Demographic Characteristics

This study included 126 participants, consisting of 63 individuals with RCCs and an equal number of age- and sex-matched controls.

The RCCs group had a mean age of 43.6±12.8 years (21-68 years), whereas the control group averaged 42.9±13.4 years (20-70 years). This difference was not statistically significant (p=0.78). The RCCs group included 39 females (61.9%) and 24 males (38.1%), whereas the control group included 37 females (58.7%) and 26 males (41.3%). The gender distribution between groups was comparable (p=0.71).

Distribution of Sphenoid Sinus Pneumatization Types

The pattern of sphenoid sinus aeration differed markedly between the RCCs and the control groups (χ^2: 23.42, df: 3, $p<0.05$). In patients with RCCs, incomplete sellar pneumatization was the most frequent pattern (58.73%, n=37), while complete sellar aeration accounted for 31.75% (n=20). Presellar types (6.35%, n=4) and conchal types (3.17%, n=2) were observed much less frequently.

In contrast, the control group demonstrated a higher prevalence of the complete sellar type (52.38%, n=33), with lower prevalences of the incomplete sellar type (28.57%, n=18), presellar type (17.46%, n=11), and conchal type (1.59%, n=1).

This difference indicates that incomplete sellar pneumatization is more frequently associated with RCCs, whereas complete sellar pneumatization is more common in individuals without sellar pathology (Table 1).

Discussion

In this study, we identified a significant difference in sphenoid sinus pneumatization patterns between patients with RCCs and matched controls. Incomplete sellar pneumatization was markedly more frequent among individuals with RCCs, whereas complete sellar pneumatization predominated in the control population. This finding suggests a potential anatomical or developmental relationship between sphenoid sinus aeration and the presence of RCCs, which has not been previously emphasized in the literature.

Although no prior studies have directly examined the association between RCCs and sphenoid sinus pneumatization, previous radiological investigations have clarified how the degree of sinus aeration influences the configuration of the sella turcica and surrounding structures (12). Recent CT-based analyses have demonstrated that extensive pneumatization correlates with a thinner sellar floor and altered relationships with the internal carotid artery, optic nerve, and other parasellar elements (5,12). Dogan et al. (5) showed that sellar and postsellar pneumatization are the dominant patterns in the general adult population, while incomplete aeration represents a smaller minority. Similarly, Tavakoli et al. (11), using cone-beam CT, reported that sellar and postsellar configurations together accounted for over 70% of cases. In contrast, our cohort of patients with RCCs exhibited a striking predominance of the incomplete sellar pattern, suggesting that patients with RCCs may differ systematically from the general population in the anatomical development of the sphenoid sinus. However, differences in classification systems may influence this apparent discrepancy. Previous studies, such as those by Dogan et al. (5) and Tavakoli et al. (11), often grouped sellar and postsellar pneumatization patterns together, whereas the present study subdivided these into incomplete and complete sellar types. When these two categories are considered jointly in our control group, the overall distribution is broadly consistent with prior reports in the general adult population. Therefore, the observed differences should be interpreted in the context of classification methodology rather than as a direct contradiction with existing literature.

Table 1. Distribution of sphenoid sinus pneumatization subtypes in RCC and control groups

Sphenoid sinus pneumatization type	RCC group (n=63)		Control group (n=63)		p value
	n	%	n	%	
Conchal type	2	3.17	1	1.59	
Presellar type	4	6.35	11	17.46	
Incomplete sellar type	37	58.73	18	28.57	
Complete sellar type	20	31.75	33	52.38	
Total	**63**	**100**	**63**	**100**	**<0.05**

Data are presented as the number of cases (n) and the percentage (%). A significant difference was observed between groups (χ^2: 23.42, df: 3, $p<0.05$). The incomplete sellar type was the most frequent pattern among RCC patients, whereas the complete sellar type predominated in controls. RCC: Rathke's cleft cyst

This observation may be interpreted within the context of the shared embryologic and anatomical evolution of the sellar region. The sphenoid sinus begins to pneumatize during early childhood and usually reaches the sella turcica by the age of seven, continuing to expand through puberty (13). Variability in the extent of this pneumatization influences the thickness of the sellar floor and the position of the pituitary fossa relative to the sinus cavity (14). In individuals with limited or incomplete sellar pneumatization, the bony sellar floor remains thicker, providing a denser barrier between the pituitary gland and the sinus. Because RCCs arise from epithelial remnants of Rathke's pouch at the junction of the anterior and posterior pituitary, such structural differences may influence the persistence, expansion, or presentation of these cystic remnants. The thicker bony confines and smaller sellar volume associated with incomplete pneumatization could restrict inferior expansion toward the sinus, causing RCCs to enlarge superiorly or remain intrasellar. As a result, these cysts may produce symptoms such as headache, visual field deficits, or endocrine dysfunction at smaller sizes, leading to earlier detection on imaging and thus overrepresentation in symptomatic cohorts such as ours (15,16).

Beyond mechanical constraint, developmental coupling between the processes of sinus pneumatization and sellar ossification may also contribute. Both occur in close temporal and spatial proximity during embryogenesis and depend on local osteogenic and epithelial-mesenchymal interactions. Subtle alterations in local signaling pathways (e.g., bone morphogenetic protein activity) or in vascular remodeling might delay or limit pneumatization and simultaneously influence the microenvironment of Rathke's pouch remnants. A less pneumatized sphenoid may also yield different local pressure gradients, venous drainage characteristics, or mucosal-osseous interactions, creating a milieu more favorable for cyst persistence or enlargement. Conversely, in a fully pneumatized sinus, increased aeration and mucosal exposure might facilitate micro-drainage or resorption of cystic fluid, potentially reducing cyst visibility or size on imaging. This interplay of developmental timing, regional mechanics, and tissue microenvironment offers a plausible embryologic framework linking incomplete pneumatization with RCCs formation or manifestation (17).

The current findings are consistent with the broader literature on RCCs' morphology and behavior. Recent reviews have underscored that RCCs are benign, epithelial cysts of variable clinical course, often stable but sometimes enlarging due to intermittent fluid accumulation or inflammation (2,3). Imaging studies have documented considerable heterogeneity in cyst size, location, and wall characteristics, supporting the idea that local anatomic context influences disease expression (18). Case reports of intrasphenoidal or ectopic RCCs further illustrate how developmental variations in sinus and sellar anatomy can modify cyst location. Therefore, the higher frequency of incomplete sellar pneumatization observed in our RCC cohort may represent a developmental variation similar to that proposed for ectopic cyst locations (19,20).

From a clinical perspective, the recognition of this anatomical relationship carries several implications. For surgical planning, incomplete sellar pneumatization is associated with a thicker bony barrier and altered landmarks, which require careful preoperative assessment to optimize transsphenoidal access. Awareness of this pattern may help anticipate technical difficulty and tailor drilling strategies. For radiologists, identifying an incomplete sellar sinus in the presence of a sellar cyst should raise awareness of possible RCCs and guide the differential diagnosis, distinguishing RCCs from other cystic lesions such as cystic adenomas or arachnoid cysts. In the context of conservative management, the possibility that incomplete pneumatization predisposes to earlier symptom onset could explain why some RCCs become clinically apparent despite small size, while others in fully pneumatized sinuses remain quiescent (21-23).

Study Limitations

This study has several limitations that should be acknowledged. First, its retrospective design limits causal inference between sphenoid sinus pneumatization patterns and the presence of RCCs. Second, the sample was drawn from a single İstanbul University Faculty of Medicine, which may have introduced selection bias toward symptomatic, referred, or more clinically apparent cases. Therefore, the RCC cohort may not fully represent the general population or incidentally detected lesions. Third, we did not include quantitative morphometric measurements (e.g., sellar depth, volume, or floor thickness), and this omission limits our ability to directly support the proposed developmental and anatomical interpretations. These parameters may act as important intermediate variables linking sphenoid pneumatization to the development of RCCs. Additionally, the four-type classification of sphenoid sinus pneumatization did not account for lateral or clival extension variants, which may also influence sellar anatomy. Another limitation is that the statistical analysis was limited to univariate comparisons. Multivariate methods, such as logistic regression, were not applied to control for potential confounding variables. Therefore, the observed association between pneumatization patterns and the presence of RCCs should be interpreted with caution, as it may be influenced by unmeasured or residual confounders. Although two neuroradiologists (Y.B.T. and M.B.) reviewed the imaging studies, interobserver agreement was assessed qualitatively rather than using quantitative reliability metrics. Future research incorporating prospective designs, larger and more diverse populations, and comprehensive morphometric and volumetric analyses would strengthen understanding of the developmental and anatomical relationships suggested by this study.

Conclusion

Our results indicate that individuals with RCCs more frequently exhibit incomplete sellar-type aeration of the sphenoid sinus. This relationship likely reflects a combination of developmental coupling and mechanical constraint within the sellar–sphenoid complex. By providing new evidence on anatomical factors that may influence the occurrence and presentation of RCCs, this study enhances understanding of the development of the pituitary region and underscores the importance of detailed radiological evaluation of sphenoid pneumatization patterns when assessing sellar lesions.

Ethics

Ethics Committee Approval: This study was approved by the İstanbul University Non-Interventional Clinical Research Ethics Committee (decision number: 23, date: 14.11.2025).

Informed Consent: Informed consent was waived by the Ethics Committee due to the retrospective nature of the study and the use of anonymized imaging data.

Acknowledgments

The authors express their sincere gratitude to the radiology department team for their expert contributions to image acquisition and interpretation throughout the study.

Footnotes

Authorship Contributions: Surgical and Medical Practices - D.D.B., C.İ.G.; Concept - D.D.B., C.İ.G., S.Ö., M.B., İ.D., A.S., T.C.Ü.; Design - D.D.B., C.İ.G., S.Ö., Y.B.T., M.B., İ.D., A.S., T.C.Ü.; Data Collection or Processing - D.D.B., S.Ö., Y.B.T., M.B.; Analysis or Interpretation - M.B., İ.D., A.S., T.C.Ü.; Literature Search - C.İ.G., S.Ö., Y.B.T.; Writing - C.İ.G., S.Ö.

Conflict of Interest: No conflict of interest was declared by the authors.

Financial Disclosure: The authors declared that this study received no financial support.

References

1. Voelker JL, Campbell RL, Muller J. Clinical, radiographic, and pathological features of symptomatic Rathke's cleft cysts. J Neurosurg. 1991; 74: 535-44.
2. Aydin S, Darko K, Detchou D, Barrie U. Rathke's cleft cysts: from pathophysiology to management. Neurosurg Rev. 2024; 47: 522.
3. Menéndez-Torre EL, Gutiérrez-Hurtado A, Ollero MD, Irigaray A, Martín P, Parra P, et al. Natural history and surgical outcomes of Rathke's cleft cysts: a Spanish multicenter study. Front Endocrinol (Lausanne). 2024; 15: 1413810.
4. Alsavaf MB, Gosal JS, Wu KC, Varthya SB, Abouammo MD, Prevedello LM, et al. Growth dynamics of Rathke's cleft cyst: a risk score system for surgical decision making. Acta Neurochir (Wien). 2024; 166: 407.
5. Dogan ME, Kotanlı S, Yavuz Y, Wahjuningrum DA, Pawar AM. Computed tomography-based assessment of sphenoid sinus and sella turcica pneumatization analysis: a retrospective study. PeerJ. 2023; 11: e16623.
6. Şimşek S, İşlek A. Pneumatization of the sphenoid sinus is the major factor determining the variations of adjacent vital structures. Egypt J Otolaryngol. 2024; 40: 2.
7. Açar G, Gökşan AS, Aydoğdu D. Computed tomography based evaluation of the association between sphenoid sinus pneumatization patterns and variations of adjacent bony structures in relation to age and gender. Neurosurg Rev. 2024; 47: 349.
8. Karadayi Buyukozsoy A, Karatay E, Tastekin Toz H. Evaluation of sphenoid sinus pneumatization subtypes in posteroanterior and lateral directions on CT imaging. J Kermanshah Univ Med Sci. 2024; 28: e131911.
9. Parameshwar Keerthi BH, Savagave SG, Sakalecha AK, Reddy V, L YU. The evaluation of variations in patterns of sphenoid sinus pneumatization using computed tomography in a South Indian Population. Cureus. 2022; 14: e23174.
10. Famurewa OC, Ibitoye BO, Ameye SA, Asaleye CM, Ayoola OO, Onigbinde OS. Sphenoid sinus pneumatization, septation, and the internal carotid artery: a computed tomography study. Niger Med J. 2018; 59: 7-13.
11. Tavakoli M, Jafari-Pozve N, Aryanezhad SS. Sphenoid sinus pneumatization types and correlation with adjacent neurovascular structures using cone-beam computed tomography. Indian J Otolaryngol Head Neck Surg. 2023; 75: 2245-50.
12. Hassan NA, Ah Mahdi M, Irhyyim NS. Correlation between sphenoid sinus pneumatization and sella turcica dimensions using computed tomography. J Int Med Res. 2024; 52: 3000605241287021.
13. Ilków W, Waligóra M, Kunc M, Kucharzewski M. Pneumatization of the sphenoid sinus, dorsum sellae and posterior clinoid processes in computed tomography. Pol J Radiol. 2018; 83: e366-71.
14. Lee S, Fernandez J, Mirjalili SA, Kirkpatrick J. Pediatric paranasal sinuses-development, growth, pathology, & functional endoscopic sinus surgery. Clin Anat. 2022; 35: 745-61.
15. Gandhi K, Patil ST, Kumar B, Patel M, Chawre P, Ahmad M, et al. Morphometry and intracranial relations of the sphenoid sinus in context to endoscopic transnasal transsphenoidal surgery. Cureus. 2023; 15: e40187.
16. Ominde BS, Ikubor J, Igbigbi PS. Pneumatization Patterns of the sphenoid sinus in adult Nigerians and their clinical implications. Ethiop J Health Sci. 2021; 31: 1295-302.
17. Baloiu AI, Filipoiu F, Toader C, Covache-Busuioc RA, Munteanu O, Serban M. Sphenoid sinus hyperpneumatization: anatomical variants, molecular blueprints, and AI-augmented roadmaps for skull base surgery. Front Endocrinol (Lausanne). 2025; 16: 1634206. Erratum in: Front Endocrinol (Lausanne). 2026; 17: 1781516.
18. Larkin S, Karavitaki N, Ansorge O. Rathke's cleft cyst. Handb Clin Neurol. 2014; 124: 255-69.
19. De Sousa Machado A, Silva A, Silva J, Brandão JR, Meireles L. Intrasphenoidal Rathke's cleft cyst: an uncommon feat. Cureus. 2023; 15: e33206.
20. Petersson M, Berinder K, Eden Engström B, Tsatsaris E, Ekman B, Wahlberg J, et al. Natural history and surgical outcome of Rathke's cleft cysts-a study from the Swedish Pituitary Registry. Clin Endocrinol (Oxf). 2022; 96: 54-61.
21. Schmutzer-Sondergeld M, Weller J, Thorsteinsdottir J, Schichor C, Rachinger W, Thon N, et al. Long-term outcome of surgically treated and conservatively managed Rathke cleft cysts. Acta Neurochir (Wien). 2024; 166: 159.
22. Yoshimoto H, Kato M, Ishida A, Shiramizu H, Matsuoka G, Tanabe N, et al. Recovery of pituitary and visual function after Rathke's cleft cyst decompression: an 80-case institutional experience. J Endocr Soc. 2025; 9: bvaf093.
23. Kinoshita Y, Taguchi A, Yamasaki F, Tominaga A, Arita K, Horie N. Natural course of Rathke's cleft cysts and risk factors for progression. J Neurosurg. 2022; 138: 1426-32.

İstanbul Med J 2026; 27(3): 194-8
DOI: 10.4274/imj.galenos.2026.61326

Effects of Physical Therapy on Pain Severity and Knee Related Symptoms in Knee Osteoarthritis with or without Neuropathic Pain

Feride Sabırlı[1], Derya Buğdaycı[1], İlhan Karacan[1], Nurdan Paker[1], Ayşegül Kılıç[2], Zozan Songur Erarslan[3]

[1]University of Health Sciences Türkiye, İstanbul Physical Therapy Rehabilitation Training and Research Hospital, Department of Physical Therapy and Rehabilitation, İstanbul, Türkiye
[2]University of Health Sciences Türkiye, Gülhane Training and Research Hospital, Department of Physical Therapy and Rehabilitation, Ankara, Türkiye
[3]Aydın Atatürk State Hospital, Clinic of Physical Therapy and Rehabilitation, Aydın, Türkiye

ABSTRACT

Introduction: There is increasing awareness of the existence of neuropathic pain (NP) symptoms in addition to mechanical pain in knee osteoarthritis (OA). The aim of this study is to evaluate the effect of physical therapy on NP in women with OA.

Methods: Forty-one women with symptomatic OA according to American College of Rheumatology criteria who underwent 15 sessions of physical therapy were included in this retrospective study. Pain severity was evaluated using the Numeric Pain Rating Scale (NPRS). PainDETECT was used to assess NP. Those with a PainDETECT score between 13 and 38 were considered to have NP. Patients without NP were classified as group 1, and patients with NP were classified as group 2. The Knee Injury and Osteoarthritis Outcome Score (KOOS) was used to evaluate knee-related conditions.

Results: Mean age was 57.8±5.9 years. Mean duration of pain was 24 months (median 108) in group 1 and 54 months (median 102) in group 2 (p=0.163). NP was detected in 14 patients (34%). Mean NPRS scores at baseline were 6.0 (3.0) and 10.0 (0.3) in groups 1 and 2, respectively. Mean NPRS scores after treatment were 3.0 (3.0) and 8.0 (2.5) in groups 1 and 2, respectively. The mean NPRS score decreased significantly in both groups ($p<0.05$). Mean NPRS scores one month later were 2.0 (3.0) and 7.5 (3.0) in groups 1 and 2, respectively ($p<0.05$). In group 1, a significant improvement was observed in all KOOS domains after treatment and at the 1st-month control ($p<0.05$). However, significant increases were observed only in the KOOS pain and activities of daily living subgroups of group 2 after treatment ($p<0.05$). Multiple linear regression analysis revealed that NP was a negative predictive factor for improvement in KOOS symptom and quality-of-life subscores after treatment and at the end of the first month (p=0.001, p=0.032).

Conclusion: In this study, NP was present in almost 1/3 of OA cases and negatively affected pain relief after physical therapy. Furthermore, NP was a negative predictive factor for improvement in knee-related function and quality of life.

Keywords: Knee osteoarthritis, physical therapy, neuropathic pain

Introduction

Knee osteoarthritis (OA) is a progressive degenerative joint disease primarily characterized by chronic pain and functional impairment. While knee OA pain is predominantly nociceptive, it can sometimes have nociplastic or neuropathic characteristics (1). A previous meta-analysis reported rates of possible neuropathic pain (NP) and probable NP in patients with knee OA assessed with the PainDETECT questionnaire as 40% and 20%, respectively (2). In another study, NP prevalence has been reported 23% in knee or hip OA (3). A previous study by Güngör Demir et al. (4) using the Douleur Neuropathique-4 (DN4) questionnaire reported a NP rate of 49% in patients with knee OA. Moreover, Golob et al. (5), concluded that 14.8% of the patients with knee OA had possible NP, whereas 24.6% had probable NP using the PainDETECT questionnaire.

Classic treatment for knee OA primarily involves patient education, protective measures, and physical therapy interventions. Simple analgesics are generally used as first-line treatment. However, it has been suggested that simple analgesics are less effective in individuals with NP (5). In symptomatic patients with a NP component, adding centrally acting analgesics to the treatment regimen is usually more beneficial than regimens without them. Psychological and physical methods are frequently used together in the treatment of NP. However, there is a paucity of rigorous studies evaluating the efficacy and safety of these

Address for Correspondence: Feride Sabırlı, MD, University of Health Sciences Türkiye, İstanbul Physical Therapy Rehabilitation Training and Research Hospital, Department of Physical Therapy and Rehabilitation, İstanbul, Türkiye
E-mail: fsabirli@gmail.com **ORCID ID:** orcid.org/0000-0001-7048-2197
Cite this article as: Sabırlı F, Buğdaycı D, Karacan İ, Paker N, Kılıç A, Songur Erarslan Z. Effects of physical therapy on pain severity and knee related symptoms in knee osteoarthritis with or without neuropathic pain. İstanbul Med J. 2026; 27(3): 194-8

Received: 09.01.2026
Accepted: 11.06.2026
Publication Date: 03.08.2026

therapeutic interventions (6). Physical therapy methods, consisting of various physical activities and exercises, can improve function and alleviate pain. However, a previous study on individuals with lower extremity OA suggested that improvement was less pronounced after a 12-week exercise program in those who had NP-like symptoms prior to treatment (7). The cornerstone of knee OA treatment includes patient education, alongside optimizing body weight and engaging in exercises (8).

Antidepressant medications have demonstrated only minimal improvements in pain and function among patients with OA (9). However, they should be used with caution due to potential side effects.

A limited body of research examines the effects of physical therapy interventions on individuals with NP secondary to OA. This study aims to evaluate improvement in pain following physical therapy in this population.

Methods

Forty-one women who were admitted to the outpatient clinics of University of Health Sciences Türkiye, İstanbul Physical Therapy Rehabilitation Training and Research Hospital between 01.08.2018 and 31.12.2018 with symptomatic knee OA according to American College of Rheumatology criteria and who were scheduled for 15 sessions of physical therapy [hot pack, transcutaneous electrical nerve stimulation (TENS), short-wave diathermy or ultrasound] were included in this retrospective study. Patients with additional comorbidities that could cause NP were excluded from the study. This study was approved by the University of Health Sciences Türkiye, Bakırköy Dr. Sadi Konuk Training and Research Hospital Clinical Research Ethics Committee (protocol code: 2020/111, decision number: 2020-05-16, date: 02.03.2020). Patients participating in the study were asked to sign an informed consent form. Demographic and clinical characteristics before treatment, at the end of treatment, and 1 month after treatment were recorded. Numeric Pain Rating Scale (NPRS), Turkish version of PainDETECT questionnaire for NP and Turkish version of knee injury and Osteoarthritis Outcome Score (KOOS) scores were completed from the patients' files. Those with a PainDETECT score between 13 and 38 were considered to have NP. Patients without NP were classified as group 1, and patients with NP were classified as group 2.

Numeric Pain Rating Scale

NPRS is an 11-point metric ranging from 0 to 10, where 0 indicates the complete absence of pain and 10 represents the maximum possible pain. Within this framework, patients are required to verbally designate a numerical value that best reflects the intensity of pain experienced during the preceding 24-hour period. Additionally, a written format is commonly used, with values from 0 to 10 expressed in words. The NPRS demonstrates commendable sensitivity while yielding data amenable to statistical analysis (10).

PainDETECT Questionnaire

The PainDETECT questionnaire, initially created for chronic low back pain, has been adapted for knee OA and shown to be effective in detecting NP components. This assessment includes seven weighted sensory-descriptive questions and two items illustrating the temporal and propagation aspects of pain. The overall score ranges from 0 to 38 points. For NP, a score of ≤12 indicates low probability; scores within 13-18 indicate indeterminate probability; and a score of ≥19 indicates high probability (11). In our study, the Turkish version of PainDETECT Questionnaire was used (12).

Knee Injury and Osteoarthritis Outcome Score

The KOOS consists of five dimensions relevant to patients, each assessed individually: pain, symptoms, activities of daily living (ADL), sports and recreational functions, and overall quality of life. It employs a Likert scale, providing five possible response options rated from 0 (indicating no issues) to 4 (indicating severe issues); the score for each of the five dimensions is the total of the respective items, where a score of 0 reflects a significant knee problem, while a score of 100 indicates no knee issues (13). The reliability and validity of the KOOS-Turkish version have been evaluated in individuals with knee OA (14).

Statistical Analysis

The Shapiro-Wilk test was used to assess whether the data conformed to a normal distribution for statistical analysis. The Friedman and Wilcoxon tests were used to compare means within groups, while the Mann-Whitney U test was used to compare means between groups. To evaluate the impact of potential confounding variables on improvements as measured by KOOS and NPRS, a multiple linear regression analysis was conducted. Data analysis was performed using the SPSS 22.0 software. A p value of less than 0.05 was regarded as statistically significant.

Results

Demographic and clinical features are outlined in Table 1. The average duration of knee pain was 67.0±72.3 months. An NP component was identified in 14 (34%) patients based on assessments using the PainDETECT score. No statistically significant differences were found between the two groups in the patients' demographic, anthropometric, and clinical characteristics (Table 1).

The intensity of pain assessed using the NPRS score showed a significant reduction following treatment and at the end of the first month in patients without NP (group 1) ($p=0.0001$) (Table 2). In group 2, a notable decrease in pain was observed after treatment ($p=0.003$) and at the end of the first month post-treatment ($p=0.001$) compared with pre-treatment levels.

Pain intensity, as measured by NPRS, decreased by 21.8% and 42.3% at the end of physical therapy in the groups with and without NP, respectively ($p=0.012$). By the first month after treatment, pain relief in the groups with and without NP was 33.7% and 48.0%, respectively ($p=0.005$).

In the group, 1 notable enhancements were seen in the KOOS pain symptom, ADL, sports activity, and quality of life sub-scores following treatment and one month after the treatment concluded ($p<0.001$) (Table 2). However, in group 2, significant improvement was found only in the KOOS pain and ADL sub-scores after treatment and at the end of the first month after treatment ($p=0.007$, $p=0.003$).

Multiple linear regression analysis was conducted to determine the effect of NP on KOOS-assessed improvement while controlling for potential confounding factors. The results demonstrated that NP was a significant determinant of clinical outcomes. Accordingly, NP was identified as a negative predictor of improvement in the KOOS symptom subscale both at the end of treatment and at 1 month post-treatment. This finding indicates that the presence of NP adversely affects improvement as measured by the KOOS symptom score (Table 3).

Furthermore, the PainDETECT score was found to be a significant negative predictor of improvement in the KOOS quality of life subscale at both the end of treatment and at 1 month post-treatment. As the NP score increased, the degree of improvement in KOOS quality of life decreased (Table 3).

Discussion

In this study, the NP rate was 34% among patients with knee OA. The severity of pain and disability was high among the knee OA patients with an NP component. Pain intensity was reduced significantly after 15 sessions of physical therapy for a total of 3 weeks in patients with and without NP, both after treatment and at the 1st-month controls.

Table 1. Demographic and clinical characteristics

	Group 1 n=27	Group 2 n=14	p value
Age (years)	57.0±7.0	57.0±10.3	0.879
BMI (kg/m^2)	32.0±10.0	35.0±8.3	0.424
Duration of education (years)	5.0±5.0	5.0±7.3	0.872
Duration of knee pain (months)	24.0 (108.0)	54.0 (102.0)	0.163
Duration of last episode of knee pain (weeks)	4.0 (5.0)	8.0 (6.5)	0.063
Kellgren-Lawrence scores-right knee	2.0 (1.0)	3.0 (1.0)	0.442
Kellgren-Lawrence scores-left knee	2.0 (1.0)	3.0 (1.0)	0.586

Data is given as median (interquartile range). Means were compared with Mann-Whitney U test. BMI: Body mass index

Table 2. KOOS and NPRS scores in two group pre-treatment, end of the treatment and after one month. The effect of physical therapy on recovery, as assessed with NPRS scores and KOOS subscores, was evaluated in groups defined by PainDETECT scores

KOOS	Group	Pre-treatment	End of the treatment	One month after treatment	p value
Pain	Group 1	53.0 (25.0)	67.0 (25.0)	78.0 (22.0)	**0.0001**
	Group 2	36.0 (16.8)	36.0 (19.8)	44.0 (20.5)	**0.007**
Symptom	Group 1	68.0 (26.0)	71.0 (24.0)	82.0 (21.0)	**0.0001**
	Group 2	54.0 (23.8)	49.5 (28.3)	57.0 (26.8)	0.726
ADL	Group 1	59.0 (32.0)	71.0 (19.0)	79.0 (24.0)	**0.0001**
	Group 2	43.5 (23.3)	43.5 (20.3)	53.5 (18.3)	**0.003**
Sport	Group 1	25.0 (25.0)	40.0 (20.0)	40.0 (25.0)	**0.002**
	Group 2	7.5 (21.3)	15.0 (23.8)	20.0 (21.3)	0.133
Quality of life	Group 1	43.0 (19.0)	50.0 (25.0)	50.0 (31.0)	**0.0001**
	Group 2	25.0 (10.8)	28.0 (16.0)	31.0 (14.3)	0.192
NPRS	Group 1	6.0 (3.0)	3.0 (3.0)	2.0 (3.0)	0.0001
	Group 2	10.0 (0.3)	8.0 (2.5)	7.5 (3.0)	0.0001

Data are presented as median (interquartile range). Means were compared using the Friedman test. KOOS: Knee Injury and Osteoarthritis Outcome Score, NPRS: Numeric Pain Rating Scale

Table 3. The effect of neuropathic pain on recovery. A regression model

Outcome variable	Predictor variable	B	Std. Beta	Sig.	Adj R^2	F	p	Durbin-Watson	VIF
KOOS symptom End of the treatment	(Constant)	8.2		0.004	0.141	7.5	0.009	2.1	
	Presense of neuropathic pain	-12.5	-0.41	0.009					1.01
KOOS symptom One month after treatment	(Constant)	12.3		0.001	0.09	4.9	0.032	2.2	
	Presense of neuropathic pain	-10.7	-0.34	0.032					1.00
KOOS-QOL End of the treatment	(Constant)	18.8		0.001	0.099	5.3	0.026	1.5	
	PainDETECT score	-1.0	-0.35	0.026					2.76
KOOS-QOL One month after treatment	(Constant)	24.3		0.001	0.095	5.2	0.028	1.7	
	PainDETECT score	-1.0	-0.34	0.028					1.00

KOOS: Knee Injury and Osteoarthritis Outcome Score, QOL: Quality of life, Std. Beta: Standardized beta coefficient, Sig.: Significance, Adj R^2: Adjusted R-squared, VIF: Variance inflation factor

Definition of NP in patients with knee OA is useful for planning the treatment (15).

A notable discovery from this research was that the group without the NP component exhibited significant improvements in KOOS pain scores, ADL, sports activity, and quality of life subgroups after treatment and at the 1st month control. However, the patients showed a significant improvement only in the KOOS pain and ADL subgroups of the NP group (Table 2). Polat et al. (16) reported that there was a significant improvement in WOMAC pain and stiffness scores ($p<0.05$) after 15 sessions of TENS and hot pack application in knee OA patients both with and without NP.

In a previous study, a poor improvement has been found after 15 sessions of physical therapy in knee OA patients with central sensitization and depression (17). In another study, the authors concluded that the patients with lower extremity OA who had NP as measured by PainDETECT questionnaire, showed a weak improvement in pain after 12-week exercise program (7).

In this study, pain severity and disability were higher in patients with an NP component. NP, pain catastrophism and central sensitization accompanies reduced knee related functional status in knee OA (18). In a study conducted by Aşkın et al. (19) with 60 patients with knee OA, NP component was detected in 66.7% of the patients according to the PainDETECT score and 46.7% according to the DN4 score. In another study conducted by Garip et al. (20), in which 150 patients participated, the prevalence of NP was reported as 44% ($p=0.00$). Similarly, Hochman et al. (21), found that the NP rate is 34% in a study with 80 knee OA patients. In another study, the NP rate was 31.1% among 109 patients with knee OA, as measured by the PainDETECT questionnaire. Scores ≥19 were accepted as likely NP, ≥13 to ≤18 as possible NP and ≤12 as unlikely NP (22). In another study conducted by Dainese et al. (23) with 96 patients, the NP rate was reported as 40% by using the PainDETECT questionnaire. In our study, this rate 34% of the patient population and was consistent with previous studies.

These results highlight the significance of considering NP in the treatment of knee OA, as it influences treatment outcomes and patient-reported improvements. The results of this study suggest that addressing NP alongside conventional OA management may be crucial for optimizing patient care and enhancing treatment efficacy. These insights contribute to a more comprehensive understanding of the multifaceted nature of knee OA and highlight the significance of tailored treatment approaches based on individual pain profiles.

Study Limitations

This study has strengths and limitations. Its strengths are that all of the tests were conducted through face-to-face interviews, both NP and pain severity were assessed, and patients were followed up after treatment. Its limitations are that it was conducted with a relatively small number of patients and a retrospective design.

Conclusion

NP in women with knee OA can significantly influence the response to physiotherapy interventions. Tailoring a special physiotherapy program to consider the NP component and pain sensitization may lead to better outcomes in knee-related pain and function in these patients.

Ethics

Ethics Committee Approval: This study was approved by the University of Health Sciences Türkiye, Bakırköy Dr. Sadi Konuk Training and Research Hospital Clinical Research Ethics Committee (protocol code: 2020/111, decision number: 2020-05-16, date: 02.03.2020).

Informed Consent: Patients participating in the study were asked to sign an informed consent form.

Footnotes

Authorship Contributions: Surgical and Medical Practices - A.K., Z.S.E.; Concept - F.S., D.B., A.K., Z.S.E.; Design - F.S., D.B.; Data Collection or Processing - F.S., D.B., A.K., Z.S.E.; Analysis or Interpretation - F.S., D.B., N.P.; Literature Search - F.S., D.B., N.P.; Writing - F.S., D.B., İ.K., N.P., A.K.

Conflict of Interest: No conflict of interest was declared by the authors.

Financial Disclosure: The authors declared that this study received no financial support.

References

1. Vanneste T, Belba A, Oei GTML, Emans P, Fonkoue L, Kallewaard JW, et al. 9. chronic knee pain. Pain Pract. 2025; 25: e13408.
2. Mougui A, Belouaham S, El Bouchti I. Neuropathic pain in patients with primary knee osteoarthritis: a cross-sectional study. Rom J Intern Med. 2023; 61: 186-94.
3. French HP, Smart KM, Doyle F. Prevalence of neuropathic pain in knee or hip osteoarthritis: a systematic review and meta-analysis. Semin Arthritis Rheum. 2017; 47: 1-8.
4. Güngör Demir U, Demir AN, Toraman NF. Neuropathic pain in knee osteoarthritis. Adv Rheumatol. 2021; 61: 67.
5. Golob M, Marković I, Zovko N, Šakić D, Gudelj-Gračanin A, Morović-Vergles J. Do we pay enough attention to neuropathic pain in knee osteoarthritis patients? Acta Clin Croat. 2018; 57: 16-21.
6. Norman-Nott N, Cashin AG, Gustin SM. Psychological, physical and complementary therapies for the management of neuropathic pain. Int Rev Neurobiol. 2024; 179: 431-70.
7. Hattori T, Shimo K, Niwa Y, Katsura Y, Tokiwa Y, Ohga S, et al. Pain sensitization and neuropathic pain-like symptoms associated with effectiveness of exercise therapy in patients with hip and knee osteoarthritis. Pain Res Manag. 2022; 2022: 4323045.
8. Dantas LO, Salvini TF, McAlindon TE. Knee osteoarthritis: key treatments and implications for physical therapy. Braz J Phys Ther. 2021; 25: 135-46.
9. Leaney AA, Lyttle JR, Segan J, Urquhart DM, Cicuttini FM, Chou L, et al. Antidepressants for hip and knee osteoarthritis. Cochrane Database Syst Rev. 2022; 10: CD012157.
10. Williamson A, Hoggart B. Pain: a review of three commonly used pain rating scales. J Clin Nurs. 2005; 14: 798-804.
11. Hochman JR, Davis AM, Elkayam J, Gagliese L, Hawker GA. Neuropathic pain symptoms on the modified painDETECT correlate with signs of central sensitization in knee osteoarthritis. Osteoarthritis Cartilage. 2013; 21: 1236-42.

12. Alkan H, Ardic F, Erdogan C, Sahin F, Sarsan A, Findikoglu G. Turkish version of the painDETECT questionnaire in the assessment of neuropathic pain: a validity and reliability study. Pain Med. 2013; 14: 1933-43.

13. Roos EM, Roos HP, Lohmander LS, Ekdahl C, Beynnon BD. Knee Injury and Osteoarthritis Outcome Score (KOOS)--development of a self-administered outcome measure. J Orthop Sports Phys Ther. 1998; 28: 88-96.

14. Paker N, Buğdaycı D, Sabırlı F, Özel S, Ersoy S. Knee injury and osteoarthritis outcome score: reliability and validation of the Turkish version. Turkiye Klinikleri J Med Sci. 2007; 27: 350-6.

15. Zolio L, Lim KY, McKenzie JE, Yan MK, Estee M, Hussain SM, et al. Systematic review and meta-analysis of the prevalence of neuropathic-like pain and/or pain sensitization in people with knee and hip osteoarthritis. Osteoarthritis Cartilage. 2021; 29: 1096-116.

16. Polat CS, Doğan A, Özcan DS, Köseoğlu BF, Koçer Akselim S, Şahin Onat Ş. The effectiveness of transcutaneous electrical nerve stimulation in knee osteoarthritis with neuropathic pain component: a randomized controlled study. Turk J Osteoporos. 2017; 23: 47-51.

17. Yüzügüldü SB, Kutlay Ş, Gök H. The relationship between inadequate response to physical therapy and central sensitization in patients with knee osteoarthritis: a prospective cohort study. Turk J Phys Med Rehabil. 2023; 69: 266-74.

18. Salaffi F, Carotti M, Farah S, Ciccullo C, Gigante AP, Bandinelli F, et al. A mediation appraisal of neuropathic-like symptoms, pain catastrophizing, and central sensitization-related signs in adults with knee osteoarthritis-a cross-sectional study. J Pers Med. 2025; 15: 22.

19. Aşkın A, Özkan A, Tosun A, Demirdal ÜS, İsnaç F. Quality of life and functional capacity are adversely affected in osteoarthritis patients with neuropathic pain. Kaohsiung J Med Sci. 2017; 33: 152-8.

20. Garip Y, Eser F, Kılıçarslan A, Bodur H. Prevalence of neuropathic pain in rheumatic disorders: association with disease activity, functional status and quality of life. Arch Rheumatol. 2015; 30: 231-7. Available from: https://archivesofrheumatology.org/index.php/pub/article/view/738

21. Hochman JR, French MR, Bermingham SL, Hawker GA. The nerve of osteoarthritis pain. Arthritis Care Res (Hoboken). 2010; 62: 1019-23.

22. Polat CS, Doğan A, Sezgin Özcan D, Köseoğlu BF, Koçer Akselim S. Is there a possible neuropathic pain component in knee osteoarthritis? Arch Rheumatol. 2017; 32: 333-8.

23. Dainese P, DE Mits S, Wittoek R, VAN Ginckel A, Huysse W, Mahieu H, et al. Neuropathic-like pain in knee osteoarthritis: exploring differences in knee loading and inflammation. A cross-sectional study. Eur J Phys Rehabil Med. 2024; 60: 62-73.

İstanbul Med J 2026; 27(3): 199-206
DOI: 10.4274/imj.galenos.2026.03083

The Association of CHA_2DS_2-VASc and CHA_2DS_2-VA Scores with Aortic Arch Calcification and Its Clinical Value in Individuals with Atrial Fibrillation

Fahri Çakan[1], Uğur Köktürk[2]

[1]Alanya Alaaddin Keykubat University Faculty of Medicine, Department of Cardiology, Antalya, Türkiye
[2]Bülent Ecevit University Faculty of Medicine, Department of Cardiology, Zonguldak, Türkiye

ABSTRACT

Introduction: This study investigates the relationship between aortic arch calcification (AAC) and the stroke risk scores, CHA_2DS_2-VASc and CHA_2DS_2-VA, in patients with atrial fibrillation (AF). It aims to evaluate the association between AAC and these scores and to assess its potential as a marker for cardiovascular risk stratification.

Methods: This cross-sectional study included 492 participants stratified by AAC severity (Grades 0-3) based on standard chest X-rays. Stroke risk scores were calculated based on clinical data. Additional parameters, including renal function, inflammatory markers, and medication use, were recorded. Statistical analyses included univariate and multivariate regression analyses, as well as receiver operating characteristic (ROC) curve analysis, to evaluate the predictive value of stroke risk scores for AAC severity.

Results: Patients with higher AAC grades demonstrated significantly elevated CHA_2DS_2-VASc and CHA_2DS_2-VA scores ($p<0.001$). AAC severity correlated with advanced age, reduced glomerular filtration rate (GFR), lower serum albumin, and anemia. Logistic regression also identified GFR, beyond the stroke risk scores, as an independent predictor of AAC severity. ROC analysis demonstrated that CHA_2DS_2-VASc [area under the curve (AUC): 0.694] and CHA_2DS_2-VA (AUC: 0.688) scores significantly predicted AAC severity, with optimal cut-off values of >3 and >2, respectively ($p<0.001$).

Conclusion: AAC is significantly associated with higher stroke risk scores in patients with AF, and may serve as an additional tool for risk stratification. Incorporating the AAC assessment into current risk models could provide additional context for cardiovascular risk stratification in patients with AF; however, prospective validation with stroke outcomes is needed.

Keywords: Aortic arch calcification, CHA_2DS_2-VASc score, cardiovascular risk

Introduction

One important field of research in contemporary clinical practice is the prevention of cerebrovascular disorders. Thrombotic or embolic events that decrease blood supply to the brain are frequently implicated in the pathophysiology of ischemic stroke. The most prevalent cardiac arrhythmia associated with stroke etiology, especially when it comes to cardioembolic processes, is atrial fibrillation (AF) (1). As a result, AF diagnosis and treatment are crucial, particularly when it comes to detecting cardiac-origin thrombi and determining the etiology of the stroke. For risk assessment in clinical practice, numerous scoring systems have been created and are now in use. Initially, the $CHADS_2$ score was utilized, which was later updated to the CHA_2DS_2-VASc score by incorporating adjustments for gender, vascular disease, and age (2). Most recently, the scoring system was changed to the CHA_2DS_2-VA score because gender has declined in importance for risk weighting (3). These scoring systems provide clinicians with a convenient method for estimating the annual risk of embolic events. For example, an individual with a CHA_2DS_2-VASc score of 5 (or a CHA_2DS_2-VA score of 4) carries an approximate 7% annual risk of ischemic stroke (2,3).

Recent studies have made recommendations to enhance the relevance and accuracy of this scoring system. According to one study, adding creatinine clearance to mortality prediction data produced more reliable results, especially for those with low creatinine clearance (4). In addition, versions that modify the effectiveness of age have also been previously studied (5). In another study, the gender component score was reversed and it was suggested that the CHA_2DS_2-VASc score may be predictive as a mortality predictor during the pandemic period (6).

Aortic arch calcification (AAC) is a clinically significant characteristic in thrombotic events and has been linked to classic cardiovascular risk factors (7-9). Specifically, there are statistically significant correlations between the severity of cardiovascular illnesses and the degree of AAC

Address for Correspondence: Asst. Prof. Fahri Çakan, MD, Alanya Alaaddin Keykubat University Faculty of Medicine, Department of Cardiology, Antalya, Türkiye
E-mail: dr.fahri.cakan@gmail.com **ORCID ID:** orcid.org/0000-0002-5427-3480
Cite this article as: Çakan F, Köktürk U. The association of CHA_2DS_2-VASc and CHA_2DS_2-VA scores with aortic arch calcification and its clinical value in individuals with atrial fibrillation. İstanbul Med J. 2026; 27(3): 199-206

Received: 13.02.2026
Accepted: 17.06.2026
Publication Date: 03.08.2026

(10,11). AAC has been thoroughly investigated in various studies as a significant indicator of active and progressive systemic atherosclerosis, rather than simply a manifestation of the aging process (7-11). Further advantages in risk assessment of patients with AF may arise from the correlation of CHA_2DS_2-VASc and CHA_2DS_2-VA scores with the extent of AAC. The aim of this study was to examine the severity of AAC in patients with AF and to evaluate a possible relationship with CHA_2DS_2-VASc and CHA_2DS_2-VA scores, which are used to predict the risk of cerebrovascular events.

Methods

This study was a cross-sectional observational study. Patients who presented to the outpatient clinic during a 6-month period were consecutively included in the study. The sample size required for inclusion in the study was calculated using the G*Power program. The study's primary variable is the degree of AAC. A sample size of at least 210 cases was determined, based on a paired Student's t-test with 95% power, an α error probability of 0.05, and a medium effect size according to Cohen.

All patients who presented to the cardiology outpatient clinic and provided consent to participate in the study underwent a comprehensive evaluation for inclusion. The exclusion criteria for the study were met if an active infection, an active malignancy, or pregnancy was detected.

A comprehensive medical history was obtained from all subjects included in the study, and comorbid cardiovascular, renal, and endocrinological conditions were documented. The body mass index [(BMI), kg/m^2] and the body surface area [(BSA), m^2] were calculated using the following formula: "weight/height²" and "SquareRoot ([height (cm) x weight (kg)]/3600)," respectively. Routine blood tests were performed on all individuals included in the study. The glomerular filtration rate (GFR) was calculated using the estimated GFR formula, and the modified Simpson method was used for the assessment of ejection fraction (12). CHA_2DS_2-VASc and CHA_2DS_2-VA scores were calculated based on the participants' data (2,3).

AACs and cardiac condition were assessed by cardiologists. At a focus-to-patient distance of 150 cm, standard chest X-rays were taken while the patient was upright. AAC received the following grade (13): There is no calcification apparent in Grade 0; there are thin calcifications or tiny calcification spots on the aortic knob in Grade 1; there are one or more thicker calcification areas in Grade 2; and there is circular calcification on the aortic knob in Grade 3 (Figure 1). Each participant's cardiothoracic index was determined using the same chest X-ray. The aorta/heart and aorta/lung ratios were also computed by dividing the aortic arch width by the heart and lung widths (as determined by the cardiothoracic index). Interobserver agreement, assessed by Cohen's kappa, was close to perfect (κ: 0.817, $p<0.001$).

For ethical compliance, approval was obtained from the Non-Interventional Ethics Committee of Tekirdağ Dr. İsmail Fehmi Cumalıoğlu City Hospital (protocol number: 43, date: 12.05.2023). All individuals included in the study were informed about the research in accordance with the ethical principles outlined in the Second Declaration of Helsinki on research involving human subjects, and their written informed consent was obtained.

Statistical Analysis

All statistical analyses were conducted using IBM SPSS Statistics software (IBM Corp. Released 2011. IBM SPSS Statistics for Windows, Version 20.0. Armonk, NY: IBM Corp). The normality of continuous variables was assessed by visual inspection of histograms and Q-Q plots and by the Shapiro-Wilk test. Continuous variables following a normal distribution were presented as mean (± standard deviation), while non-normally distributed continuous variables were reported as median (interquartile range). Categorical variables were expressed as numbers and percentages. For group comparisons, continuous variables that were normally distributed were analyzed using Student's t-test, while continuous variables that were not normally distributed were analyzed using the Mann-Whitney U test. Categorical variables were analyzed using the chi-square test or Fisher's exact test. Logistic regression analyses, both univariate and multivariate, were performed to identify predictors. Receiver operating characteristic (ROC) curve analysis was used to determine cut-off values and evaluate sensitivity and specificity. A two-sided p value <0.05 was considered statistically significant for all comparisons.

Results

A total of 492 consecutive individuals who provided consent to participate in the study were included in the analysis. First, participants were stratified into three groups based on AAC grade: absent (Grade 0, n=111), mild (Grade 1, n=211), and severe (Grade 2–3, n=170). Because clinical findings were prominent when AAC was present, significance tests were conducted on a binary basis according to the presence or absence of AAC (AAC absent, n=111; AAC present, n=381). The findings are detailed according to both AAC presence and category (Table 1).

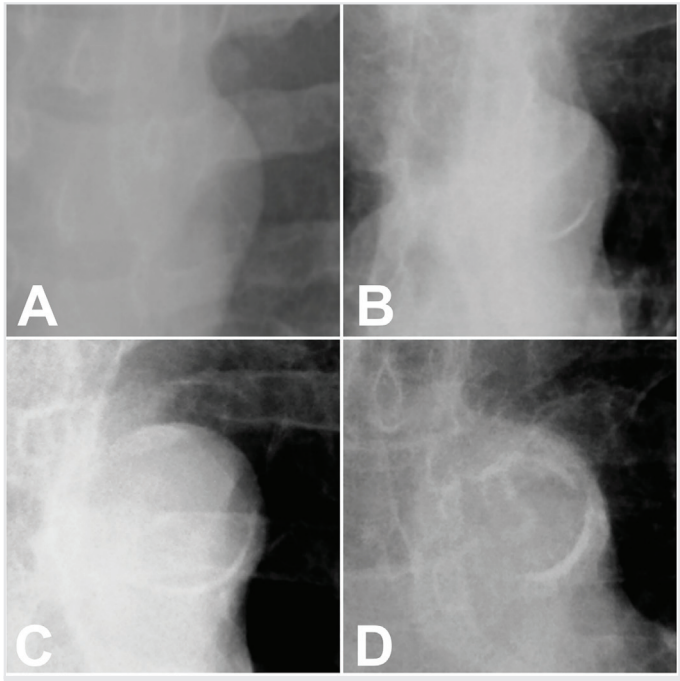

Figure 1. Aortic arch calcification grades. A) Grade 0: No calcification, B) Grade 1: Thin calcifications or tiny calcification spots, C) Grade 2: One or more thicker calcification areas, D) Grade 3: Circular calcification

Table 1. Demographic findings of study group

Parameters	Total n=492	AAC absent	AAC present			p value
		Grade 0 n=111	Mild (Grade 1) n=211	Severe (Grade 2-3) n=170	Total n=381	
Age, years	77.68±12.75	69.45±15.39	78.68±10.31	81.76±11.28	80.05±10.83	<0.001*
Gender (female)	282 (57.3%)	61 (54.9%)	117 (55.4%)	104 (61.2%)	221 (55.4%)	0.169
Body mass index, kg/m²	29.56±6.63	29.98±6.91	30.05±6.27	28.73±6.87	29.44±6.56	0.640
Body surface area, m²	1.41±0.82	1.50±0.83	1.36±0.86	1.44±0.78	1.39±0.83	0.390
Hypertension	420 (85.4%)	91 (82.0%)	179 (84.8%)	150 (88.2%)	329 (86.4%)	0.530
DM	132 (26.8%)	25 (22.5%)	54 (25.5%)	53 (31.2%)	107 (28.1%)	0.436
CAD	157 (31.9%)	27 (24.3%)	65 (30.8%)	65 (38.2%)	130 (34.1%)	0.172
CHF	65 (13.2%)	15 (13.5%)	27 (12.8%)	23 (13.5%)	50 (13.1%)	0.969
Stroke	123 (25.0%)	27 (24.3%)	52 (24.6%)	45 (26.4%)	96 (25.2%)	0.821
Hyperlipidaemia	161 (32.7%)	34 (30.9%)	64 (30.2%)	63 (37.0%)	127 (33.3%)	0.843
PAD	37 (7.7%)	8 (7.3%)	16 (7.5%)	13 (7.6%)	29 (7.6%)	0.975
CKD	51 (10.3%)	5 (4.5%)	30 (14.2%)	16 (9.4%)	46 (12.0%)	0.118
CHA_2DS_2-VASc	4.13±1.48	3.33±1.58	4.18±1.37	4.62±1.35	4.37±1.38	<0.001*
CHA_2DS_2-VA	3.56±1.41	2.78±1.56	3.63±1.26	4.00±1.29	3.79±1.28	<0.001*
RAAS blocker	280 (56.9%)	42 (37.8%)	132 (62.3%)	106 (62.4%)	238 (62.3%)	0.002*
Anti-hyperlipidaemic	146 (29.7%)	35 (31.5%)	44 (20.8%)	67 (39.4%)	111 (29.1%)	0.952
Calcium channel blocker	149 (30.3%)	24 (21.6%)	56 (26.4%)	69 (40.6%)	125 (33.6%)	0.156
Beta blocker	328 (66.7%)	76 (69.1%)	146 (68.9%)	106 (62.4%)	252 (66.0%)	0.787
Insulin	36 (7.3%)	4 (3.6%)	16 (7.5%)	18 (9.4%)	32 (8.4%)	0.370
Antiplatelet	50 (10.2%)	12 (10.9%)	18 (8.5%)	20 (11.8%)	38 (9.9%)	0.742
Digoxin	84 (17.1%)	22 (20.0%)	30 (14.2%)	32 (18.8%)	62(16.2%)	0.652
LT4	14 (2.8%)	2 (1.8%)	10 (4.7%)	2 (1.1%)	12 (3.1%)	0.511
Antithyroid	6 (1.2%)	2 (1.8%)	2 (0.9%)	2 (1.2%)	4 (1.0%)	0.890
Oral antidiabetic	114 (23.2%)	22 (20.0%)	46 (21.7%)	46 (27.1%)	92 (24.1%)	0.652
Diuretic	234 (47.6%)	38 (34.5%)	106 (50.0%)	90 (52.9%)	196 (51.3%)	0.041*
Amiodarone	28 (5.7%)	6 (5.5%)	14 (6.6%)	8 (4.7%)	22 (5.8%)	0.850
Anticoagulant						
Apixaban	144 (29.3%)	68 (30.9%)	68 (32.1%)	42 (24.7%)	110 (28.8%)	0.845
Dabigatran	12 (2.4%)	8 (3.6%)	6 (2.8%)	2 (1.2%)	8 (2.1%)	
Edoxaban	72 (14.6%)	28 (12.7%)	32 (15.1%)	26 (15.3%)	58 (15.2%)	
Rivaroxaban	234 (47.6%)	108 (49.1%)	92 (43.4%)	88 (51.8%)	180 (47.1%)	
Warfarin	30 (6.1%)	8 (3.6%)	14 (6.6%)	12 (7.1%)	26 (6.8%)	

*Statistically significant p values. AAC: Aortic arch calcification, DM: Diabetes mellitus, CAD: Coronary artery disease, CHF: Congestive heart failure, PAD: Peripheral artery disease, CKD: Chronic kidney disease, RAAS: Renin–angiotensin–aldosterone system, LT4: Levothyroxine

The cohort's average age was 77.68±12.75 years. The age difference between participants with severe AAC (81.76±11.28 years) and those without AAC (69.45±15.39 years, p<0.001) was significant. There was no discernible change in the gender distribution (p=0.169), despite a minor variation in the proportion of females between groups (56.3% in Grade 0 vs. 61.2% in Grades 2–3). Body composition measures showed no significant difference between groups (p=0.640 and p=0.390, respectively), with the mean BMI for the entire cohort being 29.56±6.63 kg/m² and the mean BSA being 1.41±0.82 m². Hypertension was the most prevalent comorbidity, affecting 85.4% of participants; however, the difference between the groups was not statistically significant (p=0.530). Diabetes mellitus was noted in 26.8% of participants; its prevalence increased with AAC severity (Grade 0: 21.8%; Grades 2–3: 31.8; p=0.436).

CHA_2DS_2-VASc and CHA_2DS_2-VA scores were significantly associated with AAC severity. The mean CHA_2DS_2-VASc score increased from 3.33±1.58 in the no AAC group to 4.62±1.35 in the severe group (p<0.001 for AAC presence). A similar pattern was observed for CHA_2DS_2-VA scores (Grade 0: 2.78±1.56 vs. Grades 2–3: 4.00±1.29, p<0.001 for AAC presence).

Laboratory parameters highlighted significant differences among AAC groups, particularly in markers of renal function, nutrition, and anemia (Table 2). GFR declined significantly with increasing AAC severity. The mean GFR was 83.80±14.75 mL/min in the absent AAC group compared to 69.79±18.79 mL/min in the AAC-present group (p<0.001). Serum albumin levels were lowest in patients with severe AAC (39.21±5.53 g/L) compared to those with no AAC (41.79±4.34 g/L, p=0.016). Haemoglobin levels showed a significant decline in patients with severe AAC (11.95±1.61 g/dL) compared to the no AAC group (13.05±1.74 g/dL, p<0.001). Lymphocyte counts were also significantly lower in AAC patients (p=0.028).

The groups were compared based on medication use. Renin–angiotensin–aldosterone system (RAAS) blockers were used by 56.9% of participants, with usage significantly lower in the absent AAC group (38.2%) compared with the mild AAC group (62.3%) and the severe AAC group (62.4%) (p=0.002). Similarly, diuretic use was higher in patients with mild AAC (50.0%) and severe AAC (52.9%) than in the absent AAC group (34.5%) (p=0.041). Other medications, including beta-blockers, oral antidiabetics, and anticoagulants, showed no significant variation across AAC groups (all p values>0.05).

Although inflammatory markers such as C-reactive protein (CRP) and lipid profiles (total cholesterol, low-density lipoprotein, high-density lipoprotein, and triglycerides) varied slightly across groups, these differences were not statistically significant. Glycated haemoglobin (HbA1c) levels, however, were significantly higher in AAC present patients (6.87±1.51%) than in the no AAC group (6.15±0.88%, p=0.031).

Univariate regression analysis identified several variables as significant predictors of AAC severity, including GFR, albumin, haemoglobin, lymphocyte count, and CHA_2DS_2-VASc score. Age was not included in the multivariate regression analysis as it was used to calculate CHA_2DS_2-VASc and CHA_2DS_2-VA scores. In the multivariate regression model, GFR emerged as an independent negative predictor of AAC severity [odds ratio (OR): 0.060, 95% confidence interval (CI): 0.010-0.362, p=0.009].

Table 2. Laboratory findings of study group

Parameters	Total	AAC absent	AAC present			p value
		Grade 0	Mild (Grade 1)	Severe (Grade 2-3)	Total	
Glucose, mg/dL	124.92±42.96	115.09±35.00	126.44±46.47	128.52±42.66	127.37±44.71	0.062
GFR, mL/min/1.73 m²	72.92±18.86	83.80±14.75	69.31±20.02	70.39±17.23	69.79±18.79	**<0.001**
ALT, IU/dL	18.71±12.31	21.09±13.16	17.47±8.92	18.73±15.02	18.03±12.01	0.105
AST, IU/dL	22.20±11.33	22.36±13.98	21.54±9.43	22.94±11.69	22.16±10.49	0.908
Sodium, mEq/L	140.46±2.97	140.48±2.29	140.55±3.11	140.35±3.21	140.46±3.15	0.961
Potassium, mEq/L	4.36±0.52	4.46±0.42	4.36±0.55	4.31±0.53	4.34±0.54	0.113
Albumin, g/L	40.16±5.19	41.79±4.34	40.13±5.15	39.21±5.53	39.71±5.33	**0.016**
C-reactive protein, mg/L	10.42±12.41	10.75±16.75	9.49±9.63	11.28±12.46	10.31±11.02	0.837
Haemoglobin, g/dL	12.32±1.76	13.05±1.74	12.25±1.80	11.95±1.61	12.12±1.72	**<0.001**
HbA1c, %	6.71±1.42	6.15±0.88	6.85±1.50	6.90±1.52	6.87±1.51	**0.031**
WBC, 10^3/µL	7.77±2.51	8.02±2.67	7.44±2.36	8.04±2.58	7.71±2.47	0.426
Neutrophils, 10^3/µL	5.07±2.19	5.11±2.45	4.83±2.05	5.37±2.18	5.07±2.12	0.908
Lymphocytes, 10^3/µL	1.89±0.95	2.14±0.74	1.82±0.70	1.83±1.28	1.82±1.00	**0.028**
Platelet, 10^3/µL	236.17±86.66	240.07±89.84	225.25±81.36	247.28±90.33	235.05±85.94	0.706
PDW, fL	16.01±2.87	16.37±2.82	16.15±3.08	15.58±2.60	15.90±2.89	0.279
RDW, %	15.69±2.39	15.33±2.35	15.60±2.33	16.06±2.47	15.80±2.40	0.192
Total cholesterol, mg/dL	179.71±42.74	187.37±44.81	179.09±41.40	175.37±42.81	177.42±41.96	0.141
Triglycerides, mg/dL	129.01±63.24	133.19±68.15	131.57±64.15	123.06±58.76	127.73±61.75	0.586
LDL, mg/dL	105.24±36.36	113.12±38.26	104.42±34.60	101.07±36.83	102.92±35.56	0.075
HDL, mg/dL	48.87±13.58	48.16±12.15	49.04±13.68	49.16±14.49	49.10±14.01	0.663
TSH, mIU/L	1.75±1.37	1.89±1.42	1.77±1.55	1.64±1.10	1.71±1.36	0.417
Aorta (mm)	40.76±5.98	40.10±5.52	41.43±6.02	40.36±6.19	40.95±6.11	0.354
CTI (fraction)	0.61±0.09	0.59±0.08	0.60±0.06	0.63±0.12	0.62±0.09	0.087
Aorta/heart (fraction)	0.23±0.03	0.24±0.03	0.23±0.03	0.23±0.03	0.23±0.03	0.488
Aorta/lung (fraction)	0.14±0.02	0.14±0.02	0.14±0.02	0.15±0.02	0.14±0.02	0.260
Ejection fraction (%)	54.37±9.5	55.20±8.65	54.52±10.33	53.64±8.99	54.13±9.74	0.463

*Statistically significant p values. AAC: Aortic arch calcification, GFR: Glomerular filtration rate, ALT: Alanine aminotransferase, AST: Aspartate aminotransferase, HbA1c: Glycated hemoglobin, WBC: White blood cells, PDW: Platelet distribution width, RDW: Red cell distribution width, LDL: Low-density lipoprotein, HDL: High-density lipoprotein, TSH: Thyroid-stimulating hormone, CTI: Cardiothoracic index

CHA_2DS_2-VA and CHA_2DS_2-VASc scores were strong positive predictors (OR: 4.763, 95% CI: 2.974-7.629, p=0.002; OR: 5.091, 95% CI: 3.039-8.527, p=0.007, respectively). Other parameters, such as haemoglobin and albumin, did not retain statistical significance in the adjusted model. Table 3 shows the univariate and multivariate regression analyses. Figure 2 shows the Forest plot of the multivariate regression analysis.

The predictive ability of CHA_2DS_2-VASc and CHA_2DS_2-VA scores for AAC severity was assessed using ROC curve analysis. For the CHA_2DS_2-VASc score, the area under the curve (AUC) was 0.694, with a sensitivity of 72.1% and a specificity of 63.6% at a cut-off score of >3. For the CHA_2DS_2-VA score, the AUC was 0.688, with higher sensitivity (83.2%) but lower specificity (45.5%) at a cut-off score of >2 (Table 4). Both scores demonstrated significant predictive value (p<0.001) for AAC severity (Figure 3).

Table 3. Regression analysis of possible variables for aortic arch calcification groups

Variable	Univariate regression analysis	Multivariate regression analysis			
	p value	p value	Odds ratio	CI lower	CI upper
Glomerular filtration rate	**<0.001**	**0.009**	0.060	0.010	0.362
Albumin	**0.016**	0.168	0.123	0.006	2.502
Haemoglobin	**<0.001**	0.218	0.119	0.004	3.511
Lymphocytes	**0.028**	0.256	0.433	0.019	9.885
HbA1c	**0.031**	0.372	0.447	0.026	7.673
Glucose	0.062				
LDL	0.075				
Cardio-thoracic index	0.087				
CHA_2DS_2-VA	**<0.001**[b]	**0.002**[b]	4.763	2.974	7.629
CHA_2DS_2-VASc	**<0.001**[b]	**0.007**[b]	5.091	3.039	8.527
Age	**<0.001**[a]				
RAAS blocker	0.179				
Diuretic	**0.030**	0.258	0.488	0.180	1.326

a: Age was not included in the analysis as it is a component of the scoring systems. b: Statistical p values were obtained from two separate multivariate models. CI: Confidence interval, HBA1c: Glycated haemoglobin, LDL: Low-density lipoprotein, RAAS: Renin–angiotensin–aldosterone system

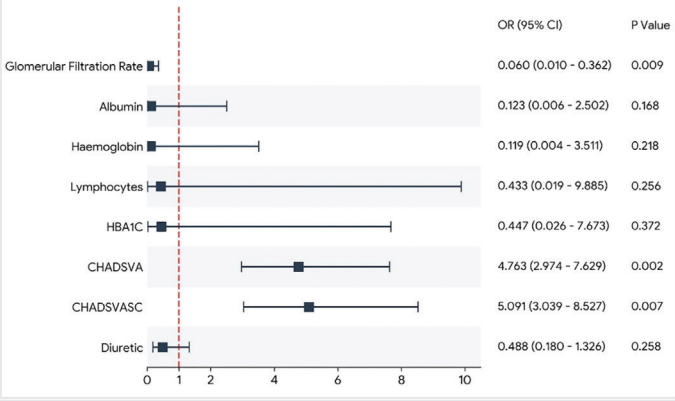

Figure 2. Forest plot of possible predictors for aortic arch calcification (multivariate analysis). OR: Odds ratio, CI: Confidence interval, HbA1c: Glycated haemoglobin

Discussion

The present study examined the association between AAC and stroke risk scores, specifically CHA_2DS_2-VASc and CHA_2DS_2-VA, in patients diagnosed with AF. Both scores demonstrated significant predictive ability, with cut-off scores of >3 and >2, respectively, showing reasonable sensitivity and specificity. The findings demonstrate a robust correlation between elevated stroke risk scores and the severity of AAC, suggesting that AAC may be used clinically as an adjunct tool for risk stratification in patients with AF. However, the moderate AUC values suggest that additional parameters, such as renal function, inflammatory markers, or imaging-based quantification of AAC, may improve predictive accuracy. This lends further support to the notion that a multi-faceted approach to risk assessment is imperative, particularly in high-risk populations such as AF patients.

The results demonstrated that individuals with prominent AAC had significantly higher CHA_2DS_2-VASc and CHA_2DS_2-VA scores compared with those without AAC. This finding aligns with previous research

Table 4. ROC curve findings for CHA_2DS_2-VASc and CHA_2DS_2-VA scores

Parameter	CHA_2DS_2-VASc	CHA_2DS_2-VA
Area under curve	0.694	0.688
Standard error	0.043	0.044
p value	<0.001	<0.001
Cut-off	3.5 (>3)	2.5 (>2)
Sensitivity	0.721	0.832
Specificity	0.636	0.455
Positive predictive value	87.3%	84.1%
Negative predictive value	39.8%	43.9%

ROC: Receiver operating characteristic

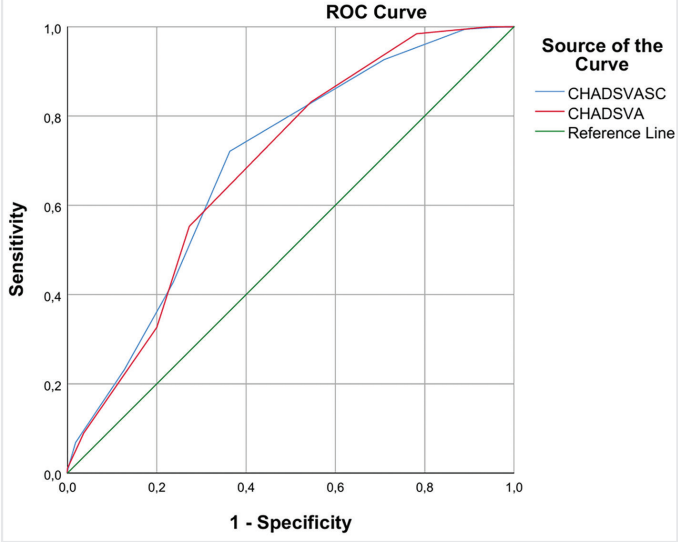

Figure 3. Receiver operating characteristic curve of aortic arch calcification for CHA_2DS_2-VASc and CHA_2DS_2-VA scores. ROC: Receiver operating characteristic

that has shown AAC as a reliable indicator of arterial stiffness, systemic atherosclerosis, and chronic inflammation, all of which have been linked to an increased risk of thromboembolism (8,9,14). The accuracy of stroke risk assessment could be enhanced by incorporating AAC assessment into existing risk prediction models, particularly for borderline or high-risk patients, for whom decisions regarding anticoagulant therapy are most challenging.

A CHA_2DS_2-VA score greater than 1 indicates an annual stroke risk of 1.5%. In light of the recent AF guidelines, this value is now considered the clinical threshold for initiating anticoagulation therapy (15). As stated in the guideline, anticoagulation therapy is recommended for patients with a score greater than 2, and this treatment has a class 1 level of evidence (15). As the score increases, so does the risk of thromboembolic events. Considering the findings of our study, the presence of AAC showed a difference of almost 1 point in the results of both scoring systems (4.37±1.38 vs. 3.33±1.58 and 3.79±1.28 vs. 2.78±1.56). This study suggests that the presence of AAC can be used as a logical indicator for initiating anticoagulation therapy, given that it can cause a 1-point difference in the scores of both scoring systems.

An important question is whether the positive correlation that AAC showed between high scores in both scoring systems can be used clinically. ROC cut-off values were considered high for both scores in clinical decision-making regarding anticoagulation. Considering the grey zone in current guidelines—such as a CHA_2DS_2-VASc score of 1 in males or 2 in females, or a score of 1 in the gender-neutral CHA_2DS_2-VA system—the clinical significance of AAC presence as an indication for initiating anticoagulation would be substantially greater. Therefore, we believe that the presence of AAC alone could be considered a tie-breaker for the use of anticoagulation.

Reduced GFR has been identified as a significant independent predictor and is strongly associated with higher AAC severity. This underscores the intricate relationship between vascular calcification and renal dysfunction (16). Chronic kidney disease (CKD) is known to accelerate vascular calcification, likely through pathways involving disturbances in calcium-phosphorus metabolism, elevated fibroblast growth factor 23 levels, and endothelial dysfunction (17). This study revealed a significant relationship between low GFR and both CHA_2DS_2-VASc and CHA_2DS_2-VA scores. These findings are consistent with prior research suggesting a strong association between declining renal function and accelerated cardiovascular calcification in AF patients (18,19).

Further clinical and laboratory findings provided valuable insights into the risk factors and systemic consequences of AAC. Patients with severe AAC exhibited lower serum albumin and haemoglobin levels, indicating the potential roles of malnutrition and anaemia in exacerbating vascular calcification (20,21). Albumin, a reliable marker of nutritional and inflammatory status, is frequently reduced in states of chronic disease and systemic inflammation, both of which may be implicated in AAC progression (20). Similarly, anaemia, a common occurrence in CKD and AF patients, has been observed to exacerbate hypoxic injury to vascular tissues, accelerating calcification (21). In the present study, univariate regression analysis revealed a significant association between hypoalbuminemia and low haemoglobin with CHA_2DS_2-VASc and CHA_2DS_2-VA scores. However, this significance was not sustained in multivariate regression analysis. The likely reasons for this are the number of study participants and selection imbalances. Given the combined roles of chronic inflammation, malnutrition, and renal failure in the progression of vascular calcification, these results are not surprising. AAC can emerge as an indicator of the cumulative burden of all these factors. We believe these findings demonstrate the clinical value of a holistic approach to AAC. Nevertheless, significant results in the initial analyses, which are in line with the literature, increase the consistency and value of this study.

It is interesting to note that higher HbA1c levels in patients with severe AAC suggest that poorly controlled diabetes is a key contributor to AAC progression (22). Persistent hyperglycaemia has been shown to exacerbate oxidative stress, promote vascular endothelial damage and accelerate calcification through non-enzymatic glycation of proteins and lipids (23). While there was no significant difference in inflammatory markers, such as CRP across AAC severity groups, the observed trend toward higher CRP levels in patients with severe AAC warrants further investigation. Chronic low-grade inflammation is a potential driver of both vascular calcification and systemic cardiovascular risk (24).

The study also explored medication use in relation to AAC severity, offering insights into current clinical management strategies. The significantly higher use of RAAS blockers and diuretics among patients with mild and severe AAC likely reflects their role in managing comorbid hypertension and heart failure. However, no significant differences in anticoagulant use were observed between AAC severity groups, suggesting that AAC is not currently considered in anticoagulation decision-making. These findings emphasise the necessity for future research to ascertain whether incorporating AAC into risk stratification tools could help guide anticoagulant therapy, particularly for intermediate-risk patients.

A potential source of confusion in this study pertains to the vascular disease component, denoted by the letter 'V' in these scoring systems. This component was defined as peripheral vascular disease, prior myocardial infarction, significant coronary artery lesion(s) with more than 50% stenosis on imaging, carotid disease and complex aortic plaque on computed tomography (CT) (25). The situation is characterised by a dichotomy. There is no ambiguity or overestimation. The definition of a complex aortic plaque is as follows: the presence of ≥4 mm in thickness, ulceration, or mobile thrombi (26). However, this study analysed the presence of any degree of AAC. Another point is that the presence of AAC could be included in this scoring system even in the absence of complex plaque. According to this study, the estimates show a difference of 1 point and the presence of AAC has been shown to be associated with recurrent ischaemic cerebral events (9,27).

The findings of this study have the potential to inform clinical practice in a number of ways. Incorporating AAC evaluation into routine risk assessment for AF patients could refine predictions of thromboembolic and cardiovascular events. This may be particularly valuable in patients with borderline or intermediate CHA_2DS_2-VASc scores, where the decision to initiate anticoagulation therapy often involves weighing the risks of thromboembolism against those of bleeding. In addition, these treatment plans have the potential to improve patient survival.

They may also generate economic, social, and psychological benefits by reducing the number of hospital admissions or shortening hospital stays. However, further studies are required to determine whether incorporating AAC into these risk scores is beneficial for calculating stroke risk in patients with AF. Furthermore, the observed associations between AAC and renal function, malnutrition, and glycemic control highlight the need for a holistic approach to managing AF patients that addresses both systemic and vascular risk factors.

Study Limitations

Despite the valuable insights this study provides, it is subject to several limitations. The study design initially included a longitudinal component; however, the current analysis focused on baseline clinical characteristics, stroke risk scores, and AAC severity and did not assess subsequent stroke incidence. This is a necessity rather than a limitation. Since the study population consisted of individuals diagnosed with AF and receiving anticoagulants for CVD prevention, minor modifications to the study cohort and a much longer follow-up are required to detect the effect of AAC in this population. Therefore, the findings should be interpreted as representing a cross-sectional association. Any assertion regarding the predictive value of AAC for stroke outcomes must be confirmed through longitudinal studies. Additionally, the number of patients included and the single-center nature of the study limit its generalizability and thus constitute significant limitations. Furthermore, the AAC grading was dependent on chest X-rays, which may understate the burden of calcification compared with more sophisticated imaging modalities such as CT, although it remains the standard criterion for aortic arch pathologies. Chest X-rays, on the other hand, are more useful and cost-effective in routine clinical practice. The relevance of the findings to other cardiovascular conditions is limited because the study population consisted exclusively of patients with AF. Additionally, bleeding, a significant endpoint of anticoagulant medications in AF patients, was not examined in the study. Should it be possible to infer an absence of a relationship with bleeding in this regard, it could further increase the diagnostic weight of AAC in CHA_2DS_2-VASc and CHA_2DS_2-VA scores.

Conclusion

This study demonstrates a substantial correlation between the severity of AAC and the stroke risk scores (CHA_2DS_2-VASc and CHA_2DS_2-VA) among individuals with AF. The results highlight the potential value of AAC as a supplementary risk stratification marker, providing a more sophisticated understanding of cardiovascular and thromboembolic risks. In addition, chest radiography offers clinicians a valuable and accessible tool for risk assessment without requiring additional radiation exposure or incurring additional cost. With a focus on enhancing patient outcomes through specialised therapy interventions, future research should seek to evaluate these findings and investigate the clinical implications of integrating AAC into risk prediction algorithms.

Ethics

Ethics Committee Approval: For ethical compliance, approval was obtained from the Non-Interventional Ethics Committee of Tekirdağ Dr. İsmail Fehmi Cumalıoğlu City Hospital (protocol number: 43, date: 12.05.2023).

Informed Consent: All individuals included in the study were informed about the research in accordance with the ethical principles outlined in the Second Declaration of Helsinki on research involving human subjects, and their written informed consent was obtained.

Footnotes

Authorship Contributions: Surgical and Medical Practices - F.Ç.; Concept - F.Ç.; Design - F.Ç., U.K.; Data Collection or Processing - F.Ç., U.K.; Analysis or Interpretation - F.Ç., U.K.; Literature Search - F.Ç., U.K.; Writing - F.Ç.

Conflict of Interest: No conflict of interest was declared by the authors.

Financial Disclosure: The authors declared that this study received no financial support.

References

1. Wyndham CR. Atrial fibrillation: the most common arrhythmia. Tex Heart Inst J. 2000; 27: 257-67.
2. Lip GY, Nieuwlaat R, Pisters R, Lane DA, Crijns HJ. Refining clinical risk stratification for predicting stroke and thromboembolism in atrial fibrillation using a novel risk factor-based approach: the euro heart survey on atrial fibrillation. Chest. 2010; 137: 263-72.
3. Champsi A, Mobley AR, Subramanian A, Nirantharakumar K, Wang X, Shukla D, et al. Gender and contemporary risk of adverse events in atrial fibrillation. Eur Heart J. 2024; 45: 3707-17.
4. Fu S, Zhou S, Luo L, Ye P. $R_{2(GFR)}CHADS_2$ and $R_{2(GFR)}CHA_2DS_2VASc$ schemes improved the performance of $CHADS_2$ and CHA_2DS_2VASc scores in death risk stratification of Chinese older patients with atrial fibrillation. Clin Interv Aging. 2017; 12:1233-8.
5. Chao TF, Lip GY, Liu CJ, Tuan TC, Chen SJ, Wang KL, et al. Validation of a modified CHA2DS2-VASc score for stroke risk stratification in Asian patients with atrial fibrillation: a nationwide cohort study. Stroke. 2016; 47: 2462-9.
6. Gunduz R, Yildiz BS, Ozdemir IH, Cetin N, Ozen MB, Bakir EO, et al. CHA2DS2-VASc score and modified CHA2DS2-VASc score can predict mortality and intensive care unit hospitalization in COVID-19 patients. J Thromb Thrombolysis. 2021; 52: 914-24.
7. Adar A, Onalan O, Cakan F, Akbay E, Karakaya E. Aortic arch calcification on routine chest radiography is strongly and independently associated with non-dipper blood pressure pattern. Arq Bras Cardiol. 2020; 114: 109-17.
8. Köktürk U, Önalan O, Somuncu MU, Çakan F, Güdül NE, Erbay İ, et al. Aortic arch calcification in predicting unfavorable angiographic outcomes for patients with ST-elevation myocardial infarction undergoing percutaneous coronary intervention. Med Princ Pract. 2024; 33: 587-96.
9. Çakan F, Sunal AS, Adar A, Onalan O. Aortic arch calcification observed on chest X-ray may serve as an independent predictor for recurrent stroke. Arq Bras Cardiol. 2024; 121: e20230805.
10. Tian WB, Zhang WS, Jiang CQ, Liu XY, Jin YL, Lam TH, et al. Aortic arch calcification and risk of all-cause mortality and cardiovascular disease: the Guangzhou Biobank Cohort Study. Lancet Reg Health West Pac. 2022; 23: 100460.
11. Hoffmann U, Massaro JM, D'Agostino RB Sr, Kathiresan S, Fox CS, O'Donnell CJ. Cardiovascular event prediction and risk reclassification by coronary, aortic, and valvular calcification in the framingham heart study. J Am Heart Assoc. 2016; 5: e003144.

12. Lang RM, Badano LP, Mor-Avi V, Afilalo J, Armstrong A, Ernande L, et al. Recommendations for cardiac chamber quantification by echocardiography in adults: an update from the American Society of Echocardiography and the European Association of Cardiovascular Imaging. J Am Soc Echocardiogr. 2015; 28: 1-39.e14.

13. Hashimoto H, Iijima K, Hashimoto M, Son BK, Ota H, Ogawa S, et al. Validity and usefulness of aortic arch calcification in chest X-ray. J Atheroscler Thromb. 2009; 16: 256-64.

14. Iribarren C, Sidney S, Sternfeld B, Browner WS. Calcification of the aortic arch: risk factors and association with coronary heart disease, stroke, and peripheral vascular disease. JAMA. 2000; 283: 2810-5.

15. Van Gelder IC, Rienstra M, Bunting KV, Casado-Arroyo R, Caso V, Crijns HJGM, et al. 2024 ESC Guidelines for the management of atrial fibrillation developed in collaboration with the European Association for Cardio-Thoracic Surgery (EACTS). Eur Heart J. 2024; 45: 3314-414. Erratum in: Eur Heart J. 2025; 46: 4349.

16. Palit S, Kendrick J. Vascular calcification in chronic kidney disease: role of disordered mineral metabolism. Curr Pharm Des. 2014; 20: 5829-33.

17. Wungu CDK, Susilo H, Alsagaff MY, Witarto BS, Witarto AP, Pakpahan C, et al. Role of klotho and fibroblast growth factor 23 in arterial calcification, thickness, and stiffness: a meta-analysis of observational studies. Sci Rep. 2024; 14: 5712.

18. Böhm M, Ezekowitz MD, Connolly SJ, Eikelboom JW, Hohnloser SH, Reilly PA, et al. Changes in renal function in patients with atrial fibrillation: an analysis from the RE-LY trial. J Am Coll Cardiol. 2015; 65: 2481-93.

19. Bautista J, Bella A, Chaudhari A, Pekler G, Sapra KJ, Carbajal R, et al. Advanced chronic kidney disease in non-valvular atrial fibrillation: extending the utility of R2CHADS2 to patients with advanced renal failure. Clin Kidney J. 2015; 8: 226-31.

20. Lee SJ, Lee IK, Jeon JH. Vascular calcification-new insights into its mechanism. Int J Mol Sci. 2020; 21: 2685.

21. Neven E, De Schutter TM, Behets GJ, Gupta A, D'Haese PC. Iron and vascular calcification. Is there a link? Nephrol Dial Transplant. 2011; 26: 1137-45.

22. Papanas N, Symeonidis G, Maltezos E, Giannakis I, Mavridis G, Lakasas G, et al. Evaluation of aortic arch calcification in type 2 diabetic patients. Vasa. 2005; 34: 113-7.

23. González P, Lozano P, Ros G, Solano F. Hyperglycemia and oxidative stress: an integral, updated and critical overview of their metabolic interconnections. Int J Mol Sci. 2023; 24: 9352.

24. Demer LL, Tintut Y. Inflammatory, metabolic, and genetic mechanisms of vascular calcification. Arterioscler Thromb Vasc Biol. 2014; 34: 715-23.

25. Zhang J, Lenarczyk R, Marin F, Malaczynska-Rajpold K, Kosiuk J, Doehner W, et al. The interpretation of CHA2DS2-VASc score components in clinical practice: a joint survey by the European Heart Rhythm Association (EHRA) Scientific Initiatives Committee, the EHRA Young Electrophysiologists, the Association of Cardiovascular Nursing and Allied Professionals, and the European Society of Cardiology Council on Stroke. Europace. 2021; 23: 314-22.

26. Suzuki M, Furuya K, Ozawa M, Miura K, Ozawa T, Matsuzono K, et al. Complex aortic arch atherosclerosis in acute ischemic stroke patients with non-valvular atrial fibrillation. J Atheroscler Thromb. 2021; 28: 776-85.

27. Cai X, Geng Y, Zhang S. The relationship between aortic arch calcification and recurrent stroke in patients with embolic stroke of undetermined source-a case-control study. Front Neurol. 2022; 13: 863450.

İstanbul Med J 2026; 27(3): 207-11
DOI: 10.4274/imj.galenos.2026.59487

Transcutaneous Laryngeal Ultrasonography for Postoperative Vocal Cord Evaluation After Thyroid and Parathyroid Surgery

Sezer Akbulut[1], Tuğba Matlım Özel[1], Aykut Çelik[1], Murat Altay[1], Begüm Bahar Yılmaz[2], Hamit Yücel Barut[3], Serkan Sarı[1]

[1]University of Health Sciences Türkiye, Başakşehir Çam and Sakura City Hospital, Clinic of General Surgery, İstanbul, Türkiye
[2]University of Health Sciences Türkiye, Başakşehir Çam and Sakura City Hospital, Clinic of Otorhinolaryngology and Head and Neck Surgery, İstanbul, Türkiye
[3]University of Health Sciences Türkiye, Başakşehir Çam and Sakura City Hospital, Clinic of Radiology, İstanbul, Türkiye

ABSTRACT

Introduction: Recurrent laryngeal nerve injury is a major complication of thyroid and parathyroid surgery and may cause vocal cord movement impairment (VCMI), which can be symptomatic or silent. Early postoperative evaluation is essential. Flexible nasolaryngoscopy (FNL) is the reference standard, but may be limited by invasiveness and practical constraints. Transcutaneous laryngeal ultrasonography (TLUS) has emerged as a non-invasive alternative, although its diagnostic performance remains controversial.

Methods: This observational study included patients undergoing thyroid or parathyroid surgery between January 2026 and April 2026. Patients younger than 18 years or those with known vocal cord pathology were excluded. All patients underwent preoperative and postoperative FNL. Postoperative TLUS was performed in a blinded manner by an experienced radiologist (H.Y.B). VCMI was defined as reduced, asymmetric, or absent vocal cord mobility. TLUS performance was evaluated using FNL as the reference standard.

Results: A total of 102 patients were included. Postoperative FNL identified VCMI in 4 patients (3.9%). TLUS suggested VCMI in 1 patient (1.0%), whereas laryngeal landmarks were visualized in all patients (100%). Using FNL as the reference standard, TLUS demonstrated a specificity of 99.0%, a negative predictive value of 96.0%, and an overall diagnostic accuracy of 95.1%. No true-positive cases were observed, and sensitivity could not be meaningfully assessed.

Conclusion: TLUS is a feasible, non-invasive adjunct for postoperative vocal cord assessment after thyroid and parathyroid surgery. It may serve as a practical complementary tool when laryngeal landmarks are adequately visualized; FNL, however remains the reference standard for definitive evaluation.

Keywords: Flexible nasolaryngoscopy, parathyroidectomy, recurrent laryngeal nerve injury, thyroidectomy, transcutaneous laryngeal ultrasound, vocal cord palsy

Introduction

Thyroidectomy remains a widely utilized surgical intervention in endocrine surgery globally and is commonly indicated for malignant thyroid disease, benign goiter, and hyperthyroidism (1). Recurrent laryngeal nerve injury continues to represent a significant postoperative concern in thyroid surgery, with transient dysfunction reported in 1% to 30% of cases and permanent impairment in 0.5% to 5% (2). Recurrent laryngeal nerve injury may result in vocal cord movement impairment (VCMI), which can lead to voice changes, airway compromise, and, in severe cases, the need for tracheostomy. Importantly, VCMI may also occur without overt clinical symptoms and therefore remain undetected in the absence of systematic postoperative evaluation (3).

Prompt identification of iatrogenic vocal cord injury in the postoperative period is essential, particularly as documentation of perioperative vocal cord function may carry medicolegal implications after thyroid or neck surgery (4). Flexible nasolaryngoscopy (FNL) remains the reference standard for vocal cord visualization and allows reliable assessment of vocal cord mobility in most patients (5). However, routine implementation of FNL may be limited by the need for otolaryngology consultation, logistical constraints at some centers, increased healthcare costs, and patient discomfort due to its invasive nature (6).

Transcutaneous laryngeal ultrasonography (TLUS) has gained attention as a non-invasive and easily accessible alternative for evaluating vocal cord mobility. Using a linear ultrasound probe placed over the thyroid

Address for Correspondence: Sezer Akbulut, MD, University of Health Sciences Türkiye, Başakşehir Çam and Sakura City Hospital, Clinic of General Surgery, İstanbul, Türkiye
E-mail: drsezerakbulut@gmail.com **ORCID ID:** orcid.org/0000-0003-4362-2240
Cite this article as: Akbulut S, Matlım Özel T, Çelik A, Altay M, Yılmaz BB, Barut HY, et al. Transcutaneous laryngeal ultrasonography for postoperative vocal cord evaluation after thyroid and parathyroid surgery. İstanbul Med J. 2026; 27(3): 207-11

Received: 27.04.2026
Accepted: 23.06.2026
Publication Date: 03.08.2026

cartilage, dynamic assessment of vocal cord motion during respiration and phonation can be performed (7). Although TLUS offers advantages in terms of patient comfort and feasibility, published data demonstrate variable diagnostic performance, with considerable heterogeneity in reported sensitivity and specificity across studies (5,8).

This study aimed to evaluate the feasibility and diagnostic performance of TLUS when performed by an experienced radiologist (H.Y.B) for assessing postoperative vocal cord mobility in patients who had undergone thyroid and parathyroid procedures. FNL was employed as the reference standard.

Methods

Study Design and Patient Selection

This observational study was carried out between January 2026 and April 2026. Patients undergoing surgical treatment for thyroid or parathyroid disorders during the study period were eligible for inclusion. Thyroid operations included lobectomy, total thyroidectomy, and procedures combined with central and/or lateral neck dissection. Parathyroid surgery consisted of parathyroid adenoma removal and four-gland exploration. Patients under 18 years of age were not included. Further exclusion criteria included isolated lateral neck dissection without accompanying thyroid surgery, prior vocal cord pathology, or previous vocal cord procedures. All thyroid and parathyroid operations were carried out with routine intraoperative nerve monitoring in accordance with institutional practice.

Laryngeal Assessment

All patients underwent preoperative FNL as part of the routine clinical evaluation to document baseline vocal cord function. In the postoperative period, FNL was repeated either on postoperative day 1 or within the first postoperative week, according to institutional practice. Following postoperative FNL, TLUS was performed in a blinded manner.

FNL was performed by experienced clinicians. Vocal cord dysfunction was defined as any departure from normal mobility, including diminished movement suggestive of weakness, asymmetry between the vocal cords, or complete absence of motion.

Transcutaneous Laryngeal Ultrasonography

TLUS was carried out using a high-frequency linear ultrasound probe. During the examination, patients were positioned supine with gentle extension of the neck to facilitate laryngeal visualization. The probe was initially placed on the anterior neck at the level of the thyroid cartilage and slowly repositioned to obtain optimal views of both vocal cords.

Identification of laryngeal anatomy was achieved by visualizing surrounding structures, including the false vocal cords and arytenoid cartilages, which served as reference landmarks when visible (Figure 1). Image settings were individually adjusted to enhance tissue contrast, allowing clear differentiation between the hyperechoic false vocal cords and the hypoechoic true vocal cords. Assessment of vocal cord mobility was performed in real time during quiet breathing and active phonation with sustained production of the vowel "ii." Normal vocal cord function was defined as the symmetric and coordinated movement of both true vocal cords during opening and closing.

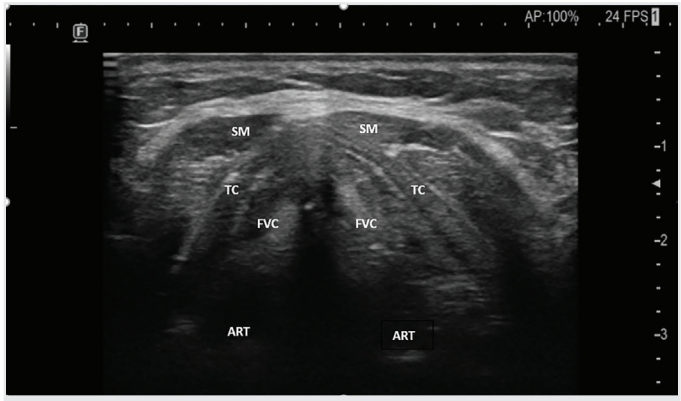

Figure 1. Anterior view of vocal cords abduction. ART: Arytenoids, FVC: False vocal cord, SM: Strap muscles, TC: Thyroid cartilage

All ultrasonographic examinations were performed by a single radiologist with extensive experience in neck ultrasonography to ensure consistency and minimize observer-related variability.

Patient-related parameters were systematically recorded, including anthropometric measurements such as neck circumference, neck length, and body mass index (BMI), and demographic variables such as age and sex. Postoperative TLUS findings were assessed for the visibility of laryngeal structures and vocal cord mobility and were categorized as either normal function or VCMI. Findings obtained from postoperative FNL were also documented for each patient.

FNL served as the reference method for identifying VCMI. The diagnostic performance of TLUS was evaluated by determining sensitivity, specificity, positive predictive value (PPV), negative predictive value (NPV), and overall accuracy, compared with FNL findings.

The study was conducted in accordance with the Declaration of Helsinki and received approval from the Institutional Ethics Committee of University of Health Sciences Türkiye, Başakşehir Çam and Sakura City Hospital (decision number: 2026-39, date: 21 January 2026). Given its observational design and reliance on routinely collected clinical data, the requirement for written informed consent was waived in line with institutional policy.

Statistical Analysis

Statistical analyses were performed using IBM SPSS Statistics version 28.0 (IBM Corp., Armonk, NY, USA). Categorical variables were expressed as numbers and percentages, and continuous variables as mean ± standard deviation. Diagnostic performance measures, including sensitivity, specificity, PPV, NPV, and overall accuracy, were calculated by comparing postoperative TLUS findings with FNL findings.

Results

The study included 102 patients who underwent thyroid or parathyroid procedures. Most patients were female (75.5%), with a mean age of 48.5±12.6 years. The average BMI was 29.0±5.3 kg/m². Mean neck circumference, neck length, and subcutaneous fat thickness measured 39.8±4.1 cm, 16.0±1.7 cm, and 3.6±1.4 mm, respectively. Postoperative

TLUS allowed visualization of laryngeal landmarks in all patients (100%). Comprehensive demographic and clinical data are summarized in Table 1.

Thyroid lobectomy was carried out in 43 patients, while 33 patients underwent total thyroidectomy alone. Total thyroidectomy combined with central neck dissection was performed in 6 patients, and total thyroidectomy with both central and lateral neck dissection was performed in 8 patients. Parathyroid procedures included adenoma excision in 10 patients and four-gland exploration in 2 patients.

Postoperative FNL identified VCMI in 4 patients (3.9%), while the remaining patients demonstrated normal vocal cord mobility.

TLUS suggested VCMI in 1 patient (1.0%), whereas 101 patients (99.0%) were classified as having normal vocal cord mobility. The comparison between TLUS and FNL findings is shown in Table 2.

When FNL was used as the reference standard, TLUS demonstrated a high specificity (99.0%), a high NPV (96.0%), and an overall diagnostic accuracy of 95.1%. No true-positive cases were observed; as none of the patients diagnosed with VCMI by FNL were identified by TLUS. Accordingly, sensitivity and PPV could not be demonstrated in this cohort.

Discussion

International guidelines highlight the importance of perioperative laryngeal assessment in patients undergoing thyroid and parathyroid procedures. The American Academy of Otolaryngology-Head and Neck Surgery recommends evaluation in both the preoperative and postoperative periods, whereas the American Thyroid Association suggests postoperative assessment particularly in patients presenting with voice-related symptoms (9,10). FNL remains the gold standard due to its direct visualization and high diagnostic accuracy (11). However, its routine use in all patients may be limited by its invasiveness, patient discomfort, and the need for otolaryngology consultation in many centers (12).

In light of these practical constraints, TLUS has been increasingly recognized as a non-invasive and cost-effective approach for the perioperative evaluation of vocal cord function. TLUS enables dynamic assessment without radiation exposure and can be performed at the bedside. Nevertheless, its diagnostic performance is known to be operator-dependent (13). Earlier prospective investigations and pooled analyses have shown that TLUS enables visualization of the vocal cords in approximately 86-96% of patients, with pooled estimates approaching 94-95.7%. Limited visualization has been associated with several patient- and anatomy-related factors, including male sex, increasing age, calcification of the thyroid cartilage, greater neck circumference, and higher BMI (14). In addition, sex-related differences have been described, with better visualization rates reported in women, likely due to thinner thyroid cartilage compared with men (15,16). The uniform visualization rate in our study may be explained by the use of a standardized examination approach and all TLUS assessments being performed by a single experienced radiologist, thereby limiting operator-related variability.

Studies comparing TLUS with flexible laryngoscopy suggest strong diagnostic performance, with sensitivities reported between 75% and 100% and specificities generally exceeding 95%. PPVs have been noted in the range of 55% to 70%, whereas NPVs are usually greater than 98% (17). In a large retrospective study of 668 patients who underwent thyroidectomy across two tertiary endocrine surgery centers, Knyazeva et al. (18) demonstrated strong postoperative diagnostic performance of TLUS, with sensitivity reaching 86% and specificity 99.1%, while PPV and NPV were 89.4% and 98.7%, respectively, highlighting its potential role in routine clinical practice.

Table 1. Demographic and clinical characteristics of the patients

Variable	Total (n=102)
Sex, n (%)	
Female	77 (75.5)
Male	25 (24.5)
Age, years (mean ± SD)	48.5±12.6
Body mass index, kg/m² (mean ± SD)	29.0±5.3
Neck circumference, cm (mean ± SD)	39.8±4.1
Neck length, cm (mean ± SD)	16.0±1.7
Subcutaneous fat thickness, mm (mean ± SD)	3.6±1.4
Visualization of laryngeal landmarks on postoperative TLUS, n (%)	102 (100)

SD: Standard deviation, TLUS: Transcutaneous laryngeal ultrasonography

Table 2. Comparison of postoperative TLUS and FNL findings in patients with evaluable vocal cords (n=102)

TLUS	FNL normal, n	FNL VCMI, n	Total, n (%)
Normal, n	97	4	101 (99.0)
VCMI, n	1	0	1 (1.0)
Total, n (%)	98 (96.1)	4 (3.9)	102 (100)

TLUS: Transcutaneous laryngeal ultrasonography; FNL: Flexible nasolaryngoscopy; VCMI: Vocal cord movement impairment

In contrast, other investigators have raised concerns regarding the limited sensitivity of TLUS, emphasizing that it cannot reliably replace laryngoscopy for detecting vocal cord dysfunction (19,20). These discrepancies across studies likely reflect variations in study design, patient characteristics, operator expertise, timing of assessment, and the underlying incidence of postoperative VCMI.

In our cohort, only four patients were diagnosed with postoperative VCMI by FNL. Consequently, no true-positive cases were identified by TLUS, precluding a meaningful assessment of sensitivity. Importantly, this finding should be interpreted in the context of the very low incidence of recurrent laryngeal nerve injury observed in a cohort with favorable surgical outcomes rather than as definitive evidence of inadequate diagnostic performance of TLUS. These findings highlight the challenges of evaluating diagnostic sensitivity when the prevalence of the target condition is very low and underscore the need for larger studies including a greater number of pathological cases.

Some studies have indicated that TLUS may demonstrate lower sensitivity and greater variability when performed by operators without dedicated training in laryngeal ultrasonography (5,21). As an example, Borel et al. (5) documented limited diagnostic performance, with TLUS showing a sensitivity of 33% and a NPV of 95% in identifying vocal cord palsy following thyroidectomy. In that study, TLUS examinations were performed by radiologists who lacked prior dedicated experience with this technique, which may have contributed to the diagnostic limitations observed.

Conversely, when TLUS is performed by surgeons with expertise in thyroid and neck ultrasonography, higher visualization success and better agreement with laryngoscopic findings have been observed (3,8,22). Surgeons may benefit from an intraoperative perspective, particularly when the recurrent laryngeal nerve is deemed to be at risk. In such situations, postoperative ultrasonographic assessment may be performed with heightened awareness of subtle vocal cord motion abnormalities. For this reason, some authors have suggested that surgeon involvement in the TLUS evaluation may enhance diagnostic performance (23).

In the present study, TLUS examinations were performed by a single radiologist with more than 30 years' experience in neck ultrasonography and dedicated practice in thyroid imaging. The complete visualization of laryngeal landmarks in all patients may be attributable, at least in part, to examiner experience and familiarity with laryngeal anatomy, meticulous probe positioning, dynamic assessment during phonation, and optimization of image settings. These factors may have helped overcome potential anatomical challenges, including increased soft tissue thickness and thyroid cartilage calcification, which have been reported to limit TLUS visualization in previous studies. These findings highlight the importance of examiner expertise in maximizing the diagnostic utility of TLUS.

The findings of this study suggest that TLUS may play a complementary role in the postoperative evaluation of vocal cord function after thyroid and parathyroid procedures. In patients with clearly visualized laryngeal landmarks and normal ultrasonographic findings, TLUS may provide reassurance regarding preserved vocal cord mobility. As a rapid and non-invasive examination that can be integrated into routine cervical ultrasonography, TLUS may serve as a practical first-line assessment tool in selected patients. In this context, TLUS could be considered an initial postoperative screening method, potentially reducing the need for routine invasive assessment. Nevertheless, FNL remains the reference standard for the definitive evaluation of vocal cord dysfunction.

Study Limitations

Our study has certain limitations that should be considered when interpreting the findings. The relatively low rate of postoperative impairment of vocal cord movement limited the ability to perform a more robust evaluation of TLUS sensitivity. In addition, the single-center design, conducted at University of Health Sciences Türkiye, Başakşehir Çam and Sakura City Hospital, a high-volume tertiary referral center, may limit the generalizability of the results to other clinical settings. As all TLUS evaluations were performed by one experienced radiologist, interobserver variability could not be assessed. Moreover, the analysis was confined to the early postoperative period; long-term functional outcomes of vocal cord mobility were not evaluated.

Conclusion

TLUS is a feasible and non-invasive method for the postoperative evaluation of vocal cord function following thyroid and parathyroid surgery. In patients with adequately visualized laryngeal landmarks, TLUS may have a complementary role in postoperative vocal cord assessment and serve as a practical first-line evaluation tool. However, the limited number of cases of postoperative VCMI in our cohort restricted the assessment of sensitivity, and TLUS should not be considered a standalone diagnostic modality. FNL remains the reference standard for the definitive evaluation of vocal cord dysfunction. Further studies involving larger patient populations are needed to better define the role of TLUS in clinical practice.

Ethics

Ethics Committee Approval: The study was conducted in accordance with the Declaration of Helsinki and received approval from the Institutional Ethics Committee of University of Health Sciences Türkiye, Başakşehir Çam and Sakura City Hospital (decision number: 2026-39, date: 21 January 2026).

Informed Consent: Given its observational design and reliance on routinely collected clinical data, the requirement for written informed consent was waived in line with institutional policy.

Footnotes

Authorship Contributions: Surgical and Medical Practices - S.A., T.M.Ö., A.Ç., M.A., B.B.Y., H.Y.B., S.S.; Concept - S.A., T.M.Ö., A.Ç., B.B.Y., H.Y.B., S.S.; Design - S.A., T.M.Ö., B.B.Y., S.S.; Data Collection or Processing - S.A., A.Ç., M.A.; Analysis or Interpretation - S.A., M.A.; Literature Search - S.A., S.S.; Writing: S.A.

Conflict of Interest: No conflict of interest was declared by the authors.

Financial Disclosure: The authors declared that this study received no financial support.

References

1. Singh H, Nelson T, Kataria K, Agarwal A, Thakur UK, Kairo A, et al. A prospective observational study on the accuracy of transcutaneous laryngeal ultrasonography in assessing vocal cord mobility before and after thyroid surgery. Iran J Otorhinolaryngol. 2025; 37: 253-9.
2. Joliat GR, Guarnero V, Demartines N, Schweizer V, Matter M. Recurrent laryngeal nerve injury after thyroid and parathyroid surgery: incidence and postoperative evolution assessment. Medicine (Baltimore). 2017; 96: e6674.
3. Rossi L, Papini P, De Palma A, Fregoli L, Becucci C, Ambrosini CE, et al. Surgeon-performed transcutaneous laryngeal ultrasound for vocal cord assessment after total thyroidectomy: a prospective study: original article. Langenbecks Arch Surg. 2024; 409: 183.
4. Wong KP, Lang BH, Chang YK, Wong KC, Chow FC. Assessing the validity of transcutaneous laryngeal ultrasonography (TLUSG) after thyroidectomy: what factors matter? Ann Surg Oncol. 2015; 22: 1774-80.
5. Borel F, Delemazure AS, Espitalier F, Spiers A, Mirallie E, Blanchard C. Transcutaneous ultrasonography in early postoperative diagnosis of vocal cord palsy after total thyroidectomy. World J Surg. 2016; 40: 665-71.
6. Patel A, Spychalski P, Polomska K, Albrahim M, Markiet K, Kurylowicz J, et al. Technical aspects of transcutaneous laryngeal ultrasonography: a review. J Voice. 2025: S0892-1997(25)00041-4.
7. Wolff S, Gałązka A, Dedecjus M. Transcutaneous laryngeal ultrasonography in vocal fold assessment before and after thyroid surgery in light of recent studies. Pol J Radiol. 2022; 87: e195-201.
8. Gambardella C, Offi C, Romano RM, De Palma M, Ruggiero R, Candela G, et al. Transcutaneous laryngeal ultrasonography: a reliable, non-invasive and inexpensive preoperative method in the evaluation of vocal cords motility-a prospective multicentric analysis on a large series and a literature review. Updates Surg. 2020; 72: 885-92.
9. Chandrasekhar SS, Randolph GW, Seidman MD, Rosenfeld RM, Angelos P, Barkmeier-Kraemer J, et al. Clinical practice guideline: improving voice outcomes after thyroid surgery. Otolaryngol Head Neck Surg. 2013; 148: S1-37.
10. Ringel MD, Sosa JA, Baloch Z, Bischoff L, Bloom G, Brent GA, et al. 2025 American Thyroid Association Management Guidelines for adult patients with differentiated thyroid cancer. Thyroid. 2025; 35: 841-985. Erratum in: Thyroid. 2025; 35: 1350.
11. Patel A, Spychalski P, Aszkiełowicz A, Mikaszewski B, Kobiela J. Transcutaneous laryngeal ultrasound for vocal cord paralysis assessment in patients undergoing thyroid and parathyroid surgery-a systematic review and meta-analysis. J Clin Med. 2021; 10: 5393.
12. Figueroa-Bohorquez D, Marulanda M, Betancourt C, Garcia C, Sanchez JG, Trujillo Y, et al. Surgeon-performed transcutaneous laryngeal ultrasonography after thyroidectomy: diagnostic accuracy and learning curve. Surgery. 2025; 188: 109779.
13. Moore CL, Copel JA. Point-of-care ultrasonography. N Engl J Med. 2011; 364: 749-57.
14. Woo JW, Suh H, Song RY, Lee JH, Yu HW, Kim SJ, et al. A novel lateral-approach laryngeal ultrasonography for vocal cord evaluation. Surgery. 2016; 159: 52-6.
15. Fung MMH, Lang BH. A prospective study evaluating the feasibility and accuracy of very early postoperative translaryngeal ultrasonography in the assessment of vocal cord function after neck surgery. Surgery. 2021; 169: 191-6.
16. Kılıç MÖ, Terzioğlu SG, Gülçek SY, Sarı E. The role of ultrasonography in the assessment of vocal cord functions after thyroidectomy. J Invest Surg. 2018; 31: 24-8.
17. Lazard DS, Bergeret-Cassagne H, Lefort M, Leenhardt L, Russ G, Frouin F, et al. Transcutaneous laryngeal ultrasonography for laryngeal immobility diagnosis in patients with voice disorders after thyroid/parathyroid surgery. World J Surg. 2018; 42: 2102-8.
18. Knyazeva P, Makarin V, Seeliger B, Chernikov R, Sleptsov I, Semenov A, et al. Transcutaneous laryngeal ultrasonography (TLUS) as an alternative to direct flexible laryngoscopy (DFL) in the perioperative evaluation of the vocal cord mobility in thyroid surgery. Langenbecks Arch Surg. 2018; 403: 1015-20.
19. Kandil E, Deniwar A, Noureldine SI, Hammad AY, Mohamed H, Al-Qurayshi Z, et al. Assessment of vocal fold function using transcutaneous laryngeal ultrasonography and flexible laryngoscopy. JAMA Otolaryngol Head Neck Surg. 2016; 142: 74-8.
20. Sidhu S, Stanton R, Shahidi S, Chu J, Chew S, Campbell P. Initial experience of vocal cord evaluation using grey-scale, real-time, B-mode ultrasound. ANZ J Surg. 2001; 71: 737-9.
21. Shah MK, Ghai B, Bhatia N, Verma RK, Panda NK. Comparison of transcutaneous laryngeal ultrasound with video laryngoscope for assessing the vocal cord mobility in patients undergoing thyroid surgery. Auris Nasus Larynx. 2019; 46: 593-8.
22. Pérez-Sánchez LE, Caballero-Rodríguez E, Orti-Rodríguez R, Soto-Sánchez A, García-Bello MÁ, Jordán-Balanza JC, et al. Cervical ultrasound for the evaluation of the vocal cords: a pilot study in an endocrine surgery unit. Cir Esp (Engl Ed). 2022; 100: 755-61.
23. Kim DH, Lee J, Seo Y, Kim SW, Hwang SH. Perioperative transcutaneous laryngeal ultrasonography to assess vocal cord function in thyroid surgery. Am J Surg. 2022; 223: 893-9.

İstanbul Med J 2026; 27(3): 212-8
DOI: 10.4274/imj.galenos.2026.90248

Prevalence and Clinical Characteristics of Pediatric Parasitic Gastroenteritis with a Comparative Analysis of Diagnostic Methods

Merve Aleyna İlteroğlu[1], Meryem Yeşil Çolak[1], Erkan Doğan[2]

[1]Karabük University Faculty of Medicine, Department of Medical Microbiology, Karabük, Türkiye
[2]Karabük University Faculty of Medicine, Department of Pediatrics, Karabük, Türkiye

ABSTRACT

Introduction: Parasitic gastroenteritis is a major cause of gastrointestinal complaints in children. The aim of this study was to determine the prevalence and clinical findings of parasitic infections in pediatric patients. We also analysed the distribution by age groups and seasonal patterns, compared the detection rate and diagnostic yield of different methods, and investigated associations between clinical findings and specific parasites.

Methods: This prospective study was conducted in 300 pediatric patients who presented to Karabük Training and Research Hospital with gastrointestinal symptoms. Demographic data, clinical symptoms, and stool characteristics (such as consistency and appearance) were systematically recorded for each patient. All clinical samples were analysed for gastrointestinal parasites using various diagnostic methods, including macroscopic examination, direct microscopy, flotation, concentration methods, and the immunochromatographic rapid test (ICT). The detection rates were compared, and correlations between clinical findings and parasite infections were analysed.

Results: Parasitic infections were detected in 26% of children, with the highest susceptibility observed in infants and young children. Among pediatric patients, the most common symptoms were diarrhoea (36.7%), abdominal pain (30.3%), fever (25.7%), and colitis (25.3%). The predominant pathogens were *Entamoeba histolytica* (22.7%), followed by *Blastocystis hominis* (6%) and *Giardia duodenalis* (4%). *Cryptosporidium parvum* appeared to be more frequently observed in patients with abdominal pain and diarrhoea; *Enterobius vermicularis* was more frequently observed in febrile patients. Rapid ICT showed a higher detection rate (23.3%) than traditional microscopy (22.7%). The consistency of watery, mucous stools was a significant clinical predictor of parasitic infection ($p<0.05$). Positive cases peaked in autumn, particularly in September.

Conclusion: ICTs showed a higher detection rate than the conventional microscopic method in this study. The correlation between stool consistency and parasitic infection serves as an important diagnostic clue for paediatricians in emergency departments and outpatient settings during clinical decision-making.

Keywords: Pediatric gastroenteritis, rapid diagnostic tests, diarrhoea, gastrointestinal parasites

Introduction

Gastrointestinal infections are the second most common infectious diseases after respiratory infections. According to World Health Organization data, there are over 1.7 billion cases of diarrheal disease worldwide each year (1). The situation is particularly critical in the pediatric age group. More than 654 million school-age children and more than 260 million preschool-age children live in areas that require treatment for parasitic infections (1,2).

The impact of gastrointestinal parasitic infections on child mortality rates is substantial. According to UNICEF 2024 data, diarrheal diseases are the third leading cause of death in children under 5 years of age, causing 443,832 child deaths annually (3). These deaths account for 9% of the total under-5 mortality rate (4,5).

The clinical impact of pediatric intestinal parasites is multidimensional, causing long-term health problems beyond acute gastrointestinal symptoms. Systematic reviews show that *Ascaris lumbricoides* is significantly associated with growth retardation (6). *Giardia duodenalis* (*G. duodenalis*) infections cause anemia and malnutrition by inhibiting the absorption of iron, vitamins, minerals, proteins, lipids, and carbohydrates, leading to physical and mental developmental delays (7). Chronic infections negatively affect school performance and result in long-term educational losses due to absenteeism (8).

Address for Correspondence: Assoc. Prof. Meryem Yeşil Çolak, PhD, Karabük University Faculty of Medicine, Department of Medical Microbiology, Karabük, Türkiye
E-mail: meryemcolak@karabuk.edu.tr **ORCID ID:** orcid.org/0000-0001-9876-935X
Cite this article as: İlteroğlu MA, Yeşil Çolak M, Doğan E. Prevalence and clinical characteristics of pediatric parasitic gastroenteritis with a comparative analysis of diagnostic methods. İstanbul Med J. 2026; 27(3): 212-8

Received: 28.11.2025
Accepted: 23.06.2026
Publication Date: 03.08.2026

Parasitic disease prevalence is affected by various factors, including environmental conditions, infrastructure, education level, water quality, hygiene practices, climate, gender, age, cleanliness habits, economic status, and dietary habits (9,10). Gastrointestinal symptoms are common causes of pediatric hospitalization, with nausea, vomiting, diarrhea, and abdominal pain accounting for a significant number of emergency department visits (11). Viral gastroenteritis causes diarrhea (92.2%), vomiting (68.7%), and abdominal pain (60.8%), while parasitic gastroenteritis presents with similar symptoms (12). The main transmission route for most intestinal parasite infections is the fecal-oral route, which is especially prevalent in countries with low socioeconomic conditions (13,14).

The most common pediatric gastrointestinal parasites are *Entamoeba histolytica* (*E. histolytica*) complex (9.28-36%), *G. duodenalis* (10-64.8%), *Blastocystis* spp. (up to 88.7% by polymerase chain reaction), and *Cryptosporidium* spp. (1.8-5%) (15,16). Distribution varies by age: children under 2 years account for 67.85% of Cryptosporidium infections, Giardia affects all pediatric age groups, and *E. histolytica* is more prevalent in children under 1 year and those aged 48-59 months (17). Diagnostic methods for gastrointestinal parasites include direct microscopy, serological and molecular methods, and rapid diagnostic tests (immunochromatographic card tests). While direct microscopic examination is the cornerstone of parasitologic diagnosis, the zinc sulfate flotation method performs better for protozoan cysts and *Hymenolepis nana*, whereas the formalin-ethyl acetate sedimentation method is superior for detecting heavy helminth eggs and larvae (14,18-23).

Our study aimed to investigate intestinal parasites in pediatric patients using various diagnostic methods (macroscopic examination, direct microscopy, zinc sulfate flotation, formalin-ethyl acetate sedimentation, rapid diagnostic tests); determine prevalence by age, sex, clinical symptoms, and seasonal distribution; and compare the detection rate and diagnostic yield of each method. These results will help to develop optimal diagnostic algorithms for pediatric gastrointestinal parasitic infections and to improve infection control.

Methods

Study Design

This prospective cross-sectional study was conducted between May 2023 and April 2024 at the Microbiology Laboratory of Karabük Training and Research Hospital. The study was approved by the Karabük University Non-Interventional Ethics Committee (decision number: 2022/787, date: 20.01.2022). Informed consent was not required, as the study used only anonymized routine clinical stool samples and associated data.

Study Population

A total of 300 pediatric patients (aged 0-18 years) presenting at the hospital's microbiology laboratory with gastrointestinal symptoms were included in the study. The study group comprised 160 (53.3%) males and 140 (46.7%) females.

Sample Collection and Processing

Fresh stool samples were collected in sterile, wide-mouthed, capped containers and transported to the laboratory. Samples were processed within 2 hours of collection. For each sample, macroscopic examination, direct microscopic examination, stool concentration methods, and immunochromatographic rapid diagnostic tests were systematically applied. Demographic data, clinical symptoms, and stool characteristics (consistency, appearance, etc.) were systematically recorded for each patient.

Laboratory Analysis

Macroscopic Examination

Stool samples were first examined macroscopically. During this evaluation, the color (yellow, green, brown, black), consistency (watery, soft, semi-solid, solid), and other macroscopic features were recorded.

Direct Microscopic Examination

Stool samples (2-3 mg) were examined by wet-mount preparation with saline and Lugol's iodine.

Zinc Sulfate Flotation Method

A stool sample (1 g) was suspended in 10 mL of distilled water, filtered, and centrifuged. After the supernatant was discarded, zinc sulfate solution was added, and the mixture was vortexed and recentrifuged. A coverslip was placed on the meniscus for 10 minutes and was then examined microscopically.

Formalin-Ethyl Acetate Sedimentation Method

Stool samples (1 g) were fixed in 10% formalin for 10 minutes, filtered, and centrifuged. After adding 7 mL of formalin and 3 mL of ethyl acetate, the mixture was shaken vigorously and centrifuged. The sediment layer from the four-layer separation was examined by wet-mount preparation.

Immunochromatographic Rapid Diagnostic Test

A commercial immunochromatographic test (ICT) (Crypto/Giardia/Entamoeba Combo Test, Monlab, Spain) was used to detect *Cryptosporidium parvum* (*C. parvum*), *G. duodenalis,* and *E. histolytica*-specific antigens according to the manufacturer's specifications. Species-level identification of *E. histolytica* was based on immunochromatographic antigen detection, which specifically detects *E. histolytica* and does not cross-react with other Entamoeba species test sensitivities were 82.4% for *E. histolytica*, *92.4%* for *G. duodenalis,* and 80.0% for *C. parvum*.

Statistical Analysis

Statistical analysis was performed using IBM SPSS Statistics 27.0 (IBM, USA). Descriptive statistics were presented as mean ± standard deviation for continuous variables and number (percentage) for categorical variables. Relationships between categorical variables were evaluated using chi-square or Fisher's exact tests, with $p<0.05$ considered statistically significant.

Results

This study included stool samples from 300 pediatric patients aged 0-18 years, of whom 160 were males (53.3%) and 140 were females (46.7%). The mean age of the study population was 6.08 years. Age distribution analysis revealed that 37% (n=111) of participants were in the 0-2 years age group, 26% (n=78) in the 6-10 years age group, 15% (n=45) in the 3-5 years age group, 11.3% (n=34) in the 15-18 years age group, and 10.7% (n=32) in the 11-14 years age group.

The most common gastrointestinal symptoms were diarrhea (36.7%, n=110), abdominal pain (30.3%, n=91), fever (25.7%, n=77), and colitis (25.3%, n=76). All stool samples were subjected to macroscopic examination, direct smear, zinc sulfate flotation, formol-ethyl acetate sedimentation, and ICT. At least one parasite species was detected in 26% (78/300) of samples.

Parasite prevalence was 27.8% (39/140) in females and 24.3% (39/160) in males, with no significant association between prevalence and gender ($p>0.05$). When the distribution of parasite-positive cases across age groups was examined as proportions of the total cohort (n=300), the largest proportion of positive cases was observed in the 0-2-year age group (27/300, 9%), followed by the 6-10-year group (22/300, 7.3%), the 3-5-year group (11/300, 3.7%), the 11-14-year group (9/300, 3%), and the 15-18-year group (9/300, 3%). These values represent the distribution of positive cases in the total cohort, and no significant association was found between age groups and parasite positivity ($p>0.05$).

Macroscopic evaluation of parasite-positive samples showed the following: watery-mucous (50%, 39/78), watery (28.2%, 22/78), mucous (11.5%, 9/78), bloody (6.4%, 5/78), mucous-bloody (2.6%, 2/78), and normal consistency (1.3%, 1/78). Watery and mucoid consistencies showed a significant association with parasite presence ($p<0.05$). Microscopic examination revealed parasite positivity in 43% (31/72) of samples with leukocytes and in 36.3% (4/11) of samples with erythrocytes; however, neither association was statistically significant ($p>0.05$).

The detected parasite species were *E. histolytica* (22.7%, 68/300), *Blastocystis hominis* (*B. hominis*) (6%, 18/300), *G. duodenalis* (4%, 12/300), *C. parvum* (2.3%, 7/300), *and Enterobius vermicularis* (*E. vermicularis*) (0.7%, 2/300). Single parasites were found in 18.3% (55/300), two species in 5.7% (17/300), and three species in 2% (6/300) of samples. The most common co-infection was *E. histolytica and B. hominis* (4.3%, 13/300). Detailed frequency distributions are presented in Table 1.

When the distribution of detected parasite species across age groups was examined as proportions of the total cohort, *E. histolytica* accounted for the largest share of positive cases in both the 0-2-year and 6-10-year age groups (21/300; 7% of the total cohort in each group) (Table 2). Statistical analysis indicated that there was no significant association between age-stratified groups and the distribution of identified parasite species ($p>0.05$).

Comparison of diagnostic methods revealed positivity rates of direct microscopy, 22.7% (68/300); zinc sulfate flotation, 16% (48/300); formol ethyl acetate sedimentation, 18.3% (55/300); and ICT, 23.3% (70/300). No parasites were detected macroscopically. By species, detection rates were highest for *E. histolytica* using both ICT and direct microscopy; for *C. parvum* and *G. duodenalis* using ICT; and for *B. hominis* and *E. vermicularis* using direct microscopy. Detailed distributions are presented in Table 3.

The most common symptoms in pediatric patients were diarrhea, abdominal pain, fever, and colitis. *E. histolytica* caused the highest diarrhea rate (16%), followed by *B. hominis* (4%) and *G. duodenalis* (3%). *C. parvum* was observed more frequently in patients with abdominal pain and diarrhea, whereas *E. vermicularis* was observed more frequently in febrile patients. No significant association was found between symptoms and parasite species ($p>0.05$). Distribution details are presented in Table 4.

When the monthly and seasonal distributions of parasite-positive cases were examined as proportions of the total cohort (n=300), September accounted for the largest share (21/300, 7%). By season, the distribution of positive cases within the total cohort was as follows: autumn 33/300 (11%), summer 22/300 (7.4%), spring 14/300 (4.7%), and winter 9/300 (3%) (Table 5). As these values represent proportions of the total cohort rather than within-month or within-season positivity rates, they reflect the temporal distribution of positive cases instead of monthly or seasonal prevalence. No significant differences were found in the monthly or seasonal distribution ($p>0.05$).

Discussion

In this study, the prevalence of intestinal parasitic infection was 26% among pediatric patients with gastrointestinal symptoms. Similar studies from Türkiye show substantial regional variation, with higher rates reported in Kocaeli and Iğdır (39% and 35%) and lower rates in Denizli and Konya (10.2% and 6.4%) (24-27). These differences likely reflect regional climate, socioeconomic conditions, hygiene levels, and diagnostic methods. International data also demonstrate heterogeneity: high prevalence in Peru and Malaysia (42% and 40.4%) indicates inadequate sanitation, whereas lower rates such as 20.1% in Chile reflect

Table 1. Distribution of the frequencies and associations of the identified parasites

Parasites	n	%
E. histolytica	68	22.7
C. parvum	7	2.3
G. duodenalis	12	4
B. hominis	18	6
E. vermicularis	2	0.7
E. histolytica + *G. duodenalis*	2	0.7
E. histolytica + *B. hominis*	13	4.3
G. duodenalis + *B. hominis*	1	0.3
E. histolytica + *Enterobius vermicularis*	1	0.3
E. histolytica + *C. parvum* + *G. duodenalis*	5	1.6
E. histolytica + *C. parvum* + *B. hominis*	1	0.3

E. histolytica: Entamoeba histolytica, G. duodenalis: Giardia duodenalis, B. hominis: Blastocystis hominis, C. parvum: Cryptosporidium parvum, E. vermicularis: Enterobius vermicularis

stronger health systems (28-30). The 30.4% prevalence reported in China is comparable to our findings (31). The epidemiological distribution of intestinal parasite infections in the pediatric age group is determined by the interaction of several factors, including environmental conditions, hygiene, and socioeconomic status. While some studies report higher positivity rates in older children, several investigations have identified peak prevalence among children aged 0-5 years (32-37). In our study, we detected that the 0-2 age group accounted for the largest share of parasite-positive cases within the total cohort. In early childhood, increased oral exploratory behaviour, immature hand hygiene, and immature immune function likely contribute to this susceptibility.

A comprehensive meta-analysis conducted in Iran found a 38% prevalence of intestinal parasites, with *E. vermicularis* (16.5%) and *G. duodenalis* (15.1%) identified as the predominant pathogens (38). In a study of 2000 pediatric patients in Bangladesh, *Entamoeba dispar* (*E. dispar*) (6.5%) and *E. histolytica* (4.2%) were found to be the main pathogens (38,39). In epidemiological studies conducted in Türkiye, regional differences were found. *G. duodenalis* was reported as the predominant parasite in Denizli (26), Van (40) and Manisa (37) provinces, while *B. hominis* was found in Iğdır (25). In another study conducted in Van, *G. duodenalis* and *B. hominis* were reported as co-dominant pathogens (36). In our study, the highest prevalence was found for *E. histolytica* (22.7%), followed by *B. hominis* (6%), *G. duodenalis* (4%), *and E. vermicularis* (0.7%). The lower prevalence of *B. hominis* compared with the rates reported in some studies in the literature (40-42) may be due to the ongoing debate about the pathogenicity of this organism and the lack of standardisation of diagnostic criteria across laboratories.

In infectious gastroenteritis caused by intestinal parasites, macroscopic examination of faecal samples is an important part of the diagnostic algorithm. In the study conducted by Çiçek and Yılmaz (40) on a pediatric cohort with gastrointestinal symptoms, it was reported that stool samples with parasite positivity were predominantly watery or excessively watery in consistency, while a mucoid character was observed less frequently. Similarly, the study by Doğan et al. (43), which investigated methodological differences in the laboratory diagnosis of intestinal parasites, emphasised that the presence of mucus in the stool has a predictive value for parasitic infection. In our study, 39 (50%) of the 78 faecal samples that were positive for parasites had a watery, mucoid

Table 2. Distribution of parasite-positive cases across age groups

Age (year)	*E. histolytica*		*C. parvum*		*E. vermicularis*		*B. hominis*		*G. duodenalis*	
	n	%	n	%	n	%	n	%	n	%
0-2	21	7	2	0.7	1	0.3	8	2.7	5	1.7
3-5	10	3.3	1	0.3	0	0	0	0	2	0.7
6-10	21	7	3	1	1	0.3	3	1	3	1
11-14	9	3	0	0	0	0	2	0.7	0	0
15-18	7	2.3	1	0.3	0	0	5	1.7	2	0.7
Total	68	22.7	7	2.3	2	0.7	18	6	12	4

All percentages reflect proportions of the total study cohort (n=300). *E. histolytica: Entamoeba histolytica, G. duodenalis: Giardia duodenalis, B. hominis: Blastocystis hominis, C. parvum: Cryptosporidium parvum, E. vermicularis: Enterobius vermicularis*

Table 3. The distribution of parasite species according to diagnostic methods

Parasites	Microscopy				Flotation				Sedimentation				ICT method			
	+	%	-	%	+	%	-	%	+	%	-	%	+	%	-	%
E. histolytica	63	21	5	1.7	45	15	23	7.7	50	16.7	18	6	63	21	5	1.7
C. parvum	6	2	1	0.3	6	2	1	0.3	6	2	1	0.3	7	2.3	0	0
E. vermicularis	2	0.7	0	0	0	0	2	0.7	1	0.3	1	0.3	0	0	2	0.7
B. hominis	17	5.7	1	0.3	11	3.7	7	2.3	12	4	6	2	0	0	18	6
G. duodenalis	9	3	3	1	9	3	3	1	10	3.3	2	0.7	11	3.7	1	0.3

ICT: Immunochromatographic rapid test, (+): Positive, (-): Negative, *E. histolytica: Entamoeba histolytica, G. duodenalis: Giardia duodenalis, B. hominis: Blastocystis hominis, C. parvum: Cryptosporidium parvum, E. vermicularis: Enterobius vermicularis*

Table 4. The distribution of parasite species according to clinical symptoms

Symptoms	*E. histolytica*		*B. hominis*		*G. duodenalis*		*C. parvum*		*E. vermicularis*	
	n	%	n	%	n	%	n	%	n	%
Nausea-vomiting	30	10	7	2.3	5	1.7	2	0.7	1	0.3
Abdominal pain	30	10	9	3	9	3	5	1.7	0	0
Diarrhea	48	16	12	4	9	3	5	1.7	1	0.3
Colitis	28	9.3	7	2.3	6	2	3	1	0	0
Fever	21	7	5	1.7	4	1.3	4	1.3	2	0.7

Table 5. Distribution of detected parasite species by months and seasons*

		E. histolytica		*C. parvum*		*G.duodenalis*		*B. hominis*		*E. vermicularis*		Total	
		n	%	n	%	n	%	n	%	n	%	n	%
Spring	March	3	1	1	0.3	2	0.7	0	0	0	0	6	2
	April	0	0	0	0	0	0	0	0	0	0	0	0
	May	7	2.3	1	0.3	0	0	5	1.7	1	0.3	8	2.7
Summer	June	6	2	2	0.7	3	1	2	0.7	0	0	6	2
	July	5	1.7	0	0	1	0.3	2	0.7	0	0	5	1.7
	August	11	3.7	0	0	0	0	1	0.3	1	0.3	11	3.7
Autumn	September	19	6.3	2	0.7	3	1	2	0.7	0	0	21	7
	October	5	1.7	0	0	0	0	2	0.7	0	0	6	2
	November	3	1	0	0	2	0.7	2	0.7	0	0	6	2
Winter	December	3	1	0	0	0	0	1	0.3	0	0	3	1
	January	4	1.3	1	0.3	1	0.3	1	0.3	0	0	4	1
	February	2	0.7	0	0	0	0	0	0	0	0	2	0.7

*All percentages reflect proportions of the total study cohort (n=300)

consistency, and this finding was statistically significant ($p<0.05$). This result indicates a significant correlation between the macroscopic characteristics of faecal samples and the presence of parasitic infection. Careful documentation of faecal consistency, the presence of mucus, and other macroscopic parameters can provide additional information for parasitological examination and thus contribute to an increased detection rate.

Laboratory diagnostic methods for intestinal parasites show considerable heterogeneity. Yula et al. (33) reported commercial test kits had the highest detection rate, Çiçek and Yılmaz (40) found trichrome staining superior, while Karakuş et al. (25) demonstrated modified acid-fast staining performed best. In our study, ICT achieved the highest detection rate, followed by native-Lugol, sedimentation, and flotation techniques.

In parasite-specific diagnostic evaluation, *E. histolytica*, the predominant pathogen, was detected at equal rates (21%) by direct microscopy and ICT. ICT was more efficient at detecting *G. duodenalis* (3.7%) and *C. parvum* (2.3%), whereas native Lugol's showed higher detection rates for *B. hominis (5.7%) and E. vermicularis* (0.7%). Çiçek and Yılmaz (40) found *Cryptosporidium* spp. (predominant pathogen) was best detected by trichrome staining. These results emphasise that the different diagnostic approaches have detection-rate profiles specific to parasite species, and that a multimodal approach is required for optimal diagnosis.

Literature reports parasite positivity most commonly in patients with abdominal pain (78%) and nausea (51.7%) (24,25), while other studies note diarrhea, fever, vomiting, growth retardation, weakness, and loss of appetite (40). In our study, the main symptoms were diarrhea, abdominal pain, fever, gastroenteritis, colitis, and nausea and vomiting. Parasite positivity was highest in diarrhea cases, followed by nausea and vomiting; however, no significant correlation was found between symptoms and parasite positivity or parasite species ($p>0.05$). Symptoms of parasitic infections are typically non-specific, requiring comprehensive medical evaluation and laboratory testing.

The seasonal distribution of parasitic infections varies depending on precipitation, climate, and geography. The literature reports that parasites of the gastrointestinal tract are most frequently detected in the summer and autumn months (35,44). In India, it has been reported that increased rainfall, flooding and contamination, especially in the summer months, can increase the parasite detection rate up to 97.4% (45). In our study, positive cases peaked in autumn, particularly in September, but no statistically significant correlation was found between the distributions by month and by season ($p>0.05$).

Study Limitations

This study has several limitations. It was conducted at a single center, which may limit the generalizability of the results. Although multiple diagnostic methods were used, microscopy remains operator-dependent, which may affect detection accuracy. The study did not include molecular tests, which could have improved the detection rate for some parasites. In particular, although the ICT used in this study specifically detects *E. histolytica* antigens, the absence of molecular confirmation represents a limitation, as the possibility of misidentification with *E. dispar* cannot be entirely excluded. Nonetheless, these limitations do not undermine the overall contribution of the study, which provides valuable data on prevalence patterns and the comparative performance of commonly used diagnostic methods in pediatric parasitic infections.

Conclusion

In this study, ICTs showed a higher detection rate for gastrointestinal parasites than conventional microscopy, suggesting that ICT may be a useful complement to microscopic methods in pediatric settings. The significant association between stool consistency, particularly watery or

mucoid stools, and parasitic infection serves as an important clinical screening indicator for pediatricians in emergency and outpatient settings. These findings emphasize the value of integrating rapid diagnostic tools with clinical evaluation to improve the accuracy, efficiency, and patient-centeredness of management for pediatric parasitic infections.

Ethics

Ethics Committee Approval: The study was approved by the Karabük University Non-Interventional Ethics Committee (decision number: 2022/787, date: 20.01.2022).

Informed Consent: Informed consent was not required, as the study used only anonymized routine clinical stool samples and associated data.

Footnotes

Authorship Contributions: Surgical and Medical Practices - M.A.İ., E.D.; Concept - M.A.İ., M.Y.Ç.; Design - M.Y.Ç.; Data Collection or Processing - M.A.İ., M.Y.Ç., E.D.; Analysis or Interpretation - M.A.İ., M.Y.Ç., E.D.; Literature Search - M.A.İ., M.Y.Ç., E.D.; Writing - M.A.İ., M.Y.Ç.

Conflict of Interest: No conflict of interest was declared by the authors.

Financial Disclosure: The research was supported by Karabük University Scientific Research Projects Coordination Unit (project number: KBUBAP-YL-063).

References

1. World Health Organization. Soil-transmitted helminth infections: fact sheet. Geneva: World Health Organization; 2024. Available from: https://www.who.int/news-room/fact-sheets/detail/soil-transmitted-helminth-infections
2. World Health Organization. Global Health Observatory data repository: soil-transmitted helminth infections. Geneva: World Health Organization; 2024. Available from: https://www.who.int/data/gho
3. UNICEF. Child mortality report 2024: levels and trends in child mortality. New York: UNICEF; 2024.
4. Black RE, Victora CG, Walker SP, Bhutta ZA, Christian P, de Onis M, et al. Maternal and child undernutrition and overweight in low-income and middle-income countries. Lancet. 2013; 382: 427-51. Erratum in: Lancet. 2013; 382: 96.
5. UNICEF. Diarrhoeal disease: fact sheet. New York: UNICEF; 2024.
6. Fauziah N, Aviani JK, Agrianfanny YN, Fatimah SN. Intestinal parasitic infection and nutritional status in children under five years old: a systematic review. Trop Med Infect Dis. 2022; 7: 371.
7. Fantinatti M, Cascais-Figueredo T, Austriaco-Teixeira P, Carvalho-Costa FA, Da-Cruz AM. Giardia lamblia-infected preschoolers present growth delays independent of the assemblage A, B or E. Mem Inst Oswaldo Cruz. 2023; 118: e230043.
8. Kunwar R, Acharya L, Karki S. Decreasing prevalence of intestinal parasitic infections among school-aged children in Nepal: a systematic review and meta-analysis. Trans R Soc Trop Med Hyg. 2016; 110: 324-32.
9. Gizaw Z, Addisu A, Dagne H. Effects of water, sanitation and hygiene (WASH) education on childhood intestinal parasitic infections in rural Dembiya, northwest Ethiopia: an uncontrolled before-and-after intervention study. Environ Health Prev Med. 2019; 24: 16.
10. Hernández PC, Morales L, Chaparro-Olaya J, Sarmiento D, Jaramillo JF, Ordoñez GA, et al. Intestinal parasitic infections and associated factors in children of three rural schools in Colombia. A cross-sectional study. PLoS One. 2019; 14: e0218681.
11. Payne DC, Vinjé J, Szilagyi PG, Edwards KM, Staat MA, Weinberg GA, et al. Norovirus and medically attended gastroenteritis in U.S. children. N Engl J Med. 2013; 368: 1121-30.
12. Platts-Mills JA, Babji S, Bodhidatta L, Gratz J, Haque R, Havt A, et al. Pathogen-specific burdens of community diarrhoea in developing countries: a multisite birth cohort study (MAL-ED). Lancet Glob Health. 2015; 3: e564-75.
13. Sánchez A, Munoz M, Gómez N, Tabares J, Segura L, Salazar Á, et al. Molecular epidemiology of *Giardia, Blastocystis* and *Cryptosporidium* among Indigenous Children from the Colombian Amazon Basin. Front Microbiol. 2017; 8: 248.
14. Garcia LS, Arrowood M, Kokoskin E, Paltridge GP, Pillai DR, Procop GW, et al. Practical guidance for clinical microbiology laboratories: laboratory diagnosis of parasites from the gastrointestinal tract. Clin Microbiol Rev. 2017; 31: e00025-17.
15. Girma A, Genet A. Prevalence and factors associated with intestinal parasitic infections among preschool-aged children in Ethiopia: a systematic review and meta-analysis. Parasite Epidemiol Control. 2024; 26: e00368.
16. Štrkolcová G, Fiľakovská Bobáková D, Kaduková M, Schreiberová A, Klein D, Halán M, et al. Intestinal parasitic infections in children from marginalised Roma communities: prevalence and risk factors. BMC Infect Dis. 2024; 24: 596.
17. Taghipour A, Javanmard E, Mohammad Rahimi H, Abdoli A, Matin S, Haghbin M, et al. Prevalence of intestinal parasitic infections in patients with diabetes: a systematic review and meta-analysis. Int Health. 2024; 16: 23-34.
18. RITCHIE LS. An ether sedimentation technique for routine stool examinations. Bull U S Army Med Dep. 1948; 8: 326.
19. Binnicker MJ. Multiplex molecular panels for diagnosis of gastrointestinal infection: performance, result interpretation, and cost-effectiveness. J Clin Microbiol. 2015; 53: 3723-8.
20. Weitzel T, Dittrich S, Möhl I, Adusu E, Jelinek T. Evaluation of seven commercial antigen detection tests for Giardia and Cryptosporidium in stool samples. Clin Microbiol Infect. 2006; 12: 656-9.
21. Akinbo FO, Okaka CE, Omoregie R. Prevalence of intestinal parasitic infections among HIV patients in Benin City, Nigeria. Libyan J Med. 2010; 5.
22. UNICEF. Diarrhoea as a cause of death [Internet]. New York: UNICEF; 2018 [cited 2025 Jul 29]. Available from: https://data.unicef.org/topic/child-health/diarrhoeal-disease
23. World Health Organization. Diarrhoeal disease: key facts [Internet]. Geneva: World Health Organization; 2017 [cited 2025 Jul 29]. Available from: http://www.who.int/news-room/fact-sheets/detail/diarrhoeal-disease
24. Yapici F, Tamer SG, Arisoy ES. Distribution of intestinal parasites in children and associated factors. Turkiye Parazitol Derg. 2008; 32: 346-50.
25. Karakuş İ, Taş Cengiz Z, Ekici A. Evaluation of ıntestinal parasites and some clinical symptoms in children with diarrhea. Turkiye Parazitol Derg. 2022; 46: 39-44. Erratum in: Turkiye Parazitol Derg. 2022; 46: 166.
26. Işık Balcı Y, Türk M, Polat Y, Erbil N. Distribution of intestinal parasites in children in Denizli. Turkiye Parazitol Derg. 2009; 33: 298-300.
27. Maçin S, Musayeva L. Investigation of the presence of Blastocystis spp. in pediatric patients admitted to our hospital with a diagnosis of gastroenteritis. Pediatr Pract Res. 2019; 7: 497-500.
28. Gilman RH, Marquis GS, Miranda E. Prevalence and symptoms of Enterobius vermicularis infections in a Peruvian shanty town. Trans R Soc Trop Med Hyg. 1991; 85: 761-4.
29. Norhayati M, Hayati MI, Oothuman P, Azizi O, Fatmah MS, Ismail G, et al. Enterobius vermicularis infection among children aged 1-8 years in a rural

area in Malaysia. Southeast Asian J Trop Med Public Health. 1994; 25: 494-7.

30. Mejías G. Infecciones enteroparasitarias en escolares rurales del Archipiélago de Chiloé, X Región, Chile [Intestinal parasite infections in rural students of Chiloé archipelago, X Region, Chile]. Bol Chil Parasitol. 1993; 48: 28-9.
31. Chang JH, Huang WH, Chen ER, Hu SC. [Survey of Enterobius vermicularis infection among school children in Tainan City]. Gaoxiong Yi Xue Ke Xue Za Zhi. 1990; 6: 587-93.
32. Aydın E, Altın N, Render DP. Evaluation of the effects of acute gastroenteritis agents on laboratory parameters in pediatric patients. Flora Infect Dis Clin Microbiol. 2022; 27: 125-34.
33. Yula E, Deveci Ö, İnci M, Tekin A. Intestinal parasites and report of etiological analysis in a state hospital. J Clin Exp Invest. 2011; 2: 74-9.
34. Şenol FF, Öner P, Aytaç Ö, Babacan A, Aşçı Toraman Z. The role of parasitic and viral agents in gastrointestinal infections. Turk Mikrobiyol Cemiy Derg. 2022; 52: 281-90.
35. Alver O, Töre O. Prevalence and distribution of intestinal parasite cases in Uludağ University Faculty of Medicine. Turkiye Parazitol Derg. 2006; 30: 296-301.
36. Jarabo MT, Garcia-Moran NP, Garcia-Moran JI. Prevalence of intestinal parasites in a student population. Enferm Infecc Microbiol Clin. 1995; 13: 464-8.
37. Demirel MM, İnceboz T, Yegane S. Investigation of intestinal parasites in patients admitted to Manisa Moris Şinasi Children's Hospital. Turkiye Parazitol Derg. 2002; 26: 282-5.
38. Daryani A, Hosseini-Teshnizi S, Hosseini SA, Ahmadpour E, Sarvi S, Amouei A, et al. Intestinal parasitic infections in Iranian preschool and school children: a systematic review and meta-analysis. Acta Trop. 2017; 169: 69-83.
39. Haque R, Faruque AS, Hahn P, Lyerly DM, Petri WA Jr. Entamoeba histolytica and Entamoeba dispar infection in children in Bangladesh. J Infect Dis. 1997; 175: 734-6.
40. Çiçek M, Yılmaz H. Prevalence of Cryptosporidium spp. and other intestinal parasites in children with diarrhea. Dicle Med J. 2011; 38: 70-5.
41. Birdal Akış F, Beyhan YE. Distribution of intestinal parasites in patients in the pediatric intensive care unit. Turkiye Parazitol Derg. 2018; 42: 113-7.
42. Reh L, Muadica AS, Köster PC, Balasegaram S, Verlander NQ, Chércoles ER, et al. Substantial prevalence of enteroparasites Cryptosporidium spp., Giardia duodenalis and Blastocystis sp. in asymptomatic schoolchildren in Madrid, Spain, November 2017 to June 2018. Euro Surveill. 2019; 24: 1900241.
43. Doğan N, Öz Y, Koçman NÜ, Nursal AF. Comparison of individual differences in direct microscopic examination in the diagnosis of intestinal parasites. Turkiye Parazitol Derg. 2012; 36: 211-4.
44. Demir A, Gümüş H. Seasonal variation of acute gastroenteritis agents in children. Van Sağlık Bil Derg. 2023; 1: 100-4.
45. Kang G, Mathew MS, Rajan DP, Daniel JD, Mathan MM, Mathan VI, et al. Prevalence of intestinal parasites in rural Southern Indians. Trop Med Int Health. 1998; 3: 70-5.

İstanbul Med J 2026; 27(3): 219-24
DOI: 10.4274/imj.galenos.2026.27096

Investigation of 25-Hydroxyvitamin D Levels in Patients with Cirrhosis: Relationship with Liver Disease Severity, Etiology, and Complications

Aykut Özmen[1], Ali Tüzün İnce[2]

[1]University of Health Sciences Türkiye, Başakşehir Çam and Sakura City Hospital, Clinic of Medical Oncology, İstanbul, Türkiye
[2]Bezmialem Vakıf University Faculty of Medicine, Department of Gastroenterology, İstanbul, Türkiye

ABSTRACT

Introduction: Vitamin D deficiency is frequently observed in people with cirrhosis, underscoring the liver's essential role in metabolizing vitamin D. This research sought to assess 25-hydroxyvitamin D [25(OH)D] levels in individuals with cirrhosis and to evaluate the association between these levels and disease extent, etiologies, and cirrhosis-related complications.

Methods: This study included 118 adult patients with cirrhosis who were evaluated at the Gastroenterology Department of Bezmialem Vakıf University. Participants ranged in age from 18 to 90 years. The study excluded individuals who were pregnant; had taken vitamin D supplements in the past six months; or had non- hepatocellular carcinoma malignancies, hematologic cancers, metabolic bone diseases, chronic kidney disease, parathyroid disorders, had undergone thyroidectomy, or other chronic conditions affecting vitamin D metabolism. The severity of liver disease was assessed using the Child-Turcotte-Pugh (Child-Pugh) classification and the Model for End-Stage Liver Disease (MELD) score. Data were examined with SPSS version 20.0.

Results: The average age of the patients was 58.7±11.8 years, with 56.8% being male. Cirrhosis was attributed to cryptogenic causes in 53.4% of cases, to hepatitis B virus in 28.80%, to hepatitis C virus in 8.50%, to alcohol in 7.60%, and to drugs in 1.70%. A deficiency in vitamin D was detected in 93.2% of the patients; 5.10% had insufficient levels, and only 1.70% had normal levels. Serum 25(OH)D levels demonstrated a positive correlation with albumin (p=0.003), total cholesterol (p=0.035), and triglycerides (p=0.006), and were negatively correlated with prothrombin time (p=0.003), international normalized ratio (p=0.011), Child-Pugh score (p=0.008), and MELD score (p=0.045). The levels of vitamin D did not significantly differ based on the cause of cirrhosis or the presence of cirrhosis-related complications.

Conclusion: Vitamin D insufficiency is a frequent problem among individuals with cirrhosis, regardless of its underlying cause. Reduced vitamin D levels are related to increasingly severe liver disease and to reduced liver function, rather than to the cause or complications of cirrhosis.

Keywords: 25-hydroxyvitamin D, cirrhosis, Child-Pugh score, MELD, liver disease severity

Introduction

Cirrhosis marked by extensive liver scarring, the development of regenerative nodules, and a progressive deterioration in liver function (1-3). It remains a key contributor to global morbidity and mortality and is associated with numerous complications (4,5).

Vitamin D, serves a vital role not solely in preserving calcium balance and bone health but also in modulating the immune system, cell growth, differentiation, and fibrogenesis (6,7). The liver is crucial for vitamin D metabolism, as it performs 25-hydroxylation and produces vitamin D-binding proteins. Therefore, it is biologically plausible that individuals with persistent liver disease may exhibit from vitamin D deficiency (6,8). Vitamin D deficiency is also extremely common among those with persistent liver disease and cirrhosis, with prevalence rates ranging from 64% to 92% (9-11).

Several factors have been identified as potential contributors to the low vitamin D levels observed in individuals with cirrhosis, including limited sunlight exposure, insufficient dietary intake, absorption issues, impaired liver hydroxylation, reduced production of vitamin D-binding proteins, and increased vitamin breakdown (8,12). Furthermore, vitamin D insufficiency may contribute to the progression of hepatic fibrosis, a diminished answer to antiviral therapy in chronic hepatitis C, an increased susceptibility to infections, and a higher risk of mortality

Address for Correspondence: Aykut Özmen, MD, University of Health Sciences Türkiye, Başakşehir Çam and Sakura City Hospital, Clinic of Medical Oncology, İstanbul, Türkiye
E-mail: draykutozmen@hotmail.com **ORCID ID:** orcid.org/0000-0003-4312-724X
Cite this article as: Özmen A, İnce AT. Investigation of 25-hydroxyvitamin D levels in patients with cirrhosis: relationship with liver disease severity, etiology, and complications. İstanbul Med J. 2026; 27(3): 219-24

Received: 21.04.2026
Accepted: 30.06.2026
Publication Date: 03.08.2026

(13-15). However, it remains unclear whether vitamin D insufficiency primarily reflects causation of cirrhosis, liver dysfunction, or complications associated with cirrhosis.

Methods

The study, which was retrospective and descriptive, examined 118 adult patients with cirrhosis evaluated at the Gastroenterology Department of Bezmialem Vakıf University between 2012 and 2016. The participants, aged 18-90 years, had chronic liver disease, including cirrhosis, and met the criteria for inclusion in the study.

Individuals between the ages of 18 and 90 with chronic liver disease or cirrhosis were considered eligible. Exclusion criteria were: pregnancy; use of vitamin supplements within the previous 6 months; non-hepatocellular carcinoma (HCC) solid malignancy; hematologic malignancy; history of metabolic bone disease; chronic kidney disease; hyperparathyroidism; hypoparathyroidism; prior thyroidectomy; and any other chronic disease that could affect vitamin D levels.

Ethics

Authorization for this research was received from the Ethics Committee of Bezmialem Vakıf University (approval number: 20/274, date: 07.11.2017). The study's retrospective nature allowed for the waiver of informed consent.

Laboratory Analysis

Venous blood samples were collected and centrifuged at 2000 × g for 10 minutes to obtain plasma. The concentration of 25-hydroxyvitamin D [25(OH)D] 3 in the blood was measured using a validated kit on a Shimadzu LC-20AT instrument. According to the Endocrine Society, vitamin D levels are classified as: deficiency,<20 ng/mL; insufficiency, 20-30 ng/mL; and normal, >30 ng/mL (16).

Clinical and Laboratory Variables

Data on patient demographics, the causes of cirrhosis, and associated complications were gathered from hospital records. The laboratory tests included measurements of glucose, white blood cell count (WBC), high-density lipoprotein (HDL), platelet count (PLT), hemoglobin (HGB), creatinine, lactate dehydrogenase (LDH), albumin, C-reactive protein (CRP), low-density lipoprotein (LDL), triglycerides, erythrocyte sedimentation rate (ESR), total cholesterol, HbA1c, ferritin, aspartate aminotransferase (AST), alanine aminotransferase (ALT), alkaline phosphatase (ALP), gamma-glutamyl transferase (GGT), prothrombin time (PT), and international normalized ratio (INR) (Table 1).

Cirrhosis-related complications included decompensation, ascites, spontaneous ascitic infection, hepatic encephalopathy, variceal bleeding, hepatorenal syndrome, portal vein thrombosis (PVT), hepatopulmonary syndrome, HCC, portal hypertension, and esophageal varices.

Assessment of Liver Disease Severity

The extent of the disease was measured using the Model for End-Stage Liver Disease (MELD) and Child-Turcotte-Pugh (Child-Pugh) scoring systems. The Child-Pugh classification was noted as stage A, B, or C (17).

Table 1. Baseline hematological and biochemical characteristics of the patients

Parameter	Mean ± SD	Median	Minimum	Maximum
Leukocyte (×10³/µL)	4.5±1.7	4.3	1.2	9.3
Hemoglobin (g/dL)	11.5±2.2	11.7	6.8	16.7
Platelet (×10³/µL)	103±59	88	27	352
Glucose (mg/dL)	118±42	106	55	325
Creatinine (mg/dL)	0.8±0.6	0.7	0.4	7.4
AST (U/L)	59.8±48.7	41.5	3	298
ALT (U/L)	47.9±48.0	32	6	266
ALP (U/L)	119.9±55.9	106	39	347
GGT (U/L)	88±133	54	8	1257
LDH (U/L)	215±65	202	62	524
25 (OH)D (ng/mL)	10.9±9.4	9.6	4	89
Total bilirubin (mg/dL)	1.4±1.6	1.0	0.2	13.0
Albumin (g/dL)	3.5±0.6	3.6	1.3	4.8
Prothrombin time (s)	17.4±3.8	16.5	11.4	32.0
INR	1.3±0.3	1.3	0.9	2.7
Total cholesterol (mg/dL)	160±56	156	53	384
Triglycerides (mg/dL)	119±77	95	33	456
LDL cholesterol (mg/dL)	98±43	97	13	251
HDL cholesterol (mg/dL)	40.9±18.7	38.5	3	87
C-reactive protein (mg/L)	0.7±1.8	0.3	0	19
HbA1c (%)	5.9±1.3	5.4	4.3	10.6
Erythrocyte sedimentation rate (mm/h)	22.9±16.1	18	3	88
Ferritin (ng/mL)	119±224	37.5	4	1649

SD: Standard deviation, AST: Aspartate aminotransferase, ALT: Alanine aminotransferase, ALP: Alkaline phosphatase, GGT: Gamma-glutamyl transferase, LDH: Lactate dehydrogenase, INR: International normalized ratio, ESR: Erythrocyte sedimentation rate, HbA1c: Hemoglobin A1c, 25(OH)D: 25-hydroxyvitamin D

Statistical Analysis

We used SPSS version 20.0 to analyze the data. We showed continuous data mean ± standard deviation or median (range), based on how they were spread out. We presented categorical data as numbers and percentages. We assessed the data distribution visually and using statistical tests. To compare two groups, we used the independent samples t-test or the Mann-Whitney U test, depending on which was appropriate. For comparisons involving three or more groups, we used one-way analysis of variance or the Kruskal-Wallis test. We used Pearson or Spearman correlation tests. A p value less than 0.05 was deemed statistically significant.

Results

Baseline Characteristics

Overall, 118 patients with cirrhosis were included in the analysis. The average age was 58.7±11.8 years (median, 59 years; range, 25-85 years). Of the patients, 67 (56.8%) were male and 51 (43.2%) were female.

The average MELD score was 9.5±2.7 and the average Child-Pugh score was 7.2±2.4. According to Child-Pugh stage, 62 patients (52.5%) were stage A, 31 (26.3%) stage B, and 25 (21.2%) stage C (Table 2).

The etiologies of cirrhosis were cryptogenic in 63 patients (53.4%), hepatitis B virus in 34 (28.8%), hepatitis C virus in 10 (8.5%), alcohol-related in 9 (7.6%), and drug-related in 2 (1.7%).

Regarding complications, portal hypertension was present in 93.2% of patients; esophageal varices in 86.4% of patients; decompensated cirrhosis in 51.7% of patients; ascites in 39.8% of patients; variceal bleeding in 31.4% of patients; hepatic encephalopathy in 25.4% of patients; PVT in 22.0% of patients; hepatorenal syndrome in 18.6% of patients; ascitic infection in 11.0% of patients; HCC in 11.0% of patients; and hepatopulmonary syndrome in 1.7% of patients (Table 3).

The mean serum vitamin D level was 10.9±9.4 ng/mL. Vitamin D deficiency was detected in 110 patients (93.2%), insufficiency in 6 patients (5.1%), and normal vitamin D levels in only 2 patients (1.7%).

When patients were stratified by Child-Pugh stage, vitamin D insufficiency was present in 91.9% of stage A patients, 96.8% of stage B patients, and 92.0% of stage C patients.

Vitamin D Levels According to Cirrhosis Etiology

Mean vitamin D levels according to etiology were as follows: cryptogenic cirrhosis, 12.6±11.7 ng/mL; hepatitis B-related cirrhosis, 9.3±5.3 ng/mL; hepatitis C-related cirrhosis, 7.5±3.6 ng/mL; alcohol-related cirrhosis, 9.9±5.4 ng/mL; and drug-related cirrhosis, 6.9±4.1 ng/mL. No statistically significant difference was found. In serum vitamin D levels among the different etiologic subgroups (p=0.210).

Vitamin D Levels and Cirrhosis-Related Complications

No notable association identified between vitamin D concentrations and decompensated cirrhosis (p=0.621), ascites (p=0.233), hepatic encephalopathy (p=0.215), variceal bleeding (p=0.988), ascitic infection (p=0.071), hepatorenal syndrome (p=0.670), hepatopulmonary syndrome (p=0.706), PVT (p=0.988), HCC (p=0.463), portal hypertension (p=0.427), or esophageal varices (p=0.794) (Table 4).

Vitamin D Levels and Laboratory Parameters

No statistically significant difference was found.among genders, with men having 10.3±6.8 ng/mL and women 11.4±10.9 ng/mL (p=0.511).

Table 2. Distribution of Child-Pugh and MELD scores of the patients

A) Continuous variables				
Parameter	**Mean ± SD**	**Median**	**Min**	**Max**
MELD score	9.5±2.7	9	6	20
Child-Pugh score	7.2±2.4	6	5	15
B) Categorical variables				
Parameter	**Category**	**n**	**%**	
Child-Pugh class	A	62	52.5	
	B	31	26.3	
	C	25	21.2	

SD: Standard deviation, MELD: Model for End-Stage Liver Disease, Min: Minimum, Max: Maximum, Child-Pugh: Child-Turcotte-Pugh

Additionally, vitamin D levels showed no significant correlation with variables such as age, WBC, HGB, PLT, glucose, creatinine, LDH, LDL, CRP, HDL, ESR, HbA1c, ferritin, GGT, AST, ALP, ALT, or bilirubin (Table 5).

Serum 25(OH)D levels displayed a positive correlation with albumin (rho: 0.271, p=0.003), total cholesterol (rho: 0.195, p=0.035), and triglycerides (rho: 0.251, p=0.006). In contrast, vitamin D levels were negatively correlated with PT (rho: -0.237, p=0.003) and INR (rho: -0.234, p=0.011).

Vitamin D Levels and Hepatic Disease Severity

Serum 25(OH)D levels were negatively associated with Child-Pugh score (rho: -0.243, p=0.008) and MELD score (rho: -0.185, p=0.045) (Table 6).

According to Child-Pugh stage, mean vitamin D levels were 11.2±6.5 ng/mL in stage A, 11.7±14.9 ng/mL in stage B, and 9.1±6.2 ng/mL in stage C. Although vitamin D levels tended to decrease with advancing Child-

Table 3. Distribution of cirrhosis-related complications

Parameter	Category	n	%
Cirrhosis status	Compensated	57	48.3
	Decompensated	61	51.7
Ascites	None	71	60.2
	Mild	15	12.7
	Moderate	8	6.8
	Severe	24	20.3
Ascitic infection	Present	13	11.0
	Absent	105	89.0
Hepatic encephalopathy	Present	30	25.4
	Absent	88	74.6
Encephalopathy stage	Stage 1–2	21	17.8
	Stage 3–4	9	7.6
Variceal bleeding	Present	37	31.4
	Absent	81	68.6
Esophageal varices	None	16	13.6
	Grade 1	34	28.8
	Grade 2	36	30.5
	Grade 3	32	27.1
Band ligation	Present	26	22.0
	Absent	92	78.0
Hepatorenal syndrome	Present	22	18.6
	Absent	96	81.4
Hepatopulmonary syndrome	Present	2	1.7
	Absent	116	98.3
Portal vein thrombosis	None	92	78.0
	Partial	24	20.3
	Complete	2	1.7
Hepatocellular carcinoma	Present	13	11.0
	Absent	105	89.0
Portal hypertension	None	8	6.8
	Stage 1–2	101	85.6
	Stage 3–4	9	7.6

PVT: Portal vein thrombosis, HCC: Hepatocellular carcinoma

Table 4. Vitamin D Levels According to cirrhosis-related complications

Complication	Category	Mean ± SD (ng/mL)	p value
Decompensated cirrhosis	Present	10.0±5.4	0.621
	Absent	11.8±12.2	
Ascites	None	10.8±6.3	0.233
	Mild	15.9±20.0	
	Moderate	7.9±4.5	
	Severe	9.1±5.7	
Hepatic encephalopathy	None	11.4±10.3	0.215
	Stage 1–2	10.4±6.0	
	Stage 3–4	7.2±3.6	
Variceal bleeding	Absent	11.3±10.8	0.988
	Present	10.1±5.1	
Ascitic infection	Absent	11.3±9.7	0.071
	Present	7.9±4.5	
Hepatorenal syndrome	Absent	11.1±10.0	0.670
	Present	10.0±5.8	
Hepatopulmonary syndrome	Absent	10.9±9.4	0.706
	Present	13.0±11.5	
Portal vein thrombosis	None	11.1±10.1	0.988
	Partial	9.9±4.9	
	Complete	16.0±16.9	
Hepatocellular carcinoma	Absent	10.9±9.8	0.463
	Present	10.7±5.0	
Portal hypertension	None	8.1±4.1	0.427
	Stage 1–2	11.3±9.9	
	Stage 3–4	8.7±4.9	
Esophageal varices	None	10.3±6.7	0.794
	Grade 1	11.2±6.4	
	Grade 2	12.4±14.6	
	Grade 3	9.3±4.4	
Band ligation	Absent	11.3±10.3	0.560
	Present	9.5±4.8	

Statistical analysis: Mann–Whitney U test and Kruskal–Wallis test were used as appropriate. SD: Standard deviation

Pugh stage, the difference among Child-Pugh stages failed to achieve statistical significance (p=0.140).

Discussion

This study found that over 90% of individuals with cirrhosis experienced vitamin D deficiency. Additionally, lower vitamin D levels were linked to signs of reduced hepatic synthetic function and increased disease severity.

These findings are consistent with previous studies indicating a elevated prevalence of inadequate vitamin D levels in those with cirrhosis (9,10,18). Our findings reveal that levels are more closely linked to the extent of hepatic dysfunction than to the underlying cause of cirrhosis. Earlier studies have also observed that vitamin D deficiency correlates

Table 5. Correlation between vitamin D levels and liver function tests

Parameter	Correlation coefficient (Rho)	p value
AST (U/L)	0.007	0.940
ALT (U/L)	0.007	0.937
ALP (U/L)	0.007	0.939
GGT (U/L)	0.092	0.322
Total bilirubin (mg/dL)	-0.080	0.390
Prothrombin time (s)	-0.237	0.003
INR	-0.234	0.011

Analysis: Spearman correlation. AST: Aspartate aminotransferase, ALT: Alanine aminotransferase, ALP: Alkaline phosphatase, GGT: Gamma-glutamyl transferase, INR: International normalized ratio

Table 6. Correlation between vitamin D levels and Child–Pugh and MELD scores

Parameter	Correlation coefficient (Rho)	p value
Child–Pugh score	-0.243	0.008
MELD score	-0.185	0.045

Analysis: Spearman correlation. MELD: Model for End-Stage Liver Disease

with disease severity rather than its etiology (11,19). The observed associations between vitamin D and albumin, PT, and INR further support the idea that a decline in liver synthetic capacity plays a critical role in the development of vitamin D deficiency. the liver is responsible for both hydroxylating vitamin D and producing binding proteins, impaired liver function could directly result in lower vitamin D levels in the blood (6,8,20). Thus, vitamin D may serve as an indirect marker of liver reserve.

While some research has indicated a link between low serum vitamin D levels and outcomes such as infection or decompensation (11,14,15), the literature is inconsistent. The lack of correlation in our study may be due to its retrospective design, modest sample size, and variation in complication profiles. The positive relationship between vitamin D and lipid parameters, including cholesterol and triglycerides, should also be considered in the context of liver function. Lower lipid levels are commonly found in progressive liver disease due to impaired synthesis (21-24). Therefore, this relationship likely reflects overall hepatic dysfunction rather than a direct metabolic interaction.

Vitamin D deficiency in cirrhosis is likely multifactorial, involving reduced sun exposure, nutritional deficiencies, impaired intestinal absorption, decreased hepatic conversion, and altered metabolism (8,20,25-27). Besides being a marker of disease severity, vitamin D may also contribute to disease progression through its roles in inflammation, fibrosis, and immune regulation (13,28-30).

Study Limitations

The present study has several limitations. First, its retrospective and observational design precludes establishing causal relationships between vitamin D levels and liver disease severity. Second, this single-center study had a relatively small sample size, which may limit the generalizability of the findings. Third, longitudinal follow-up data were unavailable;

therefore, the prognostic significance of vitamin D levels over time could not be evaluated. Fourth, the unequal distribution of certain cirrhosis-related complications may have limited the statistical power of subgroup analyses. In addition, seasonal variations in sunlight exposure, which may influence serum 25(OH)D concentrations, could not be taken into account because the timing of vitamin D measurements was not standardized. Multivariable analyses were not performed; therefore, the potential confounding effects could not be fully adjusted for.

Conclusion

Vitamin D deficiency is highly prevalent among patients with cirrhosis. Lower serum 25(OH)D levels were associated with greater liver disease severity and impaired hepatic synthetic function, rather than with the etiology or specific complications of cirrhosis. These findings suggest that vitamin D deficiency may represent a marker of disease severity in cirrhosis. However, given the observational nature of this study, these associations should not be interpreted as causal relationships. Further prospective studies are warranted to determine whether correction of vitamin D deficiency may influence clinical outcomes.

Ethics

Ethics Committee Approval: Authorization for this research was received from the Ethics Committee of Bezmialem Vakıf University (approval number: 20/274, date: 07.11.2017).

Informed Consent: The study's retrospective nature allowed for the waiver of informed consent.

Footnotes

Authorship Contributions: Concept - A.Ö., A.T.İ.; Design - A.Ö., A.T.İ.; Data Collection or Processing - A.Ö.; Analysis or Interpretation - A.Ö., A.T.İ.; Literature Search - A.Ö., A.T.İ.; Writing - A.Ö.

Conflict of Interest: No conflict of interest was declared by the authors.

Financial Disclosure: The authors declared that this study received no financial support.

References

1. Scaglione S, Kliethermes S, Cao G, Shoham D, Durazo R, Luke A, et al. The epidemiology of cirrhosis in the United States: a population-based study. J Clin Gastroenterol. 2015; 49: 690-6.
2. Schuppan D, Afdhal NH. Liver cirrhosis. Lancet. 2008; 371: 838-51.
3. Tsochatzis EA, Bosch J, Burroughs AK. Liver cirrhosis. Lancet. 2014; 383: 1749-61.
4. D'Amico G, Garcia-Tsao G, Pagliaro L. Natural history and prognostic indicators of survival in cirrhosis: a systematic review of 118 studies. J Hepatol. 2006; 44: 217-31.
5. Heidelbaugh JJ, Bruderly M. Cirrhosis and chronic liver failure: part I. Diagnosis and evaluation. Am Fam Physician. 2006; 74: 756-62.
6. Han YP, Kong M, Zheng S, Ren Y, Zhu L, Shi H, et al. Vitamin D in liver diseases: from mechanisms to clinical trials. J Gastroenterol Hepatol. 2013; 28 Suppl 1: 49-55.
7. Lim LY, Chalasani N. Vitamin D deficiency in patients with chronic liver disease and cirrhosis. Curr Gastroenterol Rep. 2012; 14: 67-73.
8. Holick MF. Vitamin D deficiency. N Engl J Med. 2007; 357: 266-81.
9. Stokes CS, Volmer DA, Grünhage F, Lammert F. Vitamin D in chronic liver disease. Liver Int. 2013; 33: 338-52.
10. Arteh J, Narra S, Nair S. Prevalence of vitamin D deficiency in chronic liver disease. Dig Dis Sci. 2010; 55: 2624-8.
11. Chen CC, Wang SS, Jeng FS, Lee SD. Metabolic bone disease of liver cirrhosis: is it parallel to the clinical severity of cirrhosis? J Gastroenterol Hepatol. 1996; 11: 417-21.
12. Fisher L, Fisher A. Vitamin D and parathyroid hormone in outpatients with noncholestatic chronic liver disease. Clin Gastroenterol Hepatol. 2007; 5: 513-20.
13. Miroliaee A, Nasiri-Toosi M, Khalilzadeh O, Esteghamati A, Abdollahi A, Mazloumi M. Disturbances of parathyroid hormone-vitamin D axis in noncholestatic chronic liver disease: a cross-sectional study. Hepatol Int. 2010; 4: 634-40.
14. Kumar R, Kumar P, Saxena KN, Mishra M, Mishra VK, Kumari A, et al. Vitamin D status in patients with cirrhosis of the liver and their relatives: a case control study from North India. Indian J Gastroenterol. 2017; 36: 50-5.
15. Putz-Bankuti C, Pilz S, Stojakovic T, Scharnagl H, Pieber TR, Trauner M, et al. Association of 25-hydroxyvitamin D levels with liver dysfunction and mortality in chronic liver disease. Liver Int. 2012; 32: 845-51.
16. Holick MF, Binkley NC, Bischoff-Ferrari HA, Gordon CM, Hanley DA, Heaney RP, et al. Evaluation, treatment, and prevention of vitamin D deficiency: an Endocrine Society clinical practice guideline. J Clin Endocrinol Metab. 2011; 96: 1911-30.
17. Petta S, Camma C, Scazzone C, Tripodo C, Di Marco V, Bono A, et al. Low vitamin D serum level is related to severe fibrosis and low responsiveness to interferon-based therapy in genotype 1 chronic hepatitis C. Hepatology. 2010; 51: 1158-67.
18. Finkelmeier F, Kronenberger B, Zeuzem S, Piiper A, Waidmann O. Low 25-hydroxyvitamin D levels are associated with infections and mortality in patients with cirrhosis. PLoS One. 2015; 10: e0132119.
19. Anty R, Tonohouan M, Ferrari-Panaia P, Piche T, Pariente A, Anstee QM, et al. Low levels of 25-hydroxy vitamin D are independently associated with the risk of bacterial infection in cirrhotic patients. Clin Transl Gastroenterol. 2014; 5: e56.
20. Bitetto D, Fabris C, Falleti E, Cussigh A, Fontanini E, Fornasiere E, et al. Vitamin D and the risk of acute allograft rejection following human liver transplantation. Liver Int. 2010; 30: 417-44.
21. Unger LW, Forstner B, Schneglberger S, Muckenhuber M, Eigenbauer E, Scheiner B, et al. Patterns and prevalence of dyslipidemia in patients with different etiologies of chronic liver disease. Wien Klin Wochenschr. 2019; 131: 395-403.
22. Peng Y, Qi X, Guo X. Child-Pugh versus MELD score for the assessment of prognosis in liver cirrhosis: a systematic review and meta-analysis of observational studies. Medicine (Baltimore). 2016; 95: e2877.
23. Matin A, Tyagi P, Sharma P, Bansal N, Agrawal D, Sharma BC. More than 90% of patients of cirrhosis have vitamin D deficiency: a cross-section study. Clin Gastroenterol Hepatol. 2015; 13: e109.
24. Malham M, Jørgensen SP, Ott P, Agnholt J, Vilstrup H, Borre M, et al. Vitamin D deficiency in cirrhosis relates to liver dysfunction rather than aetiology. World J Gastroenterol. 2011; 17: 922-5.
25. Ghadir MR, Riahin AA, Havaspour A, Nooranipour M, Habibinejad AA. The relationship between lipid profile and severity of liver damage in cirrhotic patients. Hepat Mon. 2010; 10: 285-8.
26. Phukan JP, Sinha A, Deka JP. Serum lipid profile in alcoholic cirrhosis: a study in a teaching hospital of north-eastern India. Niger Med J. 2013; 54: 5-9.

27. Kackar RR, Desai HG. Serum cholesterol in cirrhosis of liver. J Assoc Physicians India. 2004; 52: 1007.

28. Hepner GW, Roginsky M, Moo HF. Abnormal vitamin D metabolism in patients with cirrhosis. Am J Dig Dis. 1976; 21: 527-32.

29. Jung RT, Davie M, Hunter JO, Chalmers TM, Lawson DE, et al. Abnormal vitamin D metabolism in cirrhosis. Gut. 1978; 19: 290-3.

30. Pourgholami MH, Akhter J, Lu Y, Morris DL. In vitro and in vivo inhibition of liver cancer cells by 1,25-dihydroxyvitamin D3. Cancer Lett. 2000; 151: 97-102.

İstanbul Med J 2026; 27(3): 225-32
DOI: 10.4274/imj.galenos.2026.62257

Evaluation of the Potential Effects of Intra-Articular Rifamycin SV Injection into the Knee Joint on Articular Cartilage and Synovial Membrane

Yücel Bilgin[1], Elif Özkök[2], Merve Cin[3], Fevzi Birişik[4], İbrahim Doğan[5], Ahmet Sinan Kalyenci[4]

[1]Bursa Uludağ University Faculty of Medicine, Department of Orthopedics and Traumatology, Bursa, Türkiye
[2]İstanbul University, Aziz Sancar Institute of Experimental Medicine, Department of Neuroscience, İstanbul, Türkiye
[3]University of Health Sciences Türkiye, İstanbul Training and Research Hospital, Clinic of Pathology, İstanbul, Türkiye
[4]University of Health Sciences Türkiye, İstanbul Training and Research Hospital, Clinic of Orthopedics and Traumatology, İstanbul, Türkiye
[5]Binali Yıldırım University Mengücek Gazi Training and Research Hospital, Clinic of Orthopedics and Traumatology, Erzincan, Türkiye

ABSTRACT

Introduction: Rifamycin is widely used as a broad-spectrum antimicrobial agent; recent studies have demonstrated the anti-inflammatory properties of rifamycin SV. Our study aimed to determine the adverse effects of intra-articular injection of rifamycin SV on the articular cartilage and synovial membrane of the knee joint.

Methods: Thirty-two Wistar albino male rats were assigned to experimental and control groups (n=8 per group). On the first day, a single dose of 5mg/kg rifamycin SV (Rif; Koçak Farma, Türkiye) was injected into the right knee of the rats in the experimental groups (E1/E2), and a single dose of 0.9% isotonic sodium solution was injected into the right knee of the rats in the control groups (C1/C2). E1 and C1 rats were euthanized on the 7th day, and E2 and C2 rats were euthanized on the 28th day. Macroscopic and histopathological evaluations of the articular cartilage structures and synovial inflammation were performed. The histopathological grading and staging system of the Osteoarthritis Research Society International was used to evaluate the cartilage structures, with $p<0.05$ considered statistically significant.

Results: There were no statistically significant differences between the E1 and C1 groups or between the E2 and C2 groups in cartilage damage degree, stage, or score on the 7th day (p=0.117, p=0.197, p=0.197) and on the 28th day (p=0.077, p=0.061, p=0.062). When the E1 and C1 groups were examined to determine degrees of synovial inflammation, inflammation was significantly more common in the rifamycin SV (E1) group ($p<0.001$ on day 7). In contrast, degrees of synovial inflammation did not differ significantly between the E2 and C2 groups (p=0.256, day 28).

Conclusion: The intra-articular administration of rifamycin SV did not have a negative effect on articular cartilage but increased synovial inflammation on the 7th day.

Keywords: Rifamycin, knee, cartilage, isotonic sodium chloride

Introduction

Rifamycins are a group of antimicrobial drugs first discovered by Sensi at the Dow-Lepetit Research Laboratory in 1957 (1). Streptomyces mediterranei, a new Actinomyces strain isolated from a soil sample, produces molecules that primarily inhibit Gram-positive bacteria during culture. These molecules were named rifamycin A, B, C, D, and E and defined as the rifamycin complex family (2).

Rifamycins are broad-spectrum antimicrobial agents widely used to treat bacterial infections. However, recent studies indicate that rifamycin SV has anti-inflammatory and cellular protective properties (3,4). The anti-inflammatory effect of Rifamycin SV on neutrophils was also determined *in vitro* in the literature (5).

Septic arthritis is an infection of the joints. Diagnosis is made by clinical findings, gram staining, and culture of joint fluid (6). The most frequently detected pathogen is *Staphylococcus aureus* (7). Although the gold standard for treatment is surgical drainage and systemic antibiotics, arthroscopic lavage has also been described (8). In the case of inadequate treatment, cartilage damage develops, leading to permanent orthopedic sequelae. Therefore, evaluating the effect of rifamycin SV on knee joint cartilage may be important to determine its usefulness as a potential therapeutic strategy for septic arthritis.

Address for Correspondence: Asst. Prof. Yücel Bilgin, MD, Bursa Uludağ University Faculty of Medicine, Department of Orthopedics and Traumatology, Bursa, Türkiye
E-mail: yucelbilgin70@hotmail.com **ORCID ID:** orcid.org/0000-0003-0433-1918
Cite this article as: Bilgin Y, Özkök E, Cin M, Birişik F, Doğan İ, Kalyenci AS. Evaluation of the potential effects of intra-articular rifamycin SV injection into the knee joint on articular cartilage and synovial membrane. İstanbul Med J. 2026; 27(3): 225-32

Received: 01.06.2026
Accepted: 01.07.2026
Publication Date: 03.08.2026

The aim of this experimental animal study was to determine the adverse effect of the intra-articular administration of rifamycin SV on knee joint cartilage, assessed by histopathological analysis.

Methods

Ethical approval was taken for our study from the İstanbul University Animal Experiments Local Ethics Committee (decision number: 2021/17, date: 30.04.2021). The experimental part of the study was carried out at İstanbul University, the Department of Experimental Animals. The study was conducted as part of a master's thesis at İstanbul University, Institute of Health Sciences, Department of Experimental Animal Science. All experimental animals used in our study belong to İstanbul University, and the necessary permissions have been obtained for their use. The study was conducted in accordance with the ARRIVE guidelines.

Thirty-two *Wistar albino* male rats, 9-10 months old and weighing 380-420 g, were used in the study. All animals were numbered by making small ear incisions. The subjects were randomly divided into four groups of eight rats each. Randomization was performed using a table of random numbers. Two groups were designated experimental: experimental group 1 (E1) and experimental group 2 (E2). The other two groups were designated control groups 1 (C1) and 2 (C2). The groups of animals were written on labels attached to their cages. During the study, the rats were provided with a standard laboratory rodent pellet diet (ad libitum) and free access to water. The animals were housed in appropriate cages under standard room conditions with a 12-hour night, 12-hour day rhythm at a temperature of 21±2 ^{0}C and a humidity level of 55±10%. On the first day, a single dose of rifamycin SV (Rif; Koçak Farma, Türkiye) at 5 mg/kg was injected into the right knee of the rats in the experimental groups (E1, E2), and a single dose of 0.9% isotonic sodium chloride (20 microliters; Polifleks; Polifarma, Türkiye) was injected into the right knee of the rats in the control groups (C1, C2). Rifamycin SV dose was determined based on previous animal experiments in the literature (9). An intra-articular injection was administered into a normal cartilaginous knee joint. No prior pathology was identified.

Animals in the E1 and C1 groups were euthanized at the end of the 7th day, and animals in the E2 and C2 groups at the end of the 28th day. Euthanasia was performed by administering pentothal at a high dose (200 mg/kg). After euthanasia, the right lower extremities of the subjects were removed by hip disarticulation following appropriate antisepsis and preparation. Muscle tissues were separated. The right femur and tibia were preserved together with the knee joint ligaments and placed individually in appropriately labeled sample containers containing 10% formaldehyde solution. The samples were then delivered to the pathology laboratory for histopathological examination.

Injection Technique

Before the procedures, all animals were weighed and their weights recorded. For anesthesia, 5 mg/kg xylazine hydrochloride (Rompun; Bayer Healthcare, Leverkusen, Germany) and 50 mg/kg ketamine hydrochloride (Ketalar; Pfizer, Türkiye) were administered intraperitoneally. Ethical rules and animal welfare are at the forefront of experimental animal studies. Intra-articular injections were administered under anesthesia to ensure that the animal did not experience pain and that the delicate injection could be performed in accordance with the technique. Then, the right knees of the animals were shaved while the animals were in the supine position. The patella, patellar tendon, and tibial tuberosity were marked on the skin with a skin pencil. Skin antisepsis was performed using 10% povidone-iodine (Batticon; Adeka, Türkiye). Injections were administered via the transpatellar route (the same route of drug administration when needed), midway between the patella and the tuberosity of the tibia, using tuberculin syringes with a 26G needle tip. All animals in the experimental groups (E1 and E2) were injected with 5mg/kg of rifamycin SV (Rif; Koçak Farma, Türkiye), and those in the control groups (C1 and C2) were injected with 0.9% isotonic sodium chloride (20 microliters). When the anesthesia had completely taken effect, the subjects were allowed to bear weight and move freely in the cage. The criteria we used in the study to decide that the effect of anesthesia has ended are: return of reflex responses (pedaling, tail pinching, etc.), the animal regains its righting reflex, return of coordinated movements, and the animal becomes fully conscious (10). Because knee movements might be affected and gait disorders might develop following the injections, housing and care were provided for each experimental and control animal in a cage. After 24 hours, all subjects were active, showed no signs of pain, and they were moved to cages housing four animals each.

Macroscopic Evaluation

In macroscopic examination, knee joint cartilages were stained with Indian ink and evaluated for possible damage according to the criteria defined by Yoshioka et al. (11) (Table 1). To ensure blinding during macroscopic examination, the specimens were numbered and sent to the examiner. The examination was performed by a researcher who was not involved in the experimental procedures.

Histopathological Evaluation

Specimens containing femora and tibiae with preserved knee joints were decalcified in 20% hydrochloric acid for microscopic examination. Afterward, 5-micrometer-thick longitudinal sections were taken perpendicular to the joint surface using a microtome. Staining was performed using hematoxylin-eosin and safranin O, and the stained specimens were examined under a light microscope (Olympus®

Table 1. Classification of macroscopic evaluation of cartilage damage defined by Yoshioka et al. (11)

Grade	Macroscopic changes
1	İntact surface: surface appears normal and does not retain any ink;
2	Minimal fibrillation: site appears normal before staining, but retains the India ink as elongated specks or light gray patches;
3	Overt fibrillation: the cartilage is velvety in appearance and retains ink as intense black patches;
4	Erosion: loss of cartilage exposing the underlying bone.

BX51-x100). For the evaluation of the cartilage structures, the cartilage histopathological grading and staging system of the Osteoarthritis Research Society International (OARSI) was used (12) (Tables 2 and 3). In this system, cartilage damage is graded and staged, and the osteoarthritis score is calculated by multiplying the assigned grade and stage values. Histopathological evaluation of synovial inflammation was evaluated according to the 5-point scale defined by Ozyuvaci et al. (13) (Table 4).

To ensure blinding of the histopathological evaluation, specimens were sent to the laboratory with animal numbers. Histopathological examination of all samples was performed by a single pathologist.

Statistical Analysis

The SPSS 23.0 (IBM Corp. Released 2015. IBM SPSS Statistics for Windows, Version 23.0. Armonk, NY: IBM Corp.) program was used for statistical analysis, and the G Power 3.1.9.7 (Franz Faul, Germany) program was used for sample calculation.

Based on the calculation using the determined effect size (d: 0.849), 95% power, and a 5% margin of error, a total of at least 32 samples should be studied.

Table 2. Cartilage damage histopathological statiging criterias according to OARSI classification (12)

Stage	% involvement (surface, area, volume)
0	No osteoarthritis activity seen
1	<10%
2	10-25%
3	25-50%
4	>50%

Comparisons between cartilage scores and degrees of synovial inflammation were conducted using the Mann–Whitney U test. $p<0.05$ was used as the level of significance.

Results

No animal deaths were reported during the study. No problems with independent mobilization of the experimental animals were observed, and no post-injection infections occurred.

Macroscopic Findings

According to the evaluation results using the macroscopic classification ve cartilage damage defined by Yoshioka et al. (11), no difference was detected between the E1 and C1 groups consisting of rats euthanized at the end of the 7th day ($p=0.535$). No difference was observed in the degree of cartilage damage between the E2 and C2 groups, which consisted of rats euthanized at the end of day 28 ($p=0.268$).

Histopathological Findings

According to evaluation using the OARSI cartilage histopathological grading and staging system, no difference was detected in the degree of cartilage damage between the E1 and C1 groups, which consisted of rats euthanized at the end of day 7 ($p=0.117$). No difference was detected in cartilage damage stages or cartilage scores (both $p=0.197$) (Table 5; Figures 1 and 2). No difference was observed in the degree of cartilage damage between the E2 and C2 groups; both groups consisted of rats euthanized at the end of day 28 ($p=0.077$). No differences were detected with respect to cartilage damage stages ($p=0.061$) or cartilage scores ($p=0.062$) (Table 5, Figures 3 and 4).

When the E1 and C1 groups, consisting of rats euthanized on day 7, were compared for the degree of synovial inflammation, the group

Table 3. Cartilage damage histopathological graiding criterias according to OARSI classification (12)

Grade	Macroscopic changes
Grade 0: surface intact, cartilage morphology intact	Matrix: normal architecture Cells: intact, appropriate orientation
Grade 1: surface intact	Matrix: superficial zone intact, oedema and/or superficial fibrillation (abrasion), focal superficial matrix condensation Cells: death, proliferation (clusters), hypertrophy, superficial zone Reaction must be more than superficial fibrillation only
Grade 2: surface discontinuity	As above + Matrix discontinuity at superficial zone (deep fibrillation) ± Cationic stain matrix depletion (Safranin O or Toluidine Blue) upper 1/3 of cartilage ± Focal perichondronal increased stain (mid zone) ± Disorientation of chondron columns Cells: death, proliferation (clusters), hypertrophy
Grade 3: vertical fissures (clefts)	As above Matrix vertical fissures into mid zone, branched fissures ± Cationic stain depletion (Safranin O or Toluidine Blue) into lower 2/3 of cartilage (deep zone) ± New collagen formation (polarized light microscopy, Picro Sirius Red stain) Cells: death, regeneration (clusters), hypertrophy, cartilage domains adjacent to fissures
Grade 4: erosion	Cartilage matrix loss: delamination of superficial layer, mid layer cyst formation Excavation: matrix loss superficial layer and mid zone
Grade 5: denudation	Surface: sclerotic bone or reparative tissue including fibrocartilage within denuded surface. Microfracture with repair limited to bone surface
Grade 6: deformation Bone	Bone remodelling (more than osteophyte formation only). Includes: microfracture with fibrocartilaginous and osseous repair extending above the previous surface

Table 4. Grading of histopathological inflammatory changes in the knee joints of rats (13)

Grade	Histopathological changes
1	No inflammation
2	Minimal inflammation: mild congestion and oedema
3	Mild inflammation: erosion of joint surface, congestion and oedema, small number of neutrophils
4	Moderate inflammation: neutrophils and macrophages, synoviocyte hyperplasia
5	Severe inflammation: neutrophils and macrophages, synoviocyte hyperplasia, fibrin exudation

administered rifamycin SV exhibited greater synovial inflammation ($p<0.001$) (Table 6 and Figure 5). When the E2 and C2 groups, rats euthanized at the end of day 28, were compared with respect to degrees of synovial inflammation, no difference was detected between the two groups ($p=0.256$) Table 6.

Discussion

Rifamycins are a family of antimicrobials that act by inhibiting RNA polymerase. Rifamycin SV is an antimicrobial of the rifamycin group that was first used therapeutically. In addition to their antimicrobial activity, rifamycins have been reported to exert anti-inflammatory effects. It has been determined that these effects are exerted by inhibiting the synthesis of cytokines from THP-1-type monocytes and macrophages activated by lipopolysaccharide (LPS) (4). Rifamycins have also been shown to antagonize tumor necrosis factor alpha and LPS-induced nuclear factor kappa B activities and inhibit inflammatory chemokines and interleukin (IL)-8 synthesis induced through IL-1β (3).

Rifamycins are antibiotics that can be used orally or parenterally. However, the literature reports various local uses. Bruni et al. (14) reported positive results using rifamycin SV topically in the treatment of herpes zoster. Boztaş et al. (15) used rifamycin SV locally in the treatment of pilonidal sinus disease and found that it was beneficial to the treatment. For this reason, intra-articular injection was used as a alternative mode of administration in our study.

The starting point of our study was the question of whether rifamycin is safe for intra-articular use to treat intra-articular infections, because it is a broad-spectrum antimicrobial agent with anti-inflammatory effects. A review of the literature identified several studies on the intra-articular administration of rifamycins. Rifamycins were first used intra-articularly to treat rheumatoid arthritis. In a randomized, prospective study, patients with rheumatoid arthritis received a total of 525 mg of rifamycin intra-articularly once weekly for 10 weeks. In clinical findings, a significant improvement in erythrocyte sedimentation rate and C-reactive protein level was detected (16). A literature review examining 20 years of data stated that intra-articular rifamycin was effective against active synovitis and could be used together with slow-acting antirheumatic drugs (17). Rifamycin SV was compared with triamcinolone acetonide in a randomized controlled trial involving 87 patients with rheumatoid arthritis and refractory knee synovitis. It was concluded that rifamycin SV was less useful than triamcinolone acetonide in the local treatment of rheumatoid synovitis (18). In a different study, the application of rifamycin to the joint was shown to be effective in reducing pain in rheumatoid arthritis patients (19).

Rifamycins have also been used intra-articularly in the treatment of hemophilic arthropathy. A 2018 Korean study showed that chemical synovectomy with rifamycin could prevent hemarthrosis and improve clinical symptoms in patients with hemophilia. It has been found that rifamycin protects the joint, especially in the early stages of arthropathy, where there is no narrowing of the joint space (20). In 2021, Caviglia et al. (21) examined the use of intra-articular rifamycin in the treatment of hemophilic arthropathy. It has been stated that rifamycin is more effective when used in small joints (elbow and ankle) than in larger joints (knee) and that multiple injections predict failure (21).

Studies have shown that application of rifamycin to the joint reduces inflammation in rheumatological diseases and intra-articular bleeding

Table 5. Histological findings of OARSI assessment

OARSI Scores		Groups									
		E1		C1		p	E2		C2		p
		n	%	n	%		n	%	n	%	
Grade	0	4	50	7	87.5	0.117	2	25	6	75	0.077
	1	4	50	1	12.5		4	50	1	12.5	
	2	0	0	0	0		1	12.5	1	12,5	
	3	0	0	0	0		1	12.5	0	0	
Stage	0	4	50	7	87.5	0.197	2	25	6	75	0.061
	1	4	50	0	0		3	37.5	1	12.5	
	2	0	0	1	12.5		2	25	1	12.5	
	3	0	0	0	0		1	12.5	0	0	
Score	0	4	50	7	87.5	0.197	3	37.5	6	75	0.062
	1	4	50	0	0		2	25	1	12.5	
	2	0	0	1	12.5		1	12.5	0	0	
	4	0	0	0	0		0	0	1	12.5	
	6	0	0	0	0		2	25	0	0	

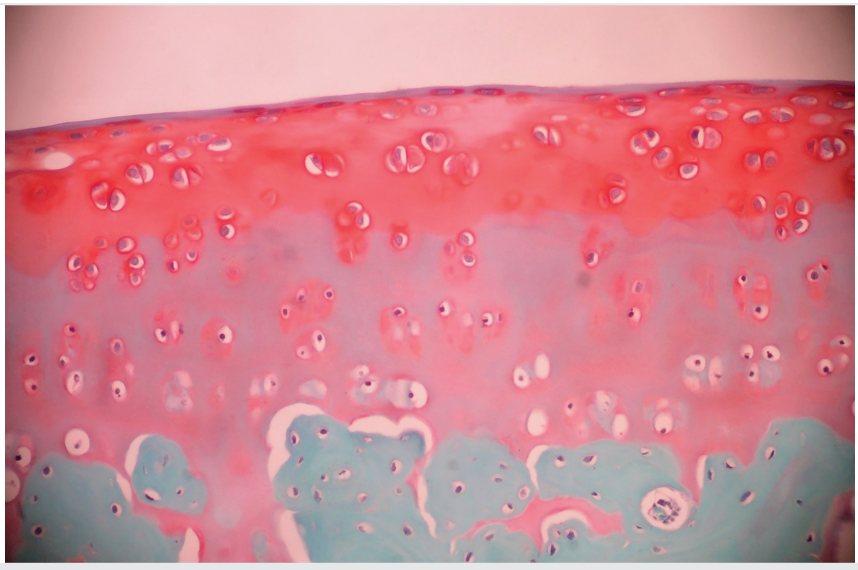

Figure 1. Histopathological appearance of the sample with grade 0 cartilage damage in group C1 (safranin-0 x100-normal architecture)

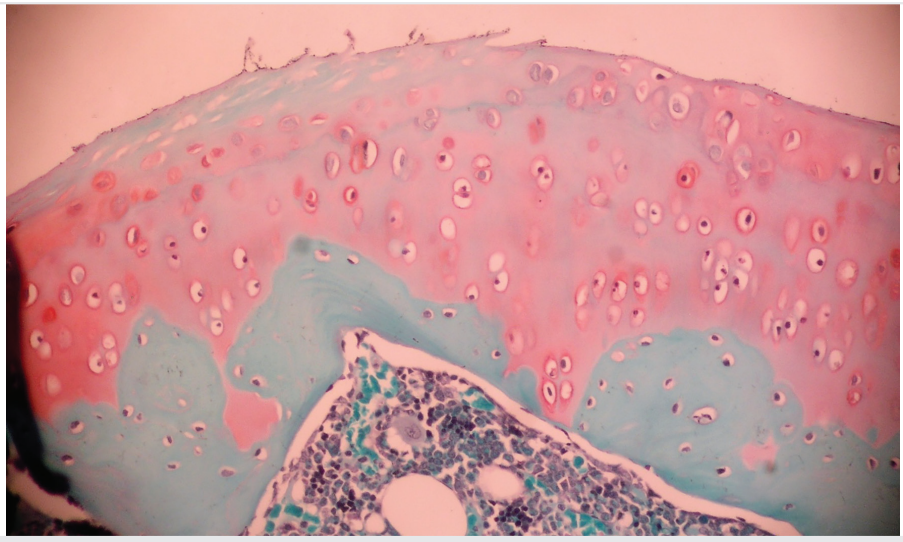

Figure 2. Histopathological appearance of the sample with grade 1 cartilage damage in group E1 (safranin-0 x100-superficial fibrillation)

in hemophilic patients. However, because cartilage destruction in these diseases appears to result from the underlying disease process, these studies do not demonstrate whether rifamycins have beneficial or harmful effects on cartilage or whether they are reliable.

In our study, cartilage structures in rats were examined using the OARSI scale after intra-articular application of rifamycin SV. This scale is a rating, staging, and scoring method (12). The animal selection and scale used were compatible with similar cartilage studies in the literature (22).

The intra-articular injection volume to be administered to rats is also important. Excessive application can damage the joint capsule and may result in drug extraction. In such cases, the effects of the drug may not be clearly observed, and additional complications may occur. Since a study conducted on this subject in the literature determined that a maximum of 30 microliters could be injected into the rat knee, 20 microliters was used as the injection volume in our study (23). Rifamycin SV is red. On macroscopic examination after euthanasia, no red discoloration was observed in the subcutaneous tissue of any sample.

The administered drug dose was determined based on previous studies. Lee et al. (9) studied a rabbit hemophilic arthropathy model and injected 10 mg rifamycin into the knees in 2000-g rabbits. In our study, the dose applied was 5 mg/kg.

Starting from a hypothesis similar to our study, Kwon et al. (24) examined the intra-articular application of rifamycin in MRSA septic arthritis. The authors stated that the local application of rifamycin may be a promising new therapeutic strategy for septic arthritis, due to the simultaneous alleviation of intra-articular inflammation and targeting of intracellular bacteria.

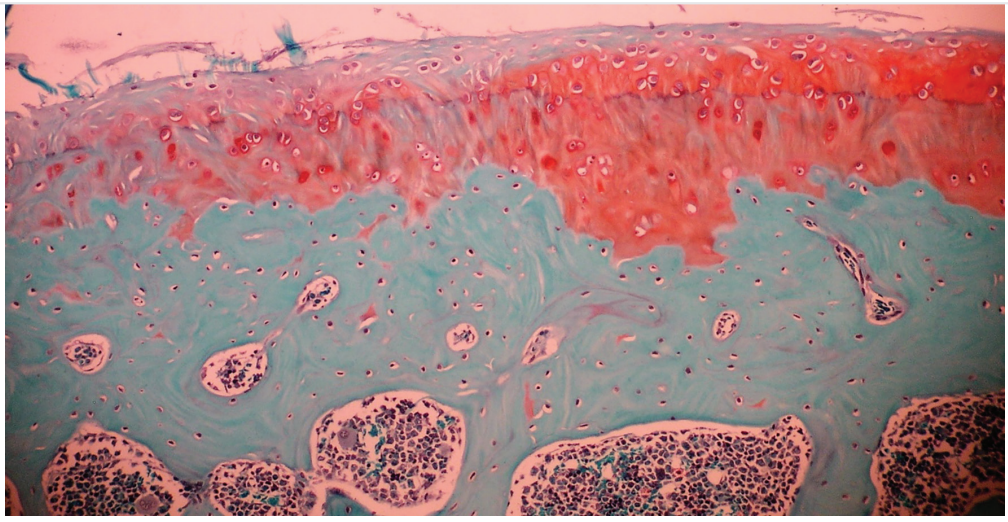

Figure 3. Histopathological appearance of the sample with grade 2 cartilage damage in group C2 (safranin-0 x100-superficial zone deep fibrillation)

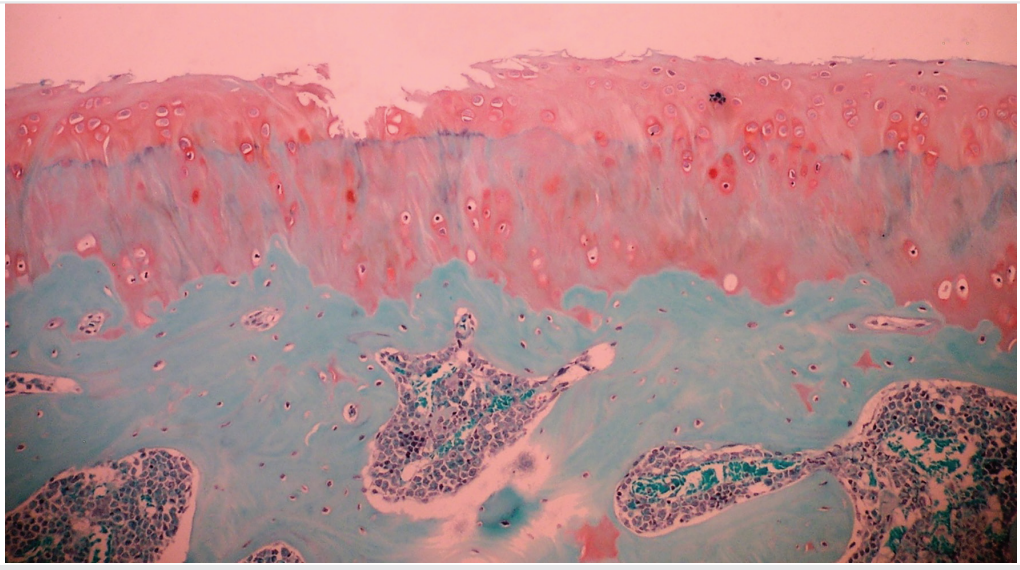

Figure 4. Histopathological appearance of the sample with grade 3 cartilage damage in group E2 (safranin-0 x100-matrix vertical fissures into mid-zone)

Table 6. Histological findings of synovial inflammation

Synovial inflammation		Groups									
		E1		C1		P	E2		C2		p
		n	%	n	%		n	%	n	%	
Grade	1	0	0	8	100	<0.001	3	37.5	6	75	0.256
	2	6	75	0	0		5	62.5	1	12.5	
	3	2	25	0	0		0	0	0	0	
	4	0	0	0	0		0	0	1	12.5	
	5	0	0	0	0		0	0	0	0	

Study Limitations

The most important limitation of our study is reliance solely on macroscopic and histopathological examinations for evaluation. The viability of cartilage cells could have been examined in the context of cartilage injury. In addition, immunohistochemical examinations and assessments of inflammatory markers to evaluate synovitis would have strengthened the study. However, these examinations could not be performed due to funding limitations. Furthermore, histopathological and macroscopic examinations were performed by a single researcher. Interobserver reliability was not investigated.

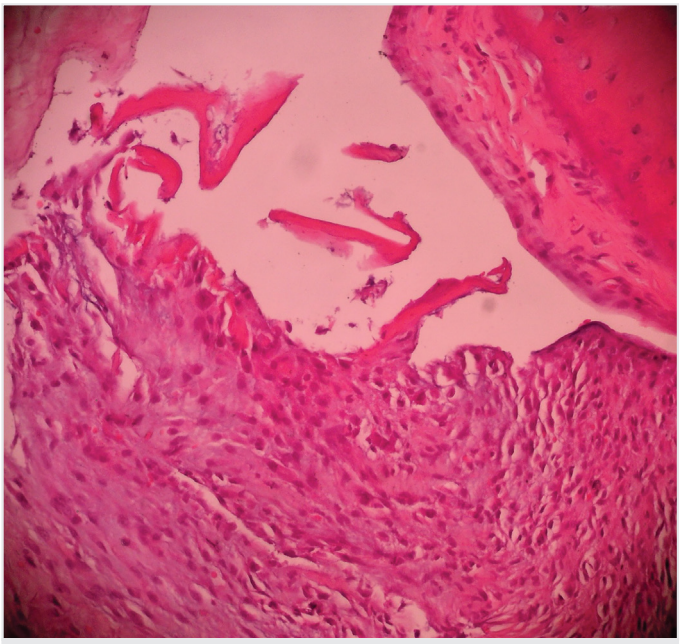

Figure 5. Histopathological appearance of the sample with grade 3 synovial inflammation in group E1 (hematoxylin eosin x100-mild synovial hyperplasia, increased vascularity, congestion, presence of rare neutrophils, focal fibrin exudation)

Conclusion

In our study, no significant difference in cartilage damage was detected compared with the control group during both the early and late periods, and intra-articular rifamycin SV was shown to be safe. However, a significant increase in synovial inflammation was observed early in the group that received rifamycin SV. Therefore, studies are needed to evaluate the reliability of rifamycin use in treating diseases that cause additional synovial inflammation, such as septic arthritis.

Ethics

Ethics Committee Approval: Ethical approval was taken for our study from the İstanbul University Animal Experiments Local Ethics Committee (decision number: 2021/17, date: 30.04.2021).

Informed Consent: Not applicable, as this study did not involve human participants.

Footnotes

Authorship Contributions: Surgical and Medical Practices - Y.B., F.B., İ.D., A.S.K.; Concept - Y.B., E.Ö., M.C., F.B.; Design - Y.B., E.Ö., M.C., F.B.; Data Collection or Processing - Y.B., M.C., İ.D., A.S.K.; Analysis or Interpretation - Y.B., E.Ö., İ.D., A.S.K.; Literature Search - Y.B., M.C., İ.D., A.S.K.; Writing - Y.B., F.B.

Conflict of Interest: No conflict of interest was declared by the authors.

Financial Disclosure: The funding of the study was covered by the author YB.

References

1. van Ingen J, Aarnoutse RE, Donald PR, Diacon AH, Dawson R, Plemper van Balen G, et al. Why do we use 600 mg of rifampicin in tuberculosis treatment? Clin Infect Dis. 2011; 52: e194-9.
2. Sensi P. History of the development of rifampin. Rev Infect Dis. 1983; 5 Suppl 3: S402-6.
3. Rosette C, Agan FJ, Rosette N, Moro L, Mazzetti A, Hassan C, et al. Rifamycin SV exhibits strong anti-inflammatory in vitro activity through pregnane X receptor stimulation and NFκB inhibition. Drug Metab Pharmacokinet. 2019; 34: 172-80.
4. Rosette C, Buendia-Laysa F Jr, Patkar S, Moro L, Celasco G, Bozzella R, et al. Anti-inflammatory and immunomodulatory activities of rifamycin SV. Int J Antimicrob Agents. 2013; 42: 182-6.
5. Spisani S, Dovigo L, Corazza G, Carletti R, Traniello S. The effect of rifamycin SV on neutrophil functions in patients with rheumatoid arthritis. Scand J Rheumatol. 1982; 11: 65-9.
6. Khodadadi RB, Damronglerd P, McHugh JW, El Zein S, Lahr BD, Yuan BJ, et al. Effect of antibiotic therapy before arthrocentesis on synovial fluid cell count and differential for diagnosis of native joint septic arthritis. Open Forum Infect Dis. 2024; 11: ofae403.
7. Swarup I, LaValva S, Shah R, Sankar WN. Septic arthritis of the hip in children: a critical analysis review. JBJS Rev. 2020; 8: e0103.
8. Sanpera I, Raluy-Collado D, Sanpera-Iglesias J. Arthroscopy for hip septic arthritis in children. Orthop Traumatol Surg Res. 2016; 102: 87-9.
9. Lee SH, Lee YA, Park EK, Kim KS, Cho YJ, Han JS, et al. The suppressive effect of rifampicin in an animal model of hemophilic synovitis. J Korean Rheum Assoc. 2007; 14: 201-9.
10. Flecknell P. Laboratory animal anaesthesia and analgesia. 5th ed. London: Academic Press; 2023.
11. Yoshioka M, Coutts RD, Amiel D, Hacker SA. Characterization of a model of osteoarthritis in the rabbit knee. Osteoarthritis Cartilage. 1996; 4: 87-98.
12. Pritzker KP, Gay S, Jimenez SA, Ostergaard K, Pelletier JP, Revell PA, et al. Osteoarthritis cartilage histopathology: grading and staging. Osteoarthritis Cartilage. 2006; 14: 13-29.
13. Ozyuvaci H, Bilgic B, Ozyuvaci E, Altan A, Altug T, Karaca C. Intra-articular injection of tenoxicam in rats: assessment of the local effects on the articular cartilage and synovium. J Int Med Res. 2004; 32: 312-6.
14. Bruni L, Tagliapietra G, Innocenti P. Herpes zoster treatments: results of a clinical trial relative to the use of rifamycin SV versus neuramide. J Int Med Res. 1984; 12: 255-60.
15. Boztaş A, Ünsal A, Ersoy Ö, Kale H, Güven H. Is intraoperative topical rifamycin application beneficial for wound healing in patients with pilonidal sinus disease? Ankara Eğit Araşt Hast Derg. 2022; 55: 233- 6.
16. Caruso I, Boccassini L, Cazzola M, Santandrea S, Montrone F, Dell'Acqua D, et al. Multiple intra-articular treatment of rheumatoid arthritis: a randomized prospective study comparing rifamycin SV with pefloxacin. J Int Med Res. 1992; 20: 27-39.
17. Caruso I. Twenty years of experience with intra-articular rifamycin for chronic arthritides. J Int Med Res. 1997; 25: 307-17.
18. Marchesoni A, Sinigaglia L, Ranza R, Varenna M, Battafarano N, Tosi S. Rifamycin SV versus triamcinolone in local treatment of rheumatoid synovitis. Scand J Rheumatol. 1993; 22: 194-8.
19. Blyth T, Stirling A, Coote J, Land D, Hunter JA. Injection of the rheumatoid knee: does intra-articular methotrexate or rifampicin add to the benefits of triamcinolone hexacetonide? Br J Rheumatol. 1998; 37: 770-2.

20. Suh HC, Kim DK, Kang SH, Seo KM, Kim HS, Lee JY, et al. Clinical and radiological evaluation after chemical synovectomy with rifampicin in hemophilic arthropathy: Korean experience with a 2-week interval protocol. Ann Rehabil Med. 2018; 42: 449-56.

21. Caviglia HA, Fernandez-Palazzi F, Galatro G, Perez-Bianco R. Chemical synoviorthesis with rifampicin in haemophilia. Haemophilia. 2001; 7 Suppl 2: 26-30.

22. Sukur E, Kucukdurmaz F. Comparison of cytotoxic effects of intra-articular use of tranexamic acid versus epinephrine on rat cartilage. Med Sci Monit. 2018; 24: 1166-70.

23. Aytekin K, Uysal M, Şahiner GG, Danışman M, Baş O, Takır S, et al. Evaluation of different intraarticular injection volumes to assess optimum efficient amount; an experimental study in rat knee joints. J Pharmacol Toxicol Methods. 2020; 101: 106658.

24. Kwon HK, Lee I, Yu KE, Cahill SV, Alder KD, Lee S, et al. Dual therapeutic targeting of intra-articular inflammation and intracellular bacteria enhances chondroprotection in septic arthritis. Sci Adv. 2021; 7: eabf2665.

İstanbul Med J 2026; 27(3): 233-7
DOI: 10.4274/imj.galenos.2026.73920

Core Circadian Clock Proteins (CLOCK and BMAL1) in Non-Muscle-Invasive Urothelial Carcinoma: Links to Histopathology and Tumor Progression

Begüm Çalım Gürbüz[1], Başak Bekiroğlu[1], Dilara Yitiz[1], Şeyma Aker[1], Emre Korkmaz[2], Halil Lütfi Canat[2]

[1]University of Health Sciences Türkiye, Başakşehir Çam and Sakura City Hospital, Clinic of Pathology, İstanbul, Türkiye
[2]University of Health Sciences Türkiye, Başakşehir Çam and Sakura City Hospital, Clinic of Urology, İstanbul, Türkiye

ABSTRACT

Introduction: This study aims to evaluate the immunohistochemical expression of core circadian clock proteins, circadian locomotor output cycles kaput (CLOCK) and brain and muscle ARNT-like protein 1 (BMAL1), in patients with non-muscle-invasive urothelial carcinoma (NMIBC) and to determine their potential role in predicting disease progression.

Methods: A total of 34 patients diagnosed with NMIBC who subsequently developed either progressive (n=20) or non-progressive (n=14) recurrence were included. Sixty-eight specimens from initial and recurrent biopsies, with a minimum 3-month interval, were analyzed. The expression of CLOCK and BMAL1 was quantified by independently assessing staining intensity and the percentage of positive cells, both of which were then used to calculate the H-score for each antibody. Statistical analyses were performed using SPSS 25.0, with significance set at $p<0.05$.

Results: The mean age of 34 patients was 64.4±10.8 years. Significant stage migration was observed between initial and subsequent biopsies ($p=0.01$), with 9% of cases progressing to muscle-invasive disease. Progressive recurrence was significantly associated with initial pathological stage and grade ($p=0.02$), particularly in non-invasive papillary urothelial carcinoma (pTa) high-grade tumors ($p=0.01$). Peritumoral inflammatory infiltration was identified in 37% of cases and was significantly more frequent in high-grade stages ($p=0.02$) and invasive stages ($p<0.01$). Strong CLOCK expression was found in 99% of cases, while BMAL1 expression was significantly milder in pTa tumors ($p=0.04$). However, changes in CLOCK or BMAL1 H-scores (ΔH-score) and shift work history were not significantly associated with time to disease progression ($p>0.05$).

Conclusion: Our findings suggest that CLOCK protein activation occurs early and remains stable during the pathogenesis of urothelial carcinoma, while BMAL1 expression correlates with the pT stage. However, within this cohort, these circadian regulators did not serve as independent prognostic markers for disease progression. Further studies with larger sample sizes are needed to elucidate the complex role of the circadian system in tumor evolution.

Keywords: Circadian rhythm, CLOCK, BMAL1, urothelial carcinoma, disease progression, immunohistochemistry, NMIBC

Introduction

Bladder cancer is one of the most common malignancies of the urinary tract, with urothelial carcinoma representing the vast majority of cases (1). At the time of initial diagnosis, approximately 75% of patients present with non-muscle-invasive urothelial carcinoma (NMIBC). Despite various treatment modalities, NMIBC is characterized by a high rate of recurrence and a significant risk of progression to muscle-invasive disease, which necessitates lifelong surveillance and impacts patient quality of life (2). Identifying reliable biomarkers that can predict the risk of progression is therefore crucial for optimizing management strategies (3).

In recent years, the role of the circadian rhythm—the internal biological clock that regulates physiological processes over a 24-hour cycle—has gained prominence in cancer research (4-7). At the molecular level, this system is governed by a set of core clock genes, including circadian locomotor output cycles kaput (CLOCK) and brain and muscle ARNT-like 1 (BMAL1). These genes form a transcriptional-translational feedback loop that regulates cell cycle progression, DNA repair, and apoptosis. Disruptions in this system, often caused by lifestyle factors such as shift work, have been classified as potential carcinogens and are increasingly linked to the development and aggressiveness of various cancers (8).

Address for Correspondence: Begüm Çalım Gürbüz, MD, University of Health Sciences Türkiye, Başakşehir Çam and Sakura City Hospital, Clinic of Pathology, İstanbul, Türkiye
E-mail: calimbegum@gmail.com **ORCID ID:** orcid.org/0000-0001-6720-0662
Cite this article as: Çalım Gürbüz B, Bekiroğlu B, Yitiz D, Aker Ş, Korkmaz E, Canat HL. Core circadian clock proteins (CLOCK and BMAL1) in non-muscle-invasive urothelial carcinoma: links to histopathology and tumor progression. İstanbul Med J. 2026; 27(3): 233-7

Received: 30.03.2026
Accepted: 01.07.2026
Publication Date: 03.08.2026

In the context of bladder cancer, the expression patterns of CLOCK and BMAL1 and their association with tumor behavior remain an area of active investigation (9). On the other hand, the molecular influence of circadian regulators on disease progression remains incompletely understood.

This study aims to evaluate the immunohistochemical expression of CLOCK and BMAL1 in patients who were diagnosed with NMIBC at their first biopsy and who subsequently developed either progressive or non-progressive recurrence. By comparing the H-scores of these markers in sequential biopsies and analyzing the relationship of these scores with clinical parameters—such as shift-work history and time to progression—we seek to determine whether circadian clock proteins have potential as prognostic indicators in the clinical course of urothelial carcinoma.

Methods

Case Selection and Preparation

This study was approved by the Scientific Research Ethics Committee No. 2 of Başakşehir Çam and Sakura City Hospital (decision no: 84, date: February 4, 2026). Due to the retrospective design of the study and the use of anonymized data, informed consent was not required in accordance with the Ethics Committee's decision and institutional regulations.

The study included 34 patients over the age of 18 who were diagnosed with NMIBC at their initial biopsy. These patients presented with either progressive or non-progressive recurrences between June 1, 2020, and January 1, 2026, at the Clinic of Pathology of University of Health Sciences Türkiye, Başakşehir Çam and Sakura City Hospital. The progression was defined solely by an increase in stage [e.g., non-invasive papillary urothelial carcinoma (pTa) to pT1/pT2]. Cases were included regardless of sex. A minimum interval of three months between the two biopsies was required, while transurethral resection (TUR) procedures performed solely for residual tumor sampling were excluded. Consequently, 68 bladder TUR and radical cystectomy specimens with sufficient tumor tissue were identified for analysis.

Clinical and Histopathological Parameters

Clinical data and archival records were retrospectively analyzed for the following parameters: age, sex, shift work history (<1 year), and survival status. Specimen-related data included the type (TUR or cystectomy) and tumor dimensions (mm), with the latter derived from cystoscopic or macroscopic measurements. Recurrence status (non-progressive vs. progressive) was determined by comparing the first and second biopsies. Other recorded variables included the inter-biopsy interval (months), pT stage, histological grade (low/high), presence of carcinoma *in situ* (CIS), and peritumoral inflammatory infiltration (PTI), categorized according to the presence of lymphocytes and plasma cells.

Immunohistochemical Staining and Evaluation

The paraffin block most representative of the tumor was selected. Sections of 2 µm thickness were prepared from these blocks and placed on positively charged slides. Staining was performed with CLOCK (JA12-33) rabbit monoclonal antibody (1/50 dilution) and BMAL1 rabbit polyclonal antibody (1/50 dilution) on the Ventana Medical System BenchMark ULTRA/ISH automated stainer, using the Ultraview Universal DAB Detection Kit. For each case, two CLOCK slides and two BMAL1 slides were obtained from both the first and second biopsies. Neural tissue served as a positive control for BMAL1, and colon adenocarcinoma served as a positive control for CLOCK.

Immunohistochemical evaluation of tumor cells was based on cytoplasmic and/or membranous staining for the CLOCK antibody and nuclear staining for the BMAL1 antibody. For both antibodies, the extent of staining in tumor cells was determined as a percentage. Staining intensity was scored as 0 (no staining), 1 (mild), 2 (moderate), and 3 (strong). The H-score was calculated using the formula (1 × 1%+) + (2 × 2%+) + (3 × 3%+), taking into account the percentage of cells corresponding to each intensity level (10). The resulting scores ranged from 0 to 300. Immunohistochemical scoring was performed by two pathologists, and interobserver agreement was assessed.

Statistical Analysis

Data analysis was performed using IBM SPSS Statistics (version 25.0). Categorical variables were expressed as frequencies and percentages, while continuous variables were presented as mean and standard deviation or median (minimum–maximum), as appropriate. The chi-square and Fisher's exact tests were employed to compare categorical data. Normality of the data was assessed using the Shapiro–Wilk test. Accordingly, the Mann–Whitney U test was used to compare non-normally distributed continuous variables. For paired categorical data, the McNemar–Bowker test of marginal homogeneity was performed. Correlation coefficients were evaluated using Spearman's rho. A p value <0.05 was considered statistically significant.

Results

Demographic and Clinical Findings

The mean age of the 34 patients was 64.4±10.8 years (range: 41-86), and 85% (n=29) were male. Seven patients (20%) had a history of shift work. Additionally, there were two deaths (6%) in the series, and the causes of death were unrelated to the primary malignancy. Of the 68 specimens collected from the initial and subsequent biopsies, 64 were obtained via TUR, and 4 were cystectomy specimens (all from the second biopsy). The mean tumor diameter was 30.4±13.4 mm. In terms of progression, 59% (n=20) of cases were classified as non-progressive and 41% (n=14) as progressive. The median interval between biopsies was 4 months (range: 3-20 months) for non-progressive cases and 3 months (range: 3-29 months) for progressive cases.

Histopathological Findings

Analysis of the 68 specimens revealed that 70% (n=48) were pTa, 26% (n=17) were invasive urothelial carcinoma involving the lamina propria (pT1), and 4% (n=3) were invasive urothelial carcinoma with muscularis propria involvement (pT2, all from cystectomy specimens). Significant stage migration was observed between the initial and

subsequent diagnoses (p=0.01). Specifically, while only 12% (n=4) of cases were classified as pT1 at the initial diagnosis, this proportion increased to 39% (n=13) at the second diagnosis. Additionally, 9% (n=3) of cases progressed to muscle-invasive bladder cancer (pT2) during follow-up.

Among the 48 pTa cases, 61% (n=29) were high-grade and 39% (n=19) were low-grade. A statistically significant association was observed between pathological stage/grade and disease progression (p=0.02). Specifically, progressive recurrence was significantly more prevalent in the pTa high-grade group than in the pTa low-grade group (p=0.01). The detailed distribution of pathological stages and grades at initial diagnosis and at recurrence is summarized in Table 1.

CIS was identified in 13 cases (19%). PTI was detected in 25 cases (37%). On initial biopsy, PTI was significantly more frequent in high-grade than in low-grade pTa cases (p=0.02) (Figure 1). Furthermore, when all biopsies were evaluated, PTI was significantly lower in pTa cases than in invasive stages (p<0.01). However, no significant associations were found between disease progression and age, sex, shift work history, survival status, or the presence of CIS or PTI (p>0.05).

Immunohistochemical Findings

CLOCK expression was similar between the first and second biopsies. Strong expression was observed in the majority of cases (99%, n=66), with mean H-scores of 281.4±37.5 in the first biopsy and 278.2±56.5 in the second.

BMAL1: The mean H-score was 94.7±85.4 in the initial biopsy and 83.5±105.7 in the subsequent biopsy. Notably, pTa cases demonstrated significantly higher rates of mild expression compared with other stages (p=0.04).

Representative images illustrating strong CLOCK and mild BMAL1 expression in a non-invasive low-grade pTa are provided in Figure 2.

Progression and H-Score Correlation

Statistical analyses (Mann-Whitney U and univariate logistic regression) showed no significant difference or association between the change in H-score (ΔH-score) and disease progression. Furthermore, Cox regression analysis indicated that CLOCK and BMAL1 ΔH-scores had no significant effect on the time to progression.

Discussion

This study is a pioneering effort examining the expression levels of CLOCK and BMAL1, core components of the circadian rhythm, and the impact of changes in these levels (ΔH-score) on disease progression in patients with NMIBC. The risk of progression remains one of the most critical factors in the surveillance and treatment planning of bladder cancer patients.

Limited epidemiological evidence exists; however, basic research consistently links circadian disruption to bladder cancers (11). In this context, circadian syndrome—exemplified by night-shift workers—has been suggested as a potential risk factor influencing the recurrence and prognosis of NMIBC (12). Despite existing literature associating circadian

Table 1. Distribution of pathological stage and grade in initial and second diagnoses, and their association with tumor progression status

Pathological stage and grade	Initial diagnosis (n=34)	Subsequent diagnosis (n=34)	p value	Non-progressive recurrence (n=20)	Progressive recurrence (n=14)	p value
pTa low-grade	10 (29%)	9 (26%)	0.01*	9 (45%)	1 (7%)	0.01**
pTa high-grade	20 (59%)	9 (26%)		8 (40%)	12 (86%)	
pT1	4 (12%)	13 (39%)		3 (15%)	1 (7%)	
pT2	0 (0%)	3 (9%)		0 (0.0%)	0 (0%)	

*McNemar-Bowker/Marginal homogeneity test, **Fisher's exact test. pTa: Non-invasive papillary urothelial carcinoma

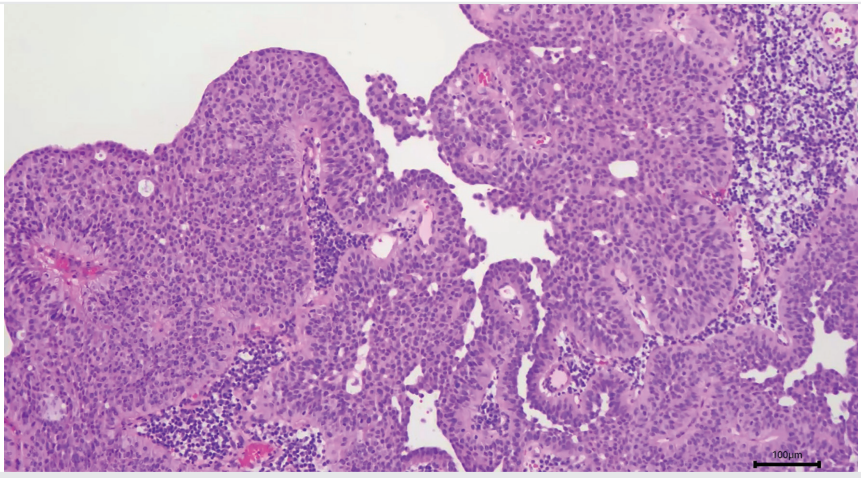

Figure 1. Lymphoplasmacytic inflammatory infiltration surrounding the peritumoral area within the papillary fibrovascular core in a non-invasive high-grade papillary urothelial carcinoma (x10)

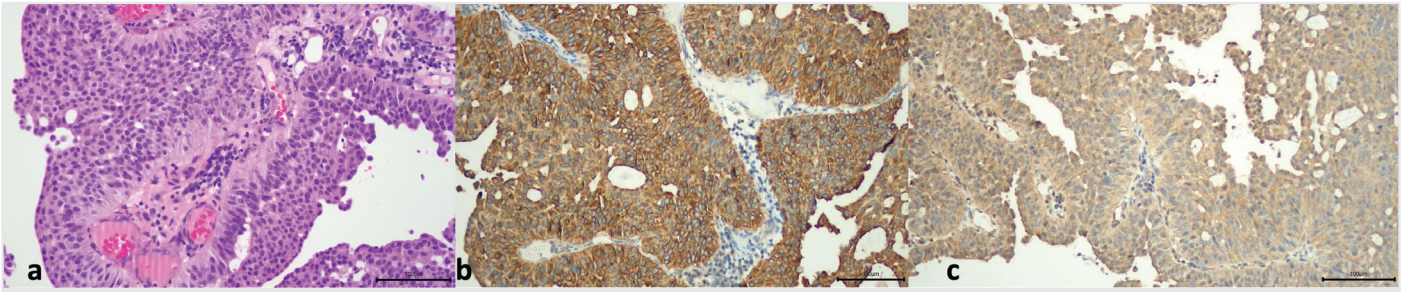

Figure 2. (a) H&E staining of non-invasive low-grade papillary urothelial carcinoma (x20). Immunohistochemical analysis showing (b) strong expression of CLOCK and (c) mild expression of BMAL1 in non-invasive low-grade papillary urothelial carcinoma (x20). H&E: Hematoxylin and eosin

rhythm disruption with increased cancer risk, our cohort did not demonstrate a statistically significant relationship between a history of night-shift work and disease progression. This discrepancy may suggest that the impact of circadian disruption is more pronounced during the tumor initiation phase than during the progression phase.

Non-muscle-invasive bladder carcinoma is characterized by a high recurrence rate; approximately 15%–61% of patients experience recurrence within one year, and 31%–78% within five years following TUR of bladder tumor (13). Non-invasive high-grade urothelial carcinoma, in particular, exhibits a high recurrence rate of up to 80% and can rapidly advance despite its initially non-invasive nature (14). Conversely, non-invasive low-grade pTa is associated with a similarly high recurrence risk (30%-80%) but carries a significantly lower risk (≤5%) of progression to muscle-invasive disease (15). A key observation in our study was the strong association between the initial pathological status and the risk of progressive recurrence. This finding aligns with established literature, which suggests that while pTa low-grade tumors frequently recur, their risk of progression to muscle-invasive disease remains relatively low. Conversely, pTa high-grade tumors represent a more heterogeneous and unpredictable group, exhibiting a significantly higher propensity for upstaging and aggressive clinical behavior.

PTI is a common immune response that frequently correlates with a more favorable prognosis and increased recurrence-free survival in high-grade urothelial carcinoma. While chronic inflammation may drive tumor progression, localized immune cell infiltration often serves as a host defense mechanism, potentially indicating better clinical outcomes (16,17). In our study, the significant association between PTI and high-grade tumors is consistent with existing literature. However, the finding that high-grade tumors with PTI did not demonstrate a significant difference in progression represents a departure from some previous reports. These results should be further validated in larger cohorts, as our current findings may be influenced by the limited sample size.

The immunohistochemical findings regarding CLOCK and BMAL1 in our study are particularly noteworthy. In contrast to the results of Litlekalsoy et al. (9), who reported a decrease in CLOCK expression and an increase in BMAL1 expression across 27 urothelial carcinoma cases—especially in high-grade instances—our study demonstrated consistently strong CLOCK expression and mild BMAL1 expression. Specifically, strong CLOCK expression was detected in 99% of cases in both the initial and recurrent biopsies. Conversely, BMAL1 expression was more variable and generally lower in pTa cases. These observations suggest that CLOCK activation in our patient group occurs early and remains a stable feature of the tumor's evolutionary process, regardless of histological grade or disease progression.

BMAL1 expression is closely associated with disease progression and prognosis in urothelial carcinoma. Generally, an increase in BMAL1 levels is linked to tumor aggressiveness and poor survival rates (18). Our finding in pTa cases with significantly reduced BMAL1 expression provides an important clue that circadian clock proteins may be associated with the invasive potential and stage of the tumor.

However, the lack of a significant difference in the change in CLOCK and BMAL1 H-scores between the progressive and non-progressive groups limits the utility of these markers standalone predictors of progression. These results indicate that although circadian proteins are present in urothelial carcinoma, progression is likely driven primarily by classical histopathological features and other molecular pathways that remain to be fully elucidated.

Study Limitations

Several limitations of this study should be noted, primarily the relatively small sample size, which limits statistical power and the generalizability of the results. The single-center retrospective design, combined with a short median interval between biopsies, may not fully reflect long-term molecular evolution or progression patterns of urothelial carcinoma. Additionally, the limited data on lifestyle factors and the semi-quantitative nature of the immunohistochemical H-score evaluation may have constrained the identification of significant associations between circadian regulators and disease progression.

Conclusion

This study explores the role of circadian rhythm components, CLOCK and BMAL1, in the progression of non-muscle-invasive bladder cancer. Our findings suggest that although these markers are widely expressed, changes in their expression over time do not independently predict disease progression. The consistently strong CLOCK expression observed across biopsies indicates that it may be an early and stable feature of bladder carcinogenesis, whereas the association of BMAL1 with pTa cases links circadian proteins to the tumor's invasive potential. Although PTI serves as a host defense mechanism in high-grade tumors, the initial pathological grade remains the most robust predictor of progressive recurrence. While circadian disruption may influence tumor initiation

rather than progression, these findings warrant further validation in larger cohorts to address the limitations of the current sample size.

Ethics

Ethics Committee Approval: This study was approved by the Scientific Research Ethics Committee No. 2 of Başakşehir Çam and Sakura City Hospital (decision no: 84, date: February 4, 2026).

Informed Consent: Due to the retrospective design of the study and the use of anonymized data, informed consent was not required in accordance with the Ethics Committee's decision and institutional regulations.

Footnotes

Authorship Contributions: Surgical and Medical Practices - B.Ç.G., E.K., H.L.C.; Concept - B.Ç.G., B.B.; Design - B.Ç.G., B.B., D.Y.; Data Collection or Processing - B.Ç.G., B.B., D.Y., Ş.A., E.K., H.L.C.; Analysis or Interpretation - B.Ç.G., B.B., D.Y., Ş.A., E.K., H.L.C.; Literature Search - B.Ç.G., B.B., Ş.A.; Writing - B.Ç.G.

Conflict of Interest: No conflict of interest was declared by the authors.

Financial Disclosure: The authors declared that this study received no financial support.

References

1. Zhang Y, Rumgay H, Li M, Yu H, Pan H, Ni J. The global landscape of bladder cancer incidence and mortality in 2020 and projections to 2040. J Glob Health. 2023; 13: 04109.
2. Manivasagam SS, Kassim A, Raman JD. Diagnosis, evaluation, and management of patients with non-muscle invasive bladder cancer. Future Sci OA. 2026; 12: 2622297.
3. Mihaila RI, Gheorghe AS, Zob DL, Stanculeanu DL. The importance of predictive biomarkers and their correlation with the response to immunotherapy in solid tumors-impact on clinical practice. Biomedicines. 2024; 12: 2146.
4. Xiao L, Chang AK, Zang MX, Bi H, Li S, Wang M, et al. Induction of the CLOCK gene by E2-ERα signaling promotes the proliferation of breast cancer cells. PLoS One. 2014; 9: e95878.
5. Aroca-Siendones MI, Moreno-SanJuan S, Puentes-Pardo JD, Verbeni M, Arnedo J, et al. Core circadian clock proteins as biomarkers of progression in colorectal cancer. Biomedicines. 2021; 9: 967.
6. Shen Z, Zhao Y, Xu X, Yang H, He S, Ma J, et al. Single-cell RNA sequencing integrated with bulk RNA sequencing analysis of clock circadian regulator with prognostic and immune microenvironment in thyroid cancer. Transl Oncol. 2025; 53: 102299.
7. Kuo KL, Chang SJ, Kwan AL, Chai CY. Correlation between levels of clock protein expression and effects on temozolomide-resistant glioblastoma and tumor progression. Hum Cell. 2025; 38: 75.
8. Fagiani F, Di Marino D, Romagnoli A, Travelli C, Voltan D, Di Cesare Mannelli L, et al. Molecular regulations of circadian rhythm and implications for physiology and diseases. Signal Transduct Target Ther. 2022; 7: 41.
9. Litlekalsoy J, Rostad K, Kalland KH, Hostmark JG, Laerum OD. Expression of circadian clock genes and proteins in urothelial cancer is related to cancer-associated genes. BMC Cancer. 2016; 16: 549.
10. Price P, Ganugapati U, Gatalica Z, Kakadekar A, Macpherson J, Quenneville L, et al. Reinventing nuclear histo-score utilizing inherent morphologic cutoffs: blue-brown color H-score (BBC-HS). Appl Immunohistochem Mol Morphol. 2023; 31: 500-6.
11. Li T, Jiang Y, Bai Y, Jiang K, Du G, Chen P, et al. A review for the impacts of circadian disturbance on urological cancers. Sleep Biol Rhythms. 2023; 22: 163-80.
12. Ren JW, Ye JJ, Bai YJ, Han P. The prognostic value of circadian syndrome in non-muscle-invasive bladder cancer: a retrospective cohort study. Int J Surg. 2026; 112: 3948-61.
13. Minato A, Jojima K, Watanabe S, Sugita Y, Mizushima Y, Matsukawa T, et al. Recurrence of low-risk non-muscle-invasive bladder cancer in patients who did not receive immediate intravesical chemotherapy. Cancer Diagn Progn. 2026; 6: 135-43.
14. Jeong SH, Han JH, Jeong CW, Kim HH, Kwak C, Yuk HD, et al. Clinical determinants of recurrence in pTa bladder cancer following transurethral resection of bladder tumor. BMC Cancer. 2022; 22: 631.
15. Isharwal S, Konety B. Non-muscle invasive bladder cancer risk stratification. Indian J Urol. 2015; 31: 289-96.
16. Offersen BV, Knap MM, Marcussen N, Horsman MR, Hamilton-Dutoit S, Overgaard J. Intense inflammation in bladder carcinoma is associated with angiogenesis and indicates good prognosis. Br J Cancer. 2002; 87: 1422-30.
17. Hodgson A, Xu B, Satkunasivam R, Downes MR. Tumour front inflammation and necrosis are independent prognostic predictors in high-grade urothelial carcinoma of the bladder. J Clin Pathol. 2018; 71: 154-60.
18. Wu YJ, Chang SJ, Huang YS, Chai CY. Overexpression of BMAL-1 is related to progression of urothelial carcinoma in arsenic exposure area. Int Urol Nephrol. 2025; 57: 1175-87.

İstanbul Med J 2026; 27(3): 238-44
DOI: 10.4274/imj.galenos.2026.02073

The Effect of Hepatitis B and Alcohol Coexistence on the Development of Hepatocellular Carcinoma in Cirrhotic Patients

Tahir Alper Cinli[1], Sezgin Vatansever[2]

[1]University of Health Sciences Türkiye, Başakşehir Çam ve Sakura City Hospital, Clinic of Hematology, İstanbul, Türkiye
[2]İzmir Atatürk Training and Research Hospital, Clinic of Gastroenterology, İzmir, Türkiye

ABSTRACT

Introduction: This study aimed to retrospectively compare the incidence of hepatocellular carcinoma (HCC), overall survival (OS), and HCC-free survival among patients with cirrhosis of different etiologies: alcohol-related, hepatitis B virus (HBV)-related, and combined HBV-alcohol-related. Additionally, the relationship between HBV viral load and HCC-free survival was evaluated in HBV-positive patients.

Methods: This retrospective single-center cohort study included 648 patients with cirrhosis followed for more than 6 months between July 2007 and April 2014. The patients were categorized into three etiological groups: alcohol-related cirrhosis (n=310), HBV-related cirrhosis (n=294), and HBV-alcohol-related cirrhosis (n=44). Clinical characteristics, HCC incidence, overall survival, and HCC-free survival were compared across these groups.

Results: During the follow-up period, HCC developed in 138 (21.3%) of the 648 patients. The prevalence of HCC differed significantly among the groups: 5.5% in the alcohol group, 34.7% in the HBV group, and 43.2% in the combined HBV-alcohol group ($p<0.001$). The 5-year cumulative HCC risk was 7% for the alcohol group, 40% for the HBV group, and 49% for the HBV-alcohol group. Despite these striking differences in HCC incidence, overall survival did not differ significantly among the etiological groups ($p=0.367$). Furthermore, in HBV-positive patients, baseline HBV DNA viral load ($<10^6$ vs. $\geq 10^6$ copies/mL) did not show a statistically significant difference in HCC-free survival ($p=0.408$).

Conclusion: HBV infection, particularly when combined with heavy alcohol use, significantly and synergistically increases the risk of HCC in patients with liver cirrhosis. The exceptionally high cumulative HCC incidence in the combined HBV-alcohol group, with 40% of patients developing HCC within the first year, underscores the critical need for close surveillance in this high-risk subgroup. Despite the differing HCC rates, overall survival remains similar across the groups, reflecting the complex and multifactorial determinants of cirrhosis-related mortality.

Keywords: Liver cirrhosis, hepatocellular carcinoma, hepatitis B virus, alcohol-related cirrhosis, survival analysis, synergistic effect

Introduction

Liver cirrhosis results from chronic inflammation and fibrosis of the liver, arising from numerous etiological factors. It causes 1.31 million deaths worldwide. The primary causes of cirrhosis include chronic viral hepatitis, alcohol, and non-alcoholic steatohepatitis (1,2). Liver damage from chronic viral hepatitis B (HBV) infection, when combined with heavy alcohol consumption, can lead to irreversible liver damage (3-5). Hepatocellular carcinoma (HCC) is the most significant complication of cirrhosis. It is the third leading cause of cancer-related deaths worldwide. Although some HCC cases can develop de novo, the vast majority (80%) develop in the setting of cirrhosis. The frequency of HCC development in the presence of cirrhosis varies according to the etiological cause of cirrhosis (4,6,7). HBV promotes carcinogenesis through integration of the viral genome into hepatocytes, causing chronic inflammation and inducing genetic instability via reactive oxygen species. In contrast, alcohol leads to HCC development by causing DNA damage through acetaldehyde, mitochondrial dysfunction, intestinal microbiota disruption, impairment of hepatic immune defense, and fibrosis secondary to hepatocyte damage (8,9). The co-occurrence of HBV and alcohol can elevate the risk of HCC to very high levels through a synergistic effect (10-12). Although the risk of HCC development, HCC-free survival, and cumulative HCC frequency in alcohol-related and HBV-related cirrhosis have been examined many times in the literature, large-scale studies demonstrating the synergistic effect of their coexistence are still needed. The outcomes of this synergistic effect are important for determining patient follow-up and surveillance intervals. International

Address for Correspondence: Tahir Alper Cinli, MD, University of Health Sciences Türkiye, Başakşehir Çam ve Sakura City Hospital, Clinic of Hematology, İstanbul, Türkiye
E-mail: tahiralper@hotmail.com **ORCID ID:** orcid.org/0000-0003-2164-9776
Cite this article as: Cinli TA, Vatansever S. The effect of hepatitis B and alcohol coexistence on the development of hepatocellular carcinoma in cirrhotic patients. İstanbul Med J. 2026; 27(3): 238-44

Received: 06.05.2026
Accepted: 01.07.2026
Publication Date: 03.08.2026

guidelines recommend six-month ultrasonographic follow-ups for all patients with cirrhosis, regardless of etiology. However, there is a need for etiologically individualized follow-up systems (13,14). Since the introduction of antiviral agents for HBV, their contribution to the risk of HCC development remains under active study. Many studies have shown that HBV viral load and high HBV DNA levels increase the population-based risk of HCC development. However, there is a need to demonstrate whether this effect continues at the same rate in a damaged hepatocyte environment, such as cirrhosis (15-17). Therefore, in this retrospective study, we compared the demographic, clinical, and laboratory values of patients with HBV-related cirrhosis, alcohol-related cirrhosis, and cirrhosis with HBV-alcohol co-occurrence. We evaluated overall survival, incidence of HCC development, and differences in HCC-free survival among these groups. Additionally, we examined the relationship between HBV viral load and HCC-free survival in the HBV-positive groups.

Methods

Study Design and Ethical Approval

The study was conducted retrospectively among patients who received inpatient or outpatient treatment at the İzmir Katip Çelebi University Atatürk Training and Research Hospital Gastroenterology Clinic. Ethics committee approval for the study was obtained from Ethics Committee of İzmir Katip Çelebi University Atatürk Training and Research Hospital on April 16, 2015 (decision number: 63). The study was conducted in accordance with the principles of the Declaration of Helsinki. Data were collected using the hospital management system.

Patient Population and Eligibility Criteria

Patients with cirrhosis who were followed up for more than 6 months, both as inpatients and outpatients at the İzmir Katip Celebi University Atatürk Training and Research Hospital Gastroenterology Clinic between July 2007 and April 2014 were included. Patients with HBV-related cirrhosis, alcohol-related cirrhosis, and HBV-alcohol coexposure-related cirrhosis were included in the study. Patients with cirrhosis due to hepatitis C, autoimmune hepatitis, non-alcoholic steatohepatitis, cholestatic liver disease, hereditary disorders related to liver disease, and accompanying additional solid malignancies were excluded from the study. A total of 648 eligible patients were included: alcohol-related cirrhosis (n=310, 47.8%), HBV-related cirrhosis (n=294, 45.4%), and HBV-alcohol-related cirrhosis (n=44, 6.8%).

Definitions and Data Collection

The diagnosis of cirrhosis was made based on clinical, ultrasonographic, computed tomography (CT), and magnetic resonance imaging (MRI) features. For etiopathological classification, serological tests [Hepatitis B surface antigen (HBsAg), HBeAg, anti-HBc, and anti-HBs] and quantitative HBV DNA levels were evaluated. For the diagnosis of alcohol-related cirrhosis, the patient's years of alcohol consumption and daily alcohol intake were evaluated. Patients with a daily alcohol consumption >80 mg were classified as heavy alcohol users. Patients meeting both criteria were included as patients with HBV-related cirrhosis and alcohol-related cirrhosis. Patient age, gender, follow-up period (months), vital status at the last follow-up, dates of death (via the death notification system), HCC development during follow-up, Child-Pugh class, baseline HBV DNA level (copies/mL), and alpha-fetoprotein (AFP, ng/mL) were recorded. The diagnosis of HCC was determined by a nodule larger than 1 cm with a characteristic contrast enhancement pattern (arterial phase hypercontrast and venous phase washout) on contrast-enhanced CT or MRI according to the radiological criteria determined by the European Association for the Study of the Liver. Overall survival (OS) was calculated as the time from the date of diagnosis to death from all causes or, in surviving patients, to the date of last follow-up. HCC-free survival was calculated as the time from the date of diagnosis to HCC diagnosis, time to last follow-up in patients without HCC, or time to date of death in patients who did not receive an HCC diagnosis but died due to non-HCC causes. Patients without an HCC diagnosis at the end of the follow-up period were censored. In HBV-positive patients, the cut-off value separating high and low viral loads was determined to be 10^6 copies/mL.

Statistical Analysis

All statistical analyses were performed using IBM SPSS Statistics (version 27.0; IBM Corp., Armonk, NY, USA). Continuous variables were expressed as mean ± standard deviation (SD) for normally distributed data and as median (minimum–maximum or interquartile range) for non-normally distributed data. Categorical variables were presented as frequencies and percentages. Normality of continuous variables was assessed using visual methods (histograms and probability plots) and the Kolmogorov-Smirnov and Shapiro-Wilk tests, as appropriate. Comparisons between two independent groups were performed using the Student's t-test for normally distributed variables and the Mann–Whitney U test for non-normally distributed variables. Comparisons among more than two groups were conducted using one-way analysis of variance or the Kruskal–Wallis test, depending on the data distribution. Categorical variables were compared using the chi-square test or Fisher's exact test, where appropriate. Adjusted residual analysis was additionally used to identify subgroup contributions to significant chi-square results in contingency tables. OS and HCC-free survival were analyzed using the Kaplan–Meier method, and differences between survival curves were evaluated using the log-rank test. Survival times were reported with 95% confidence intervals (CIs). Patients without an event during follow-up were censored at the date of the last clinical evaluation. Cumulative HCC incidence over time was evaluated using life-table analysis according to cirrhosis etiology. HBV viral load categories ($<10^6$ vs. $\geq 10^6$ copies/mL) were compared with respect to HCC-free survival using Kaplan–Meier survival analysis and the log-rank test. All tests were two-tailed, and a p value <0.05 was considered statistically significant.

Results

Baseline Characteristics

The final analysis cohort consisted of 648 patients (Table 1). The cohort was predominantly composed of males (566/648, 87.3%), which reflects the well-known gender bias of both heavy alcohol consumption and HBV-related chronic liver disease. However, gender distribution was significantly non-homogeneous across etiological groups ($p<0.001$): while male gender was nearly universal in the alcohol-related (97.4%)

and HBV-alcohol-related (95.5%) groups, the proportion of female patients was significantly higher in the HBV-related group (24.5%), which is consistent with broader demographic patterns of HBV-related liver disease. In the HBV-related cirrhosis group, the mean baseline age was 61.97±10.84 years, which was significantly higher than that in the alcohol-related cirrhosis (59.44±9.28 years; p=0.006) and HBV-alcohol-related cirrhosis (59.30±8.98 years) groups. Mean follow-up periods in the alcohol-related cirrhosis, HBV-related cirrhosis, and HBV-alcohol-related cirrhosis groups were found to be 39.0, 43.1, and 26.4 months (p=0.106). A significant difference was observed in Child-Pugh classification among the three groups (p=0.001). Patients with alcohol-related cirrhosis were more frequently identified as Child-Pugh A (31.0%), and this rate significantly exceeded the expected frequency (adjusted residual: +4.4), whereas Child-Pugh B was predominant in the HBV group (58.8%; adjusted residual: +2.2). The proportion of Child-Pugh A patients in the HBV group (15.6%) was significantly lower than expected (adjusted residual: -4.2). The distribution of Child-Pugh categories in the HBV-alcohol-related cirrhosis group did not show a significant deviation from the expected values. Neither daily alcohol consumption (alcohol group: median 140 g/day; combined group: 140 g/day; p=0.839) nor serum AFP levels (p=0.769) showed significant differences between the relevant subgroups. Median HBV DNA was generally similar between the HBV and HBV-alcohol-related groups (111.23 vs. 97.78 copies/mL; Mann-Whitney U, p=0.364). The distribution between the two HBV DNA categories ($<10^6$ vs. $\geq 10^6$ copies/mL) also showed no difference between the HBV and HBV-related cirrhosis subgroups (p=0.294).

HCC Incidence

During the follow-up period, HCC developed in 138 out of 648 patients (21.3%). HCC prevalence differed significantly among the etiological groups (chi-square test, p<0.001): 5.5% (n=17) in the alcohol group, 34.7% (n=102) in the HBV group, and 43.2% (n=19) in the HBV-alcohol-related group. These findings confirm that HBV is a strong trigger of hepatocarcinogenesis and that the combined etiology constitutes the highest absolute HCC burden.

Overall Survival Analysis

Kaplan-Meier analysis of OS (Table 2, Figure 1) showed that the mean OS was 76.06 months (95% CI: 70.54–81.58) in the alcohol group, 81.37 months (95% CI: 75.92–86.82) in the HBV group, and 74.54 months (95% CI: 59.81–89.27) in the HBV-alcohol-related group. The overall log-rank test did not reach statistical significance (χ^2: 2.005, df: 2, p=0.367). The absence of a statistically detectable difference in survival between the groups is discussed below.

Table 1. Baseline demographic, clinical and laboratory characteristics according to etiology of cirrhosis

Variable	Alcohol-related (n=310)	HBV-related (n=294)	HBV + alcohol (n=44)	p value
Sex, n (%)				<0.001
Male	302 (97.4%)	222 (75.5%)	42 (95.5%)	
Female	8 (2.6%)	72 (24.5%)	2 (4.5%)	
Age (years), mean ± SD	59.44 ± 9.28	61.97 ± 10.84	59.30 ± 8.98	0.006
Follow-up (months), median (range)*	39.0 (6–114)	43.1 (6–115)	26.4 (7–113)	0.106
Hepatocellular carcinoma, n (%)				<0.001*
Present	17 (5.5%)	102 (34.7%)	19 (43.2%)	
Absent	293 (94.5%)	192 (65.3%)	25 (56.8%)	
Alcohol consumption (g/day), median (range)*	140 (80–300)	NA	140 (80–280)	0.839
Duration of alcohol use (years), median (range)*	25 (15–45)	NA	23 (14–50)	0.003
HBV DNA (copies/mL), median*	NA	111.23	97.78	0.364
AFP (ng/mL), median**	56.25	57.80	64.03	0.769
Child-Pugh class, n (%)***				0.001
Class A	96 (31.0%)	46 (15.6%)	9 (20.5%)	
Class B	152 (49.0%)	173 (58.8%)	25 (56.8%)	
Class C	62 (20.0%)	75 (25.6%)	10 (22.7%)	

*Mann-Whitney U test applied. **Kruskal-Wallis test; n=115 with available AFP data (alcohol n=12, HBV n=87, combined n=16). ***Adjusted residuals used for cell-level post-hoc analysis. Bold p values indicate statistical significance (p<0.05). SD: Standard deviation, HBV: Hepatitis B virus, AFP: Alpha-fetoprotein, NA: Not applicable

Table 2. Kaplan-Meier overall survival estimates by etiology of cirrhosis

Cirrhosis etiology	Total n	Events n	Censored n (%)	Mean survival (months)	p value
Alcohol-related	310	113	197 (63.5%)	76.06 (70.54-81.58)	
HBV-related	294	94	200 (68.0%)	81.37 (75.92-86.82)	
HBV + alcohol	44	15	29 (65.9%)	74.54 (59.81-89.27)	0.367
Overall	648	222	426 (65.7%)	78.41 (74.64-82.18)	

HBV: Hepatitis B virus

HCC- Free Survival Analysis

Kaplan-Meier analysis of HCC-free survival (Table 3, Figure 2) paralleled the OS analysis, and the log-rank test was statistically significant across all three groups (p=0.367). However, the event rates differed significantly: 5.5% of patients in the alcohol group, 34.7% of patients in the HBV group, and 43.2% of patients in the HBV-alcohol-related group experienced HCC events. The markedly higher censoring rate in the alcohol group (94.5%), reflecting both a low HCC rate and longer event-free periods, reduced the statistical power to detect differences within the Kaplan-Meier framework.

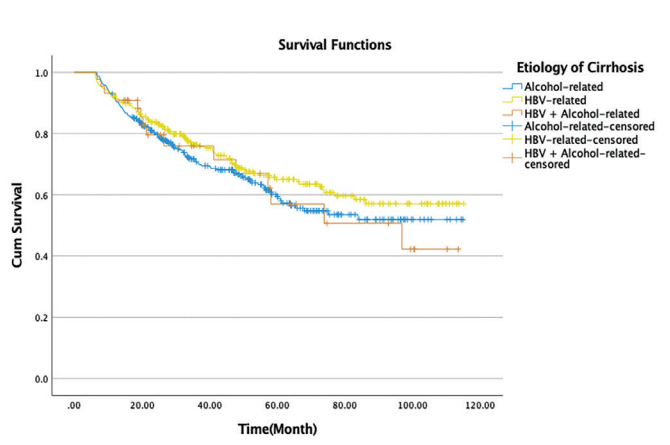

Figure 1. Kaplan-Meier overall survival estimates by etiology of cirrhosis. HBV: Hepatitis B virus

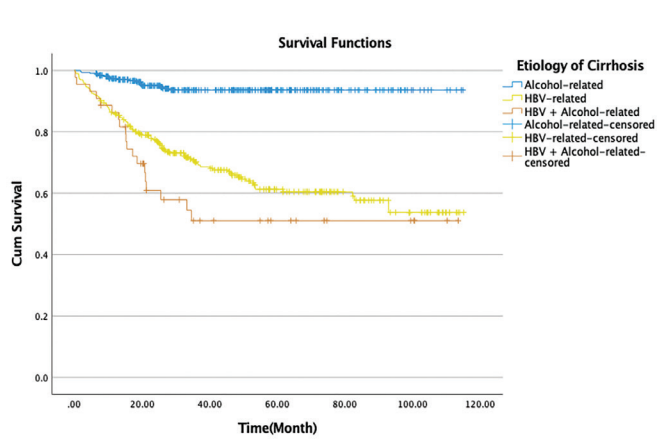

Figure 2. Kaplan-Meier HCC- free survival estimates by etiology of cirrhosis. HCC: Hepatocellular carcinoma, HBV: Hepatitis B virus

Cumulative HCC Incidence by Etiology

Life-table analysis revealed a progressive, etiology-dependent differentiation in cumulative HCC incidence rates (Table 4, Figure 3). In the alcohol group, the cumulative HCC risk was low and essentially plateaued after the first year: 5% at one year, 7% at three years, and 7% at five years. In contrast, a rapid early increase followed by continuous accumulation was observed in patients with HBV-related cirrhosis: 22% at one year, 34% at three years, and 40% at five years. The most prominent early increase in HCC risk was observed in the HBV-alcohol-related group: 40% at one year and 49% at both three and five years; this indicates that nearly half of the patients in this subgroup developed HCC and that most events occurred within the first year of the follow-up period.

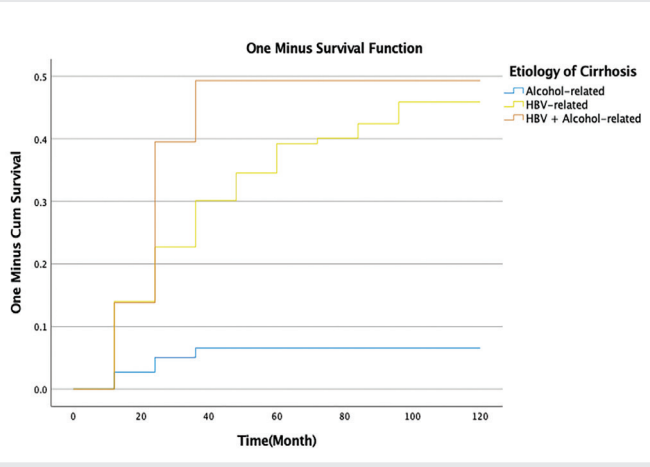

Figure 3. Cumulative HCC incidence by etiology of cirrhosis. HCC: Hepatocellular carcinoma, HBV: Hepatitis B virus

Table 3. Kaplan-Meier HCC- free survival estimates by etiology of cirrhosis

Cirrhosis etiology	n	HCC events n (%)	Censored n (%)	Mean HCC-free survival (months, 95% CI)	p value
Alcohol-related	310	17 (5.5%)	293 (94.5%)	76.06 (70.54–81.58)	
HBV-related	294	102 (34.7%)	192 (65.3%)	81.37 (75.92–86.82)	
HBV + alcohol	44	19 (43.2%)	25 (56.8%)	74.54 (59.81–89.27)	0.367

HCC: Hepatocellular carcinoma, HBV: Hepatitis B virus, CI: Confidence interval

Table 4. Cumulative HCC incidence at 1,3,5 years by etiology of cirrhosis

Etiology	1-year risk (%)	3-year risk (%)	5-year risk (%)
Alcohol-related cirrhosis	5%	7%	7%
HBV-related cirrhosis	22%	34%	40%
HBV + alcohol cirrhosis	40%	49%	49%

Cumulative risk: 1-cumulative survival, derived from life-table (actuarial) analysis at months 12, 36, and 60. HBV: Hepatitis B virus, HCC: Hepatocellular carcinoma

HBV Viral Load and HCC-Free Survival

Of the 221 HBV-positive patients with available DNA quantification data, 97 had HBV DNA $<10^6$ copies/mL and 124 had HBV DNA $\geq 10^6$ copies/mL (Table 5, Figure 4). HCC events occurred at rates of 20.6% and 28.2% in the low- and high-viral-load categories, respectively. Mean HCC-free survival was 89.85±4.66 months (95% CI: 80.70–98.99) in the low viral load group and 84.82±4.09 months (95% CI: 76.80–92.84) in the high viral load group. The log-rank test did not detect a statistically significant difference between the categories (p=0.408).

Discussion

This large, retrospective, single-center cohort study of 648 patients with HBV-, alcohol-, and combined HBV-alcohol-related cirrhosis demonstrates that etiology is a critical determinant of HCC risk; the combined HBV-alcohol group showed the highest cumulative incidence (49% at 5-years), followed by HBV-related (40%) and alcohol-related cirrhosis (7%). These findings are highly consistent with and substantially extend the existing evidence base on etiology-specific HCC risk in cirrhotic populations. The strikingly low HCC incidence in the alcohol-related group (5.5%) compared with the HBV-related (34.7%) and combined (43.2%) groups aligns with published meta-analytic estimates. Huang et al. (18) reported that the annual HCC incidence in alcohol-related cirrhosis is approximately 1.0–1.5% per year (19). In contrast, the corresponding figure for HBV-related cirrhosis ranges from 2.5% to 7.5% per year, depending on the viral replication status, geographic region, and use of antiviral therapy (4). In our HBV group, the observed five-year cumulative HCC incidence was 40%, corresponding to approximately 8% per year, which falls at the upper end of previously reported estimates.

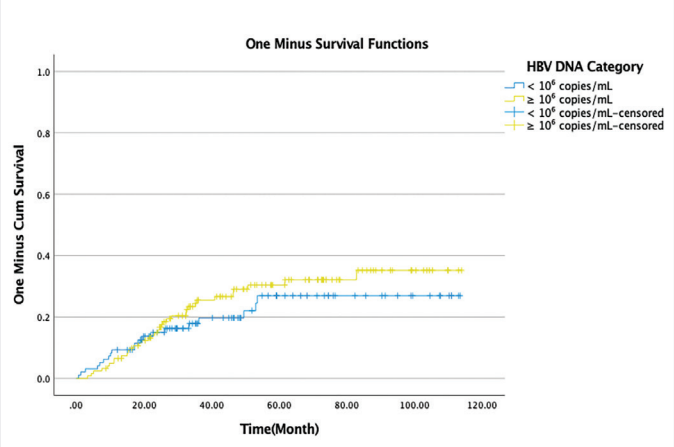

Figure 4. HCC free survival according to HBV DNA category in HBV-positive patients. HCC: Hepatocellular carcinoma, HBV: Hepatitis B virus

This likely reflects the relatively advanced disease stage at baseline in our cohort (predominance of Child-Pugh B), the inclusion of patients from the pre-antiviral era, and the Turkish epidemiological context, where HBV genotypes with high oncogenic potential are prevalent (20). The HBV-alcohol combination not only conferred the highest five-year HCC risk (49%) but also showed the steepest early accumulation; 40% of patients developed HCC within the first year. This finding is consistent with the mechanistic synergy between HBV and alcohol demonstrated in several large-scale studies. Lin et al. (21) showed that heavy alcohol use more than doubled HCC incidence in patients with HBV-related cirrhosis, and Tsai et al. (22) confirmed that the combination of heavy alcohol intake and *ALDH2* gene variants significantly increases HCC risk beyond that attributable to HBV alone. Mechanistically, alcohol accelerates HBV-mediated carcinogenesis by enhancing viral replication through acetaldehyde-induced epigenetic reprogramming, impairing HBV-specific T-cell immunity, increasing oxidative DNA damage, and pro moting fibrosis progression; together, these effects lower the threshold for malignant transformation in hepatocytes already destabilized by viral genome integration (10,16). Despite the marked differences in HCC risk, overall survival did not differ significantly among etiologic groups (log-rank p=0.367). Although it is somewhat unexpected that a four- to eightfold difference in HCC incidence does not translate into a statistically detectable difference in OS, several explanations are plausible. First, overall survival in cirrhosis is shaped by multiple complications: portal hypertensive events (bleeding, spontaneous bacterial peritonitis, hepatorenal syndrome), sepsis, hepatic decompensation, and comorbid conditions; none of these are systematically less severe in the alcohol group, despite its lower HCC risk. Second, the possibility cannot be excluded that antiviral therapy in HBV patients—systematically unrecorded in this dataset—may have improved overall survival in the HBV group while at the same time limiting HCC-related mortality (23,24). Third, the limited sample size of the HBV–alcohol group (n=44) reduces the statistical power to detect between-group differences in overall survival. Taken together, these factors suggest that while etiology strongly shapes HCC risk, its impact does not necessarily translate into discernible differences in OS (25). The lack of a statistically significant association between HBV viral load categories and HCC-free survival (p=0.408) warrants cautious interpretation. Large prospective studies, such as REVEAL, have identified HBV DNA levels as an independent dose–response determinant of HCC in asymptomatic HBsAg carriers (15,16). However, the relationship between HBV DNA and HCC has been established largely in populations without established cirrhosis. In patients with pre-existing cirrhosis, the hepatic microenvironment is already highly permissive to carcinogenesis. HCC may arise independently of current viral replication status, particularly after prolonged periods of persistently high-level viremia that may have occurred prior to the study

Table 5. HCC free survival according to HBV DNA category in HBV-positive patients

HBV DNA category	N	HCC events n (%)	Mean HCC-free survival (months ± SE)	p value
$<10^6$ copies/mL	97	20 (20.6%)	89.85±4.66 (80.70–98.99)	0.408
$\geq 10^6$ copies/mL	124	35 (28.2%)	84.82±4.09 (76.80–92.84)	
Total	221	55 (24.8%)	86.96±3.09 (80.89–93.03)	

Kaplan-Meier analysis with log-rank test. Only patients with available HBV DNA data (n = 221) are included. SE: Standard error, CI: Confidence interval, HCC: Hepatocellular carcinoma, HBV: Hepatitis B virus

entry point (26). In our study, HBV DNA measurement reflected a cross-sectional value at the time of cirrhosis diagnosis. Regression analysis and dynamic monitoring of viral load after treatment could not be evaluated because of the study's retrospective design. Furthermore, HBV DNA data were available for only 221 of 338 HBV-positive patients, introducing potential selection bias that may have attenuated the observed association. Future studies incorporating serial HBV DNA measurem ents and detailed antiviral treatment data will be critical to fully charac terize this relationship in cirrhotic populations (27,28). The observed sex distribution across groups—near-universal male predominance in the alcohol and HBV–alcohol–related groups (97.4% and 95.5%, resp ectively) and a markedly higher proportion of women in the HBV group (24.5%)—is consistent with well-documented epidemiological data on heavy alcohol use disorder and HBV infection. Globally, the male-to-female ratio for alcohol-related cirrhosis ranges from approximately 4:1 to 10:1 (18,19). By contrast, HBV infection affects both sexes without a similarly pronounced imbalance, and in endemic settings, women with HBV-related cirrhosis may constitute a larger proportion of clinical cohorts. The higher mean age observed in the HBV group (61.97 years vs. approximately 59 years in the other groups) likely reflects the prolonged natural course of chronic HBV infection, in which cirrhosis typically develops after decades of subclinical disease. In contrast, liver disease related to heavy alcohol consumption tends to follow a more rapidly progressive course (3,4). The differing distribution of Child–Pugh classes between groups may be explained by earlier detection of alcohol-related cirrhosis at a compensated stage, resulting in a predominance of Child–Pugh A in the alcohol group. In contrast, the characteristically silent nature of HBV infection, with few early clinical symptoms, often leads to diagnosis at a more advanced stage, which likely underlies the predominance of Child–Pugh B in the HBV-related cirrhosis group (25). The extremely high HCC incidence in the HBV–alcohol-related cirrhosis group (40% within one year), irrespective of hepatic reserve, suggests that this subgroup requires imaging surveillance at intervals shorter than six months. International guidelines currently recommend ultrasonography surveillance every six months for all patients with c irrhosis; however, the dramatic early HCC burden in the combined group suggests that contrast-enhanced cross-sectional imaging (CT or MRI) ma y be necessary as the primary surveillance modality for these high-risk individuals (13,14). The lower five-year HCC risk in the alcohol-related cirrhosis group (7%) indicates that, even in the setting of established cirrhosis, alcohol abstinence may confer meaningful protection against HCC and underscores the importance of alcohol use disorder interventions as an integral component of cirrhosis management. The substantial HCC risk observed even in the low viral load group indicates that HBV-infected patients with cirrhosis should receive treatment with nucleos(t)ide analogs irrespective of the viral load.

Study Limitations

This study has several limitations. Its retrospective, single-center design limits generalizability and introduces risks of selection and information bias. Patients with missing baseline data were excluded, which may have shifted the analytic sample toward individuals with more complete medical records. HBV DNA measurement was cross-sectional rather than serial, and antiviral treatment data were not systematically captured; both factors constrain the interpretation of the viral load analysis. Alcohol use was assessed based on patient history and chart review rather than objective biomarkers (e.g., phosphatidylethanol). Moreover, assessment of additional comorbid factors such as body mass index, metabolic syndrome, and other coexisting conditions was incomplete due to the retrospective design.

Conclusion

This retrospective study demonstrates that HBV infection, particularly when combined with heavy alcohol use, significantly increases HCC risk in patients with liver cirrhosis. The HBV-alcohol combination group exhibited the highest five-year cumulative HCC incidence (49%), with 40% of patients developing HCC within the first year, underscoring the importance of close surveillance in this subgroup. Despite differing HCC rates, overall survival did not differ significantly among etiologic groups, reflecting the complex, multifactorial determinants of cirrhosis-related mortality. HBV viral load did not independently predict HCC-free survival in this cirrhotic cohort, a finding that warrants further investigation in prospective studies incorporating serial viral load assessments and comprehensive antiviral treatment data. These results support etiology-specific, risk-stratified approaches to HCC surveillance and highlight the critical importance of effective antiviral therapy for HBV-positive cirrhotic patients and of alcohol cessation counseling for all patients with alcohol-related or alcohol-concomitant liver disease.

Ethics

Ethics Committee Approval: Ethics committee approval for the study was obtained from Ethics Committee of İzmir Katip Çelebi University Atatürk Training and Research Hospital on April 16, 2015 (decision number: 63).

Informed Consent: Data were collected using the hospital management system.

Footnotes

Authorship Contributions: Surgical and Medical Practices - S.V.; Concept - S.V.; Design - T.A.C., S.V.; Data Collection or Processing - T.A.C.; Analysis or Interpretation - T.A.C., S.V.; Literature Search - T.A.C.; Writing - T.A.C.

Conflict of Interest: No conflict of interest was declared by the authors.

Financial Disclosure: The authors declared that this study received no financial support.

References

1. Juanola A, Pose E, Ginès P. Liver cirrhosis: ancient disease, new challenge. Med Clin (Barc). 2025; 164: 238-46.
2. Manthey J, Shield KD, Rylett M, Hasan OSM, Probst C, Rehm J. Global alcohol exposure between 1990 and 2017 and forecasts until 2030: a modelling study. Lancet. 2019; 393: 2493-502.
3. GBD 2017 Cirrhosis Collaborators. The global, regional, and national burden of cirrhosis by cause in 195 countries and territories, 1990–2017: a systematic analysis for the Global Burden of Disease Study 2017. Lancet Gastroenterol Hepatol. 2020; 5: 245-66.

4. Sankar K, Gong J, Osipov A, Miles SA, Kosari K, Nissen NN, et al. Recent advances in the management of hepatocellular carcinoma. Clin Mol Hepatol. 2024; 30: 1-15.
5. Seitz HK, Bataller R, Cortez-Pinto H, Gao B, Gual A, Lackner C, et al. Alcoholic liver disease. Nat Rev Dis Primers. 2018; 4: 16.
6. Mancebo A, González-Diéguez ML, Cadahía V, Varela M, Pérez R, Navascués CA, et al. Annual incidence of hepatocellular carcinoma among patients with alcoholic cirrhosis and identification of risk groups. Clin Gastroenterol Hepatol. 2013; 11: 95-101.
7. Jee SH, Ohrr H, Sull JW, Samet JM. Cigarette smoking, alcohol drinking, hepatitis B, and risk for hepatocellular carcinoma in Korea. J Natl Cancer Inst. 2004; 96: 1851-6.
8. Mackowiak B, Fu Y, Maccioni L, Gao B. Alcohol-associated liver disease. J Clin Invest. 2024; 134: e176345.
9. Rehm J, Samokhvalov AV, Shield KD. Global burden of alcoholic liver diseases. J Hepatol. 2013; 59: 160-8.
10. Poorolajal J, Shadi Y, Heshmati B. Interaction between hepatitis B, hepatitis C and alcohol in the development of hepatocellular carcinoma: a systematic review and meta-analysis. J Viral Hepat. 2025; 31: e14042.
11. Ganesan M, Eikenberry A, Poluektova LY, Kharbanda KK, Osna NA. Role of alcohol in pathogenesis of hepatitis B virus infection. World J Gastroenterol. 2020; 26: 883-903.
12. Kulik L, El-Serag HB. Epidemiology and management of hepatocellular carcinoma. Gastroenterology. 2019; 156: 477-91.
13. European Association for the Study of the Liver. EASL Clinical Practice Guidelines on the management of hepatocellular carcinoma. J Hepatol. 2025; 82: 315-74.
14. Hwang SY, Danpanichkul P, Agopian V, Mehta N, Parikh ND, Abou-Alfa GK, et al. Hepatocellular carcinoma: updates on epidemiology, surveillance, diagnosis and treatment. Clin Mol Hepatol. 2025; 31: S228-54.
15. Harputluoglu M, Carr BI. Hepatitis B before and after hepatocellular carcinoma. J Gastrointest Cancer. 2021; 52: 1206-10.
16. El-Serag HB. Epidemiology of viral hepatitis and hepatocellular carcinoma. Gastroenterology. 2012; 142: 1264-73.
17. Lyu X, Liu K, Chen Y, Wang Z, Yao J, Cai G, et al. Analysis of risk factors associated with the development of hepatocellular carcinoma in chronic HBV-infected Chinese: a meta-analysis. Int J Environ Res Public Health. 2016; 13: 604.
18. Huang DQ, Terrault NA, Tacke F, Gluud LL, Arrese M, Bugianesi E, et al. Global epidemiology of cirrhosis - aetiology, trends and predictions. Nat Rev Gastroenterol Hepatol. 2023; 20: 388-98.
19. Huang DQ, Mathurin P, Cortez-Pinto H, Loomba R. Global epidemiology of alcohol-associated cirrhosis and HCC: trends, projections and risk factors. Nat Rev Gastroenterol Hepatol. 2023; 20: 37-49.
20. Abassa KK, Wu XY, Xiao XP, Zhou HX, Guo YW, Wu B. Effect of alcohol on clinical complications of hepatitis virus-induced liver cirrhosis: a consecutive ten-year study. BMC Gastroenterol. 2022; 22: 140.
21. Lin CW, Lin CC, Mo LR, Chang CY, Perng DS, Hsu CC, et al. Heavy alcohol consumption increases the incidence of hepatocellular carcinoma in hepatitis B virus-related cirrhosis. J Hepatol. 2013; 58: 730-5.
22. Tsai MC, Yang SS, Lin CC, Wang WL, Hsu YC, Chen YS, et al. Association of Heavy Alcohol Intake and ALDH2 rs671 Polymorphism with hepatocellular carcinoma and mortality in patients with hepatitis B virus-related cirrhosis. JAMA Netw Open. 2022; 5: 2223511.
23. Sung JJY, Tsoi KKF, Wong VWS, Li KCT, Chan HLY. Meta-analysis: treatment of hepatitis B infection reduces risk of hepatocellular carcinoma. Aliment Pharmacol Ther. 2008; 28: 1067-77.
24. Wong GL, Chan HL, Mak CW, Lee SK, Ip ZM, Lam AT, et al. Entecavir treatment reduces hepatic events and deaths in chronic hepatitis B patients with liver cirrhosis. Hepatology. 2013; 58: 1537-47.
25. Morgan TR, Mandayam S, Jamal MM. Alcohol and hepatocellular carcinoma. Gastroenterology. 2004; 127: 87-96.
26. Ioannou GN, Green P, Kerr KF, Berry K. Models estimating risk of hepatocellular carcinoma in patients with alcohol or NAFLD-related cirrhosis for risk stratification. J Hepatol. 2019; 71: 523-33.
27. Jepsen P, Ott P, Andersen PK, Sørensen HT, Vilstrup H. Risk for hepatocellular carcinoma in patients with alcoholic cirrhosis: a Danish nationwide cohort study. Ann Intern Med. 2012; 156: 841-7.
28. Huang DQ, Tan DJH, Ng CH, Amangurbanova M, Sutter N, Lin Tay PW, et al. Hepatocellular carcinoma incidence in alcohol-associated cirrhosis: systematic review and meta-analysis. Clin Gastroenterol Hepatol. 2023; 21: 1169-77.

İstanbul Med J 2026; 27(3): 245-51
DOI: 10.4274/imj.galenos.2026.52284

Magnetic Resonance Imaging Texture Analysis for Predicting Chemoradiotherapy Response in Locally Advanced Rectal Cancer

Murat Özoğul[1], Kamil Canpolat[2], Eşref Başaran[3], Murat Baykara[4]

[1]University of Health Sciences Türkiye, İstanbul Training and Research Hospital, Clinic of Radiology, İstanbul, Türkiye
[2]Medicalpark İzmir Hospital, Clinic of Radiology, İzmir, Türkiye
[3]University of Health Sciences Türkiye, Sultan 2. Abdülhamid Han Training and Research Hospital, Clinic of Radiology, İstanbul, Türkiye
[4]University of Health Sciences Türkiye, Haydarpaşa Numune Training and Research Hospital, Clinic of Radiology, İstanbul, Türkiye

ABSTRACT

Introduction: This study investigated the predictability of treatment response to neoadjuvant chemoradiotherapy (nCRT) using texture analysis derived from pre-treatment magnetic resonance imaging (MRI) in patients diagnosed with locally advanced rectal cancer (LARC).

Methods: A total of 47 patients (28 males and 19 females) diagnosed with LARC who received nCRT between 2018 and 2025 were retrospectively reviewed in the hospital archives. Texture analysis was performed on pretreatment MR images, specifically on T2-weighted images, apparent diffusion coefficient (ADC) maps, and contrast-enhanced T1-weighted images. For the assessment of treatment response, patients were classified according to the modified Ryan tumor regression grading system: those with Ryan grades 0 and 1 were assigned to the favorable response group, while those with Grades 2 and 3 were assigned to the poor response group. Statistical analysis was conducted using the Mann-Whitney U test, receiver operating characteristic curve analysis, and multivariable logistic regression.

Results: Statistically significant differences were detected between the responding and non-responding groups across 44 texture parameters in the three sequences. The multivariable logistic regression model was statistically significant ($p<0.001$). A combined predictive model, including the contrast of matrix from the ADC sequence and the contrast of matrix and energy of matrix from the contrast-enhanced T1-weighted sequence, explained 74.3% of the variance in treatment response and correctly classified 91.3% of the patients.

Conclusion: Texture analysis derived from pre-treatment magnetic MR imaging can predict the response to neoadjuvant therapy with high accuracy in patients with LARC. This non-invasive approach demonstrates considerable potential as a clinical tool to guide personalized treatment strategies, thereby facilitating the selection of optimal therapeutic regimens for patients who are unlikely to benefit from standard protocols.

Keywords: Rectal cancer, magnetic resonance imaging, texture analysis, radiomics, chemoradiotherapy

Introduction

Colorectal cancer is the third most frequently diagnosed cancer worldwide, with rectal cancer accounting for approximately 40% of all cases. It ranks third in incidence among men, whereas among women, it is the second most common malignancy (1,2). The incidence of colorectal cancer is disproportionately higher in Western countries, a trend that has been consistently associated with lifestyle-related risk factors such as obesity, metabolic syndrome, and dietary patterns rich in red and processed meats but low in fiber (3).

In patients with suspected rectal cancer, magnetic resonance imaging (MRI) has emerged as the modality of choice for the diagnosis of rectal cancer because of its superior soft tissue contrast and multiplanar imaging capabilities. MRI allows accurate evaluation of tumor size, local extension, and circumferential resection margin involvement, as well as precise assessment of regional lymph nodes and potential metastatic disease. Furthermore, MRI is invaluable for monitoring treatment response after neoadjuvant therapy and detecting local recurrence following surgical resection, thereby playing a central role in guiding treatment strategies and long-term patient management (4-6).

Address for Correspondence: Murat Özoğul, MD, University of Health Sciences Türkiye, İstanbul Training and Research Hospital, Clinic of Radiology, İstanbul, Türkiye
E-mail: muratozogl@gmail.com **ORCID ID:** orcid.org/0000-0001-5825-911X
Cite this article as: Özoğul M, Canpolat K, Başaran E, Baykara M. Magnetic resonance imaging texture analysis for predicting chemoradiotherapy response in locally advanced rectal cancer. İstanbul Med J. 2026; 27(3): 245-51

Received: 22.04.2026
Accepted: 06.07.2026
Publication Date: 03.08.2026

The standard treatment protocol for locally advanced rectal cancer (LARC) consists of neoadjuvant chemoradiotherapy (nCRT) followed by total mesorectal excision (TME). Pathological evaluations performed after CRT have demonstrated not only a complete response in some patients but also downstaging of tumor stage. Clinical follow-up of patients who achieved a complete response revealed that their 5 year recurrence and metastasis rates were approximately three times lower than those with a partial response (7-9).

Assessment following nCRT is critical for determining subsequent treatment strategies and predicting the disease course. Although conventional MRI plays a central role in evaluating the extent of disease prior to treatment, it has certain limitations in the post-CRT setting, particularly in distinguishing the primary tumor from radiation-induced fibrosis. MRI assessment in this context is most performed using T2 weighted sequences and apparent diffusion coefficient (ADC) maps derived from diffusion-weighted imaging (DWI) (10). Texture analysis is fundamentally based on computer-assisted data processing, in which statistical parameters are derived from imaging datasets. In recent years, it has been increasingly applied across a broad range of clinical domains, particularly in the field of oncological imaging. In digital images, each pixel and voxel is represented by a specific gray-level intensity value. Quantitative statistical features can be extracted by evaluating the distribution and interrelationships of these gray levels using various mathematical approaches. These parameters provide objective information that facilitates the interpretation of digital medical images and contributes to a more comprehensive image analysis (11,12).

This study aimed to employ texture analysis as a novel imaging method to predict the direction and magnitude of response to nCRT in patients with LARC prior to therapy.

Methods

Ethical approval was obtained from, University of Health Sciences Türkiye, Haydarpaşa Numune Training and Research Hospital on September 11, 2023 (decision number: HNEAH-KAEK 2023/163, HNEAH-KAEK 2023/KK/163). Given the retrospective design of the study, the requirement to obtain written informed consent from the patients was waived by the committee.

Study Population

Patients diagnosed with LARC between 2018 and 2025 were retrospectively reviewed using Haydarpaşa Numune Training and Research Hospital institutional Picture Archiving and Communication System (PACS) database. Individuals with locally advanced disease who received nCRT were eligible for inclusion. Patients with a histopathological diagnosis of mucinous adenocarcinoma, patients without available pathological confirmation, and patients who had undergone surgery at an external institution were excluded from the analyses. Haydarpaşa Numune Training and Research Hospital is equipped with two different MRI scanners; for the purposes of this study, only the cohort imaged with the scanner that contributed to the greater number of examinations was evaluated. Patients imaged with heterogeneous or non-standard MRI sequences were excluded. Ultimately, 47 patients who fulfilled the inclusion criteria were enrolled in this study.

In summary, patients meeting any of the following criteria were excluded from the study:

- Histopathological diagnosis of mucinous adenocarcinoma
- Imaging performed with a non-standard MRI protocol
- Receipt of neoadjuvant therapy at an external institution
- Surgical resection performed at an external institution
- Inability to tolerate or complete the planned nCRT regimen
- Insufficient image quality for appropriate diagnostic evaluation

Image Acquisition

MRI was performed using a 1.5-T scanner (General Electric, Milwaukee, WI, USA) with a standard imaging protocol. Following completion of nCRT, post-treatment MRI examinations were performed within 6-8 weeks prior to surgical resection. The protocol included a T2-weighted fast spin-echo sequence [repetition time/echo time (TR/TE), 4556/100 ms; field of view (FOV), 380 × 380 mm; matrix, 224 × 192; slice thickness, 3 mm], an axial DWI sequence (b values, 0, 400, and 800 s/mm^2; TR/TE, 2500/65 ms; FOV, 380 × 380 mm; matrix, 224 × 192; slice thickness, 6 mm), and axial T1-weighted images (TR/TE, 4.4/2.1 ms; FOV, 380 × 380 mm; matrix, 300 × 192; slice thickness, 1 mm). Quantitative ADC maps were generated using a monoexponential decay model applied to three b values. Images were obtained in planes oriented perpendicular and parallel to the long axis of the rectal tumor.

Histopathological Examination

The pathological response (pCR) was assessed in the resection specimens by a pathologist (15 years experience) with extensive expertise in gastrointestinal pathology, ensuring a high level of diagnostic accuracy and consistency. Following detailed histopathological examination, the collected data were systematically categorized according to the pathological TNM classification system, which provides a standardized framework for tumor staging. Furthermore, the degree of response to neoadjuvant treatment was evaluated using the tumor regression grading system proposed by Ryan et al. (13).

Neoadjuvant Chemoradiotherapy Scheme

All patients received preoperative concurrent CRT. The treatment regimen consisted of a total radiotherapy dose of approximately 52 Gy delivered over a 5-week period, administered five days per week, with an additional boost as indicated. Chemotherapy was administered concurrently either as 5-fluorouracil (425 mg/m^2/day) administered during the 1st and 5th weeks of radiotherapy or as capecitabine (825 mg/m^2/day) administered 5 days per week throughout the 5-week course of radiotherapy. Surgical resection was performed 6-8 weeks after CRT completion.

Analysis of Images

Magnetic resonance images, including axial T2 weighted, ADC, and axial contrast enhanced T1 weighted sequences, were exported in Digital Imaging and Communications in Medicine (DICOM) 3.0 format to the Windows 10 operating system (Microsoft Corporation, Seattle, WA, USA), with each sequence processed separately. Image analysis was

performed using the ROIEX 3.1 software. A circular ROI was manually drawn on the slice where the tumor was most clearly visualized, covering approximately two-thirds of the lesion to minimize the inclusion of artifacts. Imaging data were retrieved from the PACS in DICOM format and transferred to a Windows 10 workstation (Microsoft Corporation, Seattle, WA, USA) for subsequent analysis. All eligible images were processed using a custom in-house analysis pipeline developed in MATLAB (R2023b; MathWorks, Natick, MA, USA) (Figure 1).

Statistical Analysis

The data obtained in this study are presented as mean ± standard deviation (SD). Statistical analyses were conducted using IBM SPSS for Windows version 26.0 (IBM Statistics, IBM Corporation, Armonk, NY, USA). The Kolmogorov-Smirnov and chi-square tests were applied to assess the normality of the data distribution. Depending on the results, group comparisons were performed using the Mann-Whitney U test. For parameters showing statistical significance ($p<0.05$), receiver operating characteristic (ROC) curve analysis was conducted to determine the sensitivity and specificity. Logistic regression analysis was performed to further assess the predictive value of significant parameters.

To evaluate the treatment response in a standardized and reproducible manner, patients were stratified into two distinct groups according to the tumor regression grading system proposed by Ryan et al. (13). Specifically, patients classified as grade 0 (no viable cancer cells) or grade 1 (single cells or small groups of cancer cells) were assigned to the first group, which was defined as a favorable response to neoadjuvant therapy. In contrast, patients graded as 2 (residual cancer with evident tumor regression but more than single cells or rare groups of cancer cells) or grade 3 (extensive residual cancer with no evidence of regression) were assigned to the second group, which was considered to reflect a poor or unfavorable response to neoadjuvant chemotherapy. This dichotomization allowed for a clear comparison between patients demonstrating effective tumor regression and those exhibiting limited or absent responses to treatment.

Results

A total of 47 patients diagnosed with LARC were enrolled in this study. Upon evaluation of the collected data, 28 and 19 patients were identified as male and female, respectively, and no statistically significant difference in treatment response was detected between the two sexes.

Texture analysis was conducted on magnetic resonance images obtained from three distinct sequences: T2-weighted imaging, ADC maps, and contrast-enhanced T1-weighted imaging.

In the T2 weighted sequence, the parameters mean, root mean square, root sum of squares, 10th percentile, 25th percentile, 90th percentile, 95th percentile, 97th percentile, entropy, and contrast of matrix were significantly lower in the treatment-responsive group. In contrast, the energy of matrix, homogeneity of matrix and Higuchi Fractal dimension of matrix were significantly higher among responders (Table 1).

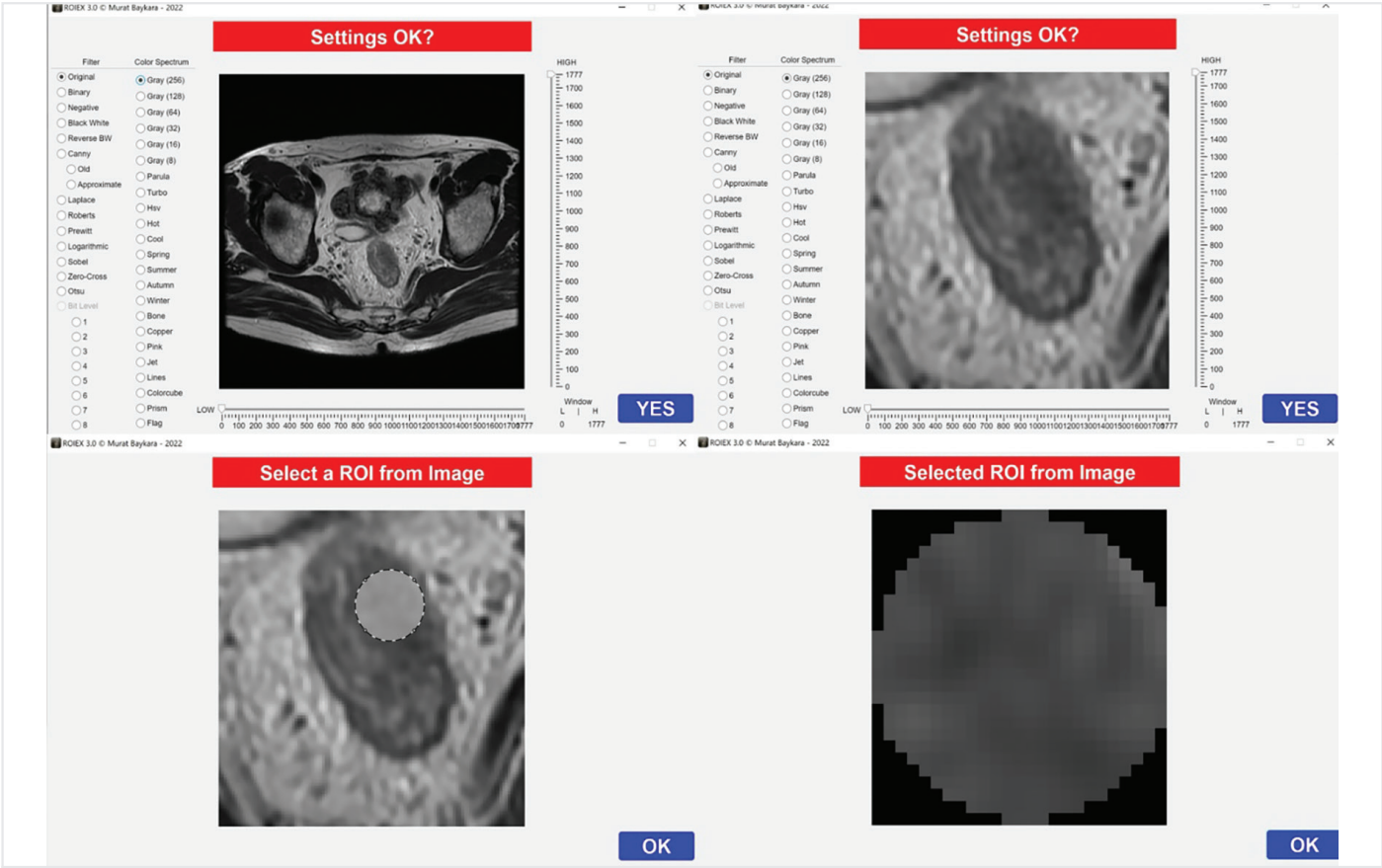

Figure 1. ROI selection steps on the DICOM image from the slice in which the tumor is most clearly visualized. ROI: Region of interest, DICOM: Digital Imaging and Communications in Medicine

Table 1. Parameters showing a statistically significant difference

Group statistics	No response	(27)	Response	(20)	p values
	Mean	SD	Mean	SD	
T2-mean of histogram	381.1469	69.3931	340.3331	76.6852	0.037
T2-root-mean-square level of histogram	383.6346	69.2325	342.8661	76.8468	0.039
T2-root-sum-of-squares level of histogram	5762.7972	2577.1566	3684.8846	1370.2391	0.001
T2-10th percentile of histogram	330.4222	69.4563	288.4700	72.1472	0.034
T2-25th percentile of histogram	354.3889	70.0191	311.9625	73.6861	0.031
T2-90th percentile of histogram	434.5407	74.1257	392.5950	88.6851	0.037
T2-95th percentile of histogram	453.8889	78.6010	410.3600	92.6228	0.032
T2-97th percentile of histogram	465.5100	83.5031	421.3390	95.9464	0.045
T2-entropy of histogram	6.3832	0.5270	5.9762	0.4984	0.011
T2-contrast of matrix	41.7244	33.7833	20.2681	10.5748	0.001
T2-energy of matrix	0.0060	0.0036	0.0108	0.0056	0.001
T2-homogeneity of matrix	0.2591	0.0566	0.3051	0.0438	0.009
T2-Higuchi fractal dimension of matrix	1.4483	0.0822	1.5209	0.1391	0.045
ADC-minimum of histogram	739.0769	211.0175	906.0500	213.6523	0.010
ADC-1st percentile of histogram	743.4665	209.5699	910.4635	211.8027	0.011
ADC-3rd percentile of histogram	774.8658	208.4411	934.6525	205.2943	0.012
ADC-5th percentile of histogram	796.7981	212.2147	960.6175	209.5846	0.012
ADC-10th percentile of histogram	840.9000	217.7492	1008.3700	225.2577	0.015
ADC-25th percentile of histogram	926.9615	231.0978	1096.8500	241.7372	0.022
ADC-entropy of histogram	5.7332	0.4331	5.1167	0.5817	<0.001
ADC-entropy of matrix	5.0015	0.3554	4.6278	0.5114	0.007
ADC-uniformity of matrix	0.4067	0.1078	0.4694	0.0897	0.028
ADC-mean local entropy of matrix	4.4500	0.2090	4.2794	0.3330	0.049
ADC-contrast of matrix	13.4676	5.9924	8.2755	5.3938	<0.001
ADC-energy of matrix	0.0163	0.0060	0.0277	0.0111	<0.001
ADC-homogeneity of matrix	0.3393	0.0535	0.4053	0.0542	<0.001
ADC-low gray-level zone emphasis of GLSZM	0.1150	0.0586	0.0845	0.0431	0.039
ADC-absolute gradient skewness of histogram-"Sobel"	1.2490	0.5924	0.9503	0.3893	0.049
ADC-absolute gradient skewness of histogram-"Prewitt"	1.2490	0.5924	0.9503	0.3893	0.049
ADC-absolute gradient skewness of matrix-"Sobel"	0.1927	0.3552	-0.1374	0.3784	0.012
ADC-absolute gradient skewness of matrix-"Prewitt"	0.1991	0.3417	-0.1205	0.3646	0.007
ADC-absolute gradient skewness of matrix-"Central"	0.1696	0.5578	-0.2682	0.5758	0.016
ADC-AR model - initial states of state-space realization	879.7952	381.8013	630.8040	344.1450	0.020
T1+C-mean of histogram	858.0034	297.4355	957.8116	173.7738	0.045
T1+C-root-mean-square level of histogram	862.5253	297.2398	963.0566	175.4708	0.048
T1+C-25th percentile of histogram	802.3889	292.4160	897.9875	166.2323	0.047
T1+C-75th percentile of histogram	913.2222	307.0603	1020.0375	196.8879	0.047
T1+C-entropy of histogram	6.5048	0.5482	6.2189	0.3923	0.023
T1+C-mean local range of matrix	381.0235	15.5574	471.3626	87.6760	0.007
T1+C-mean local standard deviation of matrix	153.5272	64.3133	191.2951	34.6884	0.006
T1+C-contrast of matrix	33.4492	18.1704	21.0826	8.6546	0.013
T1+C-energy of matrix	0.0072	0.0052	0.0096	0.0044	0.016
T1+C-homogeneity of matrix	0.2715	0.0557	0.3032	0.0458	0.037
T1+C-AR model - estimated "A" polynomial parameters	-0.9947	0.0106	-0.9925	0.0102	0.037

SD: Standard deviation, ADC: Apparent diffusion coefficient, GLSZM: Gray level size zone matrix

In the ADC sequence, the following features were significantly lower in the treatment-responsive group: entropy of histogram; entropy of matrix; mean local entropy of matrix; contrast of matrix; low gray-level zone emphasis of gray level size zone matrix; absolute gradient skewness of histogram; absolute gradient skewness of matrix-"Sobel"; absolute gradient skewness of matrix-"Prewitt"; ADC-absolute gradient skewness of matrix-"Central"; and ADC-AR model-initial states of state-space realization. Conversely, the minimum of histogram, 1st, 3rd, 5th, 10th, and 25th percentiles, uniformity of matrix, energy of matrix, and homogeneity of matrix were significantly higher in the responder group (Table 1).

In the contrast enhanced T1 weighted sequence, the Entropy of Histogram and Contrast of Matrix were significantly lower in patients who responded to therapy. Meanwhile, the mean of histogram, root mean square level, 25th percentile of histogram, 75th percentile of the histogram, mean local range of the matrix, mean local SD of the matrix, energy of the matrix, homogeneity of the matrix, and AR model-estimated "A" polynomial were significantly higher in the treatment-responsive group (Table 1).

For all other assessed texture parameters, no statistically significant differences were identified between the treatment-responsive and non-responsive groups.

ROC analyses were performed for several parameters that exhibited strong statistical significance, and the corresponding area under the curve, sensitivity, and specificity values obtained at the optimal cut-off thresholds for discriminating between the two groups are summarized in (Figures 2-4).

The logistic regression analysis was statistically significant [χ^2 (9): 37.183, $p<0.001$]. The ENTER model accounted for 74.3% of the variance in treatment response, as indicated by the Nagelkerke R^2 value, and correctly classified 91.3% of patients with respect to their response to the therapy. These findings demonstrate that the model possesses substantial explanatory power and a high level of predictive accuracy, supporting its utility in identifying individuals who are likely to respond to the treatment. In the constructed model, an increase in the contrast of matrix parameter within the ADC sequence and decreases in the contrast of matrix and energy of matrix parameters within the contrast-enhanced T1- weighted sequence were identified as significant contributors to the model's predictive capacity. These texture features demonstrated meaningful associations with the treatment response and played an important role in enhancing the discriminative performance of the model.

Discussion

In this study, we aimed to predict the therapeutic response in patients with LARC who underwent nCRT by performing a comprehensive texture analysis of pretreatment MRI scans. The overarching objective was to determine whether quantitative imaging biomarkers derived from baseline MRI could reliably characterize tumor heterogeneity and serve

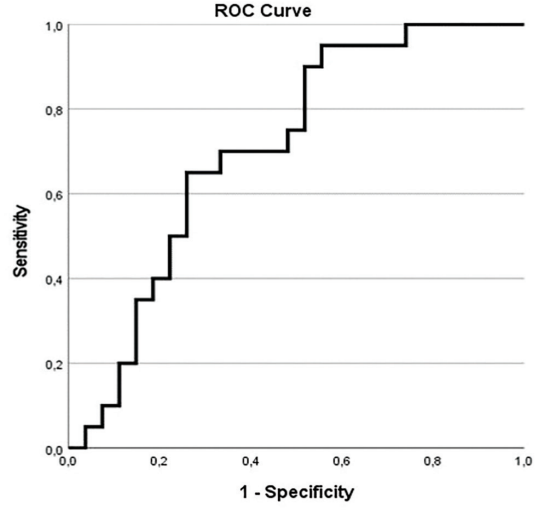

Figure 3. Receiver operating characteristic (ROC) curve for the contrast-enhanced T1 energy of the matrix parameter

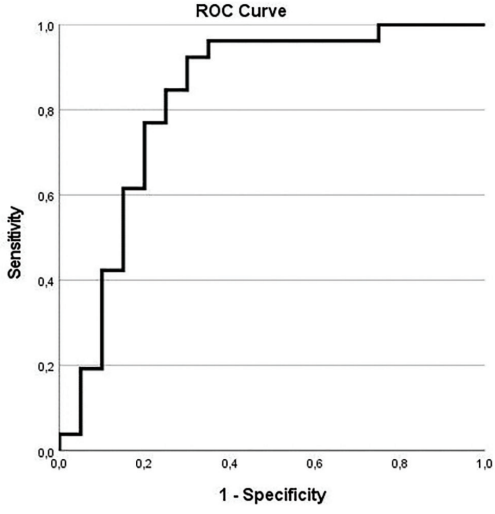

Figure 2. Receiver operating characteristic (ROC) curve for the apparent diffusion coefficient contrast of the matrix parameter

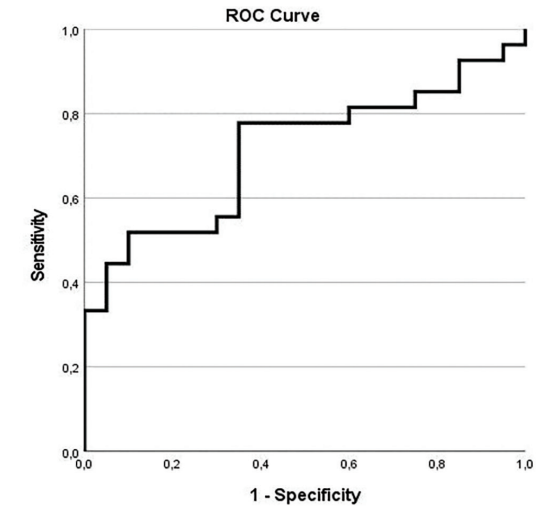

Figure 4. Receiver operating characteristic (ROC) curve for the contrast-enhanced T1 contrast of the matrix parameter

as predictors of subsequent treatment response. This approach aims to contribute to the development of precision medicine strategies that enable individualized treatment planning and improved clinical outcomes for patients with LARC.

For treatment response assessment, pre-treatment MRI images were analyzed using texture analysis across three different sequences, with 277 texture features being extracted from each sequence. Among all evaluated features, 44 parameters demonstrated statistically significant differences between the response groups. In the multivariate analysis, three parameters emerged as independent predictors of therapeutic response (Table 2).

In current oncological practice, the standard treatment approach for LARC consists of nCRT, followed by TME. This combined strategy aims to reduce the tumor burden, facilitate surgical resection, and minimize the risk of local recurrence (8). Pathological assessment after CRT isthe most reliable method for determining the extent of therapeutic response. In a subset of patients, this evaluation revealed a complete pCR or tumor downstaging, reflecting a significant reduction or even disappearance of viable tumor cells. These findings not only demonstrate the biological effectiveness of CRT but also highlight the heterogeneity of individual treatment responses among patients with rectal cancer. Moreover, numerous studies have shown that patients who achieve a pCR exhibit markedly improved clinical outcomes, including lower rates of local recurrence and distant metastasis, as well as higher overall survival rates,compared to those with partial or poor response. These observations underscore the prognostic value of treatment response following nCRT (9,10).

In recent years, numerous studies have focused on tissue evaluation using texture analysis, and its clinical adoption has steadily increased, reflecting its growing value as a quantitative imaging biomarker (14,15). The utility of this methodology extends across a wide clinical continuum, encompassing conditions from neurological spectrum disorders to complex oncological processes. This breadth of application underscores its ability to quantify subtle tissue alterations across diverse pathologies, thereby contributing to more precise diagnostic assessment, refined disease stratification, and optimized therapeutic decision-making (16,17).

Malignant tumors inherently exhibit intratumoral heterogeneity owing to their intrinsic biological structures. As a result of this heterogeneity, tumors may vary considerably in both prognosis and response to administered treatments. Texture analysis allows the quantitative evaluation of these heterogeneous intratumoral patterns and may enable the early identification of potential resistance to nCRT (18,19).

In contrast enhanced T1weighted sequences, the energy of matrix value was higher in the responder group, and a decrease in this value strengthened the prediction of treatment response. Similarly, Meng et al. (20) reported in their study that energy values were higher among patients responding to treatment. Our findings indicate that T2 weighted histogram entropy did not independently predict treatment response, yet responders exhibited lower values, corroborating another study (21). The minimum histogram value on the ADC sequence differed between responders and non-responders, consistent with the findings of a previous study (22). In another previous study (23), the minimum ADC histogram values at the 10^{th} and 25^{th} percentiles differed significantly according to treatment response. Similarly, in our cohort, we observed significant differences in these parameters between responders and non-responders. Moreover, we found that the 10^{th} and 25^{th} percentile values also differed significantly in the T2-weighted sequence, which may further underscore the potential relevance of T2-weighted imaging in response assessment. In contrast, the skewness and kurtosis derived from the ADC did not differ significantly between the two groups (24).

Based on the findings of the present study, the predictive model we developed demonstrated a robust capacity to discriminate between responders and non-responders prior to the initiation of therapy. By integrating key radiomic features with clinically relevant parameters, the model achieved a high level of accuracy, indicating that subtle textural and structural characteristics captured on pretreatment imaging harbor meaningful information regarding tumor biology and treatment susceptibility of the tumor. These results highlight the value of advanced image-based analytics in characterizing intratumoral heterogeneity and underscore the feasibility of using such quantitative metrics for individualized treatment planning. Importantly, the ability of the model to reliably predict treatment response before therapy initiation has significant clinical implications.

Study Limitations

The present study had some limitations that warrant consideration. The cohort size was relatively small, whereas radiomics studies typically require larger populations to ensure robust and generalizable results. Additionally, ROI delineation was performed in two dimensions on the para-axial plane, and the inclusion of complementary planes may improve the reliability of the extracted features. Manual segmentation also introduces potential inter-observervariability and may increase measurement errors, particularly among less experienced readers. Future studies should evaluate deep learning–based segmentation frameworks to mitigate these limitations.

Conclusion

Radiomics and mathematical modeling are attracting increasing attention in the medical community because of theirpotential to support clinicians in several ways. In this context, in patients diagnosed with LARC, early identification based on pre-nCRT imaging of those

Table 2. Logistic regression analysis findings

Parameters	b	SE	Wald	df	Sig.	Exp (B)
ADC-contrast of matrix	0.708	0.322	4.846	1	0.028	2.031
T1+C-contrast of matrix	-0.418	0.201	4.315	1	0.038	0.658
T1+C-energy of matrix	-1121.178	470.201	5.686	1	0.017	0.011

ADC: Apparent diffusion coefficient, SE: Standard error, Sig.: Significance, Exp.: Exponentiated

who are unlikely to benefit from standard protocols may facilitate timely modification of treatment strategies, prevent unnecessary toxicity, and enable a more efficient allocation of healthcare resources. Taken together, these findings suggest that radiomics-based predictive modeling may serve as a non-invasive decision support tool for the personalized management of patients undergoing neoadjuvant therapy. We also believe that studies conducted in larger cohorts may achieve higher accuracy in predicting treatment response.

Ethics

Ethics Committee Approval: Ethical approval was obtained from, University of Health Sciences Türkiye, Haydarpaşa Numune Training and Research Hospital on September 11, 2023 (decision number: HNEAH-KAEK 2023/163, HNEAH-KAEK 2023/KK/163).

Informed Consent: Given the retrospective design of the study, the requirement to obtain written informed consent from the patients was waived by the committee.

Footnotes

Authorship Contributions: Concept - M.Ö., K.C., E.B., M.B.; Design - M.Ö., K.C., M.B.; Data Collection or Processing - M.Ö., K.C., E.B.; Analysis or Interpretation - M.Ö., K.C., M.B.; Literature Search - M.Ö., K.C., E.B.; Writing - M.Ö., K.C.

Conflict of Interest: No conflict of interest was declared by the authors.

Financial Disclosure: The authors declared that this study received no financial support.

References

1. Siegel RL, Miller KD, Goding Sauer A, Fedewa SA, Butterly LF, Anderson JC, et al. Colorectal cancer statistics, 2020. CA Cancer J Clin. 2020; 70: 145-64.
2. Ferlay J, Colombet M, Soerjomataram I, Dyba T, Randi G, Bettio M, et al. Cancer incidence and mortality patterns in Europe: Estimates for 40 countries and 25 major cancers in 2018. Eur J Cancer. 2018; 103: 356-87.
3. Horvat N, Carlos Tavares Rocha C, Clemente Oliveira B, Petkovska I, Gollub MJ. MRI of rectal cancer: tumor staging, imaging techniques, and management. Radiographics. 2019; 39: 367-87.
4. Siddiqui MRS, Simillis C, Hunter C, Chand M, Bhoday J, Garant A, et al. A meta-analysis comparing the risk of metastases in patients with rectal cancer and MRI-detected extramural vascular invasion (mrEMVI) vs mrEMVI-negative cases. Br J Cancer. 2017; 116: 1513-9.
5. Lord AC, D'Souza N, Pucher PH, Moran BJ, Abulafi AM, Wotherspoon A, et al. Significance of extranodal tumour deposits in colorectal cancer: a systematic review and meta-analysis. Eur J Cancer. 2017; 82: 92-102.
6. Al-Sukhni E, Milot L, Fruitman M, Beyene J, Victor JC, Schmocker S, et al. Diagnostic accuracy of MRI for assessment of T category, lymph node metastases, and circumferential resection margin involvement in patients with rectal cancer: a systematic review and meta-analysis. Ann Surg Oncol. 2012; 19: 2212-23.
7. Sauer R, Becker H, Hohenberger W, Rödel C, Wittekind C, Fietkau R, et al. Preoperative versus postoperative chemoradiotherapy for rectal cancer. N Engl J Med. 2004; 351:1731-40.
8. Glimelius B, Tiret E, Cervantes A, Arnold D; ESMO Guidelines Working Group. Rectal cancer: ESMO Clinical Practice Guidelines for diagnosis, treatment and follow-up. Ann Oncol. 2013; 24 Suppl 6: vi81-8.
9. Martin ST, Heneghan HM, Winter DC. Systematic review and meta-analysis of outcomes following pathological complete response to neoadjuvant chemoradiotherapy for rectal cancer. Br J Surg. 2012; 99: 918-28.
10. Kim SH, Lee JM, Hong SH, Kim GH, Lee JY, Han JK, et al. Locally advanced rectal cancer: added value of diffusion-weighted MR imaging in the evaluation of tumor response to neoadjuvant chemo- and radiation therapy. Radiology. 2009; 253: 116-25.
11. Scapicchio C, Gabelloni M, Barucci A, Cioni D, Saba L, Neri E. A deep look into radiomics. Radiol Med. 2021; 126: 1296-311.
12. Castellano G, Bonilha L, Li LM, Cendes F. Texture analysis of medical images. Clin Radiol. 2004; 59: 1061-9.
13. Ryan R, Gibbons D, Hyland JM, Treanor D, White A, Mulcahy HE, et al. Pathological response following long-course neoadjuvant chemoradiotherapy for locally advanced rectal cancer. Histopathology. 2005; 47: 141-6.
14. Baykara M, Baykara S. Texture analysis of dorsal striatum in functional neurological (conversion) disorder. Brain Imaging Behav. 2022; 16: 596-607.
15. Baykara M, Yildirim M. Differentiation of multiple myeloma and metastases with apparent diffusion coefficient map histogram analysis. North Clin Istanb. 2022; 9: 256-60.
16. Baykara M, Baykara S. Is the caudate, putamen, and globus pallidus the delusional disorder's trio? A texture analysis study. Actas Esp Psiquiatr. 2024; 52: 256-67.
17. Azamat S, Karaman Ş, Azamat IF, Ertaş G, Kulle CB, Keskin M, et al. Complete response evaluation of locally advanced rectal cancer to neoadjuvant chemoradiotherapy using textural features obtained from T2 weighted imaging and ADC maps. Curr Med Imaging. 2022; 18: 1061-9.
18. Fu F, Nowak MA, Bonhoeffer S. Spatial heterogeneity in drug concentrations can facilitate the emergence of resistance to cancer therapy. PLoS Comput Biol. 2015; 11: e1004142.
19. Hardiman KM, Ulintz PJ, Kuick RD, Hovelson DH, Gates CM, Bhasi A, et al. Intra-tumor genetic heterogeneity in rectal cancer. Lab Invest. 2016; 96: 4-15.
20. Meng Y, Zhang C, Zou S, Zhao X, Xu K, Zhang H, et al. MRI texture analysis in predicting treatment response to neoadjuvant chemoradiotherapy in rectal cancer. Oncotarget. 2017; 9: 11999-2008.
21. Staal FCR, van der Reijd DJ, Taghavi M, Lambregts DMJ, Beets-Tan RGH, Maas M. Radiomics for the prediction of treatment outcome and survival in patients with colorectal cancer: a systematic review. Clin Colorectal Cancer. 2021; 20: 52-71.
22. Cantürk A, Yarol RC, Tasak AS, Gülmez H, Kadirli K, Bişgin T, et al. Comparative analysis of tumor and mesorectum radiomics in predicting neoadjuvant chemoradiotherapy response in locally advanced rectal cancer. Diagn Interv Radiol. 2026; 32: 365-75.
23. Choi MH, Oh SN, Rha SE, Choi JI, Lee SH, Jang HS, et al. Diffusion-weighted imaging: apparent diffusion coefficient histogram analysis for detecting pathologic complete response to chemoradiotherapy in locally advanced rectal cancer. J Magn Reson Imaging. 2016; 44: 212-20.
24. Enkhbaatar NE, Inoue S, Yamamuro H, Kawada S, Miyaoka M, Nakamura N, et al. MR imaging with apparent diffusion coefficient histogram analysis: evaluation of locally advanced rectal cancer after chemotherapy and radiation therapy. Radiology. 2018; 288: 129-37.

İstanbul Med J 2026; 27(3): 252-8
DOI: 10.4274/imj.galenos.2026.74271

Transient Decline and Recovery of Renal Function Following Unilateral Adrenalectomy for Primary Aldosteronism

Şebnem Burhan[1], Aslıhan Pekmezci[1], Aykut Çelik[2], Mutlu Niyazoğlu[1], Esra Hatipoğlu[1]

[1]University of Health Sciences Türkiye, Başakşehir Çam and Sakura City Hospital, Clinic of Endocrinology and Metabolism, İstanbul, Türkiye
[2]University of Health Sciences Türkiye, Başakşehir Çam and Sakura City Hospital, Division of Endocrine Surgery, Clinic of General Surgery, İstanbul, Türkiye

ABSTRACT

Introduction: A transient decline in the estimated glomerular filtration rate (eGFR) is frequently observed following adrenalectomy for primary aldosteronism (PA), reflecting the unmasking of aldosterone-mediated renal injury previously concealed by glomerular hyperfiltration. The temporal pattern of this decline and its associated preoperative predictors remain poorly characterized.

Methods: We retrospectively analyzed 38 consecutive patients with confirmed PA who underwent unilateral adrenalectomy. Serial changes in eGFR and serum creatinine were evaluated using the Friedman test with Durbin-Conover post-hoc comparisons. Correlations between postoperative renal function and preoperative clinical and biochemical variables were assessed using Spearman's rank correlation and the Mann-Whitney U test.

Results: A statistically significant overall difference in eGFR was observed during the first three postoperative months (χ^2: 9.04, p=0.03), driven by a significant decline at month 3 relative to both the preoperative baseline (p=0.03) and postoperative day 1 (p=0.003). When the 6-month measurement was incorporated, the overall difference was no longer significant (χ^2: 6.52, p=0.16). The eGFR decline at month 3 was significantly more pronounced in patients with spontaneous hypokalemia (-22.2% vs. -4.76%, p=0.04). Month 6 eGFR was negatively correlated with baseline aldosterone concentration, aldosterone-to-renin ratio, and age, and was positively correlated with preoperative eGFR and systolic blood pressure.

Conclusion: Adrenalectomy for PA was associated with a transient decline in eGFR at postoperative month 3, with values approaching baseline by month 6, and with no evidence of persistent deterioration. Spontaneous hypokalemia and a higher aldosterone burden identify patients at greater risk of postoperative decline in renal function.

Keywords: Primary aldosteronism, adrenalectomy, glomerular filtration rate, renal function, hypokalemia

Introduction

Primary aldosteronism (PA) is a common cause of secondary hypertension. Conn's syndrome is characterized by autonomous aldosterone overproduction that is independent of renin-angiotensin regulation. The main causes of PA include aldosterone-producing adenomas and bilateral adrenal hyperplasia, while rarer forms are associated with genetic mutations. Among these, an aldosterone-producing adenoma is the most common and is generally located on one side of the adrenal gland. Unilateral adrenalectomy is the treatment of choice for patients with lateralized PA and represents the only potentially curative intervention (1).

Chronic aldosterone overproduction exerts direct nephrotoxic effects independent of its hemodynamic actions (which include glomerular hypertension); these effects include tubular injury and progressive renal fibrosis. Consequently, individuals with PA are more prone to chronic kidney disease (CKD) and have an elevated risk of worsening kidney function compared to those with essential hypertension, even when their blood pressure levels are similar (2,3). Notably, the true extent of aldosterone-mediated renal damage may remain underestimated in the preoperative setting, as concurrent hemodynamic adaptations to chronic aldosterone excess, most importantly, glomerular hyperfiltration, can partially mask underlying renal dysfunction, rendering standard measures of kidney function deceptively reassuring (3).

Despite the growing body of evidence characterizing postoperative decline in estimated glomerular filtration rate (eGFR) in PA, data from centers where renal function is preserved or improved after adrenalectomy remain limited. Furthermore, most published studies originate from East Asian cohorts, and population-specific differences in PA phenotype, duration of disease at diagnosis, and preoperative management may substantially influence postoperative renal outcomes. However, whether these findings are generalizable to other ethnic groups, including

Address for Correspondence: Şebnem Burhan, MD, University of Health Sciences Türkiye, Başakşehir Çam and Sakura City Hospital, Clinic of Endocrinology and Metabolism, İstanbul, Türkiye
E-mail: drsebnemburhan@gmail.com **ORCID ID:** orcid.org/0000-0001-9260-5696
Cite this article as: Burhan Ş, Pekmezci A, Çelik A, Niyazoğlu M, Hatipoğlu E. Transient decline and recovery of renal function following unilateral adrenalectomy for primary aldosteronism. İstanbul Med J. 2026; 27(3): 252-8

Received: 04.05.2026
Accepted: 07.07.2026
Publication Date: 03.08.2026

Turkish patients, remains unclear. Therefore, the present study aimed to evaluate changes in eGFR following unilateral adrenalectomy for PA and to identify preoperative clinical and biochemical factors associated with postoperative renal function in a Turkish institutional cohort.

Methods

Study Population

We retrospectively reviewed the medical records of patients with PA who underwent unilateral adrenalectomy between September 2020 and February 2026. Initially, 46 patients were enrolled in the study. After excluding patients with autonomous cortisol co-secretion and those with insufficient clinical data, the final study population comprised 38 patients. The study was conducted in accordance with the ethical standards of the 1975 Declaration of Helsinki and was approved by the Local Ethics Committee of University of Health Sciences Türkiye, Başakşehir Çam and Sakura City Hospital (decision number: 48, date: 21.01.2026). The ethics committee waived the requirement for informed consent due to the retrospective nature of the study and the use of anonymized data.

Diagnosis PA

Before screening for PA, medications known to interfere with the renin-angiotensin-aldosterone system were either discontinued for the appropriate wash-out period or switched to non-interfering alternatives. Serum potassium levels were normalized in all patients via replacement therapy before blood sampling to prevent false-negative results. After ensuring adequate sodium intake for several days, participants were screened using morning, seated measurements of serum or plasma aldosterone and plasma renin activity (PRA). A positive screening result was defined as an aldosterone level ≥10 ng/dL (by immunoassay), a PRA ≤1 ng/mL/h, and an aldosterone-to-PRA ratio >20 (4). Confirmatory testing was omitted in patients with overt biochemical evidence of autonomous aldosterone production, defined as a PRA below 0.2 ng/mL/h in conjunction with a plasma aldosterone concentration exceeding 20 ng/dL. In the remaining patients with a positive screening result who did not fulfill these criteria, intravenous saline infusion test was performed to establish the diagnosis of PA (4). Adrenal vein sampling (AVS) was performed in patients who did not meet the criteria for a high pretest probability of unilateral aldosterone-producing adenoma. These included patients aged 35 years or older and those whose computed tomography (CT) demonstrated normal adrenal morphology, bilateral adrenal abnormalities, or non-specific findings such as lesions of 1.0 cm or smaller or bilateral gland thickening (4). For patients in whom bilateral adrenal venous sampling was unsuccessful, the decision for surgical lateralization was based on a combination of CT findings and the contralateral suppression index, calculated as the ratio of the aldosterone-to-cortisol ratio in the successfully cannulated adrenal vein relative to that in the inferior vena cava sample (5). A markedly suppressed ratio on the successfully cannulated side, together with a unilateral adenoma identified on CT, was considered indicative of contralateral aldosterone hypersecretion and supported lateralization to the contralateral non-cannulated side.

Tumor localization was confirmed in all participants using preoperative cross-sectional imaging, including abdominal CT or magnetic resonance imaging (MRI).

Histopathological examination of the surgical specimens from all 38 patients confirmed adrenocortical adenoma.

Measurement of Clinical Data

Collected clinical data included age, sex, body mass index (BMI) (kg/m^2), duration of hypertension, preoperative systolic and diastolic blood pressure, number of antihypertensive medications (excluding mineralocorticoid receptor antagonists), and preoperative hypokalemia. All patients with preoperative hypokalemia were rendered normokalemic before surgery. Smoking, diabetes mellitus, and hyperlipidemia were additionally recorded as potential covariates known to influence renal function. The eGFR was calculated using the CKD-EPI 2021 creatinine-based equation. Plasma aldosterone concentration was measured by radioimmunoassay. Postoperative eGFR was assessed on day 1 and at 1, 3, and 6 months following adrenalectomy. The percentage change in eGFR from baseline was calculated as [(postoperative eGFR-preoperative eGFR)/preoperative eGFR] × 100, with negative values indicating a decline and positive values indicating an improvement relative to the preoperative baseline. Of the 38 patients who underwent adrenalectomy, 29 (76.3%) attended the postoperative month 3 visit and were included in serial eGFR analyses at that time point. The remaining 9 patients did not present for scheduled follow-up and were therefore excluded from the month-3 analyses.

Biochemical and blood pressure outcomes were classified according to the Primary Aldosteronism Surgical Outcome consensus criteria. Complete biochemical success was defined as the correction of hypokalemia (if present preoperatively) and normalization of the aldosterone-to-renin ratio based on local laboratory reference intervals. Partial biochemical success was defined as correction of hypokalemia, with a persistently elevated aldosterone-to-renin ratio and a ≥50% reduction in baseline plasma aldosterone concentration relative to preoperative values. Absent biochemical success was defined as persistent hypokalemia or a persistently elevated aldosterone-to-renin ratio without a meaningful reduction in aldosterone concentration (6).

Postoperative blood pressure response was classified into three categories: complete clinical response, defined as a blood pressure below 140/90 mmHg without any antihypertensive medication; partial clinical response, defined as a reduction in the number or dose of antihypertensive agents with a blood pressure remaining at or above 140/90 mmHg; and absent clinical response, defined as a blood pressure of 140/90 mmHg or higher with an unchanged or increased antihypertensive medication requirement (6).

Statistical Analysis

Continuous variables were tested for normality using the Shapiro-Wilk test and expressed as median [interquartile range (IQR)] or mean ± standard deviation, as appropriate. Categorical variables are reported as frequencies and percentages. Serial changes in eGFR and serum creatinine levels across postoperative time points were evaluated

using the Friedman test. Two separate analyses were performed: the first included four time points (preoperative, postoperative day 1, and postoperative months 1 and 3), and the second included the 6-month time point. Post-hoc pairwise comparisons were conducted using the Durbin-Conover test, which is specifically designed to follow the Friedman test and incorporates an internal adjustment for multiple comparisons. Correlations between clinical and biochemical variables were assessed using Spearman's rank correlation coefficient. Differences between categorical groups were evaluated using the Mann-Whitney U test. A two-sided p value <0.05 was considered statistically significant for all analyses. Statistical analyses were performed using Jamovi (version 2.6).

Results

A total of 38 participants were included in this study. Of these, 25 (65.8%) were female and 13 (34.2%) were male. The median age at diagnosis was 48.5 years (IQR: 44.5-56.0). The median BMI was 29.9 (IQR: 26.4-32.6). The median duration of hypertension was 10.0 years (IQR: 4.75-15.0). The median number of antihypertensive medications was 3 (IQR: 2-3). The baseline systolic and diastolic blood pressures were 146 mmHg (IQR: 136–160) and 87 mmHg (IQR: 80.3-92.0), respectively. The median baseline heart rate was 77 bpm (IQR: 70.8-86.3 bpm). Spontaneous hypokalemia was observed in 20 patients (52.6%). The median total clinical follow-up duration was 35.5 months (IQR: 19.8-50.3). The baseline clinical characteristics of the study cohort are presented in Table 1.

AVS was performed in 27 patients; successful bilateral cannulation was achieved in 13 patients, yielding a median lateralization index of 14.0 (IQR: 2.0-43.0). Given the limited number of patients with complete AVS data, the lateralization index was not included as a study variable in further analyses.

Of the 38 patients, 24 (63.2%) underwent laparoscopic adrenalectomy and 14 (36.8%) underwent robotic adrenalectomy. No patient required a postoperative blood transfusion. Detailed perioperative renal function data and 3-month biochemical outcomes are shown in Table 2.

The Friedman test applied to four time points (preoperative, postoperative day 1, and postoperative months 1 and 3) revealed a statistically significant overall difference in eGFR (χ^2: 9.04, df: 3, p=0.03). Post-hoc pairwise comparisons using the Durbin-Conover test demonstrated that eGFR at postoperative month 3 was significantly lower than both the preoperative baseline (p=0.03) and the postoperative day 1 value (p=0.003). No significant difference was observed between the preoperative and postoperative day 1 eGFR (p=0.35), preoperative and postoperative month 1 eGFR (p=0.43), or postoperative day 1 and month 1 eGFR (p=0.09).

When the 6-month eGFR measurement was incorporated into the analysis, the overall Friedman test was no longer statistically significant (χ^2: 6.52, df: 4, p=0.16). Accordingly, no individual pairwise comparisons reached statistical significance at this stage, including the comparisons between preoperative and postoperative month 3 eGFR (p=0.06), and between postoperative day 1 and month 3 eGFR (p=0.02). Postoperative changes in eGFR are shown in Figure 1.

Serum creatinine levels did not differ significantly across the four time points by the Friedman test (χ^2: 5.28, df: 3, p=0.153). However, post-hoc Durbin-Conover pairwise comparisons revealed that serum creatinine at postoperative month 3 was significantly higher than at postoperative day 1 (p=0.03), mirroring the pattern observed for eGFR. No significant difference was detected in any other pairwise comparison of serum creatinine (all p>0.05).

When the 6-month creatinine measurement was incorporated into the analysis, the overall Friedman test result was no longer statistically significant (χ^2: 5.02, df: 4, p=0.28); no individual pairwise comparison reached statistical significance, including the comparison between postoperative day 1 and month 3 creatinine levels (p=0.05). These findings are consistent with the eGFR results and further support the conclusion that the transient rise in serum creatinine observed at postoperative month 3 resolved by month 6, with no sustained impairment of renal function following adrenalectomy. Postoperative changes in serum creatinine levels are shown in Figure 2.

The median percentage change in eGFR from baseline to postoperative month 3 was -6.0% (IQR: -15.0 to +1.0). No significant correlations were observed between the 3-month percentage change in eGFR and any of

Table 1. Baseline clinical characteristics of the study cohort (n=38)

Variable	Value
Demographics	
Sex: female, n (%)	25 (65.8%)
Sex: male, n (%)	13 (34.2%)
Age at diagnosis (years)	48.5 [44.5–56.0]
Body mass index (kg/m^2)	29.9 [26.4–32.6]
Clinical follow-up duration (months)	35.5 [19.8–50.3]
Hypertension and medications	
Duration of hypertension (years)	10.0 [4.75–15.0]
Antihypertensive medications ACEi/ARB Diuretics Dihydropyridine CCB Non-dihydropyridine CCB Beta-blocker MRA	 24 (64.9%) 13 (35.1%) 24 (64.9%) 12 (32.4%) 11 (29.7%) 3 (8.1%)
Spontaneous hypokalemia, n (%)	20 (52.6%)
Diabetes mellitus, n (%)	8 (21.1%)
Dyslipidemia, n (%)	5 (13.2%)
Smoking	8 (21.1%)
Baseline hemodynamics	
Systolic BP (mmHg)	146 [136–160]
Diastolic BP (mmHg)	87 [80.3–92.0]
Heart rate (bpm)	77 [70.8–86.3]
Aldosteron (ng/dL)	50.0 [29.5–68.2]
PRA (ng/mL/h)	0.33 [0.28–0.60].
ARR	99.2 [54.4–195.0].

Data expressed as median [interquartile range] or n (%). ACEi: Angiotensin-converting enzyme inhibitor, ARB: Angiotensin II receptor blocker, CCB: Calcium channel blocker, MRA: Mineralocorticoid receptor antagonist, BP: Blood pressure, bpm: Beats per minute, PRA: Plasma renin activity, ARR: Aldosterone-to-renin ratio, IQR: Interquartile range

Table 2. Perioperative renal function and postoperative outcomes

Variable	n	Median (IQR)
Renal function-eGFR (mL/min/1.73 m^2)		
Preoperative	38	78.0 (67.3-106.0)
Postoperative day 1	38	82.5 (65.3-106.0)
Postoperative month 1	29	83.0 (66.0-103.0)
Postoperative month 3	29	77.0 (60.0-98.0)
Postoperative month 6	35	86.0 (62.5-102.0)
Renal function-serum creatinine (mg/dL)		
Preoperative	38	0.860 (0.660-1.000)
Postoperative day 1	38	0.840 (0.652-1.080)
Postoperative month 1	29	0.890 (0.715-1.080)
Postoperative month 3	29	0.940 (0.735-1.190)
Postoperative month 6	35	0.920 (0.735-1.090)
3-month postoperative biochemical and clinical parameters		
Aldosterone (ng/dL)	29	9.43 (5.15-19.3)
PRA (ng/mL/h)	29	1.03 (0.700-2.59)
ARR	29	9.70 (3.46-33.5)
Systolic BP (mmHg)	29	130 (120-145)
Diastolic BP (mmHg)	29	80 (70-90)
Serum potassium (mmol/L)	29	4.80 (4.69-5.04)

IQR: Interquartile range, eGFR: Estimated glomerular filtration rate, PRA: Plasma renin activity, ARR: Aldosterone-to-renin ratio, BP: Blood pressure

the following: age at diagnosis, sex, baseline eGFR, baseline aldosterone concentration, PRA, or aldosterone-to-renin ratio (all p>0.05). It was significantly greater in patients with spontaneous hypokalemia than in those without spontaneous hypokalemia [-22.2% (IQR: -33.5 to -10.7) vs -4.76% (IQR: -11.95 to +5.61), p=0.04].

Although eGFR did not differ significantly from baseline values by postoperative month 6, the 6-month eGFR was negatively correlated with baseline aldosterone concentration (r: -0.52, p=0.003) and aldosterone-to-renin ratio (r: -0.39, p=0.02), and positively correlated with preoperative eGFR (r: 0.51, p=0.002). Additionally, the 6-month eGFR was positively correlated with baseline systolic blood pressure (r: 0.37, p=0.02) and negatively correlated with age at diagnosis (r: -0.5, p=0.002). The results are shown in Table 3.

At the 3-month follow-up, 14 patients (36.8%) achieved a complete blood-pressure response. A partial blood pressure response was observed in 22 (57.9%) patients. Two patients (5.2%) showed no blood pressure response. Preoperatively, spontaneous hypokalemia was present in 20 (52.6%) patients. Following adrenalectomy, serum potassium levels normalized in all patients without potassium supplementation. Biochemical outcomes were assessed at postoperative month 3 in 29 patients; complete biochemical response was achieved in 20 (69.0%), partial biochemical response in 7 (24.1%), and no biochemical response in 2 (6.9%). A repeated-measures analysis of variance was performed to compare patients who achieved complete biochemical remission with those who did not and to assess whether eGFR and creatinine differed according to biochemical remission status. For eGFR, no significant between-subjects effect of remission status was observed in either the four-time-point (preoperative, day 1, month 1, month 3; p=0.62) or

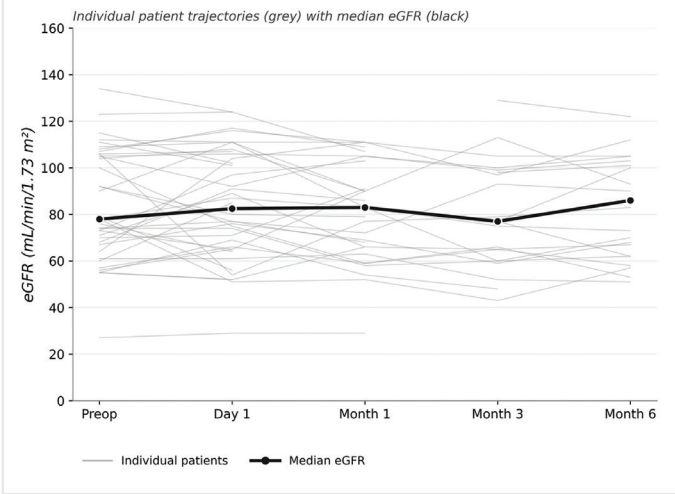

Figure 1. Individual patient trajectories of estimated glomerular filtration rate (eGFR) following unilateral adrenalectomy for primary aldosteronism. Grey lines represent individual patients; the black line represents the group median. eGFR is expressed in mL/min/1.73 m^2

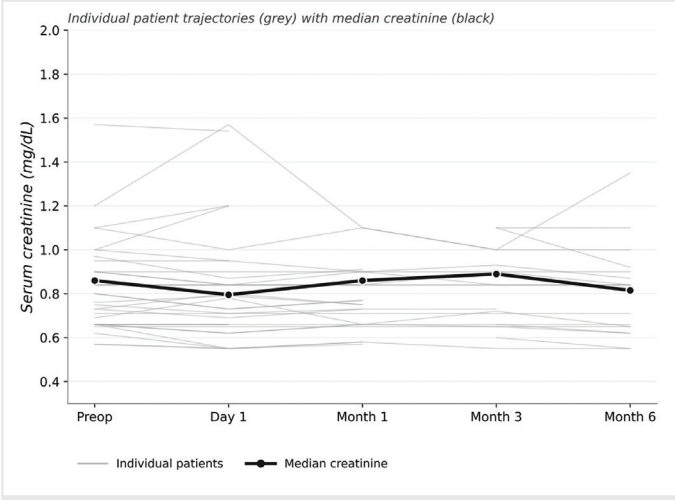

Figure 2. Individual patient trajectories of serum creatinine following unilateral adrenalectomy for primary aldosteronism. Grey lines represent individual patients; the black line represents the group median. Serum creatinine is expressed in mg/dL

Table 3. Predictors of postoperative eGFR at 6 month

Variable	eGFR 6 month	
	Spearman's r	p value
Age at diagnosis (years)	-0.5	0.002
BMI (kg/m^2)	0.14	0.41
Systolic BP (mmHg)	0.37	0.02
Preoperative eGFR	0.51	0.002
Baseline aldosterone (ng/dL)	-0.52	0.003
Baseline PRA (ng/mL/h)	0.1	0.57
Baseline ARR	-0.39	0.02

eGFR: Estimated glomerular filtration rate, BMI: Body mass index, BP: Blood pressure, PRA: PPlasma renin activity, ARR: Adosterone-to-renin ratio

the five-time-point (preoperative, day 1, month 1, month 3, month 6; p=0.36) comparison. Similarly, no significant between-subjects effect of remission status on serum creatinine was observed in either the four-time-point (p=0.24) or the five-time-point (p=0.24) comparison. Detailed results are presented in Table 4.

Discussion

In the present study, unilateral adrenalectomy for PA was associated with a transient decline in eGFR at postoperative month 3, with values approaching preoperative levels by month 6, and with no evidence of persistent deterioration in renal function. A parallel pattern was observed for serum creatinine, which showed a transient increase at month 3 that was no longer evident by month 6. The magnitude of postoperative eGFR at month 6 was significantly correlated with the baseline aldosterone concentration, aldosterone-to-renin ratio, preoperative eGFR, baseline systolic blood pressure, and age at diagnosis, highlighting the role of the preoperative disease burden in determining renal outcomes. With respect to clinical outcomes, complete blood pressure response was achieved in 36.9% of patients and complete biochemical remission was achieved in 69% of patients, with serum potassium normalizing in all patients with preoperative hypokalemia.

In PA, excess aldosterone alters kidney hemodynamics and structure. After adrenalectomy, many patients experience a decrease in eGFR. Across studies, this is consistently interpreted as unmasking pre-existing renal damage rather than as new surgical kidney injury. Excess aldosterone promotes sodium retention, volume expansion, and glomerular hypertension through afferent arteriolar vasoconstriction, resulting in sustained glomerular hyperfiltration (7,8). Hyperfiltration and glomerular hypertension can mask a true reduction in kidney function preoperatively by maintaining normal or elevated eGFR despite structural damage (3,7). Long-term aldosterone exposure causes renal fibrosis, glomerular sclerosis, and microvascular lesions, leading to CKD even when eGFR appears normal (8-10). In this study, the transient decline in eGFR observed at postoperative month 3, with values approaching preoperative levels by month 6, is consistent with the well-established pathophysiological consequences of aldosterone excess on renal hemodynamics. The nadir observed at month 3 is consistent with the timeline reported in the literature because the renin-angiotensin-aldosterone system requires weeks to months to re-equilibrate after abrupt withdrawal of autonomous aldosterone secretion, and tubular adaptation to the altered hemodynamic milieu is similarly gradual. Notably, the absence of a persistent eGFR decline by month 6 distinguishes our cohort from series reporting sustained postoperative renal function impairment. It may reflect a relatively small degree of irreversible structural renal damage induced by aldosterone in our patients at the time of surgery. This interpretation is supported by the relatively preserved preoperative eGFR and potassium levels in our cohort, compared with those in previously published series, suggesting that surgical intervention was undertaken at an earlier stage of aldosterone-mediated renal injury, before the development of irreversible fibrotic changes.

Table 4. eGFR and serum creatinine according to biochemical remission status

Variable	No remission median (IQR)	Complete remission median (IQR)
eGFR (mL/min/1.73 m^2)		
Preoperative	89.0 (69.5–105.0)	92.0 (72.0–107.5)
Postoperative day 1	89.0 (76.2–98.8)	97.0 (68.5–111.0)
Postoperative month 1	83.0 (69.0–90.0)	86.5 (66.5–106.0)
Postoperative month 3	75.0 (62.5–96.0)	77.0 (62.5–88.0)
Postoperative month 6	90.0 (73.0–103.0)	80.5 (62.2–103.0)
Serum creatinine (mg/dL)		
Preoperative	0.775 (0.665–0.937)	0.830 (0.635–0.975)
Postoperative day 1	0.795 (0.683–0.885)	0.770 (0.615–1.150)
Postoperative month 1	0.890 (0.715–1.080)	0.905 (0.747–1.050)
Postoperative month 3	0.970 (0.720–1.040)	0.915 (0.775–1.230)
Postoperative month 6	0.810 (0.715–0.985)	0.930 (0.730–1.140)

No statistically significant difference in eGFR or creatinine was observed between groups at any time point (all p>0.05). IQR: Interquartile range, eGFR: Estimated glomerular filtration rate

In the present study, the decline in eGFR at postoperative month 3 was significantly more pronounced in patients with spontaneous hypokalemia compared with those without spontaneous hypokalemia (p=0.04). These observations are consistent with those of Lu et al. (11), who identified hypokalemia as an independent predictor of postoperative renal function impairment in a large Taiwanese cohort of 328 patients, and with Tomiie et al. (7), who demonstrated that lower preoperative serum potassium concentrations were independently associated with a clinically significant drop in GFR category after adrenalectomy. These findings suggest that spontaneous hypokalemia, as a marker of severe and prolonged aldosterone excess, identifies patients with PA who are at higher risk of postoperative renal function decline and may serve as a preoperative indicator to guide patient counseling and nephrological follow-up.

Among the preoperative variables examined, baseline aldosterone concentration and aldosterone-to-renin ratio were significantly and negatively correlated with eGFR at postoperative month 6 (r: -0.52, p=0.003, and r: -0.39, p=0.02, respectively), indicating that patients with a greater degree of autonomous aldosterone excess had lower absolute renal function at 6 months postoperatively. This finding is consistent with the concept that higher aldosterone levels reflect more severe and potentially longer-standing mineralocorticoid-mediated renal injury, including glomerulosclerosis, tubular atrophy, and interstitial fibrosis, all of which reduce the kidney's functional capacity in the postoperative period (3,12,13). The positive correlation between preoperative eGFR and 6-month eGFR (r: 0.51, p=0.02) was expected and reflected the strong tracking of renal function over time; patients with better baseline renal function tended to maintain higher postoperative eGFR values. Collectively, these findings suggest that preoperative aldosterone levels are key determinants of postoperative renal function and that patients with overt biochemical hyperaldosteronism may warrant closer nephrological surveillance postoperatively.

The negative correlation between age at diagnosis and month 6 eGFR (r: -0.50, p=0.002) likely reflects the progressive age-related decline in the renal functional reserve, which limits the kidney's capacity to

maintain adequate filtration following the resolution of aldosterone-driven hyperfiltration. In older patients, the nephron mass available for functional recovery is inherently reduced, and the superimposed structural damage from chronic aldosterone excess and hypertension may compound this age-related vulnerability, resulting in lower absolute eGFR values at 6 months postoperatively compared with younger patients. Multiple cohort studies and meta-analyses have identified older age as a significant predictor of long-term eGFR decline or postoperative CKD after adrenalectomy for PA (5,8,14). The observed positive correlation between baseline systolic blood pressure and eGFR at six months (r: 0.37, p=0.02) may reflect glomerular hyperfiltration. However, this interpretation should be regarded as hypothesis-generating rather than a confirmed causal mechanism, given the retrospective, correlational design of this study. Patients with elevated preoperative systolic blood pressure may exhibit greater pressure-related glomerular hyperfiltration, which could contribute to a higher preoperative eGFR and, consequently, to a higher absolute eGFR at six months postoperatively, even after partial resolution of the hyperfiltration state. Further studies incorporating direct measures of glomerular hemodynamics would be needed to confirm this association.

Regarding clinical and biochemical outcomes, 69% of patients achieved complete biochemical remission at the 3-month follow-up. This result is consistent with remission rates reported in the literature for unilateral adrenalectomy in PA, which typically range from 60% to 99%, depending on how remission is defined and the duration of follow-up (15,16). Complete clinical blood pressure response, defined as normalization of blood pressure without antihypertensive medication, was observed in 36.9% of patients. By comparison, the majority (57.9%) achieved a partial response, characterized by a reduction in antihypertensive medication burden. The two patients who did not achieve a biochemical response also showed no clinical blood pressure response, suggesting persistent autonomous aldosterone secretion as the underlying mechanism of treatment failure in these cases. Across cohorts and meta-analyses, 20-30% of PA patients become normotensive without drugs (6,17,18); about half have improved BP and/or lower medication needs (6,18,19); and roughly 10-20% show little clinical BP benefit, despite very high biochemical cure rates (6,20). Our findings are in line with those reported in large multicenter series. The prevalence of a partial hypertensive response post-adrenalectomy may indicate that the underlying essential hypertension coexists with PA, potentially limiting the degree of blood pressure resolution following surgical cure. Remarkably, serum potassium levels returned to normal in all 20 patients who experienced spontaneous hypokalemia before surgery without requiring supplementation. This outcome confirms the complete reversal of the condition of mineralocorticoid excess and highlights one of the most consistent and reproducible advantages of surgical intervention in PA.

Study Limitations

Several limitations of the present study warrant acknowledgment. First, the retrospective single-center design limits the generalizability of the findings to other institutional settings and patient populations. Second, the relatively small sample size restricts the statistical power of correlation analyses and precludes robust multivariable regression modeling for identifying independent predictors of postoperative renal function. This limitation was particularly evident in the subgroup comparison between patients with and without complete biochemical remission, in which no significant difference in postoperative eGFR or change in creatinine was detected. However, the limited number of patients available for this comparison substantially restricted the statistical power to detect a clinically meaningful difference between groups; therefore, this negative finding should be interpreted with caution. Furthermore, eGFR data at postoperative month 3 were available for only 29 of 38 patients (76.3%), as the remaining 9 patients did not attend their scheduled follow-up visit. However, no systematic clinical difference was apparent between those with available data and those without; the possibility of informative loss to follow-up cannot be entirely excluded. Third, AVS was performed in 27 patients; however, successful bilateral cannulation was achieved in only 13 patients, and the lateralization index was therefore not included as a primary study variable. Fourth, the absence of long-term follow-up beyond 6 months precludes conclusions regarding the durability of renal function recovery and the potential long-term renoprotective benefit of adrenalectomy. Fifth, preoperative serum potassium data were recorded after potassium supplementation in most patients, precluding a reliable assessment of the true nadir potassium concentration. This variable is a stronger predictor of postoperative eGFR decline than the immediate preoperative value.

Conclusion

Unilateral adrenalectomy for PA was associated with a transient decline in eGFR at postoperative month 3; values approached baseline by month 6, and there was no evidence of persistent deterioration. This decline was more significant in patients with spontaneous hypokalemia, and the postoperative eGFR was associated with initial aldosterone levels, pre-surgery kidney function, and patient age. Complete biochemical remission was achieved in 69.0% of patients, and potassium levels normalized in all hypokalemic patients following surgery. These findings support the renal safety of adrenalectomy in appropriately selected patients with PA and highlight spontaneous hypokalemia as a clinically useful preoperative indicator of postoperative renal vulnerability. Early diagnosis and treatment are essential to optimizing long-term renal and cardiovascular outcomes.

Ethics

Ethics Committee Approval: The study was conducted in accordance with the ethical standards of the 1975 Declaration of Helsinki and was approved by the Local Ethics Committee of University of Health Sciences Türkiye, Başakşehir Çam and Sakura City Hospital (decision number: 48, date: 21.01.2026).

Informed Consent: The ethics committee waived the requirement for informed consent due to the retrospective nature of the study and the use of anonymized data.

Footnotes

Authorship Contributions: Surgical and Medical Practices - A.P., A.Ç.; Concept - Ş.B., M.N., E.H.; Design - Ş.B., M.N., E.H.; Data Collection

or Processing - Ş.B., A.P., A.Ç.; Analysis or Interpretation - Ş.B., M.N.; Literature Search - Ş.B., A.P., A.Ç.; Writing - Ş.B., A.P., E.H.

Conflict of Interest: No conflict of interest was declared by the authors.

Financial Disclosure: The authors declared that this study received no financial support.

References

1. Vaidya A, Mulatero P, Baudrand R, Adler GK. The expanding spectrum of primary aldosteronism: implications for diagnosis, pathogenesis, and treatment. Endocr Rev. 2018; 39: 1057-88.
2. Rossi GP, Bernini G, Desideri G, Fabris B, Ferri C, Giacchetti G, et al. Renal damage in primary aldosteronism: results of the PAPY Study. Hypertension. 2006; 48: 232-8.
3. Monticone S, Sconfienza E, D'Ascenzo F, Buffolo F, Satoh F, Sechi LA, et al. Renal damage in primary aldosteronism: a systematic review and meta-analysis. J Hypertens. 2020; 38: 3-12.
4. Adler GK, Stowasser M, Correa RR, Khan N, Kline G, McGowan MJ, et al. Primary aldosteronism: an Endocrine Society Clinical Practice Guideline. J Clin Endocrinol Metab. 2025; 110: 2453-95. Erratum in: J Clin Endocrinol Metab.; 110: e3933-4.
5. Yang YS, Lee SH, Kim JH, Yoo JH, Lee JH, Lee SY, et al. Contralateral suppression at adrenal venous sampling is associated with renal impairment following adrenalectomy for unilateral primary aldosteronism. Endocrinol Metab (Seoul). 2021; 36: 875-84.
6. Williams TA, Lenders JWM, Mulatero P, Burrello J, Rottenkolber M, Adolf C, et al. Outcomes after adrenalectomy for unilateral primary aldosteronism: an international consensus on outcome measures and analysis of remission rates in an international cohort. Lancet Diabetes Endocrinol. 2017; 5: 689-99.
7. Tomiie Y, Hibi Y, Nobe R, Yokoi K, Koshima Y, Ogawa K, et al. Changes in kidney function after adrenalectomy in patients with primary aldosteronism. Fujita Med J. 2025; 11: 28-35.
8. Chen JY, Huang KH, Lin YH, Chueh JS, Wang HY, Wu VC. Association of dip in eGFR with clinical outcomes in unilateral primary aldosteronism patients after adrenalectomy. J Clin Endocrinol Metab. 2024; 109: e965-74.
9. Iwakura Y, Morimoto R, Kudo M, Ono Y, Takase K, Seiji K, et al. Predictors of decreasing glomerular filtration rate and prevalence of chronic kidney disease after treatment of primary aldosteronism: renal outcome of 213 cases. J Clin Endocrinol Metab. 2014; 99: 1593-8.
10. Yoon JH, Chung HS, Hong AR, Kim HK, Kang HC, Kim MS, et al. Is acute kidney injury after laparoscopic adrenalectomy related to the progression of chronic kidney disease in patients with primary aldosteronism? Investig Clin Urol. 2021; 62: 560-8.
11. Lu YC, Liu KL, Wu VC, Wang SM, Lin YH, Chueh SJ, et al. Factors associated with renal function change after unilateral adrenalectomy in patients with primary aldosteronism. Int J Urol. 2022; 29: 831-7.
12. Martín-Fernández B, Rubio-Navarro A, Cortegano I, Ballesteros S, Alía M, Cannata-Ortiz P, et al. Aldosterone induces renal fibrosis and inflammatory M1-macrophage subtype via mineralocorticoid receptor in rats. PLoS One. 2016; 11: e0145946.
13. Polenus P, Đuran A, Karanović Štambuk S. Aldosterone in chronic kidney disease. Biomedicines. 2025; 13: 2081.
14. Kim DH, Kwon HJ, Ji SA, Jang HR, Jung SH, Kim JH, et al. Risk factors for renal impairment revealed after unilateral adrenalectomy in patients with primary aldosteronism. Medicine (Baltimore). 2016; 95: e3930.
15. Artiles Medina A, Gómez Dos Santos V, Mínguez Ojeda C, Sanjuanbenito A, Gómez-Ramírez J, Mercader E, et al. The role of adrenal-sparing surgery in the management of aldosterone-producing adenoma: a systematic review and meta-analysis. Eur J Endocrinol. 2025; 193: S36-52.
16. Murasawa S, Kageyama K, Usutani M, Asari Y, Kinoshita N, Nakada Y, et al. Biochemical evaluation by confirmatory tests after unilateral adrenalectomy for primary aldosteronism. J Renin Angiotensin Aldosterone Syst. 2023; 2023: 5732812.
17. Marzano L, Ronco C. Clinical and biochemical outcomes after adrenalectomy for primary aldosteronism in tertiary and quaternary referral centers: data from SOPRANO study. Hypertens Res. 2024; 47: 721-34.
18. Morisaki M, Kurihara I, Itoh H, Naruse M, Takeda Y, Katabami T, et al. Predictors of clinical success after surgery for primary aldosteronism in the Japanese Nationwide Cohort. J Endocr Soc. 2019; 3: 2012-22.
19. Vorselaars WMCM, Nell S, Postma EL, Zarnegar R, Drake FT, Duh QY, et al. Clinical outcomes after unilateral adrenalectomy for primary aldosteronism. JAMA Surg. 2019; 154: e185842.
20. Zekarias K, Kohlenberg J, Ikramuddin S. Primary aldosteronism surgery outcomes under current blood pressure guidelines. Endocr Pract. 2026; 32: 31-7.

İstanbul Med J 2026; 27(3): 259-67
DOI: 10.4274/imj.galenos.2026.24886

Prognostic Role of CT-Derived Muscle and Adipose Tissue Parameters After Pancreaticoduodenectomy for Pancreatic Ductal Adenocarcinoma: An Exploratory Analysis

Olgun Erdem[1], Tolga Canbak[1], Aylin Acar[1], Sevde Nur Emir[2], Hüsna Tosun[1], Görkem Karamustafao[2], Fatih Başak[1]

[1]University of Health Sciences Türkiye, Ümraniye Training and Research Hospital, Clinic of General Surgery, İstanbul, Türkiye
[2]University of Health Sciences Türkiye, Ümraniye Training and Research Hospital, Clinic of Radiology, İstanbul, Türkiye

ABSTRACT

Introduction: Body composition abnormalities, including sarcopenia and adipose tissue alterations, have emerged as potential prognostic biomarkers in pancreatic ductal adenocarcinoma (PDAC). The present study investigated the relationship between preoperative computed tomography (CT)-derived adipose and muscle parameters and survival outcomes in patients undergoing pancreaticoduodenectomy for PDAC.

Methods: This retrospective analysis enrolled 69 patients with histologically confirmed PDAC who underwent pancreaticoduodenectomy between 2018 and 2024. Preoperative contrast-enhanced CT images acquired within 30 days before surgery were assessed at the level of the third lumbar vertebra (L3). Measurements included the area and attenuation of visceral and subcutaneous adipose tissue, as well as the area and attenuation of the psoas muscle. Overall survival (OS) and disease-free survival (DFS) were evaluated using Kaplan-Meier survival curves and Cox proportional hazards models.

Results: Median OS and DFS were 10.0 and 7.0 months, respectively. Kaplan-Meier analyses showed no statistically significant differences in survival across body composition parameters (all $p>0.05$), although several parameters exhibited consistent numerical trends in survival. In multivariable analysis, higher T stage was independently associated with worse OS [hazard ratio (HR): 1.83, 95% confidence interval (CI): 1.12-3.00, $p=0.015$], whereas adjuvant chemotherapy remained independently associated with improved OS (HR: 0.16, 95% CI: 0.07-0.34, $p<0.001$). Because of the limited number of DFS events, multivariable analysis was not performed.

Conclusion: CT-derived body composition analysis may provide complementary prognostic information in patients undergoing pancreaticoduodenectomy for PDAC. Although independent associations were not consistently demonstrated, the observed survival patterns support further investigation of CT-derived muscle and adipose tissue parameters as potential imaging biomarkers. Larger prospective multicenter studies are warranted to clarify their prognostic value.

Keywords: Pancreatic ductal adenocarcinoma, pancreaticoduodenectomy, body composition, sarcopenia, myosteatosis, computed tomography, psoas muscle attenuation, visceral adipose tissue, survival analysis, prognostic biomarkers

Introduction

Pancreatic ductal adenocarcinoma (PDAC) is among the most aggressive and difficult-to-treat malignancies owing to its biological characteristics. According to GLOBOCAN 2020, pancreatic cancer accounted for near 500,000 new cases and over 450,000 deaths worldwide, reflecting its disproportionately high mortality burden (1). Surgical resection remains the primary curative treatment; for tumors located in the pancreatic head, pancreaticoduodenectomy (Whipple procedure) is the only surgical option. Yet, even in patients who undergo resection, outcomes remain disappointing, with a substantial proportion experiencing early recurrence and limited long-term survival (2,3).

In this context, improving preoperative risk stratification has become increasingly important. Conventional prognostic factors such as tumor stage, lymph node involvement, and margin status are typically determined postoperatively, limiting their utility in preoperative decision-making. Therefore, there is growing interest in identifying non-invasive, imaging-based biomarkers that can provide prognostic information before surgery. Computed tomography (CT), routinely performed in the preoperative setting, offers an opportunity to extract such information beyond standard anatomical assessment.

Among CT-derived parameters, body composition analysis at the third lumbar vertebra (L3) level provides a reliable representation of whole-

Address for Correspondence: Olgun Erdem, MD, University of Health Sciences Türkiye, Ümraniye Training and Research Hospital, Clinic of General Surgery, İstanbul, Türkiye
E-mail: olgun.erdem@hotmail.com **ORCID ID:** orcid.org/0000-0003-1433-3431
Cite this article as: Erdem O, Canbak T, Acar A, Emir SN, Tosun H, Karamustafao G, et al. Prognostic role of CT-derived muscle and adipose tissue parameters after pancreaticoduodenectomy for pancreatic ductal adenocarcinoma: an exploratory analysis. İstanbul Med J. 2026; 27(3): 259-67

Received: 25.05.2026
Accepted: 09.07.2026
Publication Date: 03.08.2026

body tissue distribution. A single cross-sectional CT image at this level can be used to quantify both adipose and lean tissue compartments with high accuracy (4). This has enabled the use of routine imaging data for quantitative assessment of patient-specific physiological characteristics.

Adipose tissue is increasingly recognized as an active metabolic organ rather than a passive energy reservoir. Both the quantity and quality of adipose tissue—reflected by cross-sectional area and attenuation values measured in Hounsfield units (HUs)—have been associated with systemic inflammation, cachexia, and tumor progression (5). Similarly, skeletal muscle parameters such as psoas muscle area and attenuation may reflect sarcopenia and myosteatosis, both of which have been linked to impaired physiological reserve and adverse oncological outcomes (6). Importantly, these measurements can be easily derived from standard preoperative CT scans without incurring extra costs or imposing an additional burden on patients.

Evidence from gastrointestinal malignancies suggests that both adipose tissue and skeletal muscle characteristics may carry prognostic significance (7,8). Increased visceral adiposity has been associated with adverse oncologic outcomes in colorectal cancer (9), while higher visceral fat attenuation has been linked to worse survival in gastric cancer (10). Likewise, reduced muscle attenuation and myosteatosis have been associated with inferior postoperative and long-term outcomes in several gastrointestinal cancers. Nevertheless, the prognostic significance of these CT-derived body composition parameters in PDAC remains incompletely defined. In particular, the relative contributions of adipose tissue quantity and quality and of muscle-related parameters to survival outcomes remain uncertain in surgically treated PDAC patients.

Therefore, this study was designed to investigate the association between preoperative CT-derived measures at the L3 vertebral level (subcutaneous and visceral adipose tissue area, adipose tissue attenuation values, and psoas muscle area and attenuation) and overall survival (OS) in patients undergoing pancreaticoduodenectomy for PDAC. Secondary objectives included evaluating the relationship between these parameters and disease-free survival (DFS) and 30-day postoperative mortality.

Methods

Study Design and Patient Selection

This retrospective cohort study included patients who underwent pancreaticoduodenectomy (Whipple procedure) at University of Health Sciences Türkiye, Ümraniye Training and Research Hospital between January 2018 and December 2024. Eligible patients were identified using the institutional surgical registry. The study was performed and reported in compliance with the Strengthening the Reporting of Observational Studies in Epidemiology recommendations.

Patients were included if they had histopathologically confirmed PDAC, were aged 18 years or older, had a preoperative abdominal CT scan obtained within 30 days before surgery, and had available OS data.

Patients were excluded if the final histopathology was not consistent with PDAC; if preoperative CT imaging was unavailable or technically inadequate for adipose tissue analysis; if OS data were unknown; if they were younger than 18 years; or if pancreaticoduodenectomy had been performed emergently for hemorrhage. PDAC patients located in the tail of the pancreas were excluded due to differences in the surgical approach and surgical burden.

Data Collection

Demographic, clinical, operative, and pathological data were retrieved retrospectively from electronic medical records. Variables of interest, where available, included age, sex, tumor-related pathological findings, nodal status, resection margin status, and adjuvant treatment status.

Follow-up data were obtained from hospital records and other accessible institutional follow-up sources. OS status, recurrence status, and 30-day postoperative mortality were recorded. Because of the retrospective nature of the study, DFS data were not expected to be available for all patients.

CT Acquisition and Image Analysis

Preoperative contrast-enhanced abdominal CT examinations obtained within 30 days of surgery were retrospectively reviewed. Body composition analysis was performed at the level of the L3 vertebra, which served as the predefined anatomical landmark. Portal venous phase CT images were used for all body composition measurements.

On a single representative axial CT image at the L3 level, subcutaneous adipose tissue, visceral adipose tissue, and bilateral psoas muscles were evaluated. Subcutaneous and visceral adipose tissue areas were segmented using a threshold-based semi-automatic method with a predefined adipose tissue attenuation range of -190 to -30 HUs, followed by manual correction when necessary. During segmentation, bowel contents, vessels, and bone structures were carefully excluded.

For each patient, subcutaneous and visceral adipose tissue areas and their mean attenuations were recorded. All area measurements were expressed in mm^2, whereas attenuation values were expressed in HU. Representative examples of visceral adipose tissue, subcutaneous adipose tissue, and psoas muscle measurements are shown in Figure 1.

Bilateral psoas muscles were segmented on the same axial slice using a semi-automatic method followed by manual correction. The right and left psoas muscle areas were summed to obtain the total psoas muscle area. Psoas muscle attenuation was measured as the mean attenuation of the segmented bilateral psoas muscles.

All CT measurements were performed by two radiologists in consensus: an abdominal radiologist with 12 years of experience and a radiology resident with 4 years of experience. Both readers were blinded to clinical, laboratory, and survival outcome data. For each patient, a single final consensus measurement was recorded for each CT-derived body composition parameter. Total psoas muscle area was used as a pragmatic surrogate marker of skeletal muscle mass because height-normalized skeletal muscle index (SMI) measurements were not consistently available owing to the retrospective study design.

Outcomes

The primary outcome was OS, measured from the date of surgery until death from any cause or the last available follow-up.

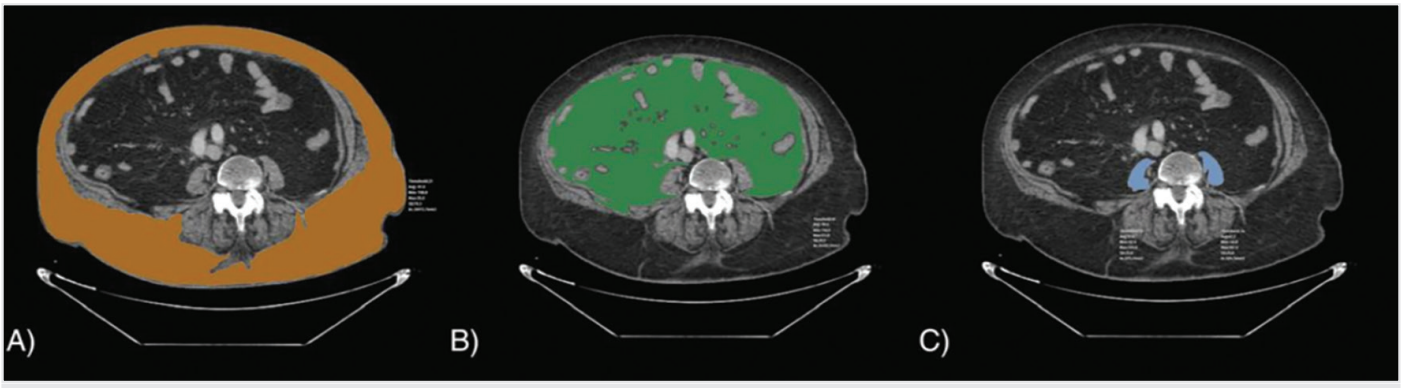

Figure 1. Computed tomography (CT)-based body composition analysis at the L3 vertebral level. Representative axial CT images showing semi-automatic segmentation of A) subcutaneous adipose tissue, B) visceral adipose tissue, and C) bilateral psoas muscles. Subcutaneous and visceral adipose tissue compartments were segmented using a predefined attenuation threshold range of -190 to -30 HU, followed by manual correction. All panels depict different tissue segmentations derived from the same axial CT slice of a single patient

Secondary outcomes included DFS, defined as the interval from surgery to recurrence, death, or last follow-up among patients with documented recurrence status; and early postoperative mortality, defined as mortality occurring within 30 days of surgery.

Ethical Approval

The study adhered to the principles of the Declaration of Helsinki and received approval from the University of Health Sciences Türkiye, Ümraniye Training and Research Hospital (decision number: 146, date: 22.04.2026). Because of the retrospective design and the exclusive use of anonymized patient data, the Institutional Ethics Committee waived the requirement for written informed consent.

Statistical Analysis

Statistical analyses were performed using IBM SPSS Statistics (version 26.0; IBM Corp., Armonk, NY, USA); data visualization and forest-plot generation were performed using RStudio (version 2025.05.1). Continuous variables were summarized as mean ± standard deviation or median with interquartile range (IQR) according to data distribution, whereas categorical variables were expressed as frequencies and percentages.

Radiological body composition parameters were primarily analyzed as continuous variables in Cox proportional hazards regression models to minimize information loss associated with dichotomization. For illustrative Kaplan–Meier analyses, body composition parameters were dichotomized according to median values. Survival curves were estimated using the Kaplan-Meier method and compared using the log-rank test. Additional Kaplan-Meier analysis was performed, stratified by adjuvant chemotherapy status, to provide an unadjusted comparison of OS.

Associations between clinicopathological variables, radiological body composition parameters, and survival outcomes were further evaluated using Cox proportional hazards regression analysis. Imaging parameters were analyzed as continuous variables in Cox models. Univariable Cox regression analyses were initially performed for both OS and DFS. Variables demonstrating statistical or borderline significance in univariable analyses were considered for multivariable Cox regression. T stage was also retained in the final model because of its established prognostic importance in PDAC and its borderline association with OS in the univariable analysis. To minimize the risk of model overfitting, the final multivariable model was restricted to a limited number of covariates. Because of the limited number of DFS events and concerns regarding model stability, multivariable Cox regression analysis was not performed.

The proportional hazards assumption was assessed using both graphical log-minus-log survival plots and formal testing based on Schoenfeld residuals.

Thirty-day postoperative mortality and complications were analyzed descriptively. Because of the limited number of early mortality events, regression analysis was not performed for the 30-day mortality endpoint.

A two-sided p value of less than 0.05 was considered statistically significant.

Results

A total of 231 patients who underwent pancreaticoduodenectomy (Whipple procedure) were screened for eligibility. Among them, 73 patients had histopathologically confirmed PDAC. Three patients were excluded because preoperative CT images were unavailable, and one patient was excluded due to loss to follow-up. Consequently, 69 patients were included in the OS analysis. Eight additional patients were excluded from DFS analysis because postoperative imaging required for recurrence assessment was unavailable, resulting in 61 patients being included in the DFS cohort (Figure 2).

The mean age of the patients was 64.0±7.8 years. Most patients had advanced pathological disease, with T2 and T3 tumors accounting for 49.3% and 36.2% of cases, respectively, while N2 nodal involvement was observed in 46.4% of patients. The mean positive lymph node count was 5.8±4.4, and the majority of tumors were grade 2 (81.2%). Margin positivity was identified in 31.9% of patients, whereas lymphovascular invasion and perineural invasion were present in 72.5% and 98.6% of cases, respectively. Adjuvant therapy was administered to 78.3% of patients, whereas only two patients (2.9%) received neoadjuvant treatment. Additional demographic, clinicopathological, biochemical, and radiological body composition characteristics are summarized in Table 1.

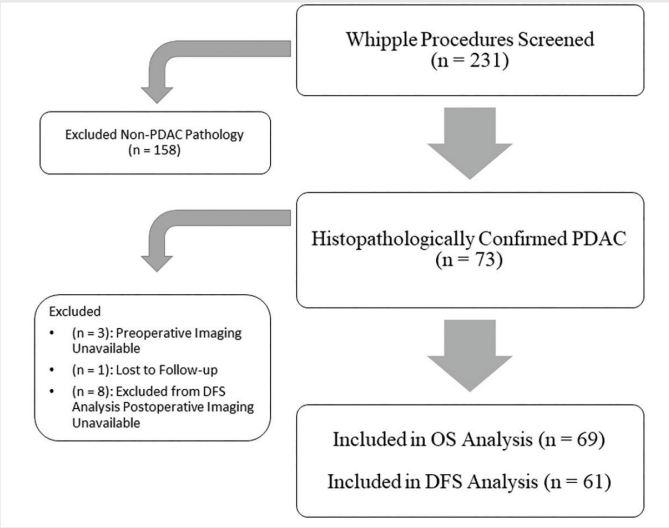

Figure 2. Flow diagram of patient selection and study cohort formation. The eight patients excluded from DFS analysis had available vital status data and were retained in the OS analysis; they were excluded solely due to unavailability of postoperative imaging required for recurrence assessment. OS: Overall survival, DFS: Disease-free survival

Postoperative pancreatic fistula developed in 21 (30.4%) patients, based on the criteria established by the International Study Group on Pancreatic Surgery, irrespective of fistula grade. Grade B/C fistulas occurred in 12 (17.3%) patients. Thirty-day mortality occurred in 5 patients (7.2%). Two deaths were attributed to sepsis secondary to pancreaticojejunostomy (PJ) leakage, while two additional patients died during intensive care follow-up after hemorrhagic complications associated with PJ leakage. One patient died from myocardial infarction on postoperative day 9, unrelated to any surgical morbidity.

Median OS was 10.0 months (IQR: 11.0), while median DFS was 7.0 months (IQR: 5.0). The median follow-up duration was 12.0 months (IQR: 10.0 months). Overall, mortality was observed in 53 patients (76.8%), and recurrence occurred in 35 patients (57.3%). The OS analysis was based on all-cause mortality.

For illustrative Kaplan-Meier analyses, body composition parameters were dichotomized according to median values. Kaplan-Meier analysis demonstrated no significant differences in OS by visceral fat area, visceral fat attenuation, subcutaneous fat area, subcutaneous fat attenuation, psoas muscle area, or psoas muscle attenuation (all $p>0.05$). Nevertheless, patients with higher visceral fat area demonstrated a non-significant trend toward longer OS than those with lower visceral fat area (median: 8.0 vs. 14.0, $p=0.161$). Similarly, a higher psoas muscle area was associated with longer OS (median: 9.0 vs. 13.0 months, $p=0.135$). Detailed OS analyses are summarized in Table 2 and Figure 3.

Likewise, DFS analyses showed no statistically significant differences in survival by visceral fat area, visceral fat attenuation, subcutaneous fat area, subcutaneous fat attenuation, psoas muscle area, or psoas muscle attenuation (all $p>0.05$). However, patients with lower psoas muscle attenuation had a numerically longer DFS (median: 9.0 vs. 7.0) than those with higher attenuation values; this difference was not statistically significant ($p=0.418$). Detailed DFS analyses are presented in Table 2 and Figure 4.

Kaplan-Meier analysis stratified by adjuvant chemotherapy status demonstrated significantly longer OS for patients who received adjuvant chemotherapy than for those who did not (log-rank $p<0.001$; Supplementary Figure 1).

Univariable Cox regression analysis for OS demonstrated borderline associations with T stage [hazard ratio (HR): 1.344, 95% confidence interval (CI): 0.855-2.113, $p=0.200$] and psoas muscle area (HR: 0.946, 95% CI: 0.894-1.000, $p=0.052$), whereas adjuvant therapy emerged as a significant protective factor (HR: 0.198, 95% CI: 0.099-0.396, $p<0.001$). In multivariable analysis, higher T stage was associated with worse OS (HR: 1.83, 95% CI: 1.12-3.00, $p=0.015$), whereas adjuvant chemotherapy was associated with improved OS (HR: 0.16, 95% CI: 0.07-0.34, $p<0.001$). Although higher psoas muscle area showed a protective effect (HR: 0.96 per 100 mm^2 increase), this association was not statistically significant (95% CI: 0.90-1.02, $p=0.200$).

Graphical assessment using log-minus-log survival plots did not demonstrate major violations of the proportional hazards assumption. Formal Schoenfeld residual testing was performed for the revised OS multivariable model. A statistically significant violation was identified for adjuvant chemotherapy ($p=0.003$), suggesting that the effect of adjuvant treatment on OS may not be constant over the entire follow-up period. Therefore, the HR for adjuvant chemotherapy should be regarded as an average effect throughout the follow-up period rather than a fixed treatment effect.

For DFS, univariate Cox regression analysis demonstrated a significant association for neoadjuvant therapy (HR: 11.326, 95% CI: 1.178-108.903, $p=0.036$), although this finding should be interpreted cautiously because only two patients received neoadjuvant therapy. Positive lymph node count ($p=0.134$), psoas muscle attenuation ($p=0.137$), and CA19-9 level ($p=0.092$) demonstrated borderline significance. Because of the limited number of DFS events and concerns regarding model stability, multivariable Cox regression analysis was not performed for DFS. Detailed Cox regression analyses are summarized in Table 3, and the OS multivariable model is visualized in Figure 5.

Table 1. Baseline demographic, clinical, and pathological characteristics of the patients

Age, years	64.0±7.8
Sex (male/female)	37/32 (53.6/46.4%)
T stage (T1/T2/T3/T4)	8/34/25/2 (11.6/49.3/36.2/2.9%)
N stage (N0/N1/N2)	13/24/32 (18.8/34.8/46.4%)
Positive lymph node count	5.8±4.4
Tumor grade (I/II/III)	6/56/7 (8.7/81.2/10.1%)

Table 1. Continued	
Positive resection margin	22 (31.9%)
Lymphovascular invasion	50 (72.5%)
Perineural invasion	68 (98.6%)
ASA score (I/II/III)	4/52/13 (5.8/75.4/18.8%)
Neoadjuvant therapy	2 (2.9%)
Adjuvant therapy	54 (78.3%)
Clavien-Dindo complication grade (0/I/II/III/IV/V)	30/15/14/5/0/5
Biochemical parameters	
CRP (mg/L)	6.7 (IQR: 17.3)
Albumin (g/L)	35.5±4.9
NLR	2.6 (IQR: 4.0)
CA 19.9 (U/mL)	60.7 (IQR: 269.5)
CT-derived body composition parameters	
Visceral adipose tissue area (mm^2)	16196.5±8507.2
Visceral adipose tissue attenuation (HU)	-75.9±15.4
Subcutaneous adipose tissue area (mm^2)	19305.8±10027.7
Subcutaneous adipose tissue attenuation (HU)	-92.0 (IQR: 14.5)
Psoas muscle area (mm^2)	1274.5 (IQR: 815.8)
Psoas muscle attenuation (HU)	45.0 (IQR: 13.0)
Survival outcomes	
Overall mortality	53 (76.8%)
Recurrence	35 (57.3%)
Overall survival, median months	10.0 months (IQR: 11.0)
Disease-free survival, median months	7.0 months (IQR: 5.0)
Median follow-up	12.0 months (IQR: 10.0)

Data are presented as mean ± standard deviation, median [interquartile range (IQR)], or n (%), as appropriate. Normally distributed continuous variables are presented as mean ± standard deviation, whereas non-normally distributed variables are presented as median (IQR). ASA: American Society of Anesthesiologists, CRP: C-reactive protein, NLR: neutrophil-to-lymphocyte ratio, CA: Carbohydrate antigen, CT: Computed tomography, HU: Hounsfield unit

Table 2. Kaplan-Meier overall survival and disease-free survival analyses according to CT-derived body composition parameters

Overall survival			
Parameter	**Cut-off**	**Median OS, months (95% CI) low vs. high**	**Log-rank p**
Visceral adipose tissue area (mm^2)	17825	8.0 (4.3-11.6) vs. 14.0 (9.4-18.5)	0.161
Visceral adipose tissue attenuation (HU)	-89	11.0 (7.8-14.1) vs. 10.0 (5.1-14.8)	0.379
Subcutaneous adipose tissue area (mm^2)	13529	10.0 (5.6-14.3) vs. 11.0 (6.1-15.6)	0.505
Subcutaneous adipose tissue attenuation (HU)	-101.5	11.0 (8.2-13.7) vs. 10.0 (5.5-14.4)	0.423
Psoas muscle area (mm^2)	1056.5	9.0 (6.9-11.1) vs. 13.0 (9.4-16.6)	0.135
Psoas muscle attenuation (HU)	42.5	10.0 (5.9-14.0) vs. 10.0 (7.3-12.7)	0.764
Disease-free survival			
Visceral adipose tissue area (mm^2)	18204.5	8.0 (4.9-11.0) vs. 10.0 (4.7-15.2)	0.249
Visceral adipose tissue attenuation (HU)	-89	8.0 (5.3-10.6) vs. 10.0 (6.1-13.8)	0.797
Subcutaneous adipose tissue area (mm^2)	12129.5	8.0 (4.0-11.9) vs. 8.0 (1.9-14.0)	0.342
Subcutaneous adipose tissue attenuation (HU)	-101.5	7.0 (3.8-10.1) vs. 8.0 (4.0-11.9)	0.968
Psoas muscle area (mm^2)	1127.5	7.0 (3.9-10.0) vs. 10.0 (6.9-13.0)	0.572
Psoas muscle attenuation (HU)	42.5	9.0 (5.8-12.2) vs. 7.0 (4.5-9.5)	0.418

Body composition parameters were dichotomized according to median values for illustrative Kaplan–Meier survival analyses. Survival outcomes are presented as median overall survival (OS) or median disease-free survival (DFS) in months, with 95% confidence intervals. Low and high groups were defined according to the corresponding cut-off values for each parameter. CT: Computed tomography, OS: Overall survival, CI: Confidence interval, HU: Hounsfield unit

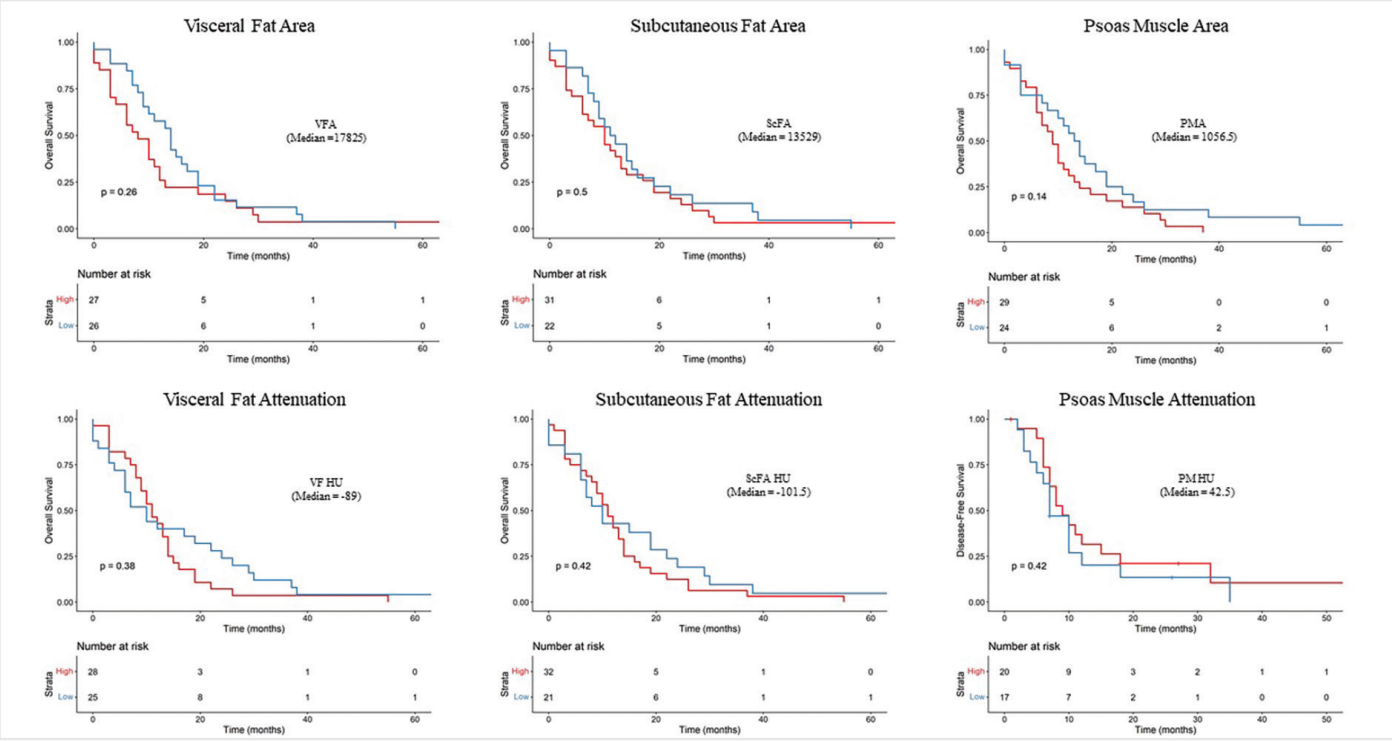

Figure 3. Kaplan-Meier overall survival curves according to computed tomography-derived body composition parameters. Kaplan-Meier overall survival curves stratified according to visceral adipose tissue area, visceral adipose tissue attenuation, subcutaneous adipose tissue area, subcutaneous adipose tissue attenuation, psoas muscle area, and psoas muscle attenuation. Body composition parameters were dichotomized at their median values for illustrative survival analyses. Red curves represent low-value groups, and blue curves represent high-value groups. The x-axis represents time in months. Number-at-risk tables are displayed beneath each survival curve. HU: Hounsfield unit

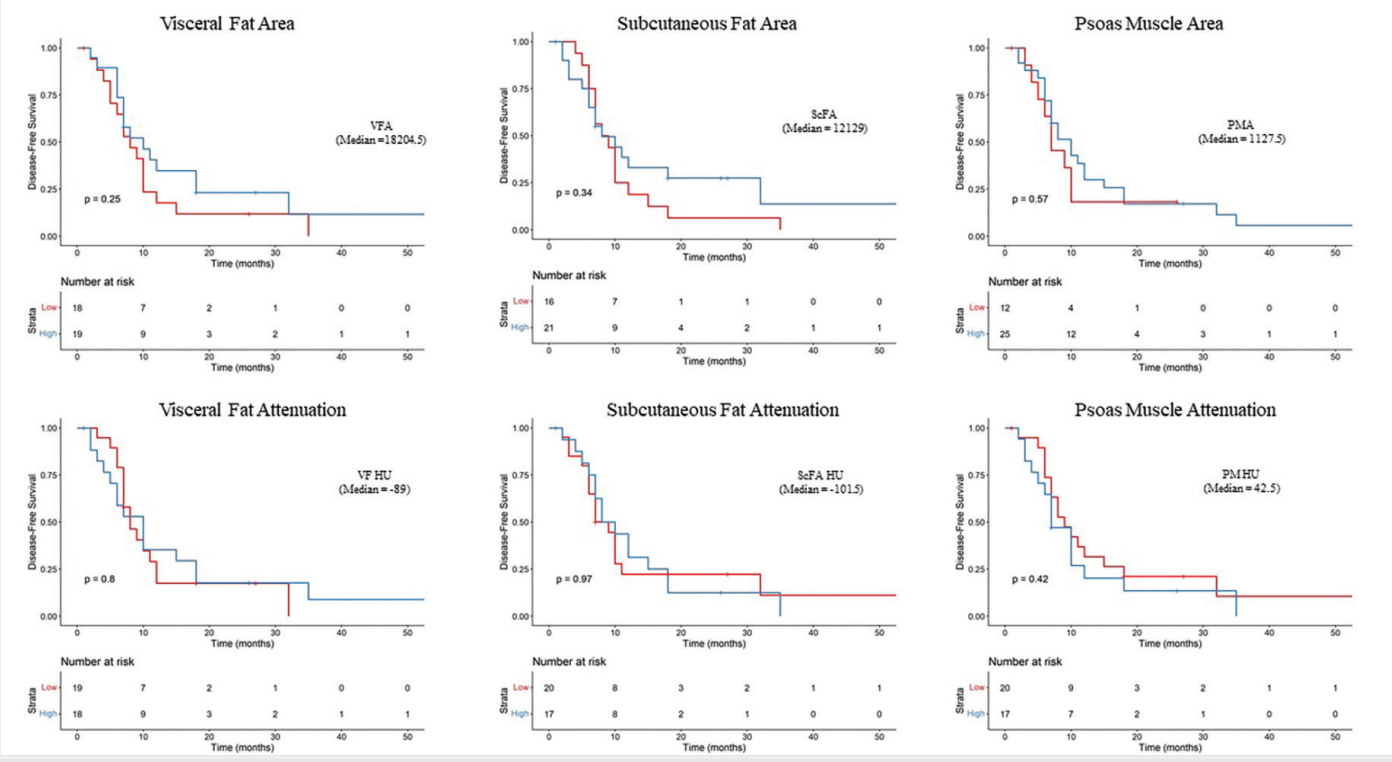

Figure 4. Kaplan-Meier disease-free survival curves according to computed tomography-derived body composition parameters. Kaplan-Meier disease-free survival curves stratified according to visceral adipose tissue area, visceral adipose tissue attenuation, subcutaneous adipose tissue area, subcutaneous adipose tissue attenuation, psoas muscle area, and psoas muscle attenuation. Body composition parameters were dichotomized according to median values for illustrative survival analyses. Red curves represent low-value groups and blue curves represent high-value groups. The x-axis represents time in months. Number-at-risk tables are displayed beneath each survival curve. HU: Hounsfield unit

Table 3. Univariate and multivariable Cox regression analyses of clinicopathological and body composition parameters for overall and disease-free survival

	Overall survival				Disease-free survival	
Variable	**Univariable HR (95% CI)**	**p**	**Multivariable HR (95% CI)**	**p**	**Univariable HR (95% CI)**	**p**
Age	1.01 (0.97-1.04)	0.593			1.01 (0.95-1.07)	0.695
T stage	1.34 (0.85-2.11)	0.200	1.83 (1.12-3.00)	0.015	1.56 (0.82-2.96)	0.166
N stage	0.98 (0.65-1.49)	0.947			1.39 (0.79-2.46)	0.246
Positive lymph node count	1.00 (0.93-1.08)	0.881			1.06 (0.98-1.16)	0.134
Tumor grade	1.04 (0.62-1.76)	0.866			1.15 (0.56-2.38)	0.689
Positive resection margin	1.64 (0.93-2.89)	0.085			0.97 (0.44-2.12)	0.951
Lymphovascular invasion	0.73 (0.37-1.44)	0.378			2.23 (0.51-9.69)	0.284
Visceral adipose tissue area (per 100 mm^2 increase)	0.98 (0.95-1.01)	0.343			0.99 (0.94-1.03)	0.726
Visceral adipose tissue attenuation	0.99 (0.97-1.00)	0.273			1.00 (0.97-1.02)	0.996
Subcutaneous adipose tissue area (per 100 mm^2 increase)	0.99 (0.96-1.02)	0.868			1.00 (0.95-1.05)	0.869
Subcutaneous adipose tissue attenuation	0.99 (0.98-1.01)	0.937			1.00 (0.97-1.02)	0.998
Psoas muscle area (per 100 mm^2 increase)	0.94 (0.89-1.00)	0.052	0.96 (0.90-1.02)	0.200	0.75 (0.35-1.46)	0.362
Psoas muscle attenuation	0.99 (0.97-1.01)	0.394			0.98 (0.95-1.00)	0.137
Adjuvant chemotherapy	0.19 (0.09-0.39)	<0.001	0.16 (0.07-0.34)	<0.001	0.18 (0.02-1.54)	0.119
ASA	1.05 (0.60-1.84)	0.843			1.31 (0.56-3.10)	0.527
CRP	1.00 (0.98-1.01)	0.652			0.99 (0.98-1.01)	0.775
Albumin	1.00 (0.95-1.05)	0.900			1.01 (0.93-1.10)	0.685
NLR	1.00 (0.99-1.01)	0.535			1.00 (0.99-1.01)	0.561
CA 19-9	1.00 (0.99-1.00)	0.472			1.00 (0.99-1.01)	0.092
Postoperative complications	1.20 (0.93-1.55)	0.148	-	-	0.97 (0.68-1.38)	0.889

Variables demonstrating statistical significance or borderline significance in univariable analyses were considered for multivariable Cox regression. The final multivariable model was refined based on clinical relevance and model stability while considering the number of observed events. Hazard ratios (HRs) for radiological body composition parameters were calculated using continuous measurements. HRs for area-based body composition parameters are expressed per 100 mm^2 increase, whereas CA 19-9 is expressed per 100 U/mL increase. Multivariable Cox regression analysis was not performed for disease-free survival because of the limited number of events and concerns regarding model stability. CI: Confidence interval, ASA: American Society of Anesthesiologists, CRP: C-reactive protein, NLR: Neutrophil-to-lymphocyte ratio, CA: Carbohydrate antigen

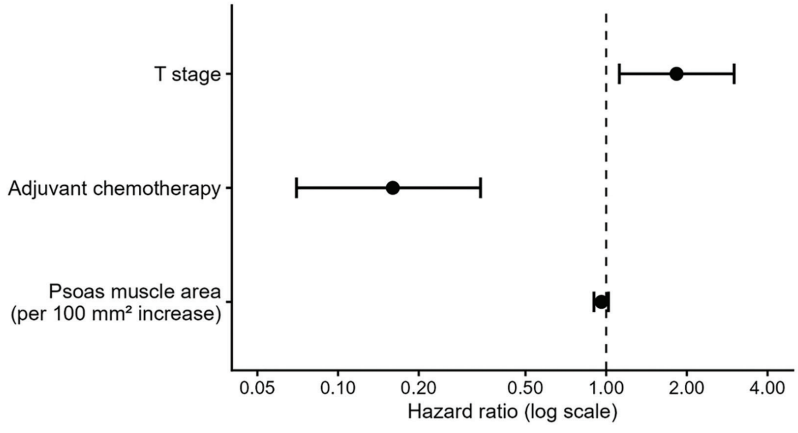

Figure 5. Forest plot of the multivariable Cox regression analysis for overall survival. Adjusted hazard ratios (HRs) and 95% confidence intervals for variables included in the final multivariable model. Psoas muscle area is expressed per 100-mm^2 increase. Hazard ratios are displayed on a logarithmic scale. The dashed vertical line indicates HR: 1.0

Discussion

In this retrospective analysis of patients undergoing pancreaticoduodenectomy for PDAC, CT-derived body composition parameters demonstrated heterogeneous associations with long-term oncological outcomes. Although most Kaplan–Meier comparisons did not reach statistical significance, several radiological markers showed consistent numerical separation of survival curves, suggesting a potential prognostic signal that may become more apparent in larger cohorts. Among the evaluated body composition parameters, psoas muscle area showed a borderline association with OS in univariable analysis and a consistently protective effect in multivariable analysis; however, this association did not remain statistically significant after adjustment. Higher T stage remained independently associated with worse OS, while adjuvant therapy consistently demonstrated a strong protective effect on OS.

Body composition analysis has attracted increasing interest in PDAC because conventional anthropometric measures often fail to capture cancer-related metabolic and muscular alterations. In particular, sarcopenia and myosteatosis have been linked to impaired functional reserve, systemic inflammation, treatment intolerance, and poorer oncological outcomes in several gastrointestinal malignancies (11,12). Recent studies have suggested that muscle quality, reflected by muscle attenuation on CT, may carry greater prognostic relevance than muscle quantity alone (13-16). A recent meta-analysis has also suggested that myosteatosis may outperform traditional sarcopenia measurements as a prognostic biomarker in pancreatic malignancies (17).

Our findings further support the growing interest in skeletal muscle characteristics as potential imaging biomarkers in PDAC. Although higher psoas muscle area showed a numerical association with longer OS in Kaplan-Meier analysis and a protective direction of effect in multivariable analysis, this association did not reach statistical significance after adjustment. Likewise, psoas muscle attenuation demonstrated a borderline association with DFS in univariable analysis but did not reach statistical significance. Overall, these findings indicate that both muscle quantity and quality may warrant further investigation as potential imaging biomarkers. Given the exploratory design and relatively small sample size, these findings should be interpreted with caution.

The relationship between adiposity and pancreatic cancer outcomes remains complex. While visceral obesity has traditionally been linked to adverse oncological biology and postoperative morbidity (18), several recent reports have suggested that severe depletion of adipose tissue may also represent an advanced catabolic state associated with poor survival (19). In our cohort, higher visceral fat area was numerically associated with longer OS and DFS, although these differences did not reach statistical significance. Rather than contradicting prior literature, these findings further support the concept that body composition in PDAC likely reflects a dynamic interaction between nutritional reserve, systemic inflammation, and tumor-related metabolic stress, and warrant further investigation in larger studies specifically designed to evaluate adipose tissue biology and distribution patterns.

Another notable finding of the present study was an independent association between adjuvant therapy and improved survival outcomes. Adjuvant chemotherapy remained independently associated with improved OS in multivariable analysis, underscoring the continued importance of systemic therapy even in surgically treated cohorts. This observation aligns closely with modern PDAC management paradigms and contemporary randomized trials demonstrating substantial survival benefits with adjuvant chemotherapy following resection (2,20). However, formal assessment of the proportional hazards assumption using Schoenfeld residual testing revealed a potential violation for adjuvant therapy in the OS model ($p=0.003$), suggesting that the effect of adjuvant treatment on survival may not be constant over time. Accordingly, the estimated hazard ratio for adjuvant therapy should be interpreted as an average effect over the follow-up period rather than a constant treatment effect.

The present study also provides clinically relevant perioperative context. Postoperative pancreatic fistula occurred in approximately one-third of patients, and early mortality was predominantly related to septic or hemorrhagic complications associated with PJ leakage. These findings reflect the continued technical and physiological complexity of pancreatic surgery, despite ongoing improvements in perioperative care. Although postoperative complications showed no significant association with OS in univariable analysis, larger studies specifically designed to evaluate postoperative morbidities are needed to better define their long-term oncological impact.

This study has several strengths. First, all body composition measurements were derived from routinely obtained preoperative CT imaging, which supports potential real-world applicability without additional cost or invasive assessment. Second, both adipose tissue and muscle-related parameters were evaluated simultaneously, allowing a more integrated assessment of body composition. Third, survival analyses incorporated both Kaplan–Meier and Cox regression approaches, enabling complementary evaluation of categorical survival patterns and continuous imaging parameters.

Study Limitations

This study has several limitations. First, its retrospective single-center design may have introduced selection bias. The relatively limited sample size and event burden may have reduced statistical power, particularly for subgroup analyses and multivariable modeling. Consequently, multivariable analysis was restricted to OS, whereas DFS was evaluated using univariable Cox regression because of concerns regarding model stability. In addition, body composition was measured at a single preoperative time point and therefore could not capture longitudinal changes in muscle or adipose tissue during treatment. Because multiple exploratory statistical comparisons were performed, the possibility of a type I error should be considered when interpreting isolated statistically significant findings.

Furthermore, total psoas muscle area was used as a surrogate for skeletal muscle mass rather than the height-normalized SMI, given the retrospective nature of the study. Although height data are typically available in medical records, SMI-based measurements were not

consistently performed; future studies should adopt standardized SMI to allow cross-study comparisons. Finally, although several radiological parameters demonstrated consistent numerical survival trends, most associations did not reach statistical significance after adjustment. Accordingly, these results should be regarded as preliminary and confirmed in larger, prospective, multicenter studies before being translated into clinical practice.

Conclusion

Overall, the present study suggests that CT-derived body composition parameters may warrant further investigation as potential imaging biomarkers in patients undergoing pancreaticoduodenectomy for PDAC. While most survival differences did not achieve statistical significance, muscle-related CT parameters showed consistent numerical associations with survival outcomes across multiple analyses, supporting their potential biological and clinical relevance. Future multicenter studies with larger cohorts and standardized radiological assessment protocols may help clarify the precise prognostic role of adipose- and muscle-related imaging biomarkers in PDAC.

Ethics

Ethics Committee Approval: The study adhered to the principles of the Declaration of Helsinki and received approval from the University of Health Sciences Türkiye, Ümraniye Training and Research Hospital (decision number: 146, date: 22.04.2026).

Informed Consent: Because of the retrospective design and the exclusive use of anonymized patient data, the Institutional Ethics Committee waived the requirement for written informed consent.

Footnotes

Authorship Contributions: Surgical and Medical Practices - O.E., T.C., A.A., S.N.E., H.T., F.B.; Concept - O.E., T.C., G.K.; Design - O.E., T.C., A.A., F.B.; Data Collection or Processing - A.A., S.N.E., H.T., G.K.; Analysis or Interpretation - O.E., S.N.E., F.B.; Literature Search - O.E.; Writing - O.E.

Conflict of Interest: No conflict of interest was declared by the authors.

Financial Disclosure: The authors declared that this study received no financial support.

Supplementary Figure Link: https://d2v96fxpocvxx.cloudfront.net/17d041fe-057c-4c8e-a75d-948e33c0152a/content-images/29059ecf-0d61-414d-a64e-7085844bc7ad.pdf

References

1. Sung H, Ferlay J, Siegel RL, Laversanne M, Soerjomataram I, Jemal A, et al. Global Cancer Statistics 2020: GLOBOCAN Estimates of incidence and mortality worldwide for 36 cancers in 185 countries. CA Cancer J Clin. 2021; 71: 209-49.
2. Conroy T, Hammel P, Hebbar M, Ben Abdelghani M, Wei AC, Raoul JL, et al. FOLFIRINOX or gemcitabine as adjuvant therapy for pancreatic cancer. N Engl J Med. 2018; 379: 2395-406.
3. Leonhardt CS, Gustorff C, Klaiber U, Le Blanc S, Stamm TA, Verbeke CS, et al. Prognostic factors for early recurrence after resection of pancreatic cancer: a systematic review and meta-analysis. Gastroenterology. 2024; 167: 977-92
4. Babic A, Rosenthal MH, Sundaresan TK, Khalaf N, Lee V, Brais LK, et al. Adipose tissue and skeletal muscle wasting precede clinical diagnosis of pancreatic cancer. Nat Commun. 2023; 14: 4317.
5. Chait A, den Hartigh LJ. Adipose tissue distribution, inflammation and its metabolic consequences, including diabetes and cardiovascular disease. Front Cardiovasc Med. 2020; 7: 22.
6. Kuwabara S, Takeuchi Y, Sato O, Mizota T, Ichinokawa M, Murakawa K, et al. Prognostic value of combined psoas muscle mass and controlling nutritional status in patients with pancreatic ductal adenocarcinoma: a retrospective cohort study. BMC Surg. 2024; 24: 116.
7. Benedek Z, Todor-Boér S, Kocsis L, Bauer O, Suciu N, Coroș MF. Psoas muscle index defined by computer tomography predicts the presence of postoperative complications in colorectal cancer surgery. Medicina (Kaunas). 2021; 57: 472.
8. Taniguchi Y, Kurokawa Y, Takahashi T, Saito T, Yamashita K, Tanaka K, et al. Impacts of preoperative psoas muscle mass and visceral fat area on postoperative short- and long-term outcomes in patients with gastric cancer. World J Surg. 2021; 45: 815-21.
9. Kamada T, Ohdaira H, Takahashi J, Aida T, Nakashima K, Ito E, et al. Effect of low visceral fat area on long-term survival of stage I-III colorectal cancer. Nutrition. 2024; 118: 112302.
10. Lee SM, Song GJ, Son MW, Yun JH, Lee MS, Lee JW. Association of increased CT-attenuation of visceral adipose tissue after surgery with poor survival outcomes in patients with stage II-III gastric cancer: a retrospective cohort study. Cancers (Basel). 2025; 17: 235.
11. Choi MH, Yoon SB. Sarcopenia in pancreatic cancer: effect on patient outcomes. World J Gastrointest Oncol. 2022; 14: 2302-12.
12. Hong S, Kim KW, Park HJ, Ko Y, Yoo C, Park SY, et al. Impact of baseline muscle mass and myosteatosis on the development of early toxicity during first-line chemotherapy in patients with initially metastatic pancreatic cancer. Front Oncol. 2022; 12: 878472.
13. Levolger S, van Vugt JL, de Bruin RW, IJzermans JN. Systematic review of sarcopenia in patients operated on for gastrointestinal and hepatopancreatobiliary malignancies. Br J Surg. 2015; 102: 1448-58.
14. Matsuo N, Yamaguchi T, Yukami H, Kodama H, Ikegami T, Kadono T, et al. Impact of skeletal muscle-related parameters on survival in patients with advanced pancreatic cancer treated with gemcitabine plus nab-paclitaxel as first-line chemotherapy. J Cancer. 2026; 17: 604-13.
15. van Dijk DP, Bakens MJ, Coolsen MM, Rensen SS, van Dam RM, Bours MJ, et al. Low skeletal muscle radiation attenuation and visceral adiposity are associated with overall survival and surgical site infections in patients with pancreatic cancer. J Cachexia Sarcopenia Muscle. 2017; 8: 317-26.
16. Peng P, Hyder O, Firoozmand A, Kneuertz P, Schulick RD, Huang D, et al. Impact of sarcopenia on outcomes following resection of pancreatic adenocarcinoma. J Gastrointest Surg. 2012; 16: 1478-86.
17. Zhang X, Wei L, Li J, Deng Y, Xu W, Chen D, et al. Influence of myosteatosis on survival of patients with pancreatic cancer: a systematic review and meta-analysis. iScience. 2024; 27: 111343.
18. Kim B, Chung MJ, Park SW, Park JY, Bang S, Park SW, et al. Visceral obesity is associated with poor prognosis in pancreatic adenocarcinoma. Nutr Cancer. 2016; 68: 201-7.
19. Yu SY, Luan Y, Dong R, Abazarikia A, Kim SY. Adipose tissue wasting as a determinant of pancreatic cancer-related cachexia. Cancers (Basel). 2022; 14: 4754.
20. Aoyama T, Hara K, Saito A, Cho H. Adjuvant treatment for resectable pancreatic cancer. Anticancer Res. 2025; 45: 1329-41.

İstanbul Med J 2026; 27(3): 268-74
DOI: 10.4274/imj.galenos.2026.91961

Real-World Outcomes of Allogeneic Hematopoietic Stem Cell Transplantation in Lymphoma Patients: A Single-Center Study

Ahmet Sarıcı[1], Emin Kaya[1], İrfan Kuku[1], Mehmet Ali Erkurt[1], İlhami Berber[1], Emine Hidayet[1], Gökhan Vakkas Çetin[2]

[1]İnönü University, Turgut Özal Medical Center, Department of Adult Hematology, Malatya, Türkiye
[2]İnönü University, Turgut Özal Medical Center, Department of Internal Medicine, Malatya, Türkiye

ABSTRACT

Introduction: Lymphomas are heterogeneous hematological malignancies, and despite effective frontline therapies, a subset of individuals develops relapsed or refractory disease. Autologous hematopoietic stem cell transplantation (HSCT) remains the standard approach; however, outcomes are poor after relapse. Allogeneic HSCT (Allo-HSCT) offers a potentially curative graft-vs.-lymphoma effect, but its use has declined due to toxicity and the emergence of novel therapies. Thus, its role in modern lymphoma management remains to be elucidated.

Methods: This retrospective investigation was performed at a single center. Patients with hodgkin lymphoma (HL) and non-HL who had undergone Allo-HSCT between January 2008 and May 2025 were evaluated for clinical characteristics, treatment outcomes, and survival parameters. A total of 25 patients were included in the study.

Results: Among the evaluated variables, only febrile neutropenia (FEN) was significantly associated with a higher mortality and shorter overall survival (OS), while other clinical and demographic factors showed no significant association. $CD34^+$ cell dose demonstrated limited predictive value for mortality (area under the curve: 0.654); the cohort's median OS was 6 months.

Conclusion: FEN emerged as the only clinical factor significantly correlated with increased mortality and with inferior OS, whereas other demographic and transplantation-related variables had no significant impact. $CD34^+$ cell dose demonstrated limited discriminative ability in predicting mortality, suggesting that post-transplant infectious complications may play a pivotal role in patient outcomes.

Keywords: Lymphoma, Allogeneic hematopoietic stem cell transplantation, survival, $CD34^+$ cell, febril neutropenia

Introduction

Lymphomas are hematological neoplasms characterized by significant clinical and biological heterogeneity (1). According to data from 2025, 89,070 lymphoma cases were reported. Lymphoma is classified as the second most frequently diagnosed malignancy among adolescents, in consideration of 19% of cases (2).

Lymphoid neoplasms arise from cells that normally differentiate into T or B lymphocytes. They are classified, according to their cellular origin, as either B-cell or T-cell neoplasms. Hodgkin lymphoma (HL) is a subtype of lymphoma characterized by the presence of neoplastic Reed-Sternberg cells and typically presents with cervical or supraclavicular lymphadenopathy. In contrast, non-HL (NHL) consists of a cohort of neoplastic abnormalities of the reticuloendothelial system, distinguished by systemic symptoms and clinical manifestations (3,4).

The primary treatment for classical HL consists of a combination of chemotherapy and radiotherapy. Autologous hematopoietic stem cell transplantation (HSCT) plays a critical association with the management of relapsed or refractory (R/R) classical HL (5). In contrast, Allogeneic HSCT (Allo-HSCT) in HL is generally reserved for medically eligible individuals who relapse after autologous HSCT and demonstrate only a partial response (PR) or progressive disease (PD) following immune checkpoint inhibition (6,7).

Most NHLs are initially treated with chemotherapy, and the majority of patients achieve remission following first-line therapy (8,9). However, a subset of individuals either relapse following complete response (CR) or exhibit resistance to initial treatment. In patients with R/R NHL, autologous HSCT is commonly employed (10,11). In contrast, Allo-HSCT is rarely used in (R/R)NHL due to its significant treatment-related toxicity and the availability of alternative therapeutic options (12).

This study was presented as an oral presentation at the 14th Annual Meet the Experts of Transplantation and Myeloma: EBMT and TCT Symposium, held in Istanbul, Türkiye, on May 8–9, 2026.

Address for Correspondence: Assoc. Prof. Ahmet Sarıcı, MD, İnönü University, Turgut Özal Medical Center, Department of Adult Hematology, Malatya, Türkiye
E-mail: ahmetsarici44@gmail.com **ORCID ID:** orcid.org/0000-0002-5916-0119

Cite this article as: Sarıcı A, Kaya E, Kuku İ, Erkurt MA, Berber İ, Hidayet E, et al. Real-world outcomes of Allogeneic hematopoietic stem cell transplantation in lymphoma patients: a single-center study. İstanbul Med J. 2026; 27(3): 268-74

Received: 01.04.2026
Accepted: 13.07.2026
Publication Date: 03.08.2026

Methods

This retrospective analysis, carried out at one institution, processed the clinical information from patients with HL and NHL who were cared for with Allo-HSCT at the Adult Stem Cell Transplantation Unit of İnönü University Turgut Özal Medical Center between January 2008 and May 2025. Clinical characteristics, treatment outcomes, overall survival (OS), progression-free survival, and prognostic factors have been evaluated through a retrospective analysis of electronic medical records.

Ethical approval for this study was obtained from the Institutional Ethics Committee from the İnönü University Health Sciences Non-Interventional Ethics Committee (approval number: 2025/7665, date: April 30, 2025). The study was conducted between May 28, 2025, and August 28, 2025. This retrospective study was conducted using anonymized patient data in accordance with the principles of the Declaration of Helsinki. As this was a retrospective study, individual informed consent was not obtained from the patients.

Information retrieved from medical records included mobilization strategies, time to neutrophil and platelet engraftment, harvested $CD34^+$ cell yield, and the number of chemotherapy cycles administered prior to autologous HSCT. Neutrophil recovery was defined as the attainment of an absolute neutrophil count greater than 0.5×10^9/L for three successive days in the absence of granulocyte colony-stimulating factor support. Platelet recovery was defined as the attainment of a platelet count exceeding 20×10^9/L without transfusion support.

The number of therapy lines received for the disease, conditioning regimens prior to HSCT, use of maintenance therapy after transplantation, and whether a second HSCT was performed were recorded.

Statistical Analysis

Statistical analyses were performed using IBM SPSS Statistics for Windows, version 25.0 (IBM Corp., Armonk, NY, USA). Summary statistics were presented as number and percentage (n, %) for categorical variables, and as mean ± standard deviation [mean ± standard deviation (SD)] and median (minimum-maximum) for continuous variables.

The Mann-Whitney U test was applied to compare two groups. Categorical variables were compared using the Pearson chi-square test, with Fisher's exact test applied when appropriate. Receiver operating characteristic (ROC) curve analysis was performed to evaluate the predictive value of CD34 for mortality. OS was assessed by the Kaplan-Meier method and compared using the log-rank test. Statistical significance was defined as $p<0.05$.

Results

The comparison of sociodemographic and hospital-based variables of individuals grouped by mortality status is presented in Table 1. The comparative analysis showed no statistically significant differences in age, sex, underlying disease type, number of prior chemotherapy lines and cycles, number of transplant procedures, conditioning regimen, pre-

Table 1. Association of sociodemographic and clinical variables with mortality

Variables	Total (n,%) n=25	Alive (n,%) n=11	Dead (n,%) n=14	p
Age				
Mean ± SD	39±11	38±13	39±10	0.701[a]
Median (min-max)	40 (19-63)	39 (20-63)	41 (19-54)	
Sex				
Female	9 (36)	4 (36)	5 (36)	1.000[b]
Male	16 (64)	7 (64)	9 (64)	
Primary disease				
NHL	14 (84)	6 (55)	8 (57)	1.000[b]
HL	11 (16)	5 (45)	6 (43)	
Number of prior chemotherapy lines before HSCT				
1	7 (28)	4 (36)	3 (21)	0.875[b]
2	9 (36)	4 (36)	5 (36)	
3	9 (36)	3 (28)	6 (43)	
Number of chemotherapy cycles prior to HSCT				
Mean ± SD	8.8±4	8.4±4.4	9±4.1	0.700[a]
Median (min-max)	8 (2-18)	8 (3-18)	10 (2-16)	
Number of HSCT				
2	22 (88)	10 (91)	12 (86)	1.000[b]
3	3 (12)	1 (9)	2 (14)	
Conditioning regime				
BU-CY	1 (4)	0 (0)	1 (7)	0.913[b]
BU-CY-E	15 (60)	6 (55)	9 (65)	
BEAM	4 (16)	2 (18)	2 (14)	
Other	5 (20)	3 (27)	2 (14)	

Table 1. Continued

Variables	Total (n,%) n=25	Alive (n,%) n=11	Dead (n,%) n=14	p
Pre-HSCT PLT				
Mean ± SD	118.5±59.7	127±57	112±63	0.701[a]
Median (min-max)	120 (20-226)	120 (53-226)	111 (20-207)	
Neutrophil engraftment time				
Mean ± SD	17±4.7	15,7±3,5	19±6	0.173[a]
Median (min-max)	16.5 (10-30)	15 (10-22)	20 (11-30)	
PLT engraftment time				
Mean ± SD	17.2±7.7	15.9±6.2	18.8±9.4	0.755[a]
Median (min-max)	14.5 (8-35)	13 (8-26)	17 (10-35)	
Disease status before HSCT				
Complete response	10 (40)	6 (55)	4 (30)	0.532[b]
Partial response	8 (32)	3 (27)	5 (35)	
Progression	7 (28)	2 (18)	5 (35)	
Occurrence of FEN				
No	10 (40)	7 (63)	3 (21)	0.049[b]
Yes	15 (60)	4 (37)	11 (79)	
Duration of hospitalization				
Mean ± SD	25.7±20.1	21.8±6.7	28.7±26.2	0.805[a]
Median (min-max)	23 (7-112)	23 (10-33)	22.5 (7-112)	
100-day all-cause mortality				
No	17 (68)			0.273[a]
Yes	8 (32)			
Second ASCT				
No	22 (88)	10 (91)	12 (86)	1.000[b]
Yes	3 (12)	1 (9)	2 (14)	
IPI score				
0	6 (24)	4 (36)	2 (14)	0.555[b]
1	10 (40)	4 (36)	6 (43)	
2	7 (28)	3 (28)	4 (29)	
3	2 (8)	0 (0)	2 (14)	
CD34+ cell count				
Mean ± SD	9.1±7.4	11.2±9.4	7.3±5.1	0.202[a]
Median (min-max)	7.1 (2.3-36.3)	7.5 (2.3-36.3)	5.2 (2.8-22.4)	
Follow-up duration (months)				
Mean ± SD	23.4±27.5	50.1±20.3	2.4±1.9	<0.001[a]
Median (min-max)	6 (1-75)	50 (14-75)	1.5 (1-7)	

[a]: Independent t-test, [b]: Pearson chi square test, [c]: Fisher's exact test, p<0.05 statistically significant. SD: Standard deviation, min–max: Minimum-maximum, NHL: Non-Hodgkin lymphoma, HL: Hodgkin lymphoma, HSCT: Hematopoietic stem cell transplantation, BU-CY: Busulfan–cyclophosphamide, BU-CY-E: Busulfan-cyclophosphamide–etoposide, BEAM: Carmustine, etoposide, cytarabine, and melphalan, PLT: Platelet, FEN: Febrile neutropenia, ASCT: Autologous stem cell transplantation, IPI: International Prognostic index

transplant platelet levels, time to neutrophil and platelet engraftment, and pre-transplant disease status (all p>0.05).

The occurrence of febrile neutropenia (FEN) was significantly associated with mortality, with an increased mortality rate observed in those presenting with FEN compared with those who did not (78.6% vs. 21.4%; p=0.049). These findings indicate that FEN may be an important predictor of mortality (Figure 1).

Patients who survived had a significantly longer follow-up duration compared to those who died (50.09±20.30 months vs. 2.42±1.98 months; p<0.001).

Collectively, these results indicate that among the variables examined, only the development of FEN and follow-up duration were significantly associated with mortality, whereas other clinical and demographic variables was not found to significantly influence mortality.

Table 2 shows the diagnostic performance of CD34 levels for discriminating mortality, evaluated by ROC analysis. According to the analysis, the area under the curve for CD34 was 0.654 (95% confidence interval: 0.422-0.886), suggesting a limited but statistically significant ability of CD34 to predict mortality (p=0.049).

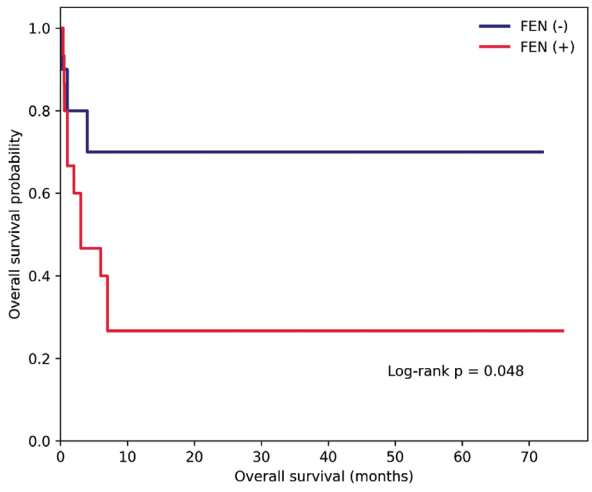

Figure 1. Comparable findings were observed between the groups with respect to length of hospital stay, second autologous transplantation status, IPI score, and CD34^{+} cell dose (all p>0.05). FEN: Febrile neutropenia

The most appropriate cut-off point was determined as ≤7.30, at which CD34 demonstrated a sensitivity of 61.5% and a specificity of 54.5% for the prediction of mortality.

In Table 3, OS outcomes were evaluated using Kaplan-Meier analysis. The median OS in the overall population was 6.00 months (0.0-12.52).

OS did not differ significantly with respect to sex; primary disease type; number of chemotherapy lines and cycles prior to transplantation; number of transplants; platelet count; neutrophil and platelet engraftment times; pre-transplant disease status; presence of a second autologous transplant; IPI score; and CD34 level (all p>0.05).

However, OS differed significantly depending on the development of FEN (p=0.048). The median OS in patients who developed FEN was 3.00 months (1.14-4.85), whereas the median OS was not estimable in those who did not develop FEN. This finding indicates that the development of FEN was associated with poorer OS.

Table 2. Assessment of the discriminative ability of CD34 for mortality

Variables	AUC	%95 CI	Cut-off	Sensitivity (%)	Specificity (%)	p
CD34	0.654	0.422–0.886	≤7.30	61.5	54.5	0.049

AUC: Area under the curve, CI: Confidence interval

Table 3. Comparison of overall survival among patients

Variables	Median (month) (%95 CI)	p
General	6 (0-1.5)	
Sex		
Female	1 (-)	0.702
Male	6 (0.1-11.8)	
Primary disease		
NHL	4 (0-11.3)	0.930
HL	6 (-)	
Number of prior chemotherapy lines before HSCT		
1	- (-)	0.666
2	7 (4.1-9.9)	
3	3 (0.1-5.9)	
Number of chemotherapy cycles prior to HSCT		
<8	7 (-)	0.673
>8	4 (0.2-7.7)	
Number of HSCT		
2	6 (-)	0.899
3	4 (2.4-5.6)	
Pre-HSCT PLT		
<120	6 (0-12.7)	0.953
>120	4 (-)	
Neutrophil engraftment time		
<16.5	- (-)	0.592
>16.5	- (-)	

Table 3. Continued

Variables	Median (month) (%95 CI)	p
PLT engraftment time		
<14.5	- (-)	0.412
>14.5	6 (0-14.7)	
Disease status before HSCT		
Complete response	- (-)	0.365
Partial response	2 (0-4.7)	
Progression	3 (0-8)	
Occurrence of FEN		
No	- (-)	0.048
Yes	3 (1.1-4.8)	
Second ASCT		
No	6 (-)	0.899
Yes	4 (2.4-5.6)	
IPI score		
0	- (-)	0.478
1	4 (0-8.6)	
2	7 (0-19.8)	
3	2 (-)	
CD34+ cell count		
<7.3	3 (0-10)	0.416
>7.3	- (-)	

Kaplan-Meier analysis and the log-rank test were used. A p value <0.05 was considered statistically significant. CI: Confidence interval, NHL: Non-Hodgkin lymphoma, HL: Hodgkin lymphoma, HSCT: Hematopoietic stem cell transplantation, PLT: Platelet, FEN: Febrile neutropenia, ASCT: Autologous stem cell transplantation, IPI: International Prognostic Index

No statistically significant differences were observed for the other variables; variations in median survival were apparent across some subgroups but did not reach statistical significance. Overall, only FEN was significantly associated with OS among the variables analyzed.

Discussion

In our study evaluating the outcomes of our Allo-HSCT patients, most sociodemographic and clinical variables—including age, sex, disease characteristics, treatment-related factors, engraftment parameters, and $CD34^+$ cell dose—had no statistically significant association with mortality or OS. In contrast, the development of FEN emerged as the only clinically relevant predictor of both increased mortality and shorter OS, highlighting its potential role as a key adverse prognostic indicator. Although $CD34^+$ cell dose demonstrated modest discriminative ability for mortality in ROC analysis, it did not translate into a difference in survival. Additionally, patients with longer follow-up were more likely to survive, as expected. Overall, these findings suggest that infectious complications, rather than baseline clinical or transplant-related variables, may exert a greater influence on outcomes in this cohort.

Rivas et al. (13) reported a multicenter analysis of 113 patients with R/R HL who received Allo-HSCT. Patients in CR had significantly improved OS and PFS (both $p \leq 0.001$) and lesser non-relapse mortality (NRM) ($p=0.04$). CR was emerged as an independent factor associated with improved OS and PFS in multivariate analysis (13).

Sureda et al. (14) analyzed 78 relapsed HL patients undergoing Allo-HSCT. NRM was 8% at day 100 and 15% at 1 year. PFS rates were 48% and 24% at 1 and 4 years, whereas OS rates were 71% and 43%. Pre-transplant CR was significantly associated with better outcomes (14).

Mercadal et al. (15) analyzed 53 recipients with B-cell NHL who underwent Allo-HSCT. Patients had a median follow-up of 72 months, with a median of 3 prior treatment lines. The 3-year PFS rate was 55%, OS was 63% and GRFS rates was 55% (15).

Doocey et al. (12) reported outcomes in 44 patients with R/R aggressive NHL undergoing Allo-HSCT. Participants had a mean age of 40 years. Five-year event-free survival (EFS) was 43, and OS was 48%. Grade III–IV acute graft-vs.-host disease proved to be the only significant predictor of both OS and EFS and was associated with poorer survival (12).

Goldberg et al. (16) retrospectively reported the results of 34 participants with NHL who had undergone Allo-HSCT at a single center. The mean follow-up duration among survivors was 45 months. The 2-year OS rate was 0.61. A Ki-67 expression ≤25% was found to be associated with superior OS ($p<0.01$), and HSCT performed in CR was associated with a reduced cumulative risk of events ($p=0.04$) (16).

Tarella et al. (17) evaluated Allo-HSCT in patients with R/R B-cell NHL, encompassing 285 transplant procedures in 281 patients. Patients had a median age at HSCT of 50 years; 94 were female. At transplantation,

47.7% were in CR, 22.3% in PR, 10.6% in SD, and 19.4% in PD. The median follow-up among survivors was 8.7 years. PFS rates at 3 and 9 years were 43.7% and 39.3%, respectively; OS rates were 50.4% and 46.6%. Pre-transplant CR was a favorable predictor of both PFS and OS (17).

Kami et al. (18) evaluated outcomes of Allo-HSCT in recipients with adult T-cell leukemia/lymphoma. The estimated 1-year OS and PFS rates were 53±30% and 45±29%, in that order (18).

Berning et al. (19) investigated 135 patients with natural killer/T-cell lymphoma who underwent Allo-HSCT. The study population had a median age of 43. After a median follow-up of 4.8 years, the 3-year PFS and OS rates were 48.6% and 55.6%, respectively. Multivariate analysis demonstrated that a shorter interval (0-12 months) from disease identification to Allo-HSCT and transplantation performed outside CR/PR were associated with poorer PFS (19).

Rigacci et al. (20) retrospectively analyzed 165 patients with NHL who underwent Allo-HSCT. Post-HSCT, CR and PR were achieved in 72 and 9 patients, respectively, with an OS rate of 49%. Rapid disease progression following HSCT was documented in 84 patients. Multivariate analysis identified remission status prior to transplantation as the only independent predictor of both OS and PFS (20).

Freytes et al. (21) analyzed 114 lymphoma patients undergoing Allo-HSCT and reported a 3-year cumulative incidence of disease progression of 52% and treatment-related mortality of 22%. Achievement of CR at transplant and the use of total body irradiation in patients with NHL were associated with reduced progression events and improved OS (21).

Further multicenter studies with larger patient cohorts, including real-world data, are needed to better define the role of allo-HSCT, particularly in patients with lymphoma.

Study Limitations

Several limitations should be acknowledged in this study. The study's retrospective design and single-center setting may predispose the study to selection bias and restrict the generalizability of the results. Second, the limited sample size may have constrained the power to detect subtle associations, potentially explaining the lack of statistically significant results for certain variables. Third, potential confounding factors—such as differences in supportive care practices, infection management, donor characteristics, and conditioning regimen intensity—could not be fully controlled. In addition, missing or incomplete data inherent to retrospective record-based analyses may have affected the accuracy of some variables. The heterogeneity of the patient population, including both HL and NHL cases with varying disease stages and prior treatment exposures, may also have influenced the outcomes. Finally, the relatively short follow-up period for some patients, particularly those who experienced early mortality, limits assessment of long-term survival outcomes.

Conclusion

FEN was the sole independent predictor significantly associated with increased mortality and reduced OS after Allo-HSCT in patients with HL and NHL. Other clinical variables, including $CD34^+$ cell dose, showed no significant impact. These findings highlight the critical role of infection management in improving outcomes.

Ethics

Ethics Committee Approval: Ethical approval for this study was obtained from the Institutional Ethics Committee from the İnönü University Health Sciences Non-Interventional Ethics Committee (approval number: 2025/7665, date: April 30, 2025).

Informed Consent: This retrospective study was conducted using anonymized patient data in accordance with the principles of the Declaration of Helsinki. As this was a retrospective study, individual informed consent was not obtained from the patients.

Footnotes

Authorship Contributions: Surgical and Medical Practices - İ.K., İ.B.; Concept - E.K., M.A.E., G.V.Ç.; Design - İ.K., İ.B.; Data Collection or Processing - A.S., İ.K., İ.B., G.V.Ç.; Analysis or Interpretation - A.S., E.K., M.A.E., E.H.; Literature Search - A.S., İ.B., E.H., G.V.Ç.; Writing - A.S., İ.K., E.H.

Conflict of Interest: No conflict of interest was declared by the authors.

Financial Disclosure: The authors declared that this study received no financial support.

References

1. Bispo JAB, Pinheiro PS, Kobetz EK. Epidemiology and etiology of leukemia and lymphoma. Cold Spring Harb Perspect Med. 2020; 10: a034819.
2. Siegel RL, Kratzer TB, Giaquinto AN, Sung H, Jemal A. Cancer statistics, 2025. CA Cancer J Clin. 2025; 75: 10-45.
3. Alaggio R, Amador C, Anagnostopoulos I, Attygalle AD, Araujo IBO, Berti E, et al. The 5th edition of the World Health Organization Classification of Haematolymphoid Tumours: lymphoid neoplasms. Leukemia. 2022; 36: 1720-48. Erratum in: Leukemia. 2023; 37: 1944-51.
4. Berber İ, Sarıcı A. Hodgkin lenfomada epidemiyoloji ve etiyoloji. In: Kaya E, editor. Hodgkin Lenfoma. 1. baskı. Ankara: Türkiye Klinikleri; 2020. p. 1-5.
5. Sarici A, Erkurt MA, Kuku I, Gok S, Bahcecioglu OF, Bicim S, et al. Selection of the mobilization regimen in lymphoma patients: a retrospective cohort study. Transfus Apher Sci. 2021; 60: 103251.
6. Rapoport AP, Meisenberg B, Sarkodee-Adoo C, Fassas A, Frankel SR, Mookerjee B, et al. Autotransplantation for advanced lymphoma and Hodgkin's disease followed by post-transplant rituxan/GM-CSF or radiotherapy and consolidation chemotherapy. Bone Marrow Transplant. 2002; 29: 303-12.
7. Rashidi A, Ebadi M, Cashen AF. Allogeneic hematopoietic stem cell transplantation in Hodgkin lymphoma: a systematic review and meta-analysis. Bone Marrow Transplant. 2016; 51: 521-8.
8. Armitage JO. How I treat patients with diffuse large B-cell lymphoma. Blood. 2007; 110: 29-36.
9. Ansell SM, Armitage J. Non-Hodgkin lymphoma: diagnosis and treatment. Mayo Clin Proc. 2005; 80: 1087-97.
10. Hill BT, Rybicki L, Bolwell BJ, Smith S, Dean R, Kalaycio M, et al. The non-relapse mortality rate for patients with diffuse large B-cell lymphoma is greater than relapse mortality 8 years after autologous stem cell transplantation and is significantly higher than mortality rates of population controls. Br J Haematol. 2011; 152: 561-9.

11. Bhatt VR, Loberiza FR Jr, Jing H, Bociek RG, Bierman PJ, Maness LJ, et al. Mortality patterns among recipients of autologous hematopoietic stem cell transplantation for lymphoma and myeloma in the past three decades. Clin Lymphoma Myeloma Leuk. 2015; 15: 409-15.e1.

12. Doocey RT, Toze CL, Connors JM, Nevill TJ, Gascoyne RD, Barnett MJ, et al. Allogeneic haematopoietic stem-cell transplantation for relapsed and refractory aggressive histology non-Hodgkin lymphoma. Br J Haematol. 2005; 131: 223-30.

13. Rivas MM, Berro M, Prates MV, Yantorno S, Fiad L, Arbelbide JA, et al. Allogeneic stem cell transplantation improves survival in relapsed Hodgkin lymphoma patients achieving complete remission after salvage treatment. Bone Marrow Transplant. 2020; 55: 117-25.

14. Sureda A, Canals C, Arranz R, Caballero D, Ribera JM, Brune M, et al. Allogeneic stem cell transplantation after reduced intensity conditioning in patients with relapsed or refractory Hodgkin's lymphoma. Results of the HDR-ALLO study - a prospective clinical trial by the Grupo Español de Linfomas/Trasplante de Médula Osea (GEL/TAMO) and the Lymphoma Working Party of the European Group for Blood and Marrow Transplantation. Haematologica. 2012; 97: 310-7.

15. Mercadal S, Mussetti A, Lee CJ, Arevalo C, Odstrcil SM, Peña E, et al. Allogeneic stem cell transplantation and CAR-T in B-cell Non-Hodgkin Lymphoma: a two-center experience and review of the literature. Ann Hematol. 2024; 103: 1717-27.

16. Goldberg JD, Chou JF, Horwitz S, Teruya-Feldstein J, Barker JN, Boulad F, et al. Long-term survival in patients with peripheral T-cell non-Hodgkin lymphomas after allogeneic hematopoietic stem cell transplant. Leuk Lymphoma. 2012; 53: 1124-9.

17. Tarella C, Sammassimo S, Frassoni S, Dominietto A, Cerretti R, Micò MC, et al. Long-term outcomes after Allogeneic hematopoietic stem cell transplantation in relapsed/refractory B-Cell Non-Hodgkin lymphoma: An Italian multicenter collaborative study. Transplant Cell Ther. 2025; 31: 806.e1-9.

18. Kami M, Hamaki T, Miyakoshi S, Murashige N, Kanda Y, Tanosaki R, et al. Allogeneic haematopoietic stem cell transplantation for the treatment of adult T-cell leukaemia/lymphoma. Br J Haematol. 2003; 120: 304-9.

19. Berning P, Schmitz N, Ngoya M, Finel H, Boumendil A, Wang F, et al. Allogeneic hematopoietic stem cell transplantation for NK/T-cell lymphoma: an international collaborative analysis. Leukemia. 2023; 37: 1511-20.

20. Rigacci L, Puccini B, Dodero A, Iacopino P, Castagna L, Bramanti S, et al. Allogeneic hematopoietic stem cell transplantation in patients with diffuse large B cell lymphoma relapsed after autologous stem cell transplantation: a GITMO study. Ann Hematol. 2012; 91: 931-9.

21. Freytes CO, Loberiza FR, Rizzo JD, Bashey A, Bredeson CN, Cairo MS, et al. Myeloablative allogeneic hematopoietic stem cell transplantation in patients who experience relapse after autologous stem cell transplantation for lymphoma: a report of the International Bone Marrow Transplant Registry. Blood. 2004; 104: 3797-803.

İstanbul Med J 2026; 27(3): 275-9
DOI: 10.4274/imj.galenos.2026.91112

Species Distribution and Antifungal Resistance in Candida Bloodstream Infections

Vahibe Aydın Sarıkaya[1], Deniz Turan[2], Sebahat Aksaray[3], Recep Balık[1], Seniha Şenbayrak[1], Asuman İnan[1], Serpil Erol[1], Nurgül Ceran[1]

[1]University of Health Sciences Türkiye, Haydarpaşa Numune Training and Research Hospital, Clinic of Infectious Diseases and Clinical Microbiology, İstanbul, Türkiye
[2]University of Health Sciences Türkiye, Haydarpaşa Numune Training and Research Hospital, Clinic of Medical Microbiology (Mycology Laboratory), Central Laboratory (ISLAB-2), İstanbul, Türkiye
[3]University of Health Sciences Türkiye, Haydarpaşa Numune Training and Research Hospital, Clinic of Medical Microbiology, İstanbul, Türkiye

ABSTRACT

Introduction: Candidemia is a serious infection with high morbidity and mortality. This study evaluated the distribution of Candida species, antifungal susceptibility outcomes, and variables associated with mortality in cases of candidemia.

Methods: Patients aged ≥18 years with candidemia diagnosed between 2024 and 2025 were retrospectively analyzed. Associations between clinical variables and 30-day mortality were examined using logistic regression analyses, including both univariable and multivariable models.

Results: The mean age of the 132 patients who developed candidemia was 68.7±15.4 years, and 46.2% were female. The dominant strain was Candida albicans, followed in order of frequency by *C. glabrata* and *C. auris*. The 30-day mortality rate was 55.3%. The highest mortality rate was observed in *C. auris* isolates (72.4%). In univariable analysis, intensive care unit (ICU) stay [odds ratio (OR): 17.26, 95% confidence interval (CI): 6.08-49.01; p<0.001], fluconazole resistance (OR: 2.92, 95% CI: 1.42-6.01; p=0.005), and amphotericin B resistance (OR: 3.57, 95% CI: 1.33-9.55; p=0.009) were significantly associated with mortality. All Candida albicans isolates were susceptible to fluconazole and echinocandins. All *C. auris* isolates were susceptible to echinocandins, while high rates of resistance to fluconazole (82.8%) and amphotericin B (89.7%) were observed. Evaluation of time to blood culture positivity showed that growth was detected in more than 90% of patients within the first two days.

Conclusion: Candidemia is associated with a high mortality rate. ICU stay emerged as an independent predictor of 30-day mortality, while resistance to fluconazole and amphotericin B may also be associated with mortality. The identification of *Candida auris* as the third most common pathogen, along with its high resistance rates to fluconazole and amphotericin B, is particularly noteworthy. The finding that all isolates, including *C. auris*, were susceptible to echinocandins supports an echinocandin-based empirical treatment approach in patients with suspected candidemia.

Keywords: Candidemia, mortality, *C. auris*, antifungal susceptibility, resistance

Introduction

Candidemia is among the leading causes of nosocomial bloodstream infections and is associated with substantial mortality, particularly in patients in intensive care units (ICUs). Despite advances in microbiological identification methods and antifungal therapy, mortality among patients with candidemia remains approximately 60%. Recent studies have demonstrated substantial inter-center variability in terms of candidemia incidence, species distribution, antifungal resistance, and mortality, and awareness of local epidemiology has been reported to reflect treatment success (1-3).

Another important epidemiological shift is the increasing prominence of non-*albicans Candida* species. Although *C. albicans* continues to be reported as the most common pathogen in many series, a notable rise has been observed in the proportions of *C. glabrata*, *C. parapsilosis*, and particularly *Candida auris*. This shift is clinically significant, as these species often exhibit reduced susceptibility to azoles or broader multidrug resistance to antifungal agents, which may complicate empirical treatment approaches and adversely affect clinical outcomes (1,2,4). Current knowledge regarding these infections in Türkiye is largely derived from a limited number of studies, leaving substantial gaps in

Address for Correspondence: Vahibe Aydın Sarıkaya, MD, University of Health Sciences Türkiye, Haydarpaşa Numune Training and Research Hospital, Clinic of Infectious Diseases and Clinical Microbiology, İstanbul, Türkiye
E-mail: dr.vahibeaydin@gmail.com **ORCID ID:** orcid.org/0009-0002-9952-1721
Cite this article as: Aydın Sarıkaya V, Turan D, Aksaray S, Balık R, Şenbayrak S, İnan A, et al. Species distribution and antifungal resistance in Candida bloodstream infections. İstanbul Med J. 2026; 27(3): 275-9

Received: 24.04.2026
Accepted: 10.07.2026
Publication Date: 03.08.2026

the evidence required to support clinical practice and public health decision-making.

This study aims to provide in-depth epidemiological insights into candidemia over a two-year period (2024-2025) at Haydarpaşa Numune Training and Research Hospital, one of the leading hospitals in İstanbul. Through detailed multivariable analyses, it seeks to identify the key risk factors associated with candidemia-related mortality. In addition, the antifungal susceptibility patterns of the isolated *Candida* species were evaluated. By providing contemporary data from Türkiye, this study may help address existing knowledge gaps and support evidence-based decisions in both clinical practice and public health.

Methods

The study protocol received institutional ethical approval from the Ethics Committee of Haydarpaşa Numune Training and Research Hospital (decision number: 2026/33, date: February 17, 2026). All research activities were carried out in accordance with internationally accepted ethical standards, including those described in the 2013 revision of the Declaration of Helsinki. Given the retrospective design of the study and the use of anonymized patient data, the requirement for obtaining individual inform consent was waived by the ethics committee.

This retrospective observational study was conducted at Haydarpaşa Numune Training and Research Hospital, in İstanbul. Patients aged ≥18 years who were hospitalized in inpatient wards and ICUs between January 1, 2024, and December 31, 2025, and had *Candida* spp. isolated from blood cultures were included. Patients with Candida isolates obtained from non-blood clinical specimens, patients in whom species-level identification could not be performed, and patients with incomplete microbiological data were excluded.

Cases were classified as candidemia when *Candida* species were identified in blood culture samples. When *Candida* was recovered again within 30 days of the initial episode, the event was classified as a continuation of the initial episode. Isolates detected after an interval greater than 30 days were considered to represent a separate episode. The survival rates of patients diagnosed with candidemia were examined during the first 30 days, and deaths within this period were considered as 30-day mortality. Data on demographic variables (age and sex), site of hospitalization, species identification, antifungal susceptibility results, time to blood culture positivity, time to initiation of empirical antifungal therapy after detection of yeast on Gram staining, administered antifungal treatment, and 30-day mortality were recorded.

Blood cultures were processed with the BD BACTEC™ FX automated detection platform (Becton Dickinson, Franklin Lakes, NJ, USA). Following a positive growth signal, Gram-stained smears were examined microscopically. Specimens containing yeast cells were then cultured on 5% sheep blood agar (Oxoid, UK) and Sabouraud dextrose agar (RTA, Türkiye) for fungal isolation. After inoculation, the culture media were maintained at 35±2 °C for 24-48 hours to allow yeast growth. Isolates obtained from the cultures were subsequently identified by MALDI-TOF MS. Antifungal susceptibility was determined with the VITEK 2 Compact platform using the AST YS08 card (bioMérieux, France). Interpretation of results was based on CLSI M27M44S criteria. To ensure the reliability of susceptibility testing, *Candida parapsilosis* (ATCC 22019) and *Candida krusei* (ATCC 6258) were incorporated as quality control reference strains. Results were retrospectively evaluated using laboratory records with categorical reporting (susceptible, intermediate, and resistant).

Time to initiation of antifungal therapy was categorized as: treatment initiated within the first 24 hours or treatment initiated after 24 hours. Time to blood culture positivity was categorized by the day on which a positive blood culture signal was detected after blood culture collection.

Statistical Analysis

All statistical analyses were performed using R version 4.5.1 (R Foundation for Statistical Computing, Vienna, Austria). According to the distributional characteristics of the variables, continuous variables were presented as mean ± standard deviation or median (minimum-maximum), whereas categorical variables were expressed as numbers and percentages. Comparisons between patients who died within 30 days and those who survived were performed using the Student's t test or the Mann-Whitney U test for continuous variables and Fisher's exact test or the chi-square test for categorical variables. Univariable logistic regression analysis was initially performed to identify variables associated with 30-day mortality. Variables with a p value <0.05 in the univariable analysis were subsequently included in a multivariable logistic regression model to identify independent risk factors associated with mortality. The results of the univariable logistic regression analyses were reported as odds ratios (ORs), whereas the results of the multivariable logistic regression analyses were presented as adjusted ORs (aORs) with corresponding 95% confidence intervals (CIs). A p value <0.05 was considered statistically significant.

Results

A total of 132 patients with candidemia were included in the study. The mean age was 68.7±15.4 years; the mean age was 67.3±14.9 years in survivors and 69.9±15.9 years in patients who died (p=0.331). Among the patients, 61 (46.2%) were female and 71 (53.8%) were male; no significant association was found between sex and mortality (p=0.484). The overall 30-day mortality rate was 55.3% (73/132). A total of 94 patients (71.2%) were followed in the ICU; the rate of ICU stay was 93.2% among patients who died vs. 44.1% among survivors, and this difference was statistically significant (p<0.001).

When antifungal susceptibility profiles were evaluated, fluconazole non-susceptible isolates were more frequent among patients who died than among survivors (56.2% vs. 30.5%; p=0.005). Similarly, resistance to amphotericin B was higher among patients who died than among survivors (28.8% vs. 10.2%; p=0.009). No echinocandin resistance was detected. There was no statistically significant difference in mortality between initiation of empirical antifungal therapy within the first 24 hours and later initiation (100.0% vs. 94.5%, respectively; p=0.128). Blood culture positivity was detected within the first two days in 95.5% of cases; this finding was not associated with mortality (98.3% vs. 93.2%, respectively; p=0.224) (Table 1, Figure 1).

The most frequently isolated species from blood cultures was Candida albicans (32.6%), followed by *C. glabrata* (23.5%) and *C. auris* (22.0)%. *C. parapsilosis* (15.2%) was identified less frequently, while *C. tropicalis*

(6.1%) and *C. krusei* (0.8%) were the least frequently isolated species (Figure 2).

All *C. auris* isolates were susceptible to echinocandins, whereas high rates of fluconazole (82.8%) and amphotericin B (89.7%) resistance were observed. In contrast, none of the Candida albicans isolates examined showed resistance to fluconazole or echinocandins; all strains were susceptible.

Species-specific mortality rates were 39.5% for *Candida albicans*, 54.8% for *C. glabrata*, 72.4% for *C. auris*, 65.0% for *C. parapsilosis*, 50.0% for *C. tropicalis*, and 100.0% for *C. krusei*. Although the highest mortality was observed in *C. auris* isolates, the mortality rate calculated for C. *krusei* was not interpretable because *C. krusei* was represented by a single isolate. Overall, the association between *Candida* species and mortality was not statistically significant (p=0.093) (Table 2).

In univariable analysis, ICU stay (OR: 17.26, 95% CI: 6.08-49.01; p<0.001), fluconazole resistance (OR: 2.92, 95% CI: 1.42-6.01; p=0.005), and amphotericin B resistance (OR: 3.57, 95% CI: 1.33-9.55; p=0.009) were significantly associated with mortality. In multivariable logistic regression analysis, only ICU stay was identified as an independent

Table 1. Baseline characteristics according to 30-day mortality

Variable	Overall (n=132)	Alive (n=59)	Died (n=73)	p value
Age, mean ± SD	68.7±15.4	67.3±14.9	69.9±15.9	0.331
Female sex, n (%)	61 (46.2)	25 (42.4)	36 (49.3)	0.484
ICU admission, n (%)	94 (71.2)	26 (44.1)	68 (93.2)	<0.001
Fluconazole non-susceptible, n (%)	59 (44.7)	18 (30.5)	41 (56.2)	0.005
Amphotericin B resistant, n (%)	27 (20.5)	6 (10.2)	21 (28.8)	0.009
Antifungal initiation within ≤24 h, n (%)	128 (97.0)	59 (100.0)	69 (94.5)	0.128
Positive signal on day 1-2, n (%)	126 (95.5)	58 (98.3)	68 (93.2)	0.224

ICU: Intensive care unit, SD: Standard deviation

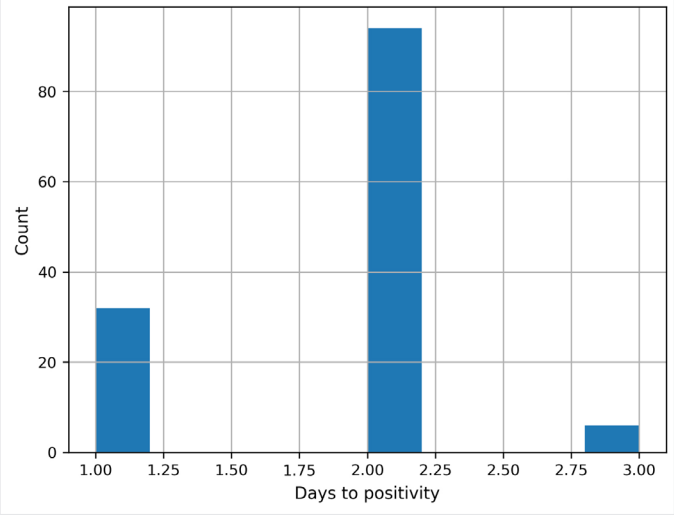

Figure 1. Time to blood culture positivity

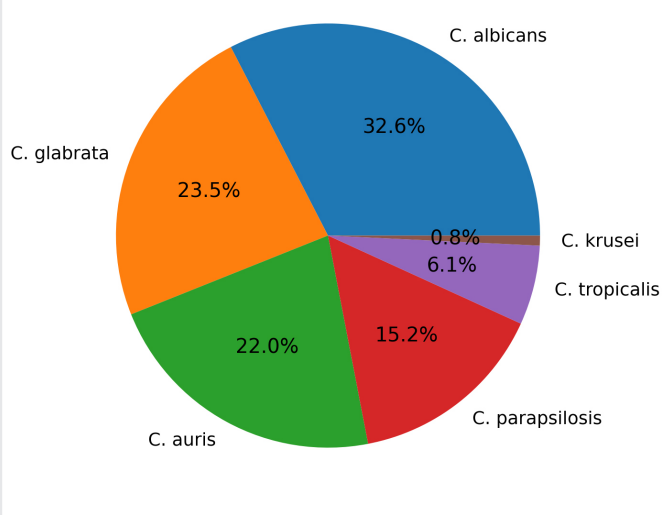

Figure 2. Species distribution of *Candida* isolates from blood cultures

Table 2. Species distribution and mortality

Species	Overall, n (%)	Alive, n (%)	Died, n (%)	Mortality, %
C. albicans	43 (32.6)	26 (44.1)	17 (23.3)	39.5
C. glabrata	31 (23.5)	14 (23.7)	17 (23.3)	54.8
C. auris	29 (22.0)	8 (13.6)	21 (28.8)	72.4
C. parapsilosis	20 (15.2)	7 (11.9)	13 (17.8)	65.0
C. tropicalis	8 (6.1)	4 (6.8)	4 (5.5)	50.0
C. krusei	1 (0.8)	0 (0.0)	1 (1.4)	100.0

Overall p value = 0.093. Mortality (%) was calculated as the proportion of deaths among patients with each *Candida* species. *C. albicans: Candida albicans, C. glabrata: Candida glabrata, C. auris: Candida auris, C. parapsilosis: Candida parapsilosis, C. tropicalis: Candida tropicalis, C. krusei: Candida krusei*

Table 3. Univariable and multivariable logistic regression analyses of factors associated with 30-day mortality

Variable	Univariable		Multivariable	
	OR (95% CI)	p value	aOR (95% CI)	p value
ICU admission	17.26 (6.08-49.01)	<0.001	15.52 (5.36-44.96)	<0.001
C. auris infection	2.57 (1.05-6.34)	0.056	–	–
Fluconazole non-susceptible	2.92 (1.42-6.01)	0.005	1.87 (0.76-4.63)	0.175
Amphotericin B resistant	3.57 (1.33-9.55)	0.009	2.24 (0.66-7.62)	0.196
Antifungal initiation >24 h	6.84 (0.35-132.06)	0.128	–	–
Blood culture positivity ≥3 days	4.26 (0.48-37.55)	0.224	–	–

Variables with a p value <0.05 in the univariable analysis were entered into the multivariable logistic regression model. OR: Odds ratio, CI: Confidence interval, aOR: Adjusted odds ratio, ICU: Intensive care unit, C. auris: Candida auris

predictor of mortality (aOR: 15.29, 95% CI: 5.27-44.42; p<0.001) (Table 3).

Discussion

In this study, the 30-day mortality rate in patients with candidemia was 55.3%. A single-center study from Türkiye published in 2024 reported a mortality rate of 59.3%, while another study published in 2025 reported a rate of 64% (2,5). Similarly, recent regional and population-based analyses indicate that mortality remains high across different healthcare systems and may vary depending on patients' clinical status, ICU burden, and the distribution of causative species. In this context, the mortality rate observed in our study appears to be consistent with the upper range of contemporary candidemia series (3,6).

When species distribution was evaluated, *C. albicans* was the most frequently identified pathogen in our study, followed by *C. glabrata* and *C. auris*. The identification of *C. auris* as the third most common species suggests that this pathogen has gained clinical significance at Haydarpaşa Numune Training and Research Hospital, which may be partially attributable to the high proportion of ICU patients. This distribution is consistent with the current literature reporting that *C. albicans* remains predominant, while non-albicans *Candida* species are increasingly encountered (1,2,7). In our study, although *C. auris* was not identified as an independent predictor of mortality, the highest mortality rate was observed in this species (72.4%) when species-specific mortality rates were evaluated. When considered together with its association with ICU settings and antifungal resistance characteristics, this finding suggests that *C. auris* retains its clinical significance and underscores the need for surveillance and infection control measures.

In our study, antifungal susceptibility patterns differed markedly among species. All *C. auris* isolates were susceptible to echinocandins, whereas fluconazole resistance was notably high at 82.8%, which is consistent with data reported in the literature. It is well established that fluconazole resistance in *C. auris* isolates exceeds 85% in most series (1,3). In contrast, a notable finding in our study was the remarkably high rate of amphotericin B resistance (89.7%, n=26). Recent studies have reported that amphotericin B resistance in *Candida auris* isolates generally ranges between 10% and 40% (8-10). In addition, differences in antifungal susceptibility testing methodologies, in interpretive criteria, and in the predominance of specific *C. auris* clades across geographic regions may have contributed to the variability in reported amphotericin B resistance rates. In this context, the high resistance rate observed in our study may be related to local epidemiological characteristics and the predominance of ICU patients. In addition, in vitro studies have demonstrated that the activity of antifungal agents against *Candida* species may vary (11). The resistance pattern observed in our center suggests that use of amphotericin B may be limited, particularly in patient populations with a high prevalence of *C. auris*; therefore, echinocandins emerge as a more appropriate option for severe candidemia and for ICU patients. Nevertheless, recent reports of emerging echinocandin-resistant *C. auris* isolates associated with mutations in the *FKS1* gene underscore the importance of ongoing antifungal susceptibility surveillance, even in centers where echinocandin susceptibility remains universal (12). Furthermore, the association between fluconazole non-susceptible isolates and mortality supports the clinical significance of azole resistance.

Our finding that all *C. albicans* isolates were susceptible to fluconazole and echinocandins indicates a clear distinction in antifungal susceptibility among species. However, no significant difference in mortality was observed between *C. auris* and other *Candida* species. This may be attributable to the susceptibility of isolates from both groups to echinocandins and the prompt initiation of empirical anidulafungin therapy following detection of yeast on Gram staining of blood cultures at our center.

The identification of ICU admission as an independent predictor of mortality represents one of the most consistent findings of our study. This observation is strongly aligned with current evidence. Recent studies from Türkiye and Kuwait have identified ICU stay as one of the strongest predictors of poor prognosis in candidemia. This association may be explained by the coexistence of broad-spectrum combination-antibiotic use, critical illness, invasive procedures, prolonged hospitalization, total parenteral nutrition, and multiple comorbidities. Our findings support that candidemia in ICU patients should be considered not only a microbiological event but also a marker of significant clinical vulnerability (1,2,13-15).

In our study, no significant association was observed between the initiation of empirical antifungal therapy within the first 24 hours after yeast detection in blood cultures and a later initiation, with respect to mortality. This finding may be explained by the close daily monitoring of ICU patients at our center and the prompt initiation of antifungal

therapy in the majority of cases (128/132) following the detection of yeast on blood culture Gram staining, which may have limited the variability in the analysis.

This study has several strengths. First, it includes a contemporary cohort and evaluates the species distribution and antifungal susceptibility patterns, along with clinically relevant 30-day mortality. In addition, the inclusion of *C. auris* in the cohort enhances the value of the findings within the current epidemiological context.

Study Limitations

As this investigation was conducted retrospectively at a single institution, the applicability of the results to other healthcare settings may be limited. In addition, some clinically relevant variables that may influence candidemia prognosis, including comorbidity burden, catheter removal, source control, septic shock status, and total duration of antifungal therapy, were not included in the analysis. Antifungal exposure before the onset of candidemia was not evaluated and may have influenced the observed antifungal resistance patterns. Similar limitations have been reported in recent single-center candidemia studies.

Conclusion

Our study demonstrates that candidemia remains a significant infection and is associated with high mortality. While *C. albicans* continues to be the predominant species, the clinical importance of non-*albicans Candida* species, particularly *C. auris*, is increasing. The finding that *C. auris* isolates were fully susceptible to echinocandins but highly resistant to amphotericin B indicates a notable susceptibility profile with important implications for treatment management. ICU admission is a major determinant of mortality. Our findings underscore the importance of local epidemiology and susceptibility patterns in guiding empirical treatment strategies.

Ethics

Ethics Committee Approval: The study protocol received institutional ethical approval from the Ethics Committee of Haydarpaşa Numune Training and Research Hospital (decision number: 2026/33, date: February 17, 2026).

Informed Consent: Given the retrospective design of the study and the use of anonymized patient data, the requirement for obtaining individual inform consent was waived by the ethics committee.

Footnotes

Authorship Contributions: Concept - V.A.S., D.T., S.A., R.B., S.Ş., A.İ., S.E., N.C.; Design - V.A.S., D.T., S.A., R.B., S.Ş., A.İ., S.E., N.C.; Data Collection or Processing - V.A.S., D.T., S.A., R.B., S.Ş., A.İ., S.E., N.C.; Analysis or Interpretation - V.A.S., D.T., S.A., R.B., S.Ş., A.İ., S.E., N.C.; Literature Search - V.A.S., D.T., S.A., S.E., N.C.; Writing - V.A.S., D.T., S.A., R.B., S.Ş., A.İ., S.E., N.C.

Conflict of Interest: No conflict of interest was declared by the authors.

Financial Disclosure: The authors declared that this study received no financial support.

References

1. Al Benwan K, Ahmed S, Al Banwan D, John M. Candidemia in a general hospital in Kuwait: epidemiology, species distribution, risk factors, and antifungal susceptibility patterns over a 10-year period (2015-2024). J Fungi (Basel). 2025; 11: 670.
2. Ünal N, Karakoyun AS, Ünal İ, Turunç T, Lass-Flörl C, Ilkit M. Epidemiological characteristics and mortality predictors of candidemia due to candida albicans: a single-center experience from Türkiye. J Fungi (Basel). 2025; 11: 788.
3. Cornely OA, Sprute R, Bassetti M, Chen SC, Groll AH, Kurzai O, et al. Global guideline for the diagnosis and management of candidiasis: an initiative of the ECMM in cooperation with ISHAM and ASM. Lancet Infect Dis. 2025; 25: e280-93. Erratum in: Lancet Infect Dis. 2025; 25: e203. Erratum in: Lancet Infect Dis. 2025; 25: e261. Erratum in: Lancet Infect Dis. 2025; 25: e684.
4. Meletiadis J, Siopi M, Spruijtenburg B, Georgiou PC, Kostoula M, Vourli S, et al. Candida auris fungaemia outbreak in a tertiary care academic hospital and emergence of a pan-echinocandin resistant isolate, Greece, 2021 to 2023. Euro Surveill. 2024; 29: 2400128.
5. Kültüral Güngör A, Yuluğkural Z. Epidemiology, clinical features and predictors of mortality in patients with candidemia in a tertiary care hospital in Türkiye: a single-center retrospective study. Phnx Med J. 2024; 6: 110-7.
6. Dai Z, Lan X, Cai M, Liao Y, Zhang J, Ye N, et al. Nineteen years retrospective analysis of epidemiology, antifungal resistance and a nomogram model for 30-day mortality in nosocomial candidemia patients. Front Cell Infect Microbiol. 2025; 15: 1504866.
7. Bhargava A, Klamer K, Sharma M, Ortiz D, Saravolatz L. *Candida auris*: a continuing threat. Microorganisms. 2025; 13: 652.
8. Laury JE, Forsberg K, Berkow EL, Jones S, Sexton DJ, Sievert DM, et al. Candida auris testing by the antimicrobial resistance laboratory network, United States, 2022-2023. Emerg Infect Dis. 2026; 32: 308-10.
9. Lockhart SR, Etienne KA, Vallabhaneni S, Farooqi J, Chowdhary A, Govender NP, et al. Simultaneous emergence of multidrug-resistant candida auris on 3 continents confirmed by whole-genome sequencing and epidemiological analyses. Clin Infect Dis. 2017; 64: 134-40. Erratum in: Clin Infect Dis. 2018; 67: 987.
10. Lyman M, Forsberg K, Sexton DJ, Chow NA, Lockhart SR, Jackson BR, et al. Worsening spread of Candida auris in the United States, 2019 to 2021. Ann Intern Med. 2023; 176: 489-95.
11. Kirkik D, Hacimustafaoğlu F, Özkanca C, Kalkanli Taş S, Elmastaş M. Assessment of the in vitro antimicrobial activity and fatty acid composition of crocodile oil from Crocodylus siamensis. Sci Rep. 2025; 15: 28673.
12. Misas E, Parnell LA, Rajeev M, López LF, Santos ARd, Mudge ZB, et al. A benchmark dataset for validating FKS1 mutations in Candida auris. Microbiol Spectr. 2025; 13: e0314724.
13. de Almeida BL, Agnelli C, Guimarães T, Sukiennik T, Lima PRP, Salles MJC, et al. Candidemia in ICU patients: what are the real game-changers for survival? J Fungi (Basel). 2025; 11: 152.
14. Sedik S, Egger M, Wolfgruber S, Salmanton-García J, Bassetti M, Mikulska M, et al. Risk factors for persistent candidemia and prognostic implications: Results from the ECMM Candida III study. J Infect. 2025; 91: 106629.
15. Colaneri M, Giusti EM, Genovese C, Galli L, Lombardi A, Gori A. Mortality of patients with candidemia and COVID-19: a systematic review with meta-analysis. Open Forum Infect Dis. 2023; 10: ofad358.